To the Graduate Council:

I am submitting herewith a thesis written by Dana Gregory Jernigan entitled "Comparative Diagenetic Histories of the Holston and Rockdell Formations, Middle Ordovician of Northeastern Tennessee." I have examined the final copy of this thesis for form and content and recommend that it be accepted in partial fulfillment of the requirements for the degree of Master of Science, with a major in Geology.

Kenneth R. Walker

Kenneth R. Walker, Major Professor

We have read this thesis and
recommend its acceptance:

Thomas L. Broadhead

Richard W. Arnseth

Accepted for the Council:

Lawrence Minkel

Vice Provost
and Dean of The Graduate School

STATEMENT OF PERMISSION TO USE

In presenting this thesis in partial fulfillment of the requirements for a Master's degree at The University of Tennessee, Knoxville, I agree that the Library shall make it available to borrowers under rules of the Library. Brief quotations from this thesis are allowable without special permission, provided that accurate acknowledgment of source is made.

Permission for extensive quotation from or reproduction of this thesis may be granted by my major professor, or in his absence, by the Head of Interlibrary Services when, in the opinion of either, the proposed use of the material is for scholarly purposes. Any copying or use of the material in this thesis for financial gain shall not be allowed without my written permission.

Signature D. Gregory Jernigan

Date July 24, 1987

COMPARATIVE DIAGENETIC HISTORIES OF THE HOLSTON AND ROCKDELL FORMATIONS, MIDDLE ORDOVICIAN OF NORTHEASTERN TENNESSEE

A Thesis

Presented for the

Master of Science

Degree

The University of Tennessee, Knoxville

Dana Gregory Jernigan

August 1987

DEDICATION

To my wife, Cheryl, who in every way is "The Wife of Noble Character" (Prov. 31:10-31).

ACKNOWLEDGMENTS

I wish to express my deepest appreciation to my major professor, Dr. Kenneth R. Walker, Carden Professor and Head of the Department of Geological Sciences, for his friendship both before and during my graduate studies at The University of Tennessee, Knoxville. Ken suggested this topic for research and encouraged, guided, and supported the work from its conception. Without Ken's guidance, the completion of this thesis would not have been possible.

I am grateful to the other members of my committee, Dr. Richard W. Arnseth and Dr. Thomas W. Broadhead. Both took time to look at my thin-sections and assisted in identification of some problematic allochems. Both also served as editors, and offered helpful criticisms in the final draft of this thesis.

I would like to thank the members of the Carbonate Bank including Eric Johnson, Mike Kozar, John Simonson, Jim Weber, and James Wedekind for their sincere and thoughtful input throughout this research. Many of the ideas presented here were developed through discussions during "Bank Meetings" over the past three years. I, as well as all present and future Bankers, am indebted to the Bankers before me. It is sometimes easy to forget that they, along with Dr. Walker, laid the framework for later diagenetic and geochemical studies in the Middle Ordovician of Eastern Tennessee.

Finally, no part of this research would have been possible without the loving encouragement of my wife, Cheryl; my mother and step-father,

Mr. and Mrs. Ross S. Jones; my father, Charles H. Jernigan; and my sister and brother-in-law, Mr. and Mrs. Edgar Floyd. I am grateful for their financial support and thankful for their unconditional love.

This research was supported by the Carden Fund for Geology, the Carden Fellowship, and the Discretionary Funds of the Department of Geological Sciences, The University of Tennessee, the Appalachian Basin Industrial Associates, and a research grant from Sigma Xi.

ABSTRACT

The Holston and Rockdell formations (Middle Ordovician) in northeastern Tennessee represent two lithologically similar, largely coeval carbonate buildup complexes which were deposited at different positions on a carbonate shelf. The Rockdell was deposited in a stable platform setting while the Holston Formation was deposited at the shelf margin (Ruppel and Walker, 1982). Each formation may be divided into three intergradational lithofacies. The Rockdell consists of: (1) bryozoan-echinoderm grainstone-packstones; (2) bryozoan-echinoderm packstones; and (3) bryozoan wackestones. The Rockdell bryozoan-echinoderm packstone lithofacies occurs predominantly in the northwestern part of the study area whereas bryozoan-echinoderm grainstone-packstones and bryozoan wackestones are best developed in the central and southeastern parts. The Holston consists of: (1) echinoderm-bryozoan grainstone-packstones; (2) bryozoan wackestone-boundstones (lime-mud mounds); and (3) echinoderm-bryozoan packstones. Rocks of the Holston Formation are limited to the southeastern part of the study area.

Petrographic and cathodoluminescence analyses allow distinction of eight cement types in the Holston and Rockdell formations: (1) radiaxial-fibrous calcite and associated cement; (2) bladed/prismatic cement; (3) turbid (inclusion-rich) syntaxial (rim) cement; (4) cryptocrystalline (micrite) cement; (5) equant (drusy) calcite; (6) clear syntaxial (rim) cement; (7) ferroan calcite; and (8) ferroan

(baroque) dolomite. Evidence suggests that radiaxial-fibrous calcite and associated cement, bladed/prismatic cement, turbid syntaxial cement, and cryptocrystalline (micrite) cement were precipitated early, in the marine diagenetic environment. The lines of evidence include: (1) high levels of trace Sr and Mg in radiaxial-fibrous calcite; (2) cement development both before and after deposition of internal marine sediment; (3) superposition within pores and cavities (cement stratigraphy); (4) microdolomite inclusions within cement crystals (suggesting a magnesian calcite precursor); and (5) comparison of cement textures, fabrics and occurrences with similar, previously studied examples. Equant (drusy) calcite and clear syntaxial cement are interpreted as meteoric in origin because they: (1) always post-date marine cement; (2) occur as pore central intrabiotic cement (equant calcite); (3) are devoid of inclusions (suggesting they were deposited as low-magnesian calcite); and (4) are similar to other previously described meteoric cement. Ferroan calcite (including the ferroan part of clear syntaxial cement) and ferroan (baroque) dolomite formed after burial under reducing conditions in the stagnant meteoric phreatic zone or much later after deep burial. A burial origin is supported by the elevated temperature of formation of baroque dolomite (60°-150°C) and the mutual occurrence of these cement phases.

Marine cement and burial cement are best developed at the shelf margin (Red House Branch and Poor Valley Creek) and, in samples from these locales, represent the predominant cementing phases. Meteoric cement is best developed at shelfward localities of the Rockdell (Cedar

Springs and Evans Ferry) where marine cement is much less abundant. Thus, two inverse cement gradients exist; marine and burial cement abundances increase basinward whereas meteoric cement abundance decreases basinward.

Depositional units at each of the study localities were dominated by either marine, meteoric, or burial cementation. Preliminary analyses of this pattern suggest that cement dominated units do not occur in random stacking order. Instead, the zones commonly occur in triplets. Each triplet consists of: (1) a lower marine cemented zone, followed by (2) a middle meteoric zone, which is capped by (3) a zone dominated by burial cement. Some cement zones may be correlative between shelf marginal and on-shelf localities.

Although their timing overlaps, the paragenetic sequence of marine cement is: (1) microcrystalline (micrite) cement; (2) bladed/prismatic cement; and (3) turbid syntaxial (rim) cement and radiaxial-fibrous calcite and associated cement. The cementation history of the Holston and Rockdell formations largely controlled other diagenetic processes. Diagenetic processes which are coeval with marine cementation, in order of earliest occurrence are: (1) macroboring and micritization of skeletal grains; (2) stromatactoid and irregular cavity formation; (3) internal sedimentation, and (4) mechanical compaction. In the meteoric diagenetic environment, equant (drusy) calcite cement and clear syntaxial (rim) cement are coeval. Diagenetic processes accompanying these cement phases, in order of their earliest occurrence, are: (1) mineralogic stabilization (magnesian calcite to low-magnesian

calcite); (2) dolomitization; (3) solution of aragonite and neomorphism; and (4) silicification (replacement by chalcedony and authigenic quartz). In the burial diagenetic environment, ferroan calcite (including ferroan zones of clear syntaxial cement) and ferroan (baroque) dolomite formed simultaneously. Other diagenetic processes which developed after burial, in temporal order, were: (1) fracturing; (2) silicification (replacement by chalcedony and authigenic quartz); and (3) chemical compaction.

TABLE OF CONTENTS

CHAPTER		PAGE
1.	INTRODUCTION	1
	Depositional Framework	3
	Purpose	5
	Stratigraphy	8
	Location of Study Area	11
	Methods of Study	14
2.	DEPOSITIONAL ENVIRONMENTS	19
	Introduction	19
	The Holston Formation Near Knoxville, Tennessee	20
	The Holston Formation in Northeastern Tennessee	26
	The Rockdell Formation Near Knoxville, Tennessee	39
	The Rockdell Formation in Northeastern Tennessee	43
	Time Relationships Between the Holston and Rockdell	53
3.	CARBONATE CEMENT	57
	Introduction	57
	Marine Cement	58
	Radiaxial-Fibrous Calcite and Associated Cement	73
	Bladed/Prismatic Cement	93
	Turbid Syntaxial (rim) Cement	98
	Cryptocrystalline (Micrite) Cement	107
	Meteoric Cement	109
	Equant (Drusy) Calcite Cement	116
	Clear Syntaxial (rim) Cement	122
	Ferroan Calcite (Fe-Calcite)	130
	Ferroan (Baroque) Dolomite	134
4.	CEMENT ABUNDANCE AND DISTRIBUTION	137
	Introduction	137
	Cement Abundance and Distribution	138
	Stratigraphic Patterns of Cementation	157
	Paragenetic Sequence of Cements	167
5.	RELATIVE TIMING OF NONCEMENTATION DIAGENETIC EVENTS	170
	Introduction	170
	Macroboring and Micritization	173
	Stromatactoid and Irregular Cavity Formation	174
	Mineralogic Stabilization and Neomorphism	178

CHAPTER PAGE

Dolomitization 180
Silicification 181
Compaction 182
Fracturing 184

6. SUMMARY AND CONCLUSIONS 186

LIST OF REFERENCES 191

LIST OF TABLES

TABLE		PAGE
1.1.	Samples Available for Use in This Study	16
2.1.	Constituent Analyses of the Echinoderm-Bryozoan Grainstone-Packstone Lithofacies of the Holston Formation	30
2.2.	Constituent Analyses of the Bryozoan Wackestone-Boundstone Lithofacies of the Holston Formation	32
2.3.	Constituent Analyses of the Echinoderm-Bryozoan Packstone Lithofacies of the Holston Formation	38
2.4.	Constituent Analyses of the Bryozoan-Echinoderm Grainstone-Packstone Lithofacies of the Rockdell Formation	45
2.5.	Constituent Analyses of the Bryozoan-Echinoderm Packstone Lithofacies of the Rockdell Formation	49
2.6.	Constituent Analyses of the Bryozoan Wackestone Lithofacies of the Rockdell Formation	51
3.1.	Articles on Marine Cementation Presented at the Bermuda Biological Station for Research in 1969 and Summarized in Bricker (1971)	59
3.2.	Trace Element Composition of Radiaxial-Fibrous Calcite Cement from Selected Samples from the Holston and Rockdell Formations	90
3.3.	Trace Element Composition of Ferroan Calcite Cement from Selected Samples from the Holston Formation	132
4.1.	Distribution of Carbonate Cement by Lithofacies in the Holston and Rockdell Formations	139
4.2.	Diagenetic Environment of Formation of Carbonate Cement Types in the Holston and Rockdell Formations in Northeastern Tennessee	161
4.3.	Stratigraphic Range of Cement Zones in the Holston and Rockdell Formations at Red House Branch	164
B.1.	Variables Observed in Constituent Analysis	219

TABLE		PAGE
C.1.	All Constituent Analysis Data	221
C.2.	Evans Ferry Samples	221
C.3.	Cedar Spring Samples	222
C.4.	Poor Valley Creek Samples	223
C.5.	Red House Branch Samples	223
C.6.	All Holston Formation Samples	224
C.7.	All Rockdell Formation Samples	224
C.8.	All Grainstones and Packstones	224
C.9.	Holston Grainstones and Packstones	225
C.10.	Rockdell Grainstones and Packstones	225
C.11.	All Wackestones, Mudstones, and Boundstones	225
C.12.	Holston Wackestones, Mudstones, and Boundstones	226
C.13.	Rockdell Wackestones, Mudstones, and Boundstones	226
D.1.	Precision Data for Strontium, Magnesium and Manganese	232
D.2.	Atomic Absorption Spectrophotometry Data	233

LIST OF FIGURES

FIGURE		PAGE
1.1.	Regional Cross-Section Through the Knoxville, Tennessee Area Illustrating the Facies Relationships of Middle Ordovician Rocks	7
1.2.	Stratigraphic Cross-Section Drawn Through the Cooper Creek Allochthon Illustrating the Stratigraphy of the Middle Ordovician Sequence Within the Study Area	9
1.3.	Palinspastic Reconstruction of the East Tennessee Area Showing the Areal Distribution of the Holston and Rockdell Formations	12
1.4.	Locations of Sections Used in This Study and the General Geology of the Study Area	13
2.1.	Environmental Model of Deposition for the Lower and Upper Holston Formation Near Knoxville, Tennessee	25
2.2.	Petrographic Features of the Holston Formation in Northeastern Tennessee	28
2.3.	Petrographic Features of the Holston and Rockdell Formations in Northeastern Tennessee	35
2.4.	Petrographic Features of the Rockdell Formation in Northeastern Tennessee	47
2.5.	Schematic Block Diagram Illustrating the Geographic and Bathymetric Relationships Between the Holston and Rockdell Formations in Northeastern Tennessee	55
3.1.	Comparison of Theoretical Cycles in Nonskeletal Carbonate Mineralogy with Sea Level Fluctuation, Climatic Episodes, and Changes in the Carbon and Oxygen Isotopic Composition of Marine Cement Through Geologic Time	68
3.2.	Theoretical First-Order "Cycles" in Nonskeletal Carbonate Mineralogy Through Geologic Time as Compared with Changes in Sea-Level, Granite Emplacement, and Climatic Episodes	69
3.3.	Petrographic and Optical Properties of: A. Radiaxial-Fibrous Calcite; B. Fascicular-Optic Calcite; and C. Radial Fibrous Calcite	76

FIGURE PAGE

3.4. Petrographic Features of Radiaxial-Fibrous Calcite and Associated Cements of the Holston and Rockdell Formations 82

3.5. Petrographic Features of Radiaxial-Fibrous Calcite and Associated Cement and Bladed/Prismatic Cement in the Holston and Rockdell Formations 86

3.6. Strontium and Magnesium Carbonate Composition of Selected Fibrous Cement from the Holston and Rockdell Formations as Compared to Published Data for Similar Ancient Fibrous Cement 91

3.7. Petrographic Features of Bladed/Prismatic Cement, Turbid Syntaxial (Rim) Cement, and Radiaxial-Fibrous Calcite and Associated Cement in the Holston and Rockdell Formations 95

3.8. Petrographic Features of Turbid Syntaxial (Rim) Cement and Micritic Cement in the Holston and Rockdell Formations 103

3.9. Characteristics of the Vadose Diagenetic Environment . . . 111

3.10. Idealized Zonation of the Meteoric Phreatic Diagenetic Environment Based on the Assumption that Saturation of Water with Respect to $CaCO_3$ Increased as Meteoric Water Moves Downward 113

3.11. Characteristics of the Freshwater Phreatic Diagenetic Environment 114

3.12. Petrographic Features of Equant (Drusy) Calcite and Clear Syntaxial (Rim) Cement in the Holston and Rockdell Formations 118

3.13. Petrographic Features of Syntaxial (Rim) Cement, Ferroan Calcite and Ferroan (Baroque) Dolomite in the Holston and Rockdell Formations 123

3.14. Idealized Pore Diagram Illustrating Compositional Zoning in "Two-Stage" Syntaxial as Revealed by Staining with Potassium Ferricyanide 127

4.1. Percent Volume Abundance of Cement Types at Red House Branch Versus Stratigraphic Position 143

4.2. Percent Volume Abundance of Cement Types at Poor Valley Creek Versus Stratigraphic Position 144

FIGURE PAGE

4.3. Percent Volume Abundance of Cement Types at Cedar Springs Versus Stratigraphic Position 145

4.4. Percent Volume Abundance of Cement Types at Evans Ferry Versus Stratigraphic Position 146

4.5. Relative Cement Abundance in Holston and Rockdell Formations Grain-Supported Rocks 149

4.6. Relative Cement Abundance in Holston and Rockdell Formations Mud-Supported Rocks 151

4.7. Relative Cement Abundance in Holston Formation Grainstones and Packstones Near Knoxville, Tennessee . . . 155

4.8. Idealized Cross-Section Across the Middle Ordovician Carbonate Shelf in Northeastern East Tennessee Illustrating the Relative Position of the Cedar Springs, Red House Branch, and Alcoa Highway Sections Relative to the Shelf Margin and the Trends in Compaction and Cementation Across the Shelf 158

4.9. Stratigraphic Cross-Section Drawn Through the Copper Creek Allochthon Illustrating the Stratigraphic Relationships Between the Holston and Rockdell Formations at Cedar Springs and Red House Branch 160

4.10. 3 x 3 Moving Averages of Marine, Freshwater, and Burial Cements Versus Stratigraphic Position in the Holston and Rockdell Formations at Red House Branch 162

4.11. 3 x 3 Moving Averages of Marine, Freshwater, and Burial Cements Versus Stratigraphic Position in the Rockdell Formation at Cedar Springs 165

4.12. Summary of the Paragenetic Sequence of Carbonate Cements in the Holston and Rockdell Formations in Northern East Tennessee 168

5.1. Sequence of Diagenetic Events in Grain-Supported Rocks of the Holston and Rockdell Formations 171

5.2. Sequence of Diagenetic Events in Mud-Supported Rocks of the Holston and Rockdell Formations 172

CHAPTER 1

INTRODUCTION

The term diagenesis, as used in this thesis, "encompasses those natural changes which occur in sediments or sedimentary rocks between the time of initial deposition and the time . . . when the changes created by elevated temperature, or pressure, or by other conditions can be considered to have crossed the threshold into the realm of metamorphism" (Murray and Pray, 1965). The processes comprising diagenesis tend to affect different sediment types to varying degrees. For example, carbonate sediment is particularly susceptible to the spectrum of diagenetic processes as compared to terrigenous clastic sediment (Wilson, 1975). Krumbein (1942) listed the basic physical and chemical processes which act on terrigenous sediment as compaction, dissolution, recrystallization, replacement, authigenesis, and cementation. Carbonate sediment may be altered by these processes as well as by stylolitization (a special form of dissolution), neomorphism, and dolomitization. The timing of diagenetic alteration is no less variable in different sediment types. The diagenetic history of carbonate sediment is a "continuing process . . . [which] begins during deposition and continues long after burial and the first stages of lithification" (Wilson, 1975).

Research conducted during the past 30 years has served to further the understanding of diagenetic processes and products in carbonate sediment so that it is apparent that diagenetic phenomena within this

type of sediment are not random. Many of the early papers which dealt with diagenetic rock fabrics were largely catalogues of diagenetic products (see Bathurst, 1958, 1959a, 1959b, 1964; Folk, 1962, 1965; and Banner and Wood, 1964). The physical and chemical processes responsible for the formation of these products were, at that time, largely unknown (Matthews, 1967). Several studies, however, were aimed at understanding diagenetic processes and products in Recent and Pleistocene carbonate sediment in an attempt to better understand ancient diagenetic phenomena (see e.g., Ginsburg, 1957; Bathurst, 1964b, 1966; Friedman, 1964; Ginsburg et al., 1967; Weyl, 1958; and Sippel and Glover, 1964).

Research dealing with carbonate diagenesis has become increasingly concerned with understanding cementation processes (see Matthews, 1967, 1968; Land, 1970, 1971, 1973; Land and Goreau, 1970; Meyers, 1974; Steinen, 1974; Harrison, 1974, 1975; James et al., 1976; Badiozamani et al., 1977; MacIntyre,1977; Hanor, 1978). The primary reason for this increased attention was that knowledge gleaned from these studies had direct application to exploration for minerals and hydrocarbons (e.g., it may be possible to predict whether porosity will be occluded or preserved in carbonate sediment deposited under different environmental conditions). Some of the studies listed above used new techniques to aid in the determination of the relative timing and environments of formation of cement generations (e.g., Meyers, 1974). These studies were used by Longman (1980) to develop predictive models (discussed in detail in Chapter 3) for the changes which occur in carbonate

sediment (with both chemically stable and unstable mineralogies) in the six major diagenetic environments from the time of initial deposition through the time of subaerial exposure or to the time of burial.

Many diagenetic studies in the past focused on single depositional units or on a narrowly defined group of strata (see for example Meyers, 1974, 1977, 1978, 1980, 1983). Only recently have studies of diagenetic processes and products in ancient carbonates been extended to large, complex sequences of carbonate rocks. This work is part of a larger, ongoing study by K.R. Walker and his associates at the University of Tennessee to examine the regional diagenetic patterns in the Middle Ordovician carbonate and terrigenous clastic rocks in East Tennessee.

Depositional Framework

Middle Ordovician strata in the Southern Appalachians were first described by Safford (1869), yet for the next 100 years, the exact stratigraphic relationships of these sediments and their environmental significance, was continually debated in the geologic literature. This was especially true for those rocks which crop out in eastern Tennessee and southwestern Virginia (see B. N. Cooper and Prouty, 1943; B. N. Cooper, 1944, 1945; B. N. Cooper and G. A. Cooper, 1946; Prouty, 1946; see also Rodgers, 1953; Twenhofel et al., 1954; G. A. Cooper, 1956; and McLaughlin, 1973). The problems encountered by these stratigraphers were twofold. First, complex structural deformation produced imbricate thrust faults, resulting in a series of northeast/southwest trending

outcrop belts. Differential displacement along these faults makes correlation between belts extremely difficult. Second, the definition and correlation of Middle Ordovician rocks by these workers was based on faunal content alone with little regard for the depositional environments of the original sediment or the three dimensional nature of the depositional systems.

Many of the problems with the stratigraphy have now been resolved by subsequent research utilizing a model for the Middle Ordovician depositional system in East Tennessee which was proposed by Walker and Alberstadt in 1973. This model, modified by Walker (1977, 1980), proposes that the Middle Ordovician sequence consists of five major stratigraphic packages representing the following depositional regimes from northwest to southeast: (1) a northwestern shallow water carbonate shelf; (2) a shelf marginal sandbank and reef complex; (3) a carbonate slope; (4) a deeper-water turbidite basin; and (5) a shallow-water, nearshore area adjacent to eroding land. Within this model, the carbonate shelf, shelf edge, and basin have received extensive research and the depositional facies within each of these major regimes have now been described in detail (see Stevenson, 1973; Ferrigno, 1973; McWilliams, 1975; Benedict and Walker, 1978; Shanmugam, 1978; Shanmugam and Walker, 1978, 1980; Sickafoose, 1979; Ruppel, 1977, 1979; Breland, 1980; McGill, 1981; Weiss, 1981; Borowski, 1982; Cantrell, 1982; Ruppel and Walker, 1982, 1984; Ewing, 1985; and Simonson, 1985). The present study concerns largely coeval, lithologically similar rocks which were deposited on-shelf and at the shelf margin, the Rockdell and Holston

Formation respectively. These two formations represent two distinct carbonate buildup complexes in eastern Tennessee (Ruppel and Walker, 1982). The similarities and differences between these two buildup complexes are discussed and a detailed treatment of their environment of deposition is presented in Chapter 2.

Purpose

The Rockdell Formation crops out exclusively in the northwestern strike belts or Chickamaugan Province (McLaughlin, 1973) of the Valley and Ridge Physiographic Province of eastern Tennessee whereas the Holston Formation crops out in both northwestern and southeastern belts or Blountian Province (McLaughlin, 1973). The Middle Ordovician rocks of the northwestern belts represent the western carbonate bank deposits and shelf marginal deposits of Walker's (1977, 1980) paleoenvironmental model and are classified together as the Chickamauga Group.

Although the paleogeography and the depositional environments of the Chickamauga Group in the northwestern belts have been extensively studied, to date there have been few detailed diagenetic studies of these rocks, and little is known concerning their postdepositional alteration. Two Chickamauga equivalent shelf edge units, deposited somewhat to the southeast in the Blountian Province and exposed near Knoxville, Tennessee, have been examined, however. McGill (1982) analyzed the diagenetic history of skeletal sand banks and lime-mud mounds in a portion of the Holston Formation which was deposited in a shelf marginal position or somewhat downslope. Her study focused

primarily on the paragenetic sequence of carbonate cement and trace elemental variations at three different localities. Cantrell (1982) and Cantrell and Walker (1985) examined the diagenetic rock fabric in an oolite body within a portion of the Ottosee Formation and proposed a model for the observed features. These depositional units are extremely different both in terms of lithology, as noted above, and time (see Figure 1.1).

The primary objective of this thesis was to compare the diagenetic history of lithologically similar, largely coeval rocks which were deposited in different positions relative to the Middle Ordovician shelf margin. To this end I have examined the rock fabric of the on-shelf Rockdell Formation and shelf marginal to slightly down-slope Holston Formation and the trace elemental distribution in selected cement phases with the following objectives:

1. Determine the relative sequence of diagenetic phenomena such as compaction, dissolution, cementation, etc.

2. Ascertain the paragenetic sequence of carbonate cements, their mineralogy, and the variables which control the distribution of these cements (such as substrate mineralogy and microstructure and pore water chemistry).

3. Determine the degree and timing of the reduction of primary porosity and permeability through cementation and compaction.

4. Compare the similarities and differences between 1, 2 and 3 above with the results of the study of Holston diagenesis near Knoxville, Tennessee by McGill (1982).

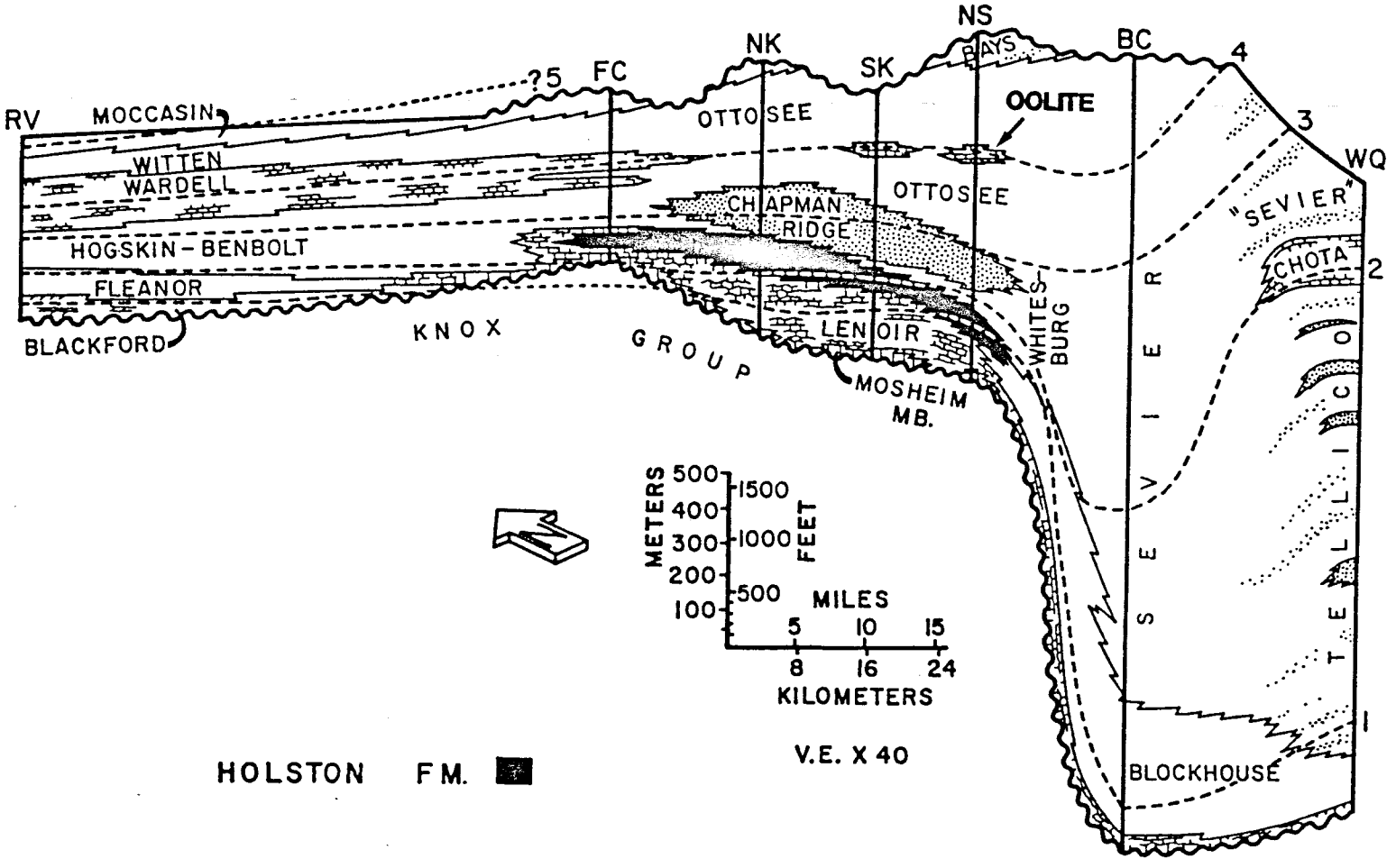


Figure 1.1. Regional cross-section through the Knoxville, Tennessee area illustrating the facies relationships of Middle Ordovician rocks. Lines 1-5 are time lines based on lithostratigraphic and biostratigraphic evidence. Note the time difference between deposition of Holston sediments and the Ottosee oolite. (From Walker, 1977).

5. Illucidate the origin of cavities within the lime-mud mounds which are common in both formations.

6. Determine the mechanisms by which these mound lithologies were stabilized and the role of diagenesis in mound development.

Stratigraphy

The original definition of the Chickamauga Group by Hayes (1891) included the entire Middle Ordovician and part of the Upper Ordovician. Subsequent redefinitions by various stratigraphers caused confusion as to the exact stratigraphic rank of these rocks (see Prouty, 1946; Rodgers, 1953; Swingle, 1964; Milici, 1973; and Milici and Smith,1969). More recently, Ruppel (1979) and Ruppel and Walker (1982, 1984) have redefined the Chickamauga Group as those Middle Ordovician strata exposed west of the Saltville Fault which lie between the unconformity at the top of the Knox Group (Lower Ordovician) and the base of the Martinsburg Formation (Upper Ordovician). Within the study area, the Chickamauga Group is comprised of ten separate formations which in ascending stratigraphic order, are: the Blackford; Five Oaks; Holston; Lincolinshire; Rockdell; Benbolt; Wardell; Bowen; Witten; and Moccasin formations. The stratigraphic relationships between these units are depicted in a stratigraphic cross-section (Figure 1.2) drawn through the Copper Creek allochthon, perpendicular to depositional strike from northwest to southeast. The three westernmost localities indicated in this diagram, Evans Ferry (EF), Cedar Springs (CS), and Red House Branch (RHB), are three of the locales used in this study. This cross-

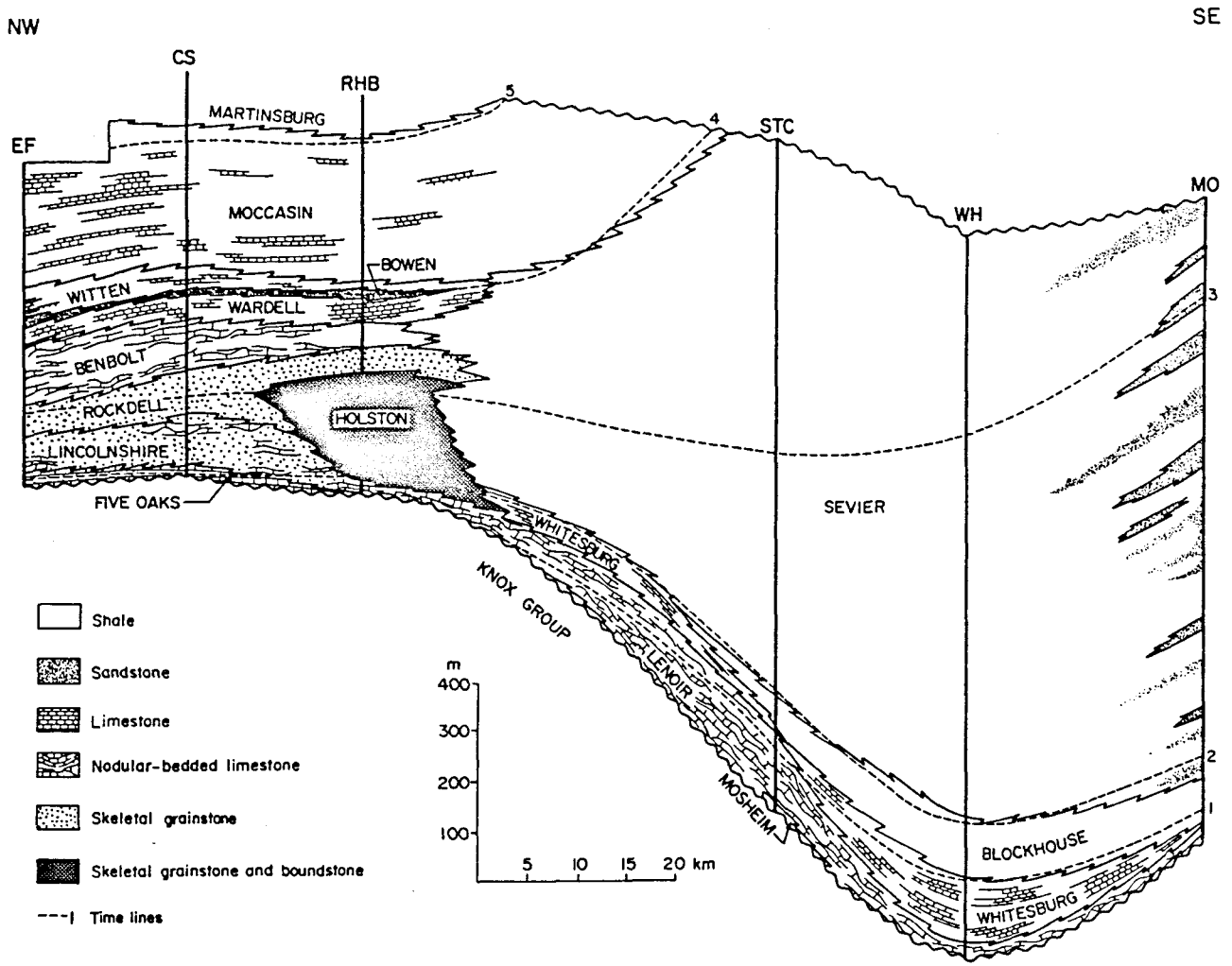


Figure 1.2. Stratigraphic cross-section drawn through the Copper Creek allochthon illustrating the stratigraphy of the Middle Ordovician sequence within the study area. Evans Ferry (EF), Cedar Springs (CS), Poor Valley Creek (PVC), and Red House Branch (RHB) are localities used in this study. (From Ruppel and Walker, 1982).

section illustrates that the Rockdell Formation and the upper part of the Holston Formation are largely coeval. Note that in the northwest, the Rockdell Formation overlies the Lincolnshire Formation, whereas, in the easternmost portion of the Copper Creek allochthon, adjacent to the Saltville fault, the Rockdell Formation overlies the Holston Formation.

Prior to the work of Ruppel (1979) and Ruppel and Walker (1982, 1984), the use of the term "Holston" and "Rockdell" had been inconsistent. In general, the "marble" industry in East Tennessee applied the term "Holston" (Keith, 1895) to all quarryable, brick-red to white, fine- to coarse-grained limestones (Ruppel, 1979). Stratigraphic studies of Middle Ordovician rocks in the Southern Appalachians, conducted in the 1940s and 1950s, suggested that these deposits more likely represented several stratigraphic units (e.g., B. N. Cooper and Prouty, 1943; B. N. Cooper, 1944; B. N. Cooper and G. A. Cooper, 1946; G. A. Cooper, 1956). The term "Rockdell" was extended southwestward from Virginia into northern East Tennessee (see G. A. Cooper, 1956) to include those generally light colored, coarse-grained limestones outcropping in the western belts of the Tennessee Valley and Ridge Province (Ruppel, 1979). Since no detailed petrographic studies of the depositional environments or faunal and floral content of these rocks were undertaken at that time, many workers continued to confuse these two units in the belief that there were no lithologic criteria for distinguishing the "Holston" from the "Rockdell" (Ruppel, 1979).

In the work of Ruppel (1979) and Ruppel and Walker (1982, 1984), emphasis was placed on determining the depositional environments of the

Rockdell and Holston formations. This research has allowed the restriction of the term "Rockdell" to the area west-northwest of the Saltville Fault (except in the area of Cuba, Tennessee) and the term "Holston" to the area adjacent to and east-southeast of the Saltville Fault based on sediment texture and fabric and on the faunal and floral content of the rocks. Figure 1.3, taken from Ruppel and Walker (1982), illustrates the spatial relationship between the two formations. The four sections used in this study have been highlighted for reference. Note the overlap of the occurrences of the formations adjacent to the Saltville Fault where the Rockdell Formation overlies the Holston Formation.

Location of Study Area

The area chosen for this study is located in northeastern Tennessee in the Copper Creek and Hunter Valley allochthons. Within this area (Figure 1.4), four stratigraphic sections, where either the Rockdell, Holston or both formations crop out, were studied. From northwest to southeast, these sections represent a transect from well on-shelf to shelf margin. Only the Rockdell Formation is exposed at Evans Ferry and Cedar Springs while the lower 38.4 m of the Holston Formation are exposed at Poor Valley Creek. At Red House Branch, the Rockdell overlies the Holston (refer to Figure 1.2, p. 9).

A study of this kind is predicated on the understanding of the regional facies patterns and paleogeography of the depositional regimes of the Rockdell and Holston formations. Often in past diagenetic

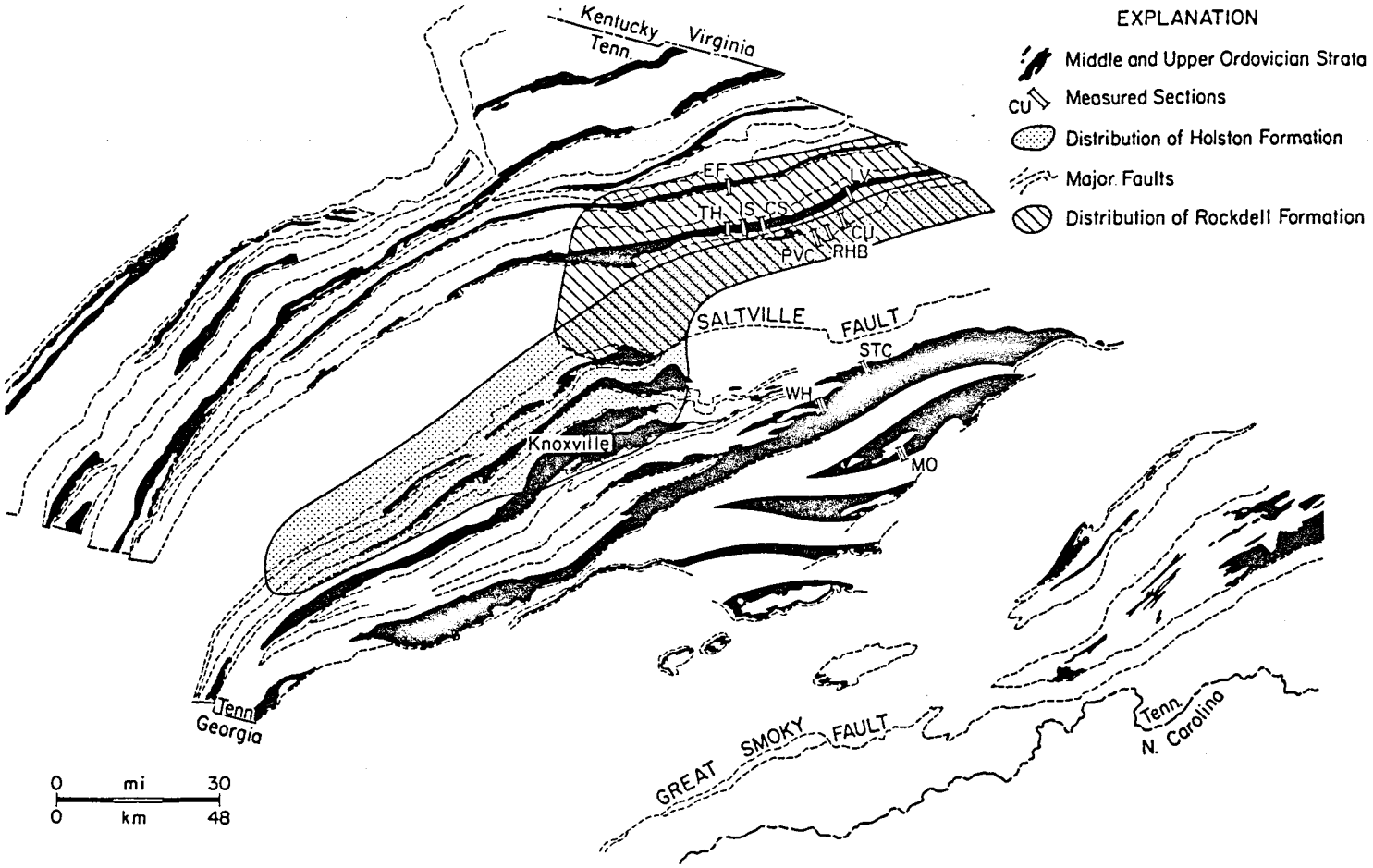


Figure 1.3. Palinspastic reconstruction of the East Tennessee area showing the areal distribution of Holston and Rockdell formations. The 4 localities used in this study are highlighted: EF--Evans Ferry; CS--Cedar Springs; PVC--Poor Valley Creek; RHB--Red House Branch. (From Ruppel and Walker, 1982).

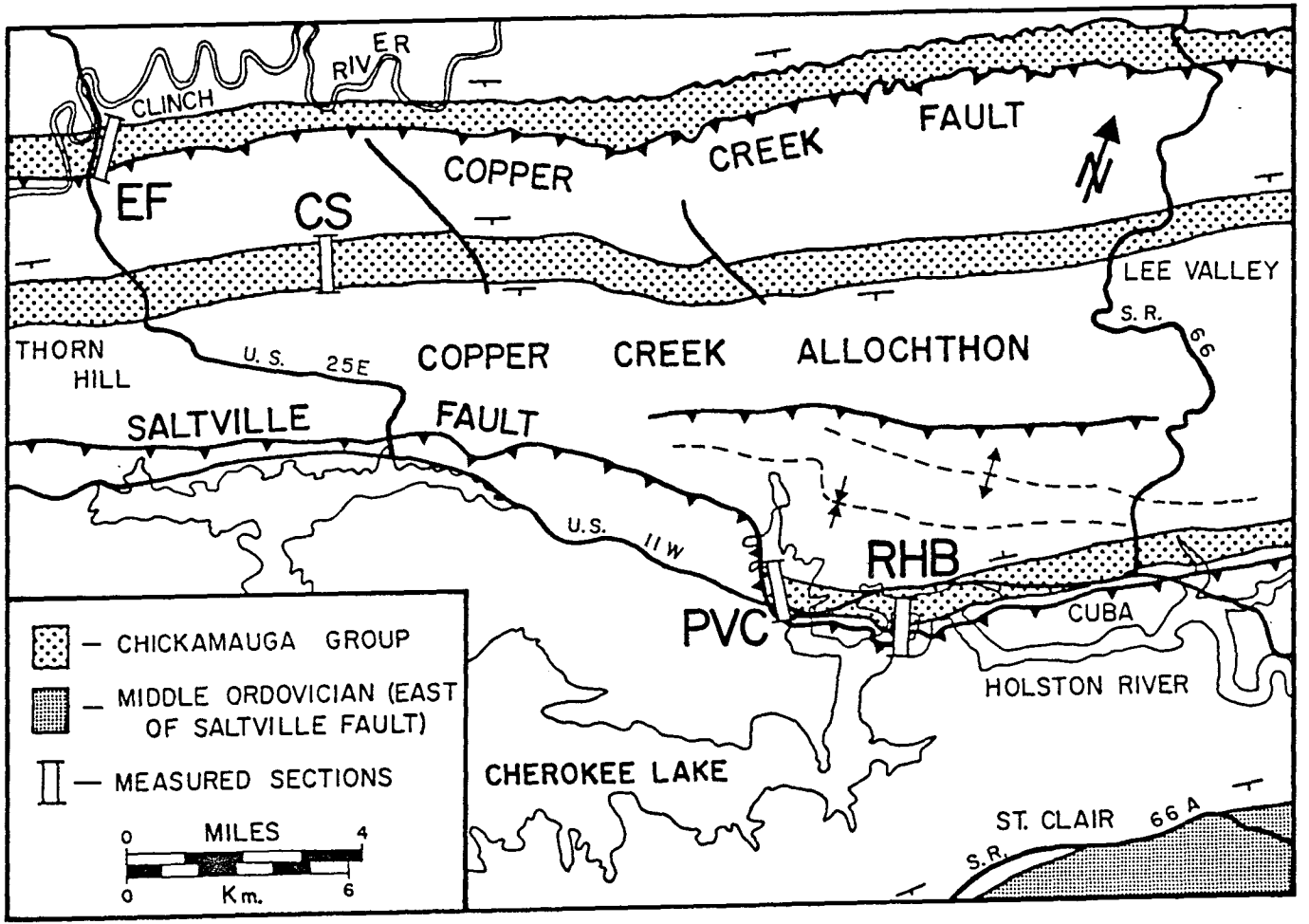


Figure 1.4. Locations of sections used in this study and the general geology of the study area. EF--Evans Ferry; CS--Cedar Springs; PVC--Poor Valley Creek; RHB--Red House Branch.

studies of other stratigraphic sequences, these parameters were poorly known or were ignored altogether. The four sections used in this study have previously been studied by faculty and students at the University of Tennessee in terms of the paleoenvironment, paleobathymetery, and to some degree, paleoecology. Thus, the control that these variables have on the variation of diagenetic products,such as cement types, may be investigated. Evans Ferry was studied by Sickafoose (1979), Sickafoose and Broadhead (1980), Ruppel (1977, 1979), and Ruppel and Walker (1982, 1984). Cedar Springs has been studied by Ruppel (1979), Ruppel, Broadhead and Walker (1980), and Ruppel and Walker (1982, 1984). The Poor Valley Creek and Red House Branch localities were studied by Ruppel (1979), and Ruppel and Walker (1982, 1984). Johnson (in prep.) is studying diagenetic effects on the trace element geochemistry of Rockdell and Holston sediments at the Cedar Springs, Poor Valley Creek and Red House Branch localities.

Methods of Study

After selecting the stratigraphic sections to be used in this investigation, thin-sections from the studies of Sickafoose (1979), Ruppel (1979) and Johnson (in prep.) were selected for diagenetic study. The sampling intervals of these previous studies were compared with the stratigraphic thicknesses of each of the four sections in order to determine if the number of available samples was sufficient for this study. Preliminary examination of sample availability indicated that the samples from the studies of Sickafoose (1979), Ruppel

(1979) and Johnson (in prep.) provided excellent coverage of the stratigraphic intervals of interest at the Evans Ferry and Cedar Springs localities (see Table 1.1). The number of available samples from the study of Ruppel (1979) was not sufficient to represent the lithologic variability of the Holston Formation at Poor Valley Creek or the Holston and Rockdell formations at Red House Branch. For this reason, the successions at the Poor Valley Creek and Red House Branch localities were remeasured and resampled.

The lithology of each unit at Poor Valley Creek and Red House Branch was described and samples were collected to include all lithologic variation noted in the field. Samples were classified in the field according to Dunham (1962) in keeping with the previous studies of the Rockdell and Holston in the study area. Eighteen samples were collected from the 38.4 m of exposed Holston Formation at Poor Valley Creek. Thirty-eight samples were collected from the Holston Formation and 12 from the Rockdell Formation at the Red House Branch locality. The 68 samples from these two southeastern sections, when combined with the samples from Evans Ferry and Cedar Springs, give a total sample size for this study of 145 (Table 1.1). Lithologic descriptions, stratigraphic thicknesses and sample locations for each of the study localities are provided in Appendix A.

The 68 samples from Poor Valley Creek and Red House Branch were cut into 2x3 inch thin-sections (similar to the thin-sections from Evans Ferry and Cedar Springs). Thin-sections from all four localities were stained with Alizarin Red-S in order to determine the distribution

Table 1.1. Samples available for use in this study. This list includes samples from Sickafoose (1979) and Johnson (in prep.).

Section	Formation	Thickness (m)	Total Samples
Evans Ferry	Rockdell	62.0	32
Cedar Springs	Rockdell	84.0	45
Poor Valley Creek	Holston	38.4	18
Red House Branch	Holston	221.0	38
Red House Branch	Rockdell	42.4	12

of dolomite within each sample and with potassium ferricyanide in order to distinguish ferroan from nonferroan carbonate cement using the procedure of Dickson (1966). Each thin-section was petrographically described in detail with emphasis being placed on the fabric and textures of the various cement types and on the overall paragenetic sequence of cement. Important cement textures and fabrics were photographed for comparison with luminescent petrography (see below). Seventy-five of the thin sections were point-counted using a cement priority technique. This method, which recognized intra-allochem cement as cement rather than as host allochem, gives a better estimate of the volume percentage of each cement type and thus, a better estimate of original porosity. Data from the petrographic constituent analyses are tabulated in Appendix B. Correlation coefficients for the entire data set and subsets of the data set were estimated using the correlation matrix procedure of the microcomputer program Stratigraphics. This procedure was used to determine the degree of association between the various point-count categories. A description of the procedure and the results of these analyses are presented in Appendix C.

Forty etched thin-sections were examined using cathodoluminescent petrography with a Nuclide Corporation Luminoscope. Using this technique, the luminescent character of the various cement phases was examined, and significant luminescent characteristics and/or growth zonation not visible using conventional petrographic techniques were recorded. Although it is generally believed that the Fe^{2+}/Mn^{2+} ratio in calcite controls the luminescent intensity and that relatively low

concentrations of manganese may cause luminescence, "the amount of manganese necessary to induce luminescence in calcite has not been clearly established . . ." (Frank et al., 1982). For this reason, luminescent data obtained using this technique has been used only as ancillary evidence in interpreting cement phases in this thesis.

The trace elemental composition of selected cement types and associated matrix material (micrite) from lime-mud mounds in the Rockdell and Holston formations at Poor Valley Creek and Red House Branch was analyzed using atomic absorption spectrophotometry in an attempt to determine the original mineralogy and environment of formation of the cement phases and to compare the trace elemental compositions of the micrite samples. The component to be analyzed was "microsampled" using carbide steel, dental drill bits mounted in a Jensen vertical milling machine. The 25 powdered samples produced by this technique were prepared using the technique of Johnson (in prep.) and were analyzed for magnesium, strontium, manganese, and sodium. A description of this procedure and a table illustrating the results are provided in Appendix D.

CHAPTER 2

DEPOSITIONAL ENVIRONMENTS

Introduction

As discussed in Chapter 1, the stratigraphic studies of Middle Ordovician strata of the Southern Appalachians conducted during the 1940s and 1950s were "based either on mapping of large lithologic units or on biostratigraphic interpretation of organisms now known to be subject to much facies control" (Walker and Ferrigno, 1973). Early researchers proposed several names for the white to brick-red "marble" deposits in eastern Tennessee including Holston, Farragut, Red Knobs, and Rockdell formations. Different names were proposed for similar rocks which crop out in different strike belts mainly because it was apparent that these rocks represented facies which were somewhat discontinuous and occurred at different stratigraphic positions within the Middle Ordovician stratigraphic sequence (see for example B. N. Cooper, 1944). These early studies, however, provided virtually no information concerning the depositional environments or resulting depositional textures and fabrics of the original sediments (Walker and Ferrigno, 1973).

This chapter concerns the depositional environments of the Holston and Rockdell formations in eastern Tennessee. For the reasons discussed above, only research subsequent to 1970 will be discussed here. The reader is referred to Walker and Ferrigno (1973), Ruppel (1979),

and Ruppel and Walker (1982) for detailed discussions of studies of these sediments conducted prior to 1970.

The Holston Formation Near Knoxville, Tennessee

The first studies of the Holston Formation which used field observations together with modern petrographic techniques were conducted in the eastern belts of the Tennessee Valley and Ridge Province near Knoxville by Walker and Ferrigno (1973), Ferrigno (1973) and Walker (1977, 1980). Walker (1977, 1980) suggested that the Holston Formation may be divided into the lower and upper Holston, based on both field observations and on petrographic characteristics of the two units. Rocks of the lower Holston Formation exhibit large scale debris-slope and avalanche type cross stratification (Walker, 1977, 1980). Also present within this unit are thin sets of wave induced cross-laminae. Local small, isolated "bryozoan-pelmatozoan organic buildups" occur but are rare within this part of the Holston (Walker, 1977, 1980). Petrographic examination of samples from the lower Holston reveal that the lithology consists of skeletal sand composed largely of pelmatozoan debris with somewhat less abundant ramose bryozoan debris. Other fossil groups such as arthropods and molluscs are present but make up only a minor part of the rock. Pelmatozoan debris is generally abraded and commonly exhibits algal and/or fungal borings. Calcareous algae, although not abundant, are present in this part of the Holston and include Girvanella, Solenopora, Contexta, and Vermiporella (Walker, 1977, 1980). The abundance of algae diminishes upward in the unit.

Walker (1977, 1980) interpreted the lower Holston as a complex of shelf marginal sand banks. The primary evidence for this interpretation was: (1) the abundance of debris-slope cross-beds, (2) the presence of current induced cross-lamination, (3) the presence of calcareous algae, and (4) the interbedded nature of the lower contact of the Holston Formation with algal-rich biomicrites of the Lenoir Formation (lagoonal facies; see Stevenson, 1973 and Benedict, 1977). Coeval basinal shale deposits are exposed just southeast of lower Holston outcrops at Martin Mill Pike (Walker 1977, 1980). The geographical relationship of these two sediment types supports a shelf marginal environment of deposition for the lower Holston skeletal sands. Water depths during deposition of these sediments were on the order of 10 m or less, but probably deepened upward (Walker, 1977, 1980).

Historically, the upper Holston Formation has been given more attention than the lower Holston in the geologic literature. Early studies of the upper Holston described its variable lithology and theorized a "reefal" origin for these deposits (see for example, Stose and Schrader, 1923). This hypothesis was based mainly on the occurrence of cross-bedded, white to pink calcarenites dipping away from and abutting against massive, dark-red limestones (Ferrigno, 1973). Walker and Ferrigno (1973), Ferrigno (1973) and Walker (1977, 1980) examined the upper Holston in an attempt to define the exact nature of the environments in which these sediments were deposited. They found that the upper Holston consists of two associated lithologies: (1) anastomosing, pink to dark-red bryozoan boundstones or lime-mud mounds which

they termed "reef core" deposits and (2) cross-bedded echinoderm packstones and grainstones (calcarenites) which they termed "reef flank" deposits. The flanking packstone and grainstone beds which fill the intervening space between boundstone masses, were shown to dip away from these mounds at high angles. These deposits generally make-up 75-80 percent of the unit with lime-mud mound lithologies comprising only 20-25 percent (Walker and Ferrigno, 1973).

Using modern petrographic techniques, Walker and Ferrigno (1973), Ferrigno (1973) and Walker (1977, 1980) characterized these two subenvironments of the upper Holston Formation. The reef core facies consists of two lithologies. The dominant lithology within this facies consists of encrusting bryozoan boundstones. Encrusting bryozoans make-up as much as 80 percent of the fauna in these rocks. Echinoderms, ramose bryozoans, arthropods (trilobites and ostracodes), brachiopods, and molluscs are also present, but generally make upless than 20 percent of the fauna. Stromatactis structures make up the second lithology within the reef core facies. These structures are characterized by horizontal planar cavities (now filled with calcite cement) in lime-mud. The floors of these cavities are generally flat whereas the roofs or upper walls are somewhat irregular or digitate. The cavities are interconnected forming a network similar to that described by Bathurst (1959). These cavities were commonly partially filled by internal sediment and are typically filled by what Ferrigno (1973) termed blade spar (this cement has been reinterpreted by Walker and his students as radiaxial fibrous cement). Often, the growth of this

cement was interrupted by subsequent depositional episodes of internal sediment. Calcareous algae are conspicuously absent from the upper Holston formation at the localities used in these studies (Walker and Ferrigno, 1973; Ferrigno, 1973; and Walker, 1977, 1980). Both the encrusting bryozoan boundstones and the stromatactis structures exhibit a high volume percentage of lime-mud (micrite) (Walker and Ferrigno, 1973; Ferrigno, 1973; and Walker, 1977, 1980). Ferrigno (1973) noted that this matrix material is uncharacteristically coarse-grained (4-12 μm). He thought that the luminescent character and the coarse-grained nature of this micrite suggests that it was derived mainly from the comminution of skeletal material such as bryozoans, echinoderms, arthropods, brachiopods, and molluscs.

The flanking packstone and grainstone beds are dominated by echinoderm debris which makes up 60-70 volume percent of the rock; ramose bryozoans make up an additional 25-30 volume percent. Other fossil groups, such as arthropods, brachiopods, molluscs and encrusting bryozoans, are present within this facies, but collectively usually account for less than 5 volume percent of the fauna. Small, angular mud clasts which contain reef core bryozoans are also present within these flanking beds. Calcareous algae are absent from this facies also (Walker and Ferrigno, 1973; Ferrigno, 1973; and Walker, 1977, 1980).

Walker and Ferrigno (1973), Ferrigno (1973) and Walker (1977, 1980) interpreted the upper Holston Formation as a "biohermal reef" (term after Nelson, et al., 1962). In three dimensions, encrusting bryozoan boundstone masses up to 3 m wide anastomose laterally and

upward through the formation (Walker and Ferrigno, 1973). These lime-mud mounds grew upward rapidly relative to the intervening calcarenite areas, often developing near vertical margins, which were encrusted by bryozoans. Cross-bedded echinoderm-bryozoan packstone and grainstone beds were shown to dip away from the boundstone masses at high angles (25°-40°). Tracing individual cross-beds away from the reef bodies suggested that they stood as much as 3-7 m above the sea-floor. The absence of calcareous algae in the upper Holston at the locales used in these studies may indicate that the sediment was deposited below the algal compensation depth (Walker and Ferrigno, 1973; Ferrigno, 1973; and Walker, 1977, 1980). Current-induced sedimentary structures are rare in the upper Holston suggesting that these sediments were deposited below effective wave base (Walker and Ferrigno, 1973; Ferrigno, 1973; Walker, 1977, 1980).

The boundstone masses were lithified at the time of deposition. Evidence for early lithification is: (1) the presence of intraclasts of core lithology within adjacent flanking deposits; (2) petrographic observation of encrusting bryozoans binding micrite and fossil material and (3) bryozoans encrusting vertical reef margins and vertical cavity walls. The boundstone masses had the ecological potential to be wave resistant and thus, fit the definition of reef given by Nelson et al. (1962) (Walker and Ferrigno, 1973; Ferrigno, 1973).

The studies of Walker and Ferrigno (1973), Ferrigno (1973), and Walker (1977, 1980) were used in the development of an environmental model for the Holston Formation (Figure 2.1) (Walker, 1977, 1980). The

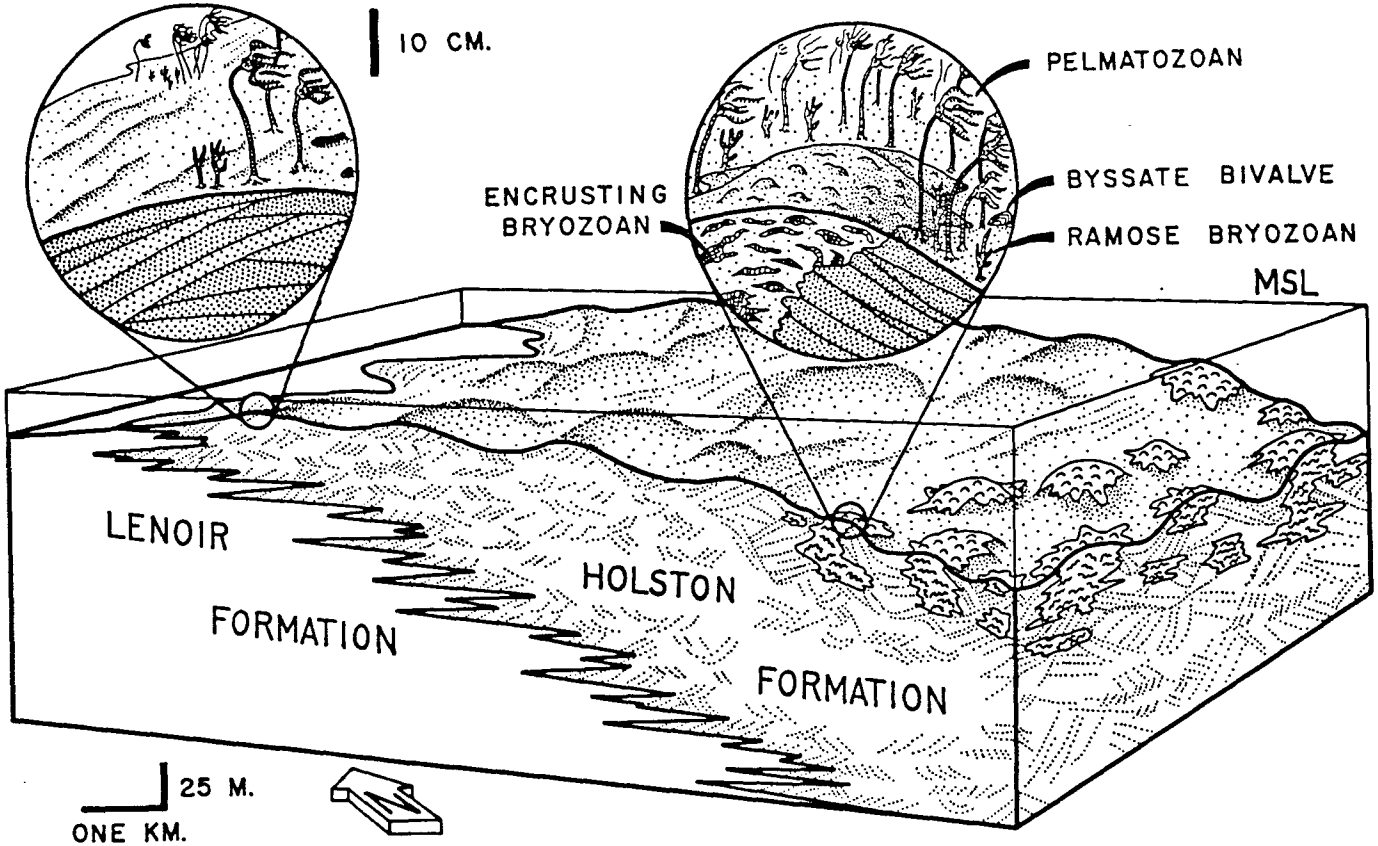


Figure 2.1. Environmental model of deposition for the lower and upper Holston formation near Knoxville, Tennessee. The lower Holston Formation sediments were deposited in a shelf marginal position in waters 10 meters deep or less while sediments of the upper Holston were deposited basinward of the lower Holston sediments in somewhat deeper water. (From Walker, 1977, 1980).

skeletal sandbanks of the lower Holston were deposited in a shelf marginal position in waters 10 m deep or less that deepened through time. The lime-mud mounds and associated lithologies of the upper Holston were deposited basinward of these skeletal sandbank deposits in waters which were approximately 50 to 100 m deep (Walker, 1977, 1980).

The Holston Formation in Northeastern Tennessee

Prior to the studies of Ruppel (1979) and Ruppel and Walker (1982, 1984), the Holston Formation had not been studied extensively at locales west of the Saltville Fault in East Tennessee. The Holston Formation was examined as part of a larger study at the University of Tennessee which was concerned with understanding the depositional environments of the Middle Ordovician shelf. These shelf deposits crop out extensively in East Tennessee. The following discussion of the depositional textures and fabrics of the Holston Formation in northeastern Tennessee is largely a summary of the studies of Ruppel (1979) and Ruppel and Walker (1982, 1984). It is, however, supplemented by observational and constituent analysis data obtained in the present study.

In northeastern Tennessee, the Holston Formation cannot be divided into upper and lower units as it is near Knoxville. Within the study area, the Holston consist of three lithofacies whose characteristics partly overlap. These lithofacies (modified after Ruppel, 1979 and Ruppel and Walker, 1982, 1984) are: (1) echinoderm-bryozoan grainstone-packstones; (2) bryozoan wackestone-boundstones (lime-mud mounds); and

(3) echinoderm-bryozoan packstones (Ruppel, 1979; Ruppel and Walker, 1982, 1984).

Echinoderm-bryozoan grainstone-packstones (Figure 2.2A) are volumetrically the least important lithofacies in the Holston Formation. These deposits are cream to red on outcrop and cross-beds are readily discernable. These rocks consist primarily of ramose bryozoan debris with subdominant abraded, well sorted echinoderm debris (Table 2.1; Figure 2.2A). However, Ruppel (1979) and Ruppel and Walker (1982) found that these rocks were dominated by echinoderm debris with subdominant ramose bryozoan debris (Table 2.1). Ruppel and Walker (1982, 1984) found that calcareous algae are absent from this lithofacies. In this study, calcareous algae were found in several samples from this lithofacies although they are uncommon.

Ruppel (1979) and Ruppel and Walker (1982, 1984) compared these grainstone-packstones to the grainstone-packstone lithofacies of the Rockdell Formation (see below). This comparison is based on the similar faunal content (other than calcareous algae), the generally abraded character of the fossil debris, and on the presence of abundant cross-beds. The echinoderm-bryozoan grainstone-packstone lithofacies, however, is also similar to the skeletal sand bank deposits of the lower Holston Formation near Knoxville, Tennessee as described by Walker (1977, 1980). Both lithologies consist of cross-bedded echinodermal grainstones with less abundant packstones. Arthropods (trilobites and ostracodes), brachiopods, and molluscs generally account for no more than 5 volume percent of the rock. The primary distinction between

Petrographic features of the Holston Formation in northeastern Tennessee.

A. Photomicrograph of echinoderm-bryozoan grainstone-packstone lithofacies showing the primary sediment constituents, abraided echinoderm debris and bryozoan fragments. Bar scale is approximately 1.0 mm. Red House Branch. (RHB'4BS2).

B. Photomicrograph of the bryozoan wackestone-boundstone lithofacies showing the common sediment constituents. Bar scale is approximately 1.0 mm. Poor Valley Creek. (PVC'2AC1MR).

C. Photomicrograph of the bryozoan wackestone-boundstone lithofacies showing a shelter void created by a trilobite carapace. The void is filled by cross-laminated, peloidal internal sediment and equant "drusy" calcite cement. Bar scale is approximately 1.0 mm. Poor Valley Creek. (PVC'2E).

D. Photomicrograph of the bryozoan wackestone-boundstone lithofacies showing a well developed stromatactoid cavity. In this example, the entire void is filled by radiaxial-fibrous calcite cement. Note that crystals growing off the roof and floor of the cavity meet along a median boundary in the center of the cavity. Bar scale is approximately 1.0 mm. Red House Branch. (RHB'2K).

E. Photomicrograph of stromatactoid cavity from the bryozoan wackestone-boundstone lithofacies showing radiaxial-fibrous calcite cement growth interrupted by internal sediment. Note also the changing inclusion density in the cement crystals growing off the layer of internal sediment. Bar scale is approximately 1.0 mm. Red House Branch. (RHB'2K).

F. Photomicrograph of a stromatactoid cavity in the bryozoan wackestone-boundstone lithofacies showing an ostracode engulfed by radiaxial-fibrous calcite cement. Note that inclusion bands in the cement crystals show that the ostracode is sitting in a low position between two longer sets of crystals. Bar scale is approximately 1.0 mm. Red House Branch. (RHB'2K).

G. Close-up of the radiaxial-fibrous cement filled cavity in Figure 2.2F. Note that the ostracode is sitting just above a prominent band of inclusions in the cement crystals. Bar scale is approximately 0.25 mm. Red House Branch. (RHB'2K).

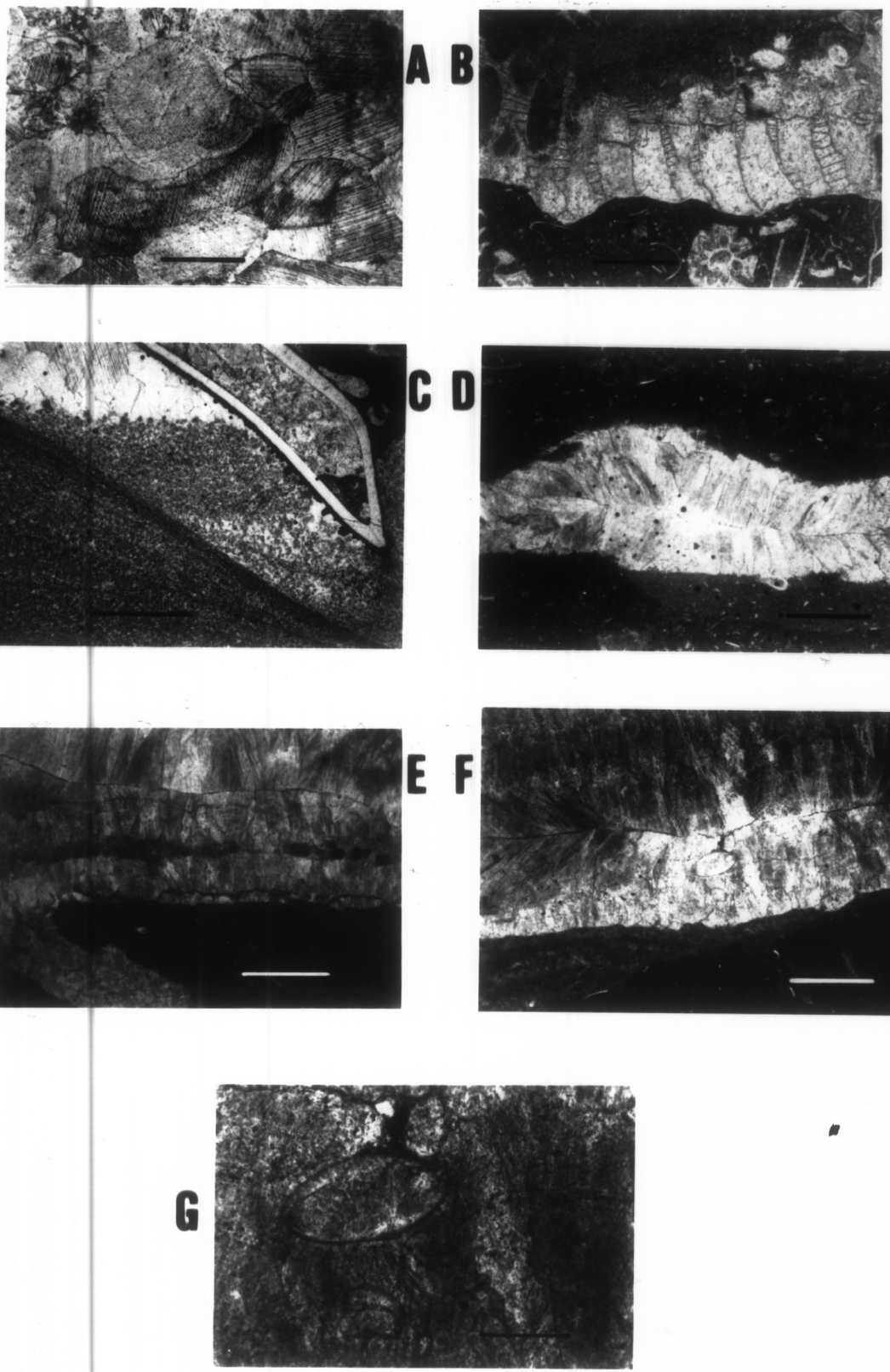

A
B
C
D
E
F
G

Figure 2.2
29
Jernigan, 1987

Table 2.1. Constituent analyses of the echinoderm-bryozoan grainstone-packstone lithofacies of the Holston Formation. NR represents a constituent which was not recorded. The numbers in parentheses represent the total number of samples.

	Holston Formation			
	(This Study) Echinoderm-Bryozoan Grainstone/ Packstone (15)		(Ruppel and Walker, 1982) Pelmatozoan-Bryozoan Grainstone/ Packstone (7)	
Constituent	Range	Average	Range	Average
Spar	20-55	37	3-51	30
Micrite	0-7	2	0-5	1
Microspar	0-5	1	NR	NR
Echinoderms	1-34	20	12-70	41
Bryozoans	18-42	31	5-70	22
Trilobites	<1-5	1	0-2	1
Ostracodes	0-1	<1	0-1	<1
Brachiopods	0-1	<1	-	-
Molluscs	-	-	-	-
Corals	-	-	-	-
Algae	0-2	<1	-	-
Sponges/spicules	-	-	-	-
Indeterminate Fossils	<1-3	2	-	-
Intraclasts	0-<1	<1	-	-
Peloids	0-<1	<1	-	-
Oncolites	-	-	-	-
Stylocumulate	0-8	3	0-14	6
Dolomite	0-6	1	0-1	<1

the grainstone/packstone lithofacies and the skeletal sand bank deposits of the lower Holston near Knoxville is that ramose bryozoans are the dominant fossil group in the grainstone/packstone lithofacies while they are the second most common fossil type in the lower Holston. The similarities between the grainstone-packstone lithofacies of the Holston, the grainstone-packstone lithofacies of the Rockdell in the study area and the skeletal sandbank deposits of the lower Holston near Knoxville suggest that this lithofacies was similarly deposited in relatively shallow water (<10 m). These rocks probably represent skeletal sandbanks which were deposited shelfward of the other lithofacies in the Holston Formation.

Bryozoan wackestone-boundstones (Figure 2.2B, C) consist of a high percentage of dark-red to maroon, coarse-grained (4-12 μm) lime-mud (20-50 volume percent). Constituent analysis data for wackestone-boundstone samples from the present study and the study of Ruppel and Walker (1982) are summarized in Table 2.2. Bryozoans dominate the fauna of the mud mounds (up to 35 volume percent of the rock material) with encrusting forms predominating. These bryozoans bind micritic matrix material as well as other fossil debris. Echinoderm and sponge debris locally occur in abundance (up to 18 and 17 volume percent, respectively). These three fossil groups commonly account for over 90 volume percent of the fauna within these lime-mud mounds. Arthropods (trilobites and ostracodes), brachiopods, molluscs and algae are also present within this lithofacies (see Appendix B). Ruppel (1979) and Ruppel and Walker (1982, 1984) have previously indicated that

Table 2.2. Constituent analyses of the bryozoan wackestone-boundstone lithofacies of the Holston Formation. NR represents a constituent which was not recorded. The numbers in parentheses represent the total number of samples.

	Holston Formation			
	(This Study) Bryozoan-Wackestone/ Boundstone (15)		(Ruppel and Walker, 1982) Bryozoan-Wackestone/ Boundstone (10)	
Constituent	Range	Average	Range	Average
Spar	8-46	24	5-67	25
Micrite	19-50	31	12-61	32
Microspar	<1-15	4	NR	NR
Echinoderms	0-18	5	<1-9	2
Bryozoans	<1-35	16	18-75	39
Trilobites	0-2	1	0-1	<1
Ostracodes	0-3	1	0-4	<1
Brachiopods	0-2	<1	0-<1	<1
Molluscs	0-1	<1	0-<1	<1
Corals	-	-	-	-
Algae	-	-	-	-
Sponges/spicules	0-17	4	0-2	<1
Indeterminate Fossils	0-2	1	0-3	<1
Intraclasts	0-1	<1	-	-
Peloids	0-2	<1	-	-
Oncolites	0-1	<1	-	-
Stylocumulate	0-9	3	0-6	2
Dolomite	0-4	<1	-	-

calcareous algae are absent from the Holston Formation in northeastern Tennessee. However, samples collected from both the bryozoan wackestone-boundstone lithofacies and the bryozoan-echinoderm packstone lithofacies have revealed the presence of several algal genera including Contexta and Dasyporella as well as several examples of algally coated grains.

Stromatactis mud mounds are common within this lithofacies. These structures are similar to those described by Walker and Ferrigno (1973) and Ferrigno (1973) which occur in the upper Holston Formation near Knoxville, Tennessee. As previously described, these structures are composed of a series of spar-filled, horizontal cavities which are separated by relatively thin layers of sparsely fossiliferous, faintly laminated, red lime mud (Figure 2.2D). Sponge spicules are commonly dispersed throughout the lime-mud matrix and represent the dominant faunal type in these structures. The cavities are commonly flat floored and have digitate upper walls. Cavity floors are usually covered by internal sediment which may be graded. This internal sediment may appear peloidal, as fine-grained micrite (<5 μm), or as crystal silt. The majority of the pore space is filled by radiaxial-fibrous calcite cement (Figure 2.2D) which nucleated on cavity walls, polycrystalline fossil debris which protrudes into the cavities, and internal sediment. Equant calcite or ferroan calcite may fill the center of these cavities. Fibrous cement growth is commonly interrupted by episodes of internal sedimentation (Figure 2.2E). Fossil debris was trapped in these cavities and in some instances engulfed in

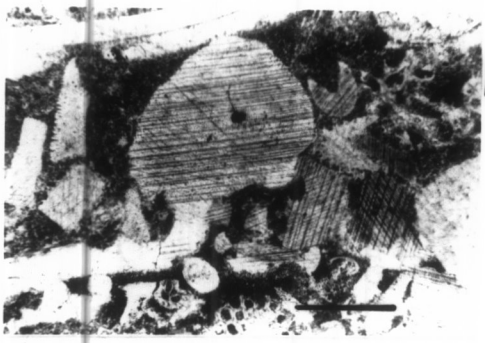
radiaxial-fibrous cement by later cement growth (Figure 2.2F, G). Stromatactoid cavities may truncate laminations in the micritic matrix.

An intriguing feature of the bryozoan wackstone-boundstone lithofacies is the abundance of not only stromatactoid cavities but of cavities of several shapes and origins. These cavities range in size from less than 1 cm to over 2 m in diameter. Relatively small (10-20 cm diameter) "subspherical" shaped cavities are apparent on outcrop (Ruppel, 1979; Ruppel and Walker, 1982, 1984). These cavities are commonly partially filled with internal sediment. The remaining portion of the cavity is filled first by what appears on outcrop to be botryoidal calcite cement and later pink equant calcite. Several examples of large (1-2 m in diameter) cavities were observed in the field. These cavities are commonly infilled by large orthocone cephalopods and dark-red lime-mud. In thin-section, small (0.50-2.0 mm) irregularly shaped cavities and shelter voids (created by elongate skeletal grains such as trilobites) are abundant. These cavities commonly exhibit geopetal infilling of internal sediment, fossil material and cement. The internal sediment commonly appears graded or cross-laminated. The origin and preservation of these cavities will be discussed in detail in Chapter 4.

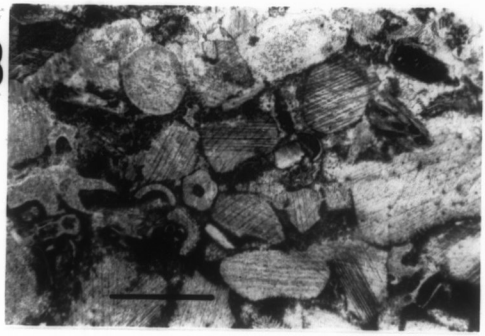
The dominant lithotacies in the Holston Formation in the study area consists of echinoderm-bryozoan packstones (Figure 2.3A, B). On outcrop, especially in the lower portions of the stratigraphic sections at Poor Valley Creek and Red House Branch, cross-beds dip away from lime mud-mounds (bryozoan wackestone-boundstones) at high angles

Figure 2.3. Petrographic features of the Holston and Rockdell Formations in northeastern Tennessee.

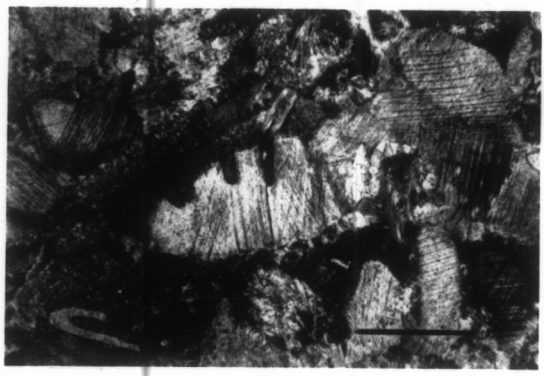
A. Photomicrograph of the echinoderm-bryozoan packstone lithofacies in the Holston Formation. Bar scale is approximately 1.0 mm. Red House Branch. (RHB'3AB).
B. Photomicrograph of the echinoderm-bryozoan packstone lithofacies in the Holston Formation. Bar scale is approximately 1.0 mm. Red House Branch. (RHB'6BBR).
C. Photomicrograph of the echinoderm-bryozoan packstone lithofacies in the Holston Formation showing macroboring of an echinoderm ossicle. Note also that the outer fringe of the ossicle shows some micritization. Bar scale is approximately 1.0 mm. Red House Branch. (RHB'6BT).
D. Photomicrograph of the echinoderm-bryozoan packstone lithofacies in the Holston Formation showing an echinoderm ossicle which has been micritized on the outer and inner surfaces. Fibrous cement (seen most clearly at the upper right on the echinoderm) is growing off the micritized surfaces. Bar scales is approximately 1.0 mm. Red House Branch. (RHB'3DS2).
E. Photomicrograph of the bryozoan-echinoderm grainstone-packstone lithofacies in the Rockdell Formation. The large, fragmented grain in the center of the field of view is the green alga Vermiporella? Bar scale is approximately 1.0 mm. Evans Ferry. (EF'45).
F. Photomicrograph of the bryozoan-echinoderm grainstone-packstone lithofacies in the Rockdell Formation showing abundant abraided echinoderm debris. Note also the micritic rims on most of the echinoderm grains in the field of view. Evans Ferry. (EF'45).
G. Enlarged photomicrograph of the micritized echinoderm grains in Figure 2.3F. Bar scale is approximately 0.25 mm. Evans Ferry. (EF'45).



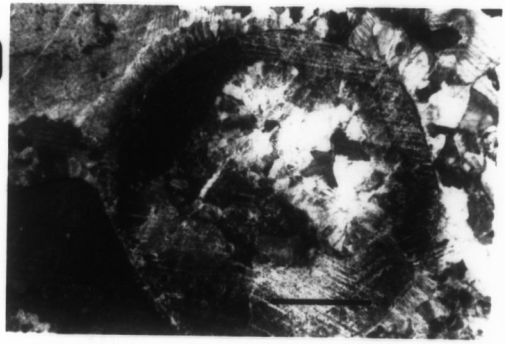
A



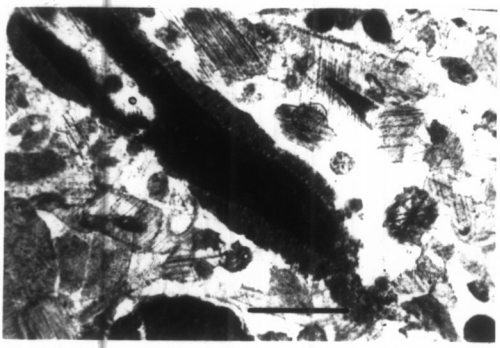
B



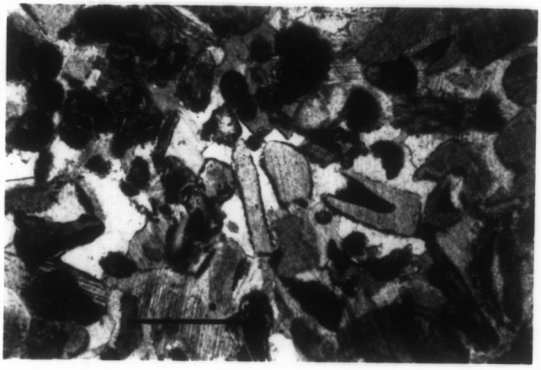
C



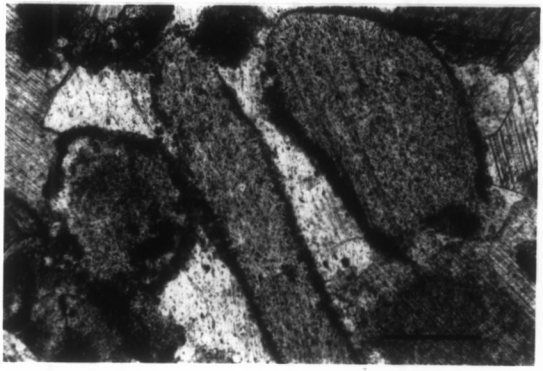
D



E



F



G

Figure 2.3
36
Jernigan, 1987

(Ruppel and Walker, 1982). Ramose and encrusting bryozoans are common in this lithofacies. Bryozoans usually dominate the fauna but in some samples, echinoderm debris is the most abundant allochem (Table 2.3). Arthropods (trilobites and ostracodes), brachiopods, molluscs together account for less than 5 volume percent of the sediment. Calcareous algae and sponge debris, although rare, were observed in several samples from this lithofacies. Intraclasts, peloids, and algally coated grains are also present but volumetrically unimportant. Intraclasts increase in abundance in this lithofacies in the upper part of the Holston at Red House Branch. Skeletal grains such as echinoderm ossicles are generally unabraded. Macroboring (Figure 2.3C) and micritization (Figure 2.3D) of echinoderm ossicles and trilobite carapaces are common. Multiplated echinoderm holdfasts are also common.The proportions of lime-mud to calcite cement in this lithofacies is highly variable.

Ruppel (1979) and Ruppel and Walker (1982, 1984) found the echinoderm-bryozoan packstone lithofacies to be intermediate in character between the echinoderm-bryozoan grainstone-packstone lithofacies and the bryozoan wackestone-boundstone lithofacies. They believed that sediment accumulated in "echinoderm-bryozoan thickets" which were associated with bryozoan wackestone-boundstones. Such environments have been postulated for many Paleozoic lime-mud mound deposits (Wilson, 1975). This interpretation is supported by field evidence in that these packstone beds were observed lateral to and abutting against bryozoan boundstone masses.

Table 2.3. Constituent analyses of the echinoderm-bryozoan packstone lithofacies of the Holston Formation. NR represents a constituent which was not recorded. The numbers in parentheses represent the total number of samples.

	Holston Formation			
	(This Study) Echinoderm-Bryozoan-Packstone (10)		(Ruppel and Walker, 1982) Bryozoan-Pelmatozoan Packstone (6)	
Constituent	Range	Average	Range	Average
Spar	19-51	31	8-23	18
Micrite	4-25	14	17-35	26
Microspar	1-14	5	NR	NR
Echinoderms	2-32	17	8-25	16
Bryozoans	10-32	21	18-50	31
Trilobites	<1-5	1	0-2	1
Ostracodes	0-1	<1	0-5	1
Brachiopods	0-2	<1	0-2	1
Molluscs	0-1	<1	0-1	<1
Corals	-	-	-	-
Algae	-	-	-	-
Sponges/spicules	-	-	-	-
Indeterminate Fossils	<1-2	1	0-1	<1
Intraclasts	0-2	<1	-	-
Peloids	0-2	<1	-	-
Oncolites	-	-	-	-
Stylocumulate	<1-8	4	0-8	4
Dolomite	0-16	2	0-1	<1

Together, the echinoderm-bryozoan packstone lithofacies and the bryozoan wackestone-boundstone lithofacies are analogous to the "reef flank" and "reef core" deposits of the upper Holston Formation near Knoxville, Tennessee (Walker, 1977, 1980). Ruppel (1979) and Ruppel and Walker (1982, 1984) have interpreted the bryozoan wackestone-boundstone lithofacies as true "'organic reefs' (Wilson, 1975), developed in large part by the activities of encrusting bryozoans" (Ruppel, 1979). The cross-bedded nature of the echinoderm-bryozoan packstones away from bryozoan boundstone masses indicates that these mounds were topographically raised relative to the surrounding sediment (Ruppel and Walker, 1982). The lime-mud mounds were lithified, at least in part, syndepositionally as evidenced by the following: (1) the binding activity of encrusting bryozoans which bound micritic matrix material as well as fossil debris; (2) the presence of marine cement-filled cavities (including stromatactoid type cavities) which required the formation of cemented marine crusts above unlithified sediment (Bathurst, 1980); and (3) the presence of bryozoans encrusting vertical cavity walls within reef core masses. Thus, these lime-mud mounds "had the potential of being wave resistant structures" (Ruppel, 1979).

The Rockdell Formation Near Knoxville, Tennessee

Breland (1980) studied the Rockdell Formation in northeastern Knox County, Tennessee. His study was conducted approximately 29 miles southeast of the present study within the same strike belt. Breland's (1980) study area consisted of a 15 mile long, 4-locality transect,

oriented normal to the Middle Ordovician shelf margin. A reentrant in the Middle Ordovician shelf (see Benedict and Walker, 1978) adjacent to the northeastern portion of this area allowed Breland (1980) to examine the lithologic and paleontologic variability in the Rockdell Formation from the inner shelf area (southwest) to an area of transition between the inner shelf and the shelf margin (northeast). Breland (1980) noted that in his study area, the Rockdell Formation consists of a complex assemblage of lithofacies including: (1) pelmatozoan-bryozoan packstone-grainstones, (2) bryozoan wackestones, and (3) bryozoan-algal boundstones. These lithofacies have been interpreted to represent: (1) skeletal sand banks with incising tidal channels, (2) lime-mud mounds; and (3) bryozoan-algal patch reefs (Breland, 1980).

The pelmatozoan-bryozoan packstone-grainstone lithofacies is developed in the southeastern portion or inner shelf area of Breland's (1980) study area. Carbonate mud generally increases shelfward as does the relative abundance of sponge debris. Bryozoan wackestones and bryozoan-algal boundstones decrease in abundance shelfward (toward the southwest) and are not present at the southwestern most locality. Bryozoan and echinoderm debris are the dominant fossil groups in the rocks of the inner shelf area (Breland, 1980).

The bryozoan wackestone and bryozoan-algal boundstone lithofacies are best developed in the northeastern portion of Breland's (1980) study area. Bryozoan wackestones generally consist of bifoliate and encrusting bryozoans. Echinoderm debris is abundant and characteristically unabraded. Red lime-mud is the dominant constituent of these

rocks. Breland (1980) observed abundant in situ pelmatozoan holdfasts on these wackestone buildups. He suggested that pelmatozoans (in thickets or meadows) acted as "current baffles" aiding in the deposition of lime-mud. Encrusting bryozoans are associated with the holdfasts on outcrop. These organisms acted as sediment binders which "stabilized" these mud mounds and allowed their further growth and development (Breland, 1980). The bryozoan wackestone lithofacies generally "interfingers both laterally and vertically" with the pelmatozoan-bryozoan packstone-grainstone lithofacies. This lithofacies consists of abundant bifoliate bryozoan debris as well as abraded pelmatozoan debris. Lime-mud is volumetrically reduced in this lithofacies in the northeastern part of Breland's study area.

The bryozoan-algal boundstone lithofacies consists of abundant encrusting bryozoans which Breland (1980) suggested acted as sediment binders helping to "stabilize" the boundstone masses. The encrusting red alga, Solenopora sp., is also abundant in this lithofacies. Breland and Walker (1980) have stated that Solenopora sp. shared the role of sediment binder with encrusting bryozoans in these boundstone buildups. These boundstone masses are similar to the bryozoan boundstones described by Ruppel (1979) and Ruppel and Walker (1982, 1984) which occur in the Holston Formation to the northeast in the same strike belt (see above discussion of Holston bryozoan wackestone-boundstones). For example, these boundstone masses are similarly cavernous; cavities may be filled with cement or internal sediment. Also, Breland (1980) noted that bryozoans encrusted cavity walls and roofs.

The bryozoan-algal boundstone lithofacies is associated with lateral (flanking) pelmatozoan-bryozoan packstone-grainstones which are similar to the packstone-grainstones associated with the bryozoan wackestone (lime-mud mound) lithofacies. This lithofacies commonly contains angular fragments of bryozoan-algal boundstone. The sediment was generally well washed and well sorted (Breland, 1980). Pelmatozoan and bryozoan debris commonly appears abraded suggesting some degree of transport.

The bryozoan wackestone (lime-mud mound) lithofacies is not considered to have been true "reef core" (Walker and Ferrigno, 1973) material due to the paucity of encrusting bryozoans (Breland, 1980). The bryozoan-algal boundstone lithofacies, on the other hand, exhibits abundant encrusting bryozoans and algae. The boundstone masses also exhibit flanking pelmatozoan-bryozoan packstone-grainstone beds which often contain angular or abraded fragments of boundstone lithology. Breland (1980) has described these boundstone masses and associated rocks as being similar to the deposits of the upper Holston Formation near Knoxville, Tennessee. Thus, the boundstone masses are described as "reef core" deposits and the flanking packstone-grainstones are described as "reef flank" deposits (terms after Walker and Ferrigno, 1973).

In the northeastern portion of his study area, Breland (1980) interpreted the Rockdell as a mosaic of sand banks, tidal channels and lime-mud mounds "which were characterized by pelmatozoan-bryozoan packstone-grainstones and bryozoan wackestone-boundstones" (Breland, 1980). The abundance of lime-mud in the packstone-grainstone

lithofacies as well as the sorted and abraded nature of the pelmatozoan and bryozoan debris in this lithofacies suggests that the current energy in this part of the study area was at least of moderate intensity. To the southeast, the environmental conditions on the inner shelf were more "restricted" due in part to the patch reef buildups which developed across the shelf to the northeast (Breland, 1980). Evidence for restricted circulation in the southwestern part of the study area is the increase in lime-mud abundance in sediment deposited southwest of the lime-mud mounds (Breland, 1980).

The Rockdell Formation in Northeastern Tennessee

The Rockdell Formation in the area of the present study has been examined by Sickafoose (1979), Ruppel (1979), and Ruppel and Walker (1982, 1984). The following discussion of the depositional textures and fabrics observed in the Rockdell Formation is largely a summary of these environmental studies, supplemented by observational and constituent analysis data obtained during the present study.

Ruppel and Walker (1982, 1984) have outlined three "intergradational lithofacies" which comprise the Rockdell within the study area. These lithofacies (modified after Ruppel and Walker, 1982, 1984) are: (1) bryozoan-echinoderm grainstone-packstones; (2) bryozoan-echinoderm packstones; and (3) bryozoan wackestones. In general, the echinoderm-bryozoan packstone lithofacies occurs dominantly toward the west-northwest portions of the study area (toward Evans Ferry). The echinoderm-bryozoan grainstone-packstone and the bryozoan wackestone

lithofacies occur most often in the central and east-southeastern portion of the study area (at Cedar Springs and Red House Branch). The primary cause for these differences in occurrence is the overall increase in abundance of lime-mud to the northeast. It is important to note that lime-mud does not occur as lime-mud "mounds" (bryozoan wackestones) at Evans Ferry, but rather is "disseminated throughout the formation" (Ruppel and Walker, 1982).

The bryozoan-echinoderm grainstone-packstone lithofacies (Figure 2.3E, F, p. 35) is typically cross-bedded. Lime-mud is present but always in low abundance (<10 volume percent) (Table 2.4). Echinoderm debris is the dominant sediment constituent averaging 28 volume percent (Ruppel and Walker, 1982). Bryozoan debris, most commonly ramose forms, are the second most common fossil group (average 17 volume percent). Arthropods (trilobites and ostracodes), brachiopods, molluscs and calcareous algae typically represent less than 10 volume percent of the rocks. Abrasion and micritization of skeletal grains is common (Figure 2.3F, G). Intraclasts, peloids, and algally coated grains are also common. The Rockdell Formation in general exhibits a diverse algal flora which includes Contexta, Kazahkstanellia, Vermiporella, and Nuia. Girvanella, Solenopora, and Hedstromeia are also present but are relatively rare. Contexta and Nuia are common in the bryozoan-echinoderm grainstone-packstone lithofacies.

Ruppel and Walker (1982, 1984) have interpreted the bryozoan-echinoderm grainstone-packstone lithofacies as skeletal sand bank

Table 2.4. Constituent analyses of the bryozoan-echinoderm grainstone-packstone lithofacies of the Rockdell Formation. NR represents a constituent which was not recorded. The numbers in parentheses represent the total number of samples.

	Rockdell Formation			
	(This Study) Bryozoan-Echinoderm Grainstone/ Packstone (8)		(Ruppel and Walker, 1982) Pelmatozoan Bryozoan Grainstone/ Packstone (12)	
Constituent	Range	Average	Range	Average
Spar	26-47	36	25-50	36
Micrite	0-6	3	0-9	4
Microspar	0-5	2	NR	NR
Echinoderms	19-36	29	15-40	28
Bryozoans	5-21	15	6-35	28
Trilobites	<1-2	1	0-5	1
Ostracodes	0-1	1	1-8	5
Brachiopods	0-2	1	0-2	<1
Molluscs	0-<1	<1	0-3	<1
Corals	-	-	-	-
Algae	0-3	1	0-13	3
Sponges/spicules	0-1	<1	-	-
Indeterminate Fossils	1-6	3	0-3	<1
Intraclasts	0-2	1	0-10	2
Peloids	0-<1	<1	0-8	1
Oncolites	0-6	1	0-5	<1
Stylocumulate	<1-8	4	0-10	2
Dolomite	0-4	1	0-4	1

deposits. The presence of abraded grains, concentric algally coated grains, as well as the paucity of lime-mud, suggests that sediment was deposited in current-agitated conditions. Girvanella oncoids indicate that this lithofacies was deposited in water depths of 10 m or less (Benedict and Walker, 1978).

The bryozoan-echinoderm packstone lithofacies (Figure 2.4A, B) differs from the bryozoan-echinoderm grainstone-packstone lithofacies primarily in the relative proportions of matrix material (Table 2.5). Lime-mud is more abundant in this lithofacies (average 14 volume percent in the present study and 25 volume percent in the study of Ruppel and Walker, 1982). Interparticle calcite cement is less abundant in this lithofacies (average 29 volume percent versus 36 volume percent in the grainstone-packstones). The most abundant fossil group is echinoderms which average 20 volume percent of the sediment. Bryozoans, principally ramose forms, represent the second most common fossil group, averaging 14 volume percent of these sediments. Arthropods (trilobites and ostracodes), brachiopods, molluscs, corals and calcareous are also commonly present in these sediments, but together usually account for less than 10 volume percent of the samples based on constituent analysis data (Ruppel, 1979; Ruppel and Walker, 1982; and from the present study). Cross-bedding is poorly developed. Abrasion and micritization (boring by endolithic algae and/or fungi) of skeletal debris is generally less common in this lithofacies relative to grainstone-packstones. The entire algal flora of the Rockdell Formation which was previously

Figure 2.4. Petrographic features of the Rockdell Formation in northeastern Tennessee.

A. Photomicrograph of the bryozoan-echinoderm packstone lithofacies. Bar scale is approximately 1.0 mm. Cedar Springs. (CS45).
B. Photomicrograph of the bryozoan-echinoderm packstone lithofacies. Bar scale is approximately 1.0 mm. Red House Branch. (RHB'8CL).
C. Photomicrograph of the bryozoan wackestone lithofacies showing the characteristic sediment constituents, bryozoans and lime-mud. Bar scale is approximately 1.0 mm. Cedar Springs. (CS8DS1).
D. Photomicrograph of the bryozoan wackestone lithofacies showing abundant sponge spicules disseminated in micrite. Bar scale is approximately 1.0 mm. Evans Ferry. (EF'28).
E. Photomicrograph of the bryozoan wackestone lithofacies showing macroboring of trilobite fragments. Bar scale is approximately 1.0 mm. Red House Branch. (RHB'4DS1).
F. Enlarged photomicrograph of the bryozoan wackestone lithofacies showing micritization of a trilobite fragment. Bar scale is approximately 0.25 mm. Evans Ferry. (EF'19).
G. Photomicrograph of a cement filled stromatactoid cavity in the bryozoan wackestone lithofacies. Note that the fibrous cement crystals growing off the roof and floor meet in the center of the cavity to form a median boundary. Bar scale is approximately 1.0 mm. Red House Branch. (RHB'8H).
H. Photomicrograph of stromatactoid cavities in the bryozoan wackestone lithofacies. Note the sponge debris disseminated in the micritic matrix. Bar scale is approximately 1.0 mm. Red House Branch. (RHB'8H).

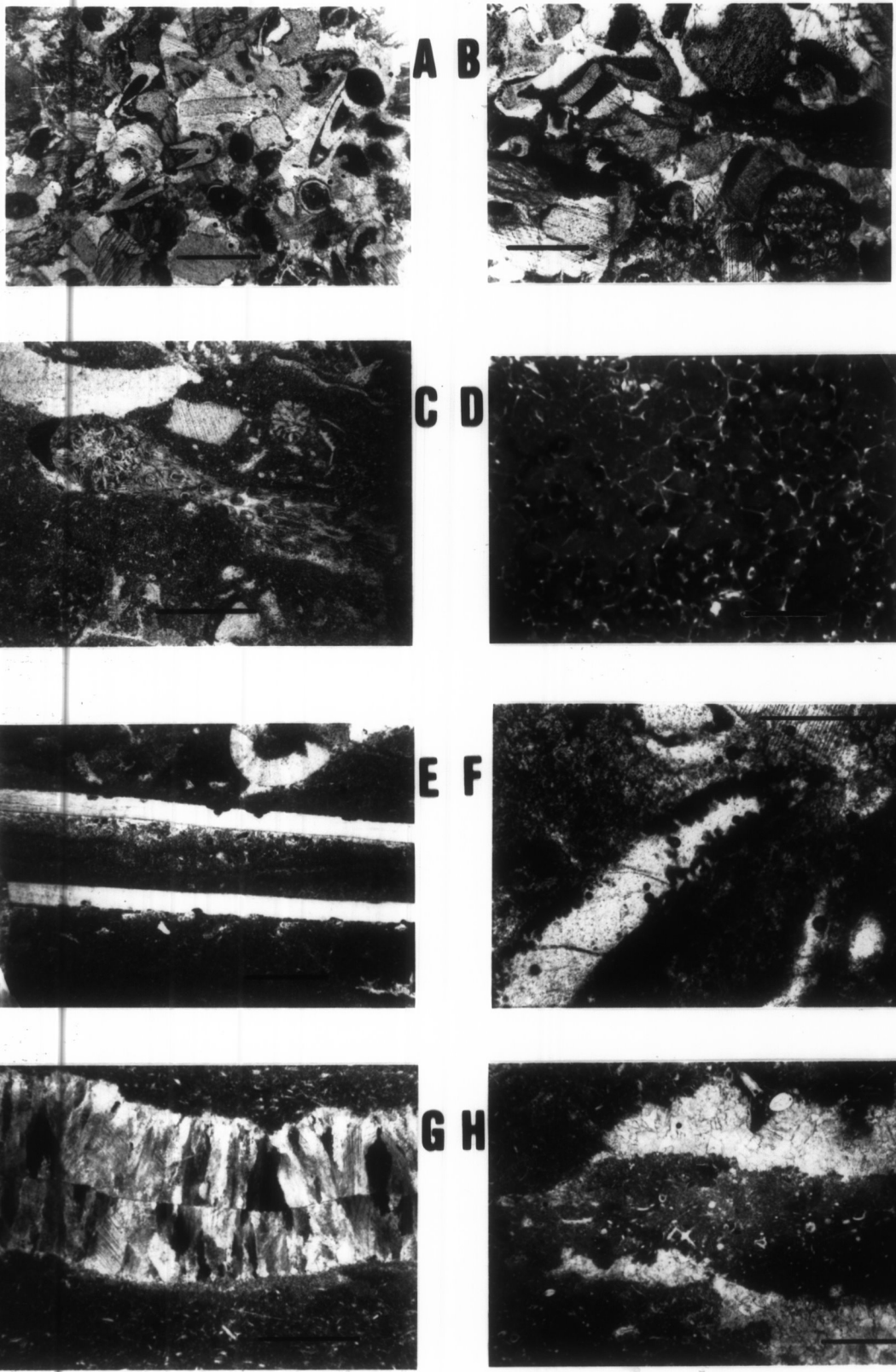

A
B
C
D
E
F
G
H

Figure 2.4
48
Jernigan, 1987

Table 2.5. Constituent analyses of the bryozoan-echinoderm packstone lithofacies of the Rockdell Formation. NR represents a constituent which was not recorded. The numbers in parentheses represent the total number of samples.

	Rockdell Formation			
	(This Study) Bryozoan-Echinoderm Packstone (14)		(Ruppel and Walker, 1982) Pelmatozoan Bryozoan Packstone (9)	
Constituent	Range	Average	Range	Average
Spar	6-43	29	5-44	21
Micrite	5-27	14	12-40	25
Microspar	<1-17	8	NR	NR
Echinoderms	11-36	20	15-31	22
Bryozoans	2-24	14	7-16	11
Trilobites	0-2	1	0-2	1
Ostracodes	0-1	<1	0-6	3
Brachiopods	0-1	<1	0-1	<1
Molluscs	0-<1	<1	0-2	1
Corals	-	-	0-35	4
Algae	0-3	<1	0-29	6
Sponges/spicules	0-8	1	0-1	<1
Indeterminate Fossils	0-5	3	0-2	<1
Intraclasts	0-1	<1	0-12	2
Peloids	0-1	<1	0-4	<1
Oncolites	0-2	<1	0-25	3
Stylocumulate	1-11	4	0-5	1
Dolomite	0-9	1	0-5	1

described is well developed in this lithofacies (Ruppel and Walker, 1982, 1984).

Ruppel and Walker (1982, 1984) have interpreted the bryozoan-echinoderm packstone lithofacies as in situ accumulations of skeletal sands and lime-mud which were deposited in bryozoan, echinoderm (pelmatozoan) "thickets." Stalked echinoderms and ramose bryozoans acted to "protect" local areas from wave and current activity, allowing deposition of lime-mud with locally derived skeletal debris. These relatively quiet-water conditions are evidenced by the unabraded nature of the skeletal material as well as the abundance of lime-mud in these deposits (Ruppel and Walker, 1982, 1984). The bryozoan-echinoderm grainstone-packstone lithofacies is thought to have resulted from winnowing and reworking of sediment of the bryozoan-echinoderm packstone lithofacies.

The bryozoan wackestone lithofacies (Figure 2.4C, D) consists of abundant bryozoans (encrusting and bifoliate), sponges, encrusting algae and abundant lime-mud (up to 80 volume percent in the study of Ruppel, 1979) (Table 2.6). Locally, encrusting bryozoans are sufficiently abundant to produce bryozoan boundstones. At Cedar Springs, lime-mud has a distinctive red color similar to the lime-mud in the Holston Formation. Echinoderms, arthropods (trilobites and ostracodes), molluscs and calcareous algae are present in this lithofacies, but only echinoderms are volumetrically important. Skeletal debris, other than bryozoans, is abraded (Ruppel, 1979; Ruppel and Walker, 1982, 1984). Macroboring (Figure 2.4E) and micritization (Figure 2.4F)

Table 2.6. Constituent analyses of the bryozoan wackestone lithofacies of the Rockdell Formation. NR represents a constituent which was not recorded. The numbers in parentheses represent the total number of samples.

	Rockdell Formation			
	(This Study) Bryozoan Wackestone (13)		(Ruppel and Walker, 1982) Bryozoan Wackestone (16)	
Constituent	Range	Average	Range	Average
Spar	1-27	11	0-22	8
Micrite	15-61	45	38-80	64
Microspar	0-37	16	NR	NR
Echinoderms	0-10	4	0-18	6
Bryozoans	<1-26	9	1-24	13
Trilobites	0-1	<1	0-5	1
Ostracodes	0-2	<1	0-5	3
Brachiopods	0-1	<1	0-1	<1
Molluscs	0-<1	<1	0-3	<1
Corals	-	-	-	-
Algae	0-3	<1	0-5	1
Sponges/spicules	0-8	2	0-8	3
Indeterminate Fossils	<1-4	2	0-9	1
Intraclasts	0-<1	<1	-	-
Peloids	0-2	1	0-10	1
Oncolites	0-<1	<1	-	-
Stylocumulate	0-19	4	0-3	1
Dolomite	0-8	1	0-1	<1

of fossil debris, especially echinoderm ossicles and trilobite carapaces, is common. All algal genera which occur in the Rockdell are represented in this lithofacies, however, oncoids are absent. Locally, irregularly shaped, filled voids or cavities occur within rocks of this lithofacies (Ruppel, 1979). These voids may be filled with geopetal internal sediment and later equant calcite. The internal sediment is usually fine-grained (<5 μm) micrite or crystal silt and may be mixed locally with fine skeletal material. Ruppel (1979) and Ruppel and Walker (1982, 1984) have interpreted these features as dissolution voids or fenestrae. At Red House Branch, stromatactoid structures (Figure 2.4G) are developed in the bryozoan wackestone lithofacies. These structures are similar to stromatactis mounds described in the Holston Formation in this study area (Ruppel, 1979; Ruppel and Walker, 1982, 1984) and near Knoxville, Tennessee (Walker and Ferrigno, 1973; Ferrigno, 1973). Cavities developed between micritic laminae are filled with internal sediment (which appears laminated or cross-laminated), multiple generation radiaxial-fibrous cement, and later by equant calcite cement. Staining with potassium ferricyanide reveals that the pore central, equant calcite is ferroan. Sponge spicules are locally disseminated in the micritic laminae (Figure 2.4H) and represent the dominant fossil in these structures (>6 volume percent of the sediment in one sample which was point-counted). It is significant to note that stromatactoid structures are only developed in the lower part of the stratigraphic section at this locality.

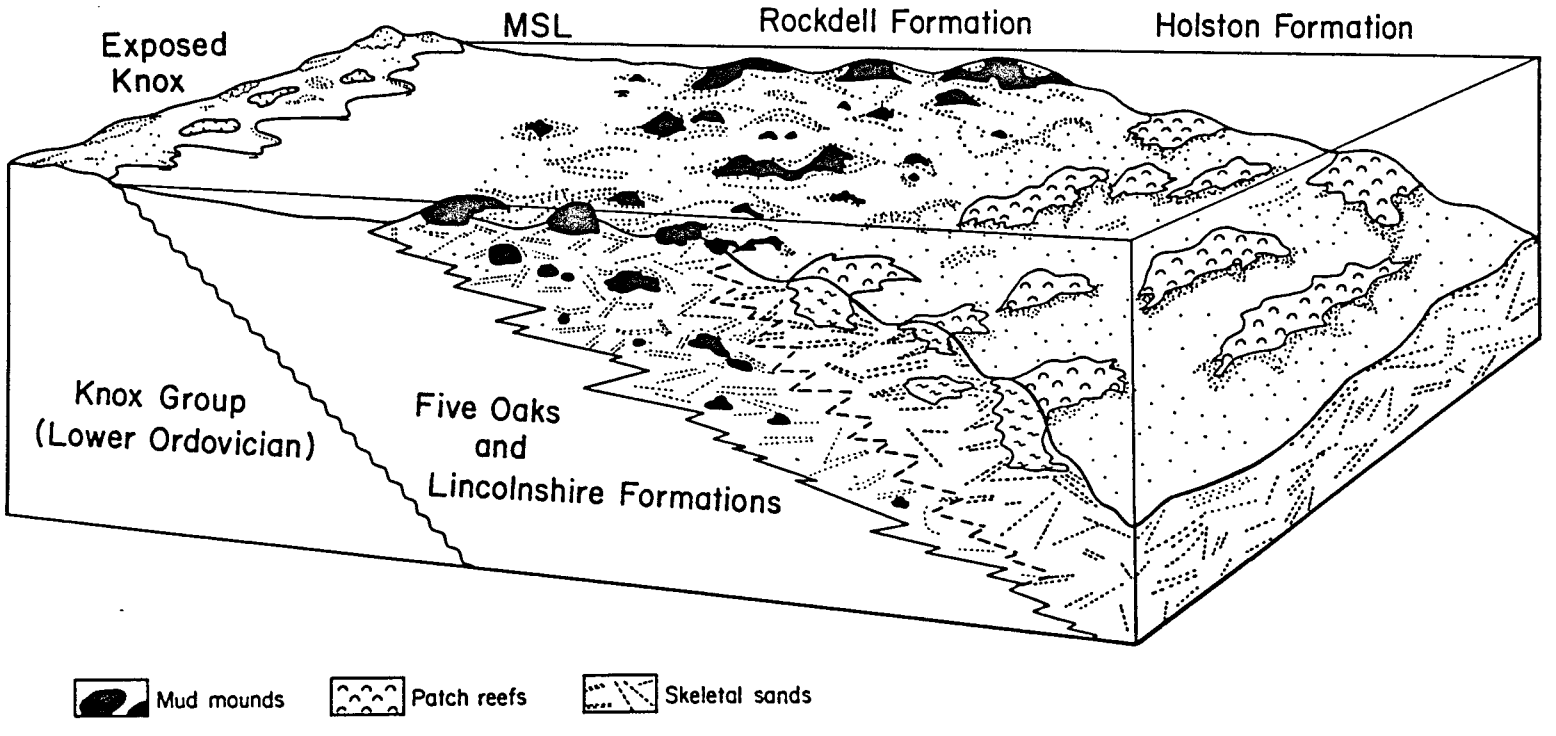
Ruppel (1979) and Ruppel and Walker (1982, 1984) suggested that the bryozoan-echinoderm wackestone lithofacies actually represents somewhat isolated lime-mud mounds developed within a "complex" of skeletal sand banks (bryozoan-echinoderm grainstone-packstones and bryozoan-echinoderm packstones). They contend that local quiet-water conditions allowed the initial deposition of carbonate mud which was later colonized by encrusting bryozoans and algae. The encrusting organisms effectively "stabilized" the mound buildups and aided further mound development. The diverse algal flora and presence of dissolution voids and tenestrae within these lime-mud mounds suggests that they may have developed in shallow water and were, at least occasionally, subaerially exposed.

Time Relationships Between the Holston and Rockdell

Ruppel (1979) and Ruppel and Walker (1982, 1984) have recognized the Holston and Rockdell formations as "two distinct buildup complexes" which were deposited in substantially different environments. The initial Holston deposition occurred at the Middle Ordovician shelf margin or slightly downslope (Ruppel, 1979; Ruppel and Walker, 1982). Ruppel and Walker (1982) have examined strata which were deposited further on-shelf relative to the Holston (e.g., the Lincolnshire Formation). Based on these investigations and on the lithologic content of Holston, they suggested that the Holston Formation was not a barrier which restricted wave and current energy shelfward but rather was deposited in deep water below normal wave-base. Initial deposition of Rockdell

sediment began in the late stages of Holston deposition (Ruppel, 1979; Ruppel and Walker, 1982). The Rockdell was initially a shelfward extension of Holston sediment deposited in shallower water, agitated conditions. These authors illustrated these geographic and bathymetric relationships between the Holston and Rockdell formations at a time which corresponds to Time Line 3 on Figure 1.2 (p. 9) (Figure 2.5). Shortly after that time, Holston deposition ceased and Rockdell sediment prograded toward the shelf margin (to the southeast) and covered the Holston (note the Red House branch locality in Figure 1.2 in which the Rockdell Formation overlies the Holston Formation). Ruppel and Walker (1982) have proposed that this basinward migration of Rockdell sediment might best be explained by a change in the configuration of the basin which facilitated the influx of terrigenous material from the east onto the Middle Ordovician carbonate shelf. There is evidence of a major diastem, marked by a thin, gray, shaley limestone which contains phosphatic and manganiferous nodules, at the top of the Holston Formation near Knoxville, Tennessee. Walker (pers. comm.) believes that this horizon may represent a rapid drop in sea level which would have exposed portions of the shelf and shelf margin. The migration of shelf environments toward the shelf margin in northeastern Tennessee may best be explained by this major fall in sea level rather than a slow-down in the "carbonate machine" due to the influx of terrigenous material.

Figure 2.5. Schematic block diagram illustrating the geographic and bathymetric relationships between the Holston and Rockdell formations in Northeastern Tennessee. Time represented is approximately that of Time Line 3 in Figure 1.2 (p. 9). (From Ruppel and Walker, 1982).


Exposed
Knox
MSL
Rockdell Formation
Holston Formation
Knox Group
(Lower Ordovician)
Five Oaks
and
Lincolnshire Formations
Mud mounds
Patch reefs
Skeletal sands

CHAPTER 3

CARBONATE CEMENT

Introduction

One of the major goals of this thesis was to determine the distribution of carbonate cement in the Holston and Rockdell formations in northeastern Tennessee and by using "accepted" texture and fabric criteria (Folk, 1974; Bathurst, 1975), determine the diagenetic environment of formation for each cement type. Cement textures and fabrics observed in the Holston and Rockdell formations are described in this chapter. The abundance and distribution of cement types are discussed in Chapter 4, along with a discussion of the observed paragenetic sequence of carbonate cement.

The term cement, as used here, includes "all passively precipitated, space-filling carbonate crystals which grow attached to a free surface" (Bathurst, 1975). Petrographic analysis has allowed the distinction of the following eight cement categories:

1. Radiaxial-fibrous calcite and associated cement;
2. Bladed/prismatic calcite cement;
3. Turbid or inclusion-rich syntaxial (rim) calcite cement;
4. Cryptocrystalline (micrite) (calcite) cement;
5. Equant (drusy) calcite cement;
6. Clear syntaxial (rim) calcite cement;
7. Ferroan calcite cement;
8. Ferroan (baroque) dolomite.

In this chapter, each cement category is presented in terms of the diagenetic environment responsible for its formation. The major diagenetic environments, marine and meteoric, are outlined as a preface to the discussion of cement types formed in those environments. In some cases, cement crystal sizes will be referred to in terms of very finely, finely, medium, coarsely, or very coarsely crystalline. A key to the actual sizes (in millimeters) corresponding to these terms is provided in Appendix B.

Marine Cement

Since the late 1960s, marine cementation has been known to occur in modern carbonate sediment. In 1969, an international conference on carbonate cementation was held at the Bermuda Biological Station for Research. Several papers given at that conference concerned marine lithification of modern carbonate sediment from widely varying geographic locations. These papers (Table 3.1) represented the state-of-knowledge at that time and served to illustrate several important aspects of submarine cementation. Fibrous (length to width ratio >6:1, Folk, 1965) and bladed cement (length to width ratio 1.5:1-6:1, Folk, 1965) are common precipitates in the shallow marine environment as are microcrystalline and micrite cement. These cement types occur as both aragonite and magnesian calcite, commonly referred to as high Mg-calcite. This mineralogy is distinctly different from the low Mg-calcite precipitated under meteoric diagenetic conditions (Milliman, 1971). The isotopic composition of marine cement was found to be

Table 3.1. Articles on marine cementation presented at the Bermuda Biological Station for Research in 1969 and summarized in Bricker (1971). Abbreviations used in the table are as follows: O = oxygen; C = carbon; A = aragonite; and Mg = magnesian calcite. Numbers in parentheses represent mole% magnesium in calcite.

				Cements			
Author	Environment	Evidence	Area	Micrite	Fibrous	Granular Drusy	Remarks
Friedman	shallow marine	79m	N. Jersey	A	A		cement promoted by CH_4
Ginsburg	subtidal	sed structs reefs, isotopes 3100 bp	Bermuda		Mg (16)		
Land	reef	75 feet C14, O, C12	Jamaica	Mg	Mg (18)		reef talus cemented
Hoskins	reef rampart	0 to 10 feet	Alacran		A ?		
Pingitore	subaerial expo. Pleistocene reefs	?	Barbados		A ?		
Glover, Pray	subtidal intraparticle	4 to 10 feet	Bahamas		Mg (15-19) A	in Mg shells in A shells	
Roberts, Moore	subtidal (no other source of grains)	10 to 12 feet	Grand Cayman	A (partly algal boring)	A		
McIntyre et al.	open marine C14 500-1500	60 feet	Barbados	Mg (20) rims	Mg (20) interiof		stronger around burrows
Shinn	subtidal (2,000 to recent lack diagnostic sed structures) O18/O16 C13/C12	5 to 90 feet	Persian Gulf	Mg in mud A (Mg) mud 15% Mg	A		due to carbonate saturated sea water, related to grain size and rate of sedimentation
Milliman	seamounts steep slopes supersaline	fossils O18, C	everywhere except N. Pac., Red Sea, Med.	Mg (10-14) A Mg (12) in veins	A (some)	Mg (10-14)	
	volcanic seamounts		world	?		Ca	filling cavities, voids pelletal matrix
McIntyre, Milliman	outer shelf 13,500-15,000	oolites, algal calcarenite	SE US BP	Mg	A Mg (12)		fine g. pelleted 1st probably beachrock when sea level lower
Friedman	1,300-1,700 m		Red Sea		A prismatic		indurated layers between calclutite
Marlowe	340-380 M		Caribbean	minor in pellts	Mg (11-14) rhomb		minor A xtals of 2-5 microns

distinct from meteoric cement (Land, 1971; Milliman, 1971). Factors which control cement mineralogy were postulated to be ion concentration, the presence of organic compounds (Mitterer, 1971), salinity (Milliman, 1971; Shinn, 1971), Mg^{2+}/Ca^{2+} ratio (Taylor and Illing, 1971; Mackenzie and Bricker, 1971), and a relatively slow rate of sedimentation (Shinn, 1971).

Subsequent researchers have found marine cement to be common in "reef" or "mound" environments. Marine cementation associated with the seaward facing margins of the Holocene barrier and atoll reefs of Belize (British Honduras) has received considerable attention. The initial analysis of the Belize reef complex by James et al. (1976) was undertaken in order to map the distribution of cement types in shallow lagoon, barrier, and atoll reefs "at or near the sediment/rock-water interface." They found that cementation in these environments was restricted to the seaward margins of barrier and atoll reefs and absent from lagoonal reefs. Aragonite cement and two forms of magnesian calcite cement were described from these sediments. Aragonite occurred only as intraskeletal cement partially or completely filling corallites of various coral species. Cementation by magnesian calcite was shown to follow a generally repetitive sequence. Initially silt-sized grains or silt- and sand-sized grains were cemented by magnesian calcite micrite (2-6 μm diameter). Sediment consisting of both silt- and sand-sized particles was then cemented by a two-phase cement which consists of "thin rinds of micrite that grade outward into bladed spar." Grainstones with interparticle pores larger than 50 μm are then

cemented by bladed magnesian calcite crystals ranging from 6 to 40 μm in length and 2-5 μm in width. James et al. (1976) inferred that the preferential occurrence of cementation along the seaward-facing margin of these reefs was controlled primarily by three factors: (1) subtidal pumping of seawater through the sediment; (2) oxidizing conditions being maintained within the sediment; and (3) low sedimentation rates.

Shortly after this study, Ginsburg and James (1976) described botryoidal aragonite cement in samples blasted from the forereef wall and from talus blocks of the forereef rise. This cement occurred in several types of cavities, often alternating with deposition of internal marine sediment. Several lines of evidence support a marine origin for the aragonite botryoidal cement. First, the cement occurred in sediment rich in magnesian calcite with no evidence of leaching or mineral transformation. Second, the growth of aragonite botryoids was associated with deposition of internal marine sediment. Third, benthic foraminifera are often engulfed by cement growth and appear as "floating" grains within the fibrous cement mosaic. Finally, strontium and sodium concentrations (8120 to 8460 ppm and 2700 to 3600 ppm, respectively) as well as carbon and oxygen isotopic ratios (+3.3 to +4.2 per mil and +0.4 to +1.1 per mil vs. PDB, respectively) of the cement are characteristic of calcium carbonate precipitated from sea water. The entire spectrum of carbonate cement types encountered within the reef complex of Belize by Ginsburg, James and their associates has been summarized in James and Ginsburg (1979).

Similar cement types (both in texture and fabric) have been described from modern coral reef complexes at numerous localities around the world. Land and Goreau (1970) found two forms of magnesian calcite cement in Jamaican reef-crest, and "forereef framework and inter-framework sediment." This cement occurs as isopachous fringes of acicular, scalenohedral magnesian calcite crystals and as laminated, peloidal magnesian calcite micrite.

Friedman, et al. (1974) observed both magnesian calcite micrite and rod- or needle-shaped aragonite (up to 50 μm in length) cement immediately below the surface of reef corals in the Red Sea. Aragonite was the dominant cement type in Red Sea reefs, a situation which is unusual in comparison to other modern reef localities. Another unusual feature of these reefs was that lithification generally increased with depth, away from the sediment-water interface. Macintyre (1977) explained this anomaly as the result of an area "where a poorly cemented surface overlies a section of the reef that had experienced a slow rate of [sediment] accumulation, or was exposed to high agitation during its formation."

Macintyre (1977) documented submarine cementation in a fringing reef at Galata Point, Panama. The most abundant cement consists of "dense submicrocrystalline" (<4 μm), microcrystalline (4-30 μm) or "porous submicrocrystalline" (<4 μm) magnesian calcite (15 to 19 mole percent $MgCO_3$) which coats or fills a variety of reef components. Aragonite is present, occurring as acicular or bladed crystals within primary cavities of corals. The data presented by Macintyre (1977)

suggests that cementation in modern reef environments occurs predominantly very near the sediment/rock-water interface and "is intensified by exposure of the reef-water interface to agitated normal marine water." An important result of this study was that the sediment accumulation rate, thought by many to be a limiting factor in marine cementation (see Shinn, 1969), was shown to be important only in regulating the length of time various parts of the reef were exposed to the agitated conditions ("near-surface conditions") "suitable for the precipitation of marine cement." Thus, Macintyre (1977) proposed that the distribution of marine cement in reef environments was controlled by two factors: (1) "the degree of agitation in various environments of deposition," and (2) sedimentation rates within each environment.

Marshall and Davies (1981) observed extensive submarine cementation on windward reef slopes of the Capricorn-Bunker Group at the southern end of the Great Barrier Reef. Fibrous aragonite (80 to 120 μm long and 10 μm wide) and bladed magnesian calcite (20 to 60 μm long and 5 to 20 μm wide) were present, most commonly as intraskeletal cement filling cavities in corals, and filling chambers in gastropods and foraminifera. Intrabiotic aragonite crystals generally grow syntaxially off the walls of corals. Bladed magnesian calcite cement generally forms isopachous rims within interparticle voids of corals and in some instances completely fills the voids. Microcrystalline magnesian calcite (1 to 6 μm in diameter) and magnesian calcite peloids (20 to 60 μm diameter) were shown to be the most abundant cement in this sediment, and the dominant interparticle void filling materials.

Bladed magnesian calcite cement is normally preceded by a magnesian calcite micrite crust (10 to 40 μm thick) forming a two phase cement which is strikingly similar to the two phase cement described by James et al. (1976) and James and Ginsburg (1979). Precipitation of cement was observed in the following sequence: (1) fibrous aragonite; (2) magnesian calcite micrite and peloids ; and (3) bladed magnesian calcite. This same sequence was shown to occur in the reef complexes of Belize (James et al., 1976) and of Panama (Macintyre, 1977).

Although marine cementation in modern reef environments has received a great deal of attention, there have been significant studies of marine cementation in other environments. Shinn (1969) described submarine hardgrounds in the Persian Gulf, where aragonite is the dominant cement in sand-sized sediment, occurring in two ("often gradational") forms: (1) "as loosely packed acicular needles perpendicular to grains," and (2) "as tightly packed fibrous cement." Magnesian calcite cement occurs as micrite or microcrystalline calcite primarily in lithified depositional aragonite muds. Shinn (1969) found that the degree of lithification in sand-sized sediment decreases with depth away from the sediment/rock-water interface, a phenomenon which produced 10-15 cm thick cemented crusts. These crusts are underlain by unlithified sediment. He attributed this to the proximity of sediment to the source of supersaturated sea water. The progressive lithification of the sediment at and just below the sediment-water interface was "thought to plug the pores to reduce water circulation, thus providing an automatic limit to the depth to which the process can penetrate."

The sedimentation rate was regarded as a limiting factor in cement formation because fast accumulation rapidly removes successive horizons from the zone of cementation. Other controls of cementation were thought to be the maintenance of normal temperature and salinity, sediment stability, and initially high sediment permeability.

Areas of modern marine cementation previously described have been characterized by low energy or "reduced tidal agitation and circulation" (Dravis, 1979). Dravis (1979) described submarine hardground formation in the high energy setting of the Schooner Cays tidal bar belt, Eleuthera Bank, Bahamas. He observed two types of lithified oolitic sediment: (1) "in situ surficial crusts" and (2) "unattached clasts (erosional crust fragments)." Previously, Ball (1967) had observed the penecontemporaneous cementation of this oolitic sediment by fibrous aragonite on Eleuthera Bank, but had not detailed cement distribution. Dravis (1979) determined that hardgrounds are forming in three ooid environments: (1) long, linear sand shoals oriented at an angle to the bank margin; (2) tidal channel floors, between sand shoals; and (3) large sand waves at the bank margin. All three of these environments are sites of active ooid formation and bottom agitation. Agitated conditions make these unusual environments for marine cement formation when compared with the studies described above.

Dravis (1979) recognized two cement types within ooid crusts. The dominant cement type is fibrous aragonite which develops as isopachous rim cement around each ooid. This cement begins as a "thin veneer 10-15 μm" in thickness surrounding grains. Continued growth of the

aragonite produces fibrous crystals up to 100 μm in length, "resulting in occlusion of much of the primary pore space." Magnesian calcite micrite cement was present generally as a second cementing phase overlying the fibrous aragonite.

Many carbonate petrographers believe that marine cementation in ancient carbonate sediment "is not a common or widespread" phenomenon (James and Choquette, 1983). In general, it appears to have been best developed in sediment deposited in ancient reef or mound environments, just as it is in modern reef environments. The similarity of occurrence in modern and ancient reefs has lead to the "uniformitarian" axiom that "as in present times, aragonite and magnesian calcite were the most common carbonates forming on shallow sea floors of the past" (James and Choquette, 1983). Recent studies have challenged that idea and at present, evidence suggests that the carbonate geochemistry of the world ocean system has changed throughout the Phanerozoic Era (Brand and Veizer, 1981; Popp et al., 1981; Mackenzie and Pigott, 1981; Pigott, 1981; Sandberg and Popp, 1981; Wilkinson, 1982; Sandberg 1983; Walker and Diehl, 1985). Further, evidence suggests that the changing ocean water chemistry resulted in the preferential precipitation of either aragonite and magnesian calcite or low-magnesian calcite at various times. The original models for these variations were linear, implying a one-time shift in atmospheric pCO_2 in early Cenozoic time (Sandberg, 1975) or in mid-Carboniferous time (Mackenzie and Pigott, 1981) which resulted in a change from conditions favoring the preferential precipitation of calcite to conditions favoring the precipitation

of aragonite and magnesian calcite. The linear models have been replaced by a nonlinear model which relates changing atmospheric pCO_2 to global sea level fluctuations (Vail et al., 1977) and global tectonics (see Fischer, 1981, 1983; Mackenzie and Pigott, 1981; Pigott,1981; Sandberg and Popp, 1981; and Sandberg, 1983).

Milliken and Pigott (1977) have coined the terms "calcite seas" and "aragonite seas" to differentiate times favoring precipitation of calcite from times favoring the precipitation of aragonite and magnesian calcite. Similarly, Fischer (1981) has coined the term "greenhouse" for periods of elevated atmospheric pCO_2 and the term "icehouse" for periods of reduced pCO_2. Greenhouse conditions are characterized by warmer earth temperatures, less continental glaciation and elevated global sea levels. Icehouse conditions are characterized by cooler earth temperatures, continental glaciation, and lower global sea levels. James and Choquette (1983) (Figure 3.1) and Sandberg (1983) (Figure 3.2) have summarized the data from Vail et al. (1977), Fischer (1981), Wilkinson (1982) and several other studies and were able to illustrate the relationships between the following, through the Phanerozoic Era:

1. "calcite" and "aragonite seas";
2. "greenhouse" and "icehouse modes" of atmospheric pCO_2;
3. fluctuations in global sea level;
4. carbon and oxygen isotopic composition of marine cement (James and Choquette, 1983); and
5. the incidence of granite emplacement (Sandberg, 1983).

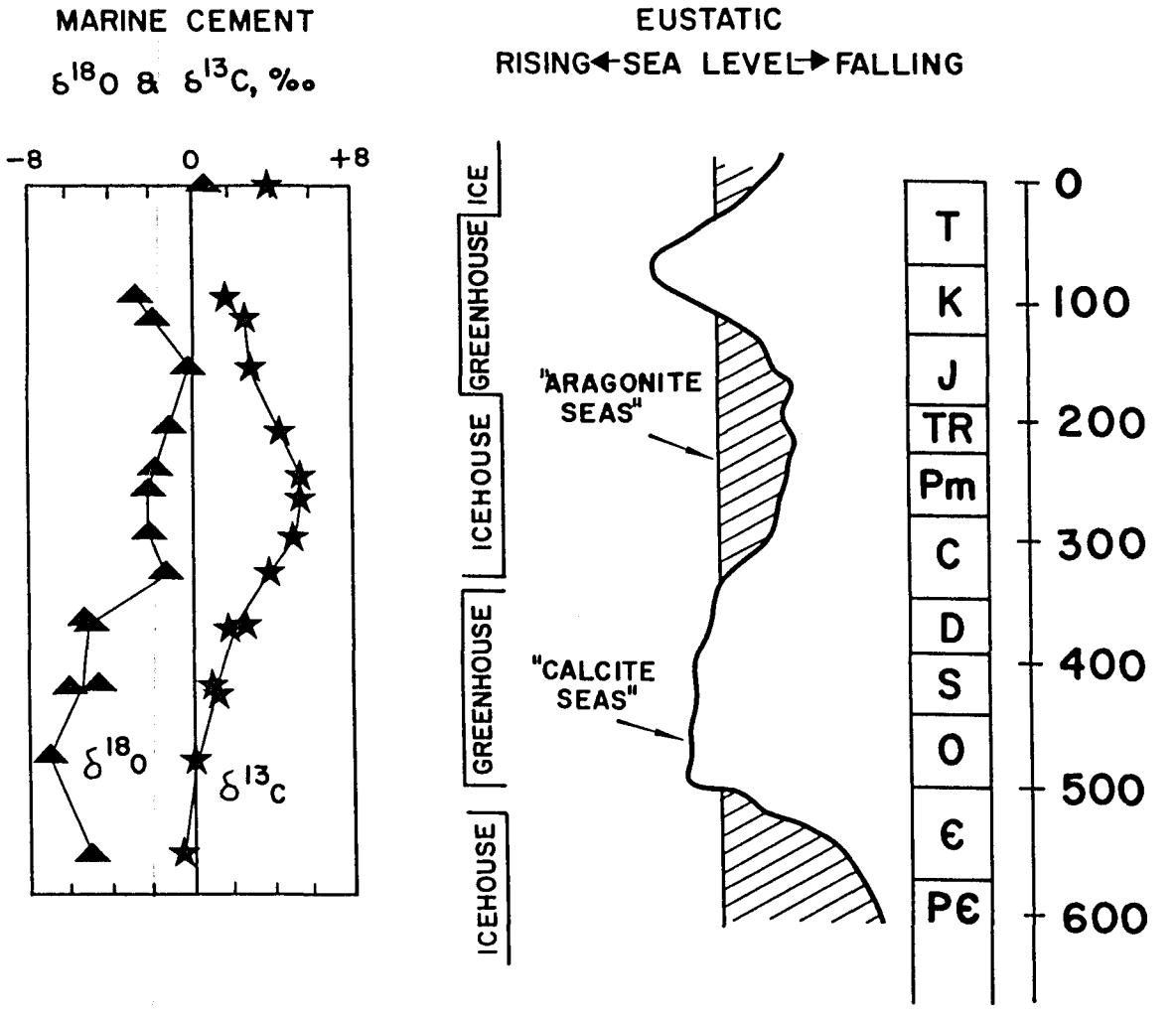


Figure 3.1. Comparison of theoretical cycles in nonskeletal carbonate mineralogy with sea level fluctuation, climatic episodes, and changes in the carbon and oxygen isotopic composition of marine cement through geologic time. Note the possible distribution of "calcite" and "aragonite seas." Data for this figure are published in James and Klappa (1983), Ross et al. (1975), Sears and Lucia (1980), Mattes and Mountjoy (1980), Walls et al. (1979), Meyers and Lohmann (1985), Lohmann (in press), Davies and Krouse (1975), Given and Lohmann (1985, 1986), Marshall and Ashton (1980), Moldovanyi and Lohmann (1982), and James and Ginsburg (1979). (From James and Choquette, 1983).

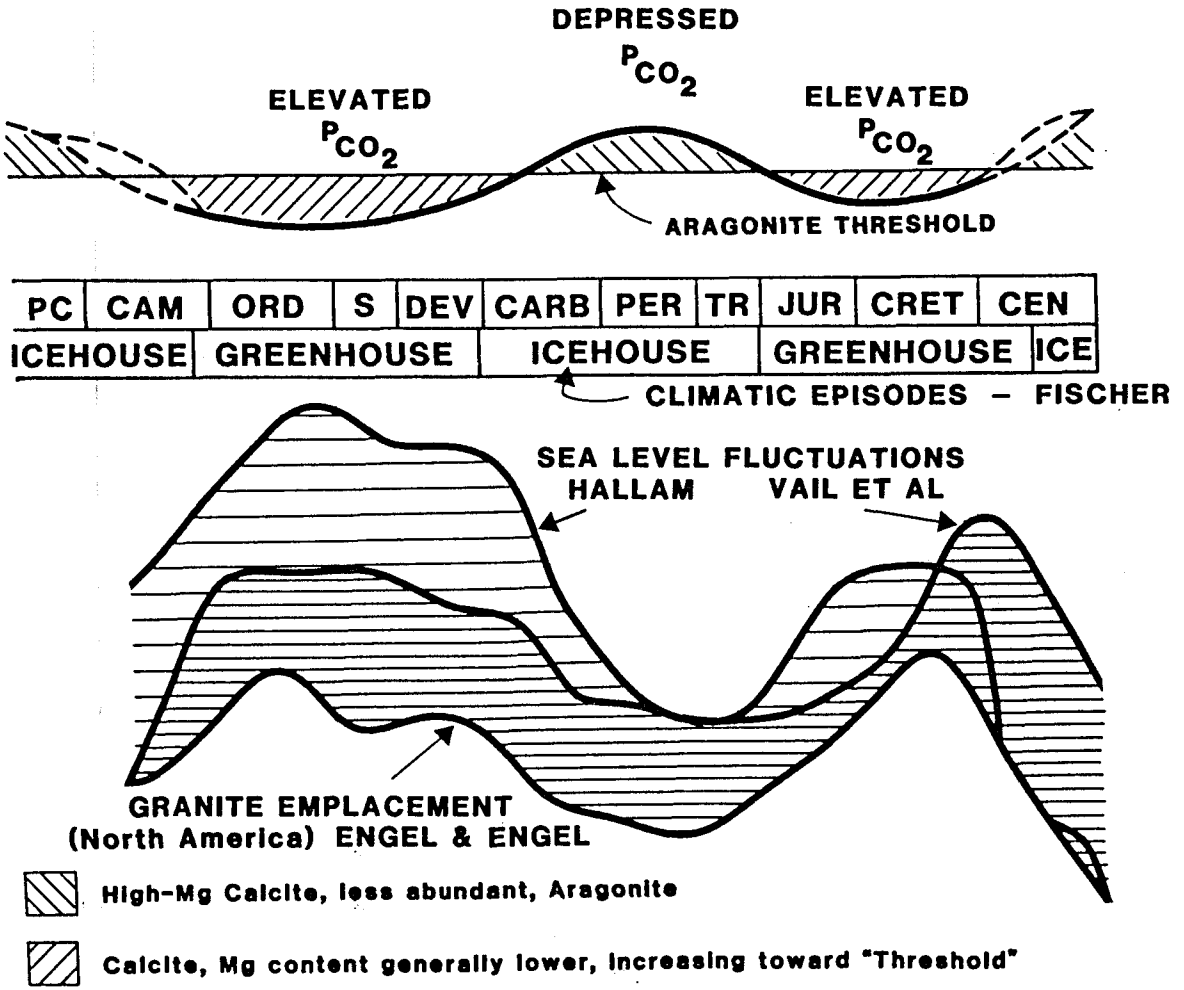


Figure 3.2. Theoretical first-order "cycles" in nonskeletal carbonate mineralogy through geologic time as compared with changes in sea-level, granite emplacement, and climatic episodes. (After Sandberg, 1983).

The nonlinear model of changing ocean-water chemistry is, at this time, essentially a hypothesis. Much more data are needed to support the range of implications set forth in the model. At present, many researchers feel that stable isotopic analysis is the best delineator of marine cement in ancient limestones. Others commonly rely on petrographic analysis of cement textures and fabrics to distinguish marine from meteoric cement. This method is particularly effective for "fibrous" cement which has been shown by other means to be mainly of marine origin (James and Choquette, 1983). The best method for distinguishing marine cement, however, would involve using isotope (carbon and oxygen) and trace element data (strontium, magnesium, sodium and manganese) with data derived from petrographic analysis.

Studies using the methods described above are common in the geologic literature so that submarine cementation in ancient carbonate sediment is becoming increasingly well documented. Since the first detailed studies in the late 1960s, marine carbonate cement has been described in rocks from the entire Phanerozoic. Purser (1969) observed marine cement in Middle Jurassic limestone of the Paris Basin. The dominant cement in the rocks he studied consisted of short, isopachous calcite crystals developed around most sediment grains. This isopachous cement was in contact with adjacent crystals through most of its length. Nonisopachous, loosely packed fibrous cement was rarely observed in these rocks. These crystals were generally not in contact with adjacent crystals, except near their bases. Individual crystals were acicular in habit and were generally much longer than the

isopachous cement crystals. Purser (1969) compared the nonisopachous, acicular to fibrous cement to Recent acicular aragonite cement from the Persian Gulf (Shinn, 1969). Syntaxial cement on echinoderm grains was interpreted as syndepositional cement because it was locally truncated by marine borings. The controversy over the origin of syntaxial cement on echinoderm grains will be discussed later in this chapter.

Davies (1977) has recognized extensive marine cementation in Middle Pennsylvanian bryozoan reefs and Pennsylvanian to Lower Permian shelf edge carbonates of the Canadian Arctic. These rocks were exposed on the northwestern side of Ellesmere Island in the Canadian Arctic Archipelago. Davies (1977) recognized two primary marine cement groups. The first and most abundant cement type consisted of radiaxial-fibrous calcite (Bathurst, 1959; Kendall and Tucker, 1973) and radial-fibrous forms of calcite. These cement types (or unstable precursor cement) were interpreted to be of marine origin based on the following five lines of evidence:

1. The cement occurred as the first cement on sedimentary grains;

2. The cement was isopachous within primary pores, showing no evidence of vadose diagenetic fabrics;

3. The cement was commonly incrusted by marine organisms;

4. The cement predated or alternated with marine internal sediment;

5. The cement exhibited a mean enrichment in the heavy carbon isotope, C^{13}, of +5.4 ± 0.8 per mil (relative to Chicago PDB).

Davies (1977) proposed that the radiaxial-fibrous and radial-fibrous cement was neomorphic after an original fibrous magnesian calcite precursor. Several lines of evidence supported his proposal. First, the radiaxial- and radial-fibrous crystals retained what Davies (1977) termed a "relict" fibrous to acicular microfabric. Second, these cement types exhibited elevated levels of magnesium (averaging 1.6 ± 0.24 mole percent $MgCO_3$) similar to levels detected in echinoderms (averaging 1.5 mole percent $MgCO_3$) which were probably originally magnesian calcite. Also, radiaxial and associated cement contained microdolomite inclusions (up to 5 μm in length) which have been described from crinoidal calcite elsewhere (Macqueen and Ghent, 1970; also see Meyers and Lohmann, 1978). The microdolomite inclusions were thought to have formed by exsolution during early diagenesis of magnesian calcite. Finally, aragonite was precluded as the mineralogy of the precursor cement because of the absence of solution-moldic replacement of the cement and the low (usually undetectable with an electron microprobe) strontium content of the fibrous crystals.

Davies' second variety of cement consisted of second generation botryoidal calcite. He interpreted this cement as marine in origin because it is: (1) interlaminated with fibrous marine cement and internal marine sediment, and (2) enriched in C^{13} by +5.7 ± 0.8 per mil (relative to PDB standard). This cement is substantially enriched in strontium (average of 7500 ± 1250 ppm) suggesting an aragonite precursor, and some botryoids show "pseudomorphs" of aragonite (tapered

crystal with blunt terminations). The botryoids also showed evidence of extensive solution, which also suggests originally unstable mineralogy.

Mazzullo and Cys (1979) described the occurrence of calcified aragonite botryoidal cement in Permian phylloid algal mounds of New Mexico. They suggested that the calcification process was a multistage phenomenon. The initially developed calcite crystals were believed to exhibit relicts of precursor fibrous aragonite crystals. If taken to completion, they proposed that the process would obliterate all relict structure of the original aragonite fibers and form large replacement crystals. Elemental analysis of the calcified botryoids showed elevated concentrations of strontium and relatively low concentrations of $MgCO_3$ suggesting that the precursor cement was in fact aragonitic.

Sandberg (1985), based on reinterpretation of samples from the study of Mazzullo and Cys (1979) showing relict aragonite in the replacement crystals, suggested that the process of replacement involved a "single-step." He also noted that high strontium concentrations would not be expected in cement subjected to repeated diagenetic alteration.

Radiaxial-Fibrous Calcite and Associated Cement

The dominant marine cement in the Holston and Rockdell formations in northeastern Tennessee is radiaxial-fibrous calcite. Bathurst (1959) originally defined the radiaxial-fibrous fabric from Carboniferous knoll-reefs of Lancashire, England. This cement fabric is common

throughout the Phanerozoic "in depositional and early diagenetic cavities in many reef biolithites, mud-mound complexes (Lees, 1964) and their associated skeletal and nonskeletal calcarenites and calcirudites" (Kendall and Tucker, 1973). Radiaxial-fibrous calcite is characterized by the occurrence of the following in each crystal:

1. Preferential elongation of the long crystallographic axis normal to the substrate;

2. Subcrystals which diverge away from the substrate (Figure 3.3A);

3. Optic axes which converge away from the substrate (recognized by an extinction shadow which sweeps in the opposite direction of microscope stage rotation) (Figure 3.3A);

4. Curved twin lamellae which are concave up (away from the substrate) (Figure 3.3A);

5. Nonplanar intercrystalline boundaries (Figure 3.3A); and

6. Inclusions which cause crystals to appear turbid (Bathurst, 1959, 1975; Kendall and Tucker 1971, 1973; Kendall, 1977, 1985).

Associated with the radiaxial-fibrous calcite in the Holston and Rockdell formations are two related cement fabrics: (1) fascicular-optic calcite (Kendall, 1977) (Figure 3.3B); and (2) radial-fibrous calcite (Davies, 1977; Mazzullo, 1980; Kendall, 1985) (Figure 3.3C). Fascicular-optic calcite cement is similar to radiaxial-fibrous calcite in that single crystals of both cement fabrics consist of several subcrystals. The major difference between these two cement fabrics is that within each fascicular-optic crystal, the optic axes diverge away

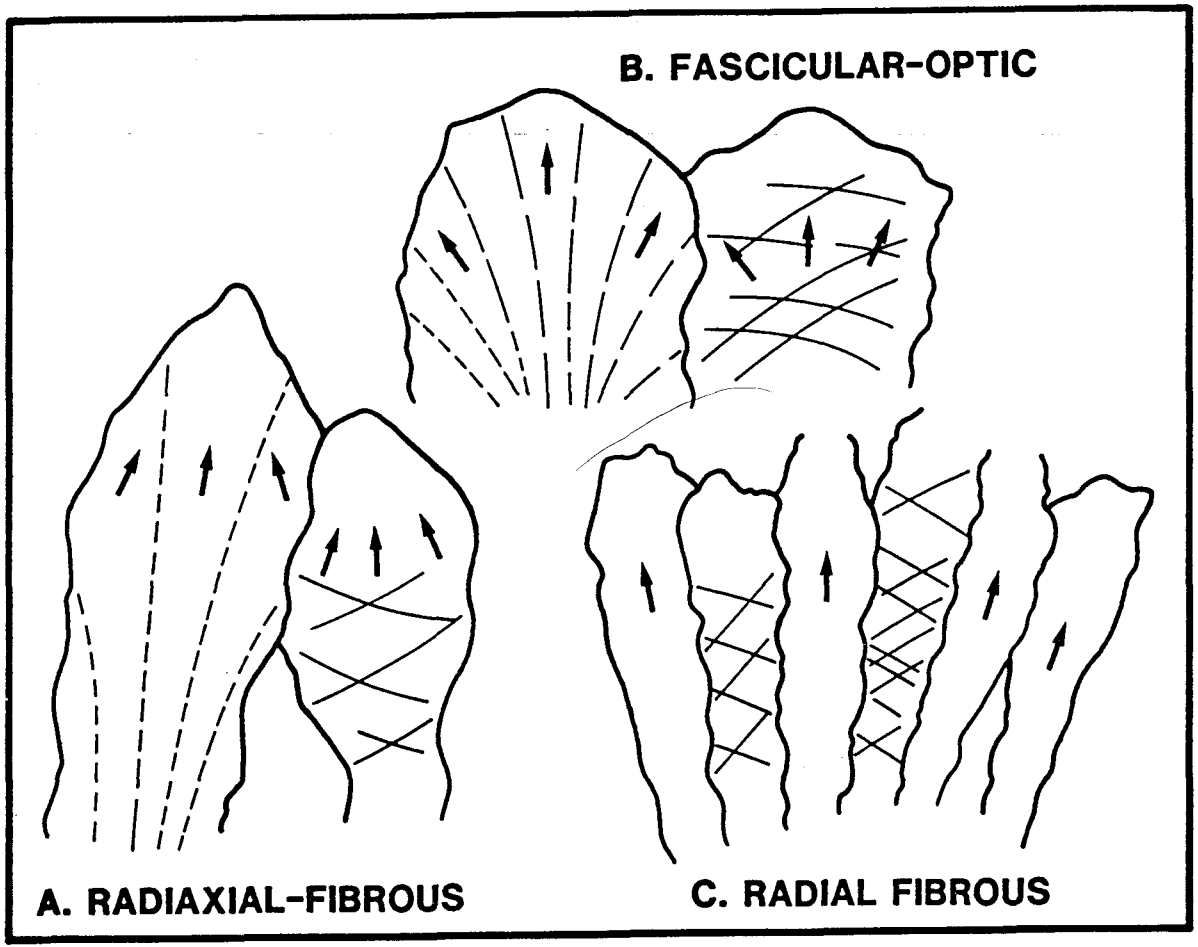


Figure 3.3. Petrographic and optical properties of: A. Radiaxial-fibrous calcite; B. Fascicular-optic calcite; and C. Radial fibrous calcite. Dashed lines represent subcrystal boundaries. Solid lines within crystals represent twin patterns. Arrows represent optic axes orientations. (After Kendall, 1985).

from the substrate (Kendall, 1977, 1985). The divergence of the "fast vibration directions" away from the substrate in fascicular-optic calcite results in curved twin lamellae which are convex up (away from the substrate). Thus, extinction in fascicular-optic crystals sweeps in the direction of stage rotation.

Radial-fibrous cement is distinguished from radiaxial-fibrous and fascicular-optic calcite by the absence of subcrystals. Also, twin lamellae are characteristically straight. In general, this cement exhibits no "marked undulose extinction" (Kendall, 1985).

There has been considerable controversy concerning radiaxial-fibrous calcite and related cement fabrics. As summarized by Kendall and Tucker (1973), early carbonate researchers interpreted the radiaxial fabric as "reef-tufa," a precipitate formed by evaporation of sea water (Dixon, 1921; Hudson, 1933; Parkinson, 1935; and Bond, 1950); as a replacement of fine-grained carbonate sediment (Black, 1952; Orme and Brown, 1963); as void-filling (primary) cement (Sander, 1951; Bathurst, 1959; Schwarzacher, 1961; Lees, 1964; Garrison, 1972); and as a replacement after a void-filling cement (Newell, 1955; Cotter, 1966; Zankl, 1971; Kendall and Tucker, 1971, 1973). The idea that radiaxial-fibrous calcite and associated cement were replacement fabrics after acicular primary cement quickly gained wide acceptance in the literature (see Kendall and Tucker, 1971, 1973; Kendall, 1977). Similarly, when fascicular-optic calcite was originally described by Kendall (1977), it was alleged to be a replacement fabric after bundled acicular cement

primarily because it occurred in the same cavities as radiaxial-fibrous calcite.

Kendall and Tucker (1973) noted several characteristics in radiaxial-fibrous calcite which suggested a primary cement origin. These characteristics included: (1) its occurrence in "depositional or early diagenetic cavities"; (2) it predates and alternates with internal marine sediment; (3) elongation of crystals normal to cavity walls; (4) a general increase in crystal size away from the substrate; and (5) presence of all criteria used to recognize cement (see Bathurst, 1971, 1975). They, however, rejected a primary origin for radiaxial-fibrous fabrics based primarily on the presence of nonplanar intercrystalline boundaries (or absence of compromise boundaries; see Buckley, 1951; Bathurst, 1975), the undulose extinction pattern of the cement crystals, and the presence of inclusions which impart a turbid and often pseudopleochroic appearance to the crystals (see Hudson, 1962).

Friedman (1964) coined the term "paramorphic replacement" to describe a process by which aragonite could be replaced by calcite "on a microscale with an intervening solution-redeposition phase" (Kendall, 1985). The process was envisioned to occur without the creation of moldic pore space and resulted in the transfer of the original cement fabric to the new crystal. Kendall and Tucker (1973) envisioned a similar process for the formation of the radiaxial-fibrous cement fabric. They proposed that a fluid film migrated from cavity walls toward the center of cavities, dissolving the acicular host crystals at the

leading edge and precipitating "a stable mineral phase (low Mg-calcite)" at the trailing edge. In their model, replacement occurred most rapidly between bundles of acicular crystals, creating composite calcite crystals which represent "parts of adjacent acicular groups (where the acicular crystals incline toward each other)." A process which they termed "crystallographic transference" allowed the replacement calcite crystals to retain the c-axes orientations of the acicular precursor crystals. Crystallographic transference then, was proposed as the cause of the curved crystal lattice and distinctive sweeping extinction pattern in radiaxial fabrics. Kendall (1977) observed lateral transitions between radiaxial-fibrous and fascicular-optic cement within cavities between pillow lavas in the Crescent Formation (Eocene) of Washington. Based on their similar fabric and occurrence, Kendall (1977) proposed a similar replacement origin for fascicular-optic calcite.

Sandberg (1985) has questioned the conclusions of Kendall and Tucker (1971, 1973) and Kendall (1977). Based on his observations of the preservation of skeletal (Sandberg, 1975a), ooid and other nonskeletal aragonite (Sandberg, 1975b), he concluded that had the original mineralogy of radiaxial-fibrous and associated cement been aragonite, then the replacement process, however small the scale, would have created "distinctive, disruptive textures." He contended that the idea of "pseudomorphic alteration or paramorphic replacement," as used by most carbonate researchers, implies "the duplication of fine crystal morphology at the ultrastructure level." The geologic record does not support

such a process. Citing studies which documented the calcification process occurring along "diagenetic fronts" (Purdy, 1969; Sandberg et al., 1973; James, 1974; Tebbutt, 1975; Pingitore, 1976; and Sandberg and Hudson, 1983), he noted that in all cases, extensive textural disruption was observed.

Sandberg (1985) believed that radiaxial-fibrous and fascicular-optic calcite represented primary pore filling cement. He observed radiaxial-fibrous calcite and fascicular-optic calcite together as cement fringes on fossil skeletal grains in "scarcely altered" Pleistocene limestone from Japan. In those rocks, the cement occurred as interbiotic cement (between aragonite and calcite skeletal grains) and within "primary pores of still aragonitic corals." The lateral gradation from radiaxial-fibrous to fascicular-optic calcite suggested that both fabrics have the same origin. On corals, locally a first stage epitaxial aragonitic cement was overlain by a fine-grained "dentate calcite cement" and then by radiaxial-fibrous/ fascicular-optic fringe cement. Sandberg (1985) concluded that it was unreasonable to postulate an alteration to produce radiaxial-fibrous and fascicular-optic calcite that would simultaneously leave the adjacent first generation aragonite cement and aragonite skeletons untouched. Thus, he proposed that the fabrics are primary. He reserved an opinion as to the environment of formation of the cement pending analysis of carbon and oxygen isotopes. However, oxygen isotope data of Hudson and Coleman (1978) and Walls et al. (1979) were cited as evidence supporting a marine origin of the cement fabrics.

Kendall (1985) has also reevaluated the work of Kendall and Tucker (1971, 1973). The replacement hypothesis, proposed by Kendall and Tucker (1973), was thought to be unsupportable based on two lines of evidence. First, often in depositional or early diagenetic cavities, radiaxial-fibrous calcite is interbedded with internal marine cement. In many cases, crystal terminations,defined by an internal sediment layer overlying radiaxial cement, were preserved suggesting that if replacement of a precursor cement occurred, it had to take place prior to the deposition of the overlying sediment layer. Second, Kendall (1985) noted that replacement crystals formed by the mechanism proposed by Kendall and Tucker (1973) should exhibit little lattice curvature toward their distal ends since, at their distal ends, "laterally interfering bundles" of acicular crystals are generally parallel. Radiaxial crystals characteristically exhibit lattice curvature (evidenced by curved twin lamellae) throughout their length.

Kendall (1985) now suggests that radiaxial-fibrous and related cement fabrics are primary calcite cement types which are precipitated as magnesian calcite or as low-magnesian calcite. He proposed a marine origin based on their occurrence in sediment which was deposited in environments where the influence of "nonmarine" fluids can be precluded: as fill material in neptunian sills in Upper Devonian rocks of the Canning Basin, Western Australia. The characteristic features of radiaxial-fibrous calcite such as composite crystals, convergent optic axes and subcrystals which diverge away from the substrate are reinterpreated as the end result of "asymmetric growth within calcite crystals

undergoing split-growth." Asymmetric growth of the "split-crystal aggregate" causes adjacent subcrystals to be deflected toward slower growing subcrystals creating lattice curvature and sweeping extinction.

In the Holston and Rockdell formations, radiaxial-fibrous calcite accounts for over 90 percent of the fibrous cement phases. Where it occurs in grain-supported rocks, this cement is isopachous, lining both intra- and interparticle pore spaces. In mud-supported lithologies, it occurs in depositional and early diagenetic (stromatactoid) cavities. Crystals are elongate normal to their substrate, and individual crystals commonly become wider at their distal ends (averaging 2 to 3 times as wide). The length:width ratio of radiaxial-fibrous and fascicular-optic cement may be as high as 12:1 but averages 6:1 to 8:1. Intercrystalline boundaries are characteristically nonplanar. Radiaxial-fibrous and associated cement are preferentially developed on polycrystalline substrates such as micrite (Figure 3.4A), bryozoans (Figure 3.4B), and intraclasts (Figure 3.4C). Rarely, they may occur on monocrystalline substrates such as turbid, syntaxial cement.

Radiaxial-fibrous and fascicular-optic calcite cement are characterized by compound crystals. Extinction between subcrystals generally varies between 2° and 10°. These cement types are always turbid with inclusions. Inclusion density is generally uniform, but rarely (in stromatactoid cavities), inclusions may define distinct growth zones forming banded cement crystals (Figure 3.4D, E). Etched thin-sections reveal that some inclusions have a rhombohedral outline suggesting that they are dolomite. Rarely, inclusions appear to be elongate parallel

Petrographic features of radiaxial-fibrous calcite and associated cements of the Holston and Rockdell Formations.

A. Plane light photomicrograph showing the variety of polycrystalline grains which act as host for radiaxial-fibrous and associated cements, in this case, internal marine sediment and a bryozoan. In this example, radiaxial-fibrous calcite occurs both prior to and after deposition of internal sediment. Bar scale is approximately 1.0 mm. Poor Valley Creek. (PVC'2D).

B. Crossed-nichol photomicrograph showing a bryozoan acting as substrate for radiaxial-fibrous calcite cement. In this example, the bryozoan is totally encased in cement. Bar scale is approximately 1.0 mm. Poor Valley Creek. (PVC'1B2L).

C. Photomicrograph in plane light showing an intraclast (left) acting as substrate for the development of radiaxial-fibrous calcite cement. At right, note fibrous cement also growing from depositional micrite. Bar scale is approximately 1.0 mm. Red House Branch. (RHB'6BBR).

D. Photomicrograph in plane light showing radiaxial-fibrous calcite cement growing within a stromatactoid cavity in the Holston Formation. The cement has nucleated on peloidal internal sediment flooring the cavity and also the cavity roof. Inclusion density in these cement crystals is nonuniform, creating distinct growth bands. Bar scale is approximately 1.0 mm. Red House Branch. (RHB'2K).

E. Close-up photomicrograph of the prominent banded fibrous cement crystal growing from the roof of the stromatactoid cavity in Figure 3.4D. The inclusion bands are also present in the smaller crystal to the right. The medial growth boundary, created by the intersection of crystals growing from the roof and floor of the cavity, is visible below the large banded crystal. Bar scale is approximately 0.25 mm. Red House Branch. (RHB'2K).

F. Photomicrograph in plane light showing a large stromatactoid cavity in the Holston Formation with radiaxial-fibrous calcite cement crystals interlayered with internal marine sediment. Both the cavity floor and internal sediment layers have acted as substrates for fibrous cement development. Note that the second layer of radiaxial-fibrous cement crystals exhibit distinct inclusion banding. This example clearly illustrates the results of an intermittent process of cement growth. Bar scale is approximately 1.0 mm. Red House Branch. (RHB'2K).

Figure 3.4 (continued).

G. Photomicrograph in plane light showing radiaxial-fibrous calcite cement interlayered with peloidal internal sediment in a large shelter void. This example illustrates that fibrous cement formation was an intermittent process. Fibrous cement is developed on the skeletal grain which created the void, the micritic portion of the roof, and the peloidal internal sediment. Bar scale is approximately 1.0 mm. Red House Branch. (RHB'2A).

H. Plane light photomicrograph of a large stromatactoid cavity in the Holston Formation showing an articulated ostracode engulfed in radiaxial-fibrous calcite cement. The ostracode appears to be "floating" in cement (see Figures 2.2F, G, p. 28, for a similar example). Bar scale is approximately 1.0 mm. Red House Branch. (RHB'2K).

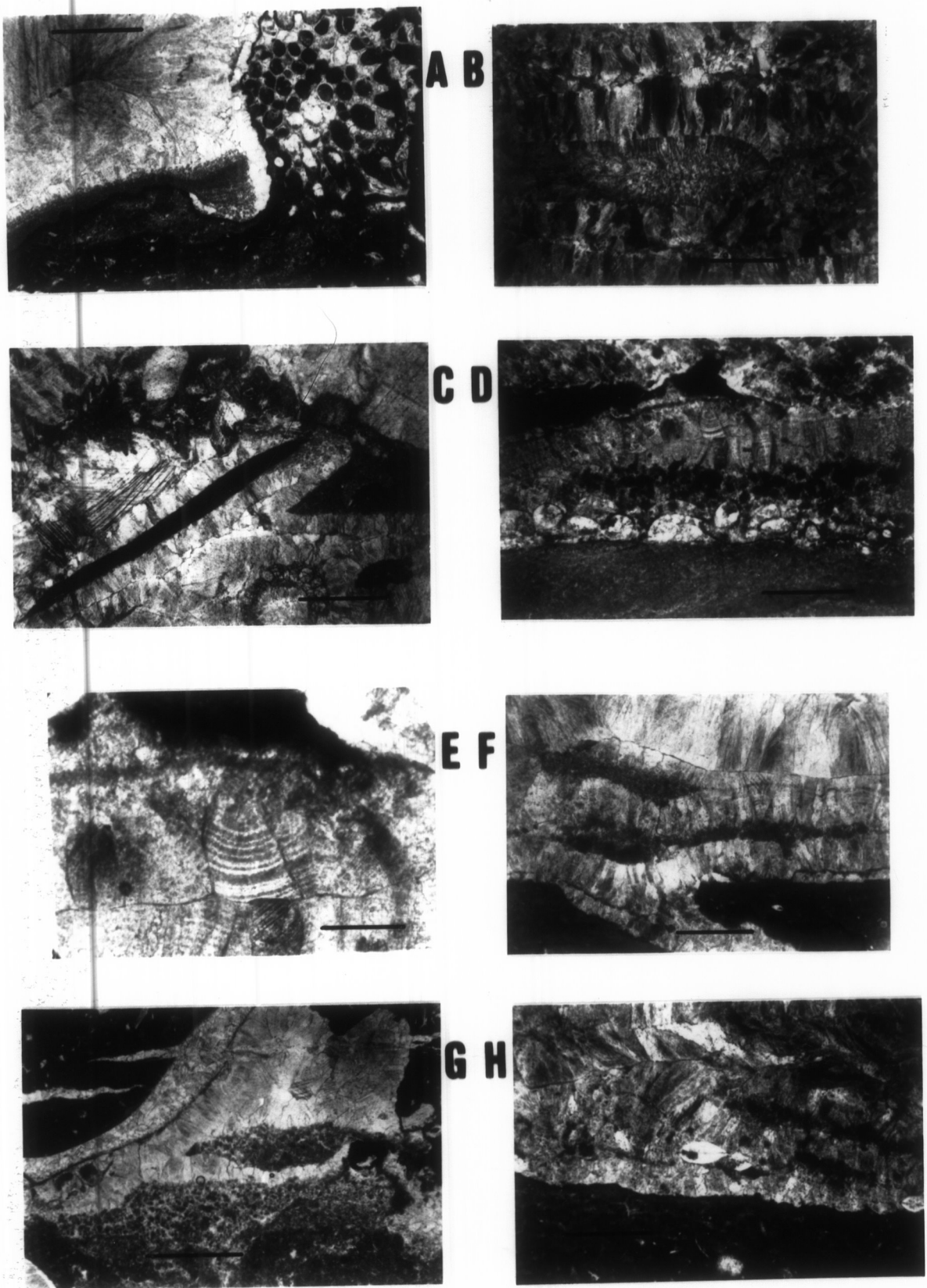

A B
C D
E F
G H

Figure 3.4
84
Jernigan, 1987

to the extinction pattern of individual crystal "fibers" similar to the inclusions observed by Kendall (1985). Other inclusions may be fluid filled although small size and irregular shape made them difficult to resolve with a petrographic microscope.

In mud-supported lithologies, radiaxial-fibrous calcite and associated cement predate and postdate deposition of internal marine sediment (Figure 3.4F, G). In some stromatactoid cavities, fossil material (particularly ostracodes, bryozoans, and trilobites) has been swept into the cavities and engulfed by later cement growth creating what appears to be "floating" fossil fragments (Figure 3.4H) (see also Black, 1952; Bathurst, 1959; Ginsburg and James, 1976; and Ruppel, 1979). In some instances, it is evident that the fossil material was sitting on a flat surface created by an initial isopachous cement cavity lining and was later engulfed by further cement growth (see Figure 2.2F, G; p. 28).

Where radiaxial-fibrous and associated cement are developed, they typically represent the first generation of carbonate cement. In some stromatactoid cavities, however, the radiaxial-fibrous cement is predated by what I have interpreted as an initial micrite cement phase (Figure 3.5A). In most cavities, radiaxial-fibrous or fascicular-optic calcite is developed both on the floor and roof of the cavity and grows toward the center of the void. Commonly, these two cement types meet in the center of the cavity and form a medial line of interference (Figure 3.5B). Crystal terminations are not developed at these interference boundaries, indicating that the cement was growing at the same

Figure 3.5. Petrographic features of radiaxial-fibrous calcite and associated cement and bladed/prismatic cement in the Holston and Rockdell Formations.

A. Photomicrograph of a complex stromatactoid cavity showing two distinct layers of micrite cement lining the floor and walls of the cavity. Note the anti-gravitational nature of the micrite cement in this example. Radiaxial-fibrous calcite cement alternates with micrite cement in this example. Bar scale is approximately 1.0 mm. Poor Valley Creek. (PVC'2D).

B. Photomicrograph under crossed-nichols showing a median growth boundary created by radiaxial-fibrous calcite cement crystals growing toward the center of a stromatactoid cavity. Distal ends of cement crystals are flat indicating growth interference. Bar scale is approximately 1.0 mm. Red House Branch. (RHB'8H).

C. Photomicrograph of rare crystal terminations in radiaxial-fibrous calcite cement. These pointed crystal terminations are distinctly inclusion-free. Overlying the radiaxial-fibrous crystals is Fe-calcite cement which is stained with potassium ferricyanide. Bar scale is approximately 0.25 mm. Poor Valley Creek. (PVC'2G).

D. Photomicrograph of "stubby," bladed cement crystals growing from a trilobite fragment. Although not apparent in plane light, these cement crystals are syntaxial with the host trilobite. Bar scale is approximately 0.25 mm. Red House Branch. (RHB'3DS1).

E. Photomicrograph under crossed-nichols of elongate bladed cement crystals growing on a brachiopod fragment. Cement crystals are syntaxial with the host brachiopod grain. Note that some crystals appear club-shaped. Bar scale is approximately 0.25 mm. Red House Branch. (RHB'4AS2BL).

F. Photomicrograph of elongate, "club-shaped," bladed cement under crossed-nichols. These crystals are 2-3 times wider at the distal ends than at their bases. Bar scale is approximately 1.0 mm. Red House Branch. (RHB'2GBL).

G. Photomicrograph of "two-stage" bladed cement crystals growing from the roof of a cavity. The first stage if represented by an inclusion-rich (turbid) phase while the second stage is inclusion-free (clear). The cement below the median interference boundary is radiaxial-fibrous calcite. Bar scale is approximately 0.25 mm. Red House Branch. (RHB'4AS1R).

Figure 3.5 (continued).

H. Photomicrograph of the same "two-stage" bladed cement under crossed-nichols. Note that the large, extinct crystal on the right is distinctly "club-shaped." Bar scale is approximately 0.25 mm. Red House Branch. (RHB'4AS1R).

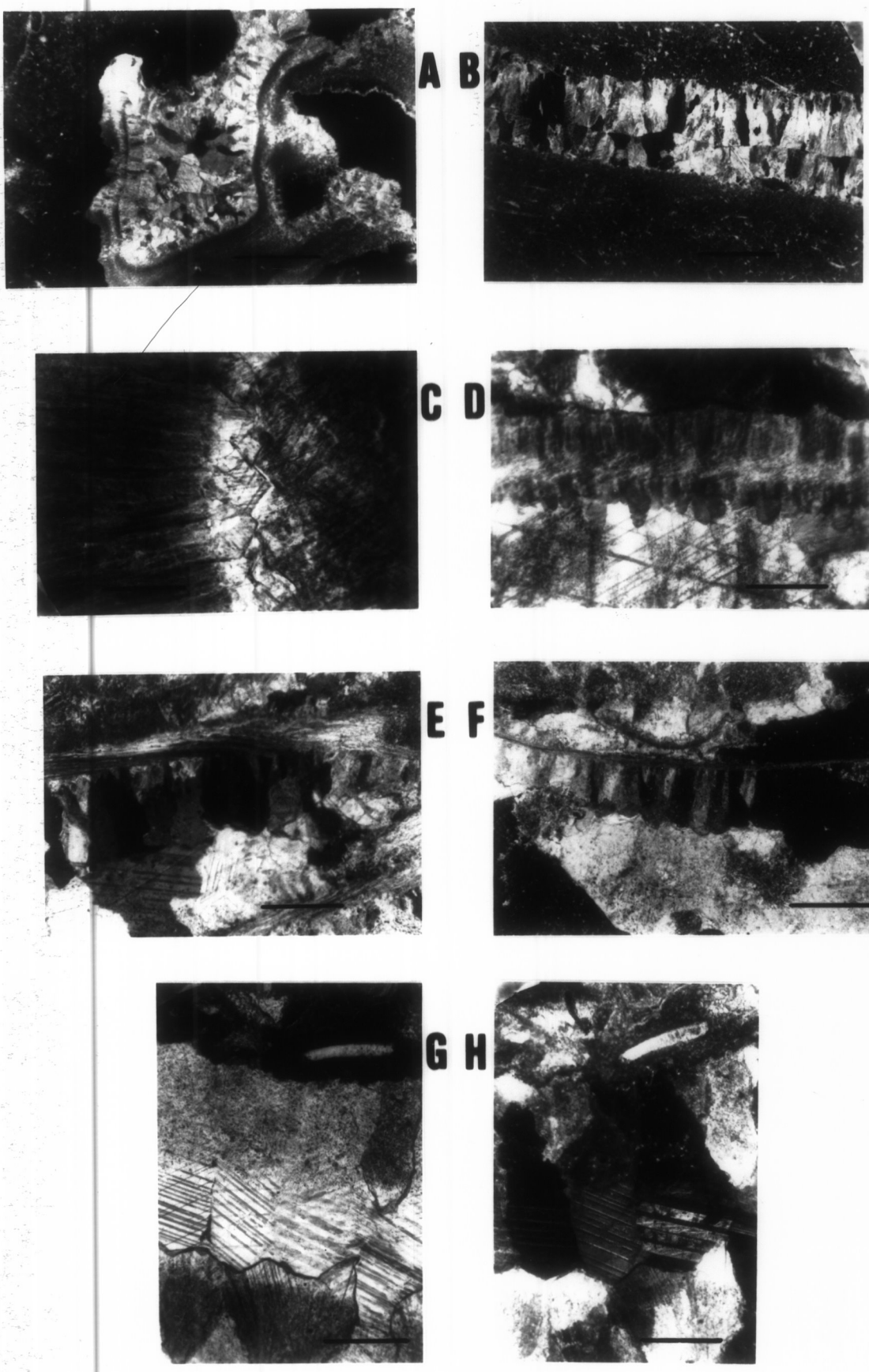

A
B
C
D
E
F
G
H

Figure 3.5
88
Jernigan, 1987

time and interfered with each other at their distal ends. In such cases, the distal ends of the radiaxial crystals are flat. Crystal terminations are typically developed only where radiaxial-fibrous or fascicular-optic calcite cement is overlain by a second generation cement phase (equant calcite or Fe-calcite) (Figure 3.5C). In these cases, the fibrous cement grew to completion forming pointed, inclusion poor crystal terminations.

Composition of Radiaxial-fibrous Calcite. The concentrations of strontium, magnesium and manganese in radiaxial-fibrous cement from the Holston and Rockdell formations averaged 239 ppm Sr, 2193 ppm Mg (0.90 mole percent $MgCO_3$) and 142 ppm Mn (Table 3.2). Strontium and magnesium concentration data from this cement type is compared to similar data for ancient "fibrous" carbonate cement from the geologic literature in Figure 3.6. Strontium values for radiaxial-fibrous calcite in the Holston and Rockdell formations fall well below the average strontium concentrations from cement interpreted as calcitized fibrous aragonite cement while the magnesium concentrations are much higher (Mazzullo, 1980). Magnesium concentrations fall well into the range of values of fibrous cement interpreted as "stabilized," originally magnesian calcite (Davies, 1977; James and Klappa, 1983; Prezbindowski, 1985). Thus, the strontium and magnesium concentrations in Holston and Rockdell radiaxial-fibrous calcite cement suggests that it was originally magnesian calcite.

The concentration of manganese in radiaxial-fibrous calcite ranged from 93 ppm to 249 ppm and averaged 142 ppm (Table 3.2). These values

Table 3.2. Trace element composition of radiaxial-fibrous calcite cement from selected samples from the Holston and Rockdell Formations. Duplicate analyses are noted in parentheses. Sample RHB'2H and RHB'8H are both stromatactis samples.

Sample No.	Sr (ppm)	Mg (ppm)	mole% $MgCO_3$	Mn (ppm)
RHB'2J	230	2640	1.09	100 (157)
RHB'2H	250	3760	1.55	124
RHB'8H	256	2670	1.10	93
PVC'2A (Proximal)	289	2670	1.10	226
PVC'2A (Distal)	180	1800	0.74	140
PVC'2F	280	1500	0.62	100
PVC'2G	200	1500	0.62	104
PVC'2J	230	1750	0.72	249 (225)
PVC'2K	240	1450	0.60	143
Average	239	2193	0.90	142

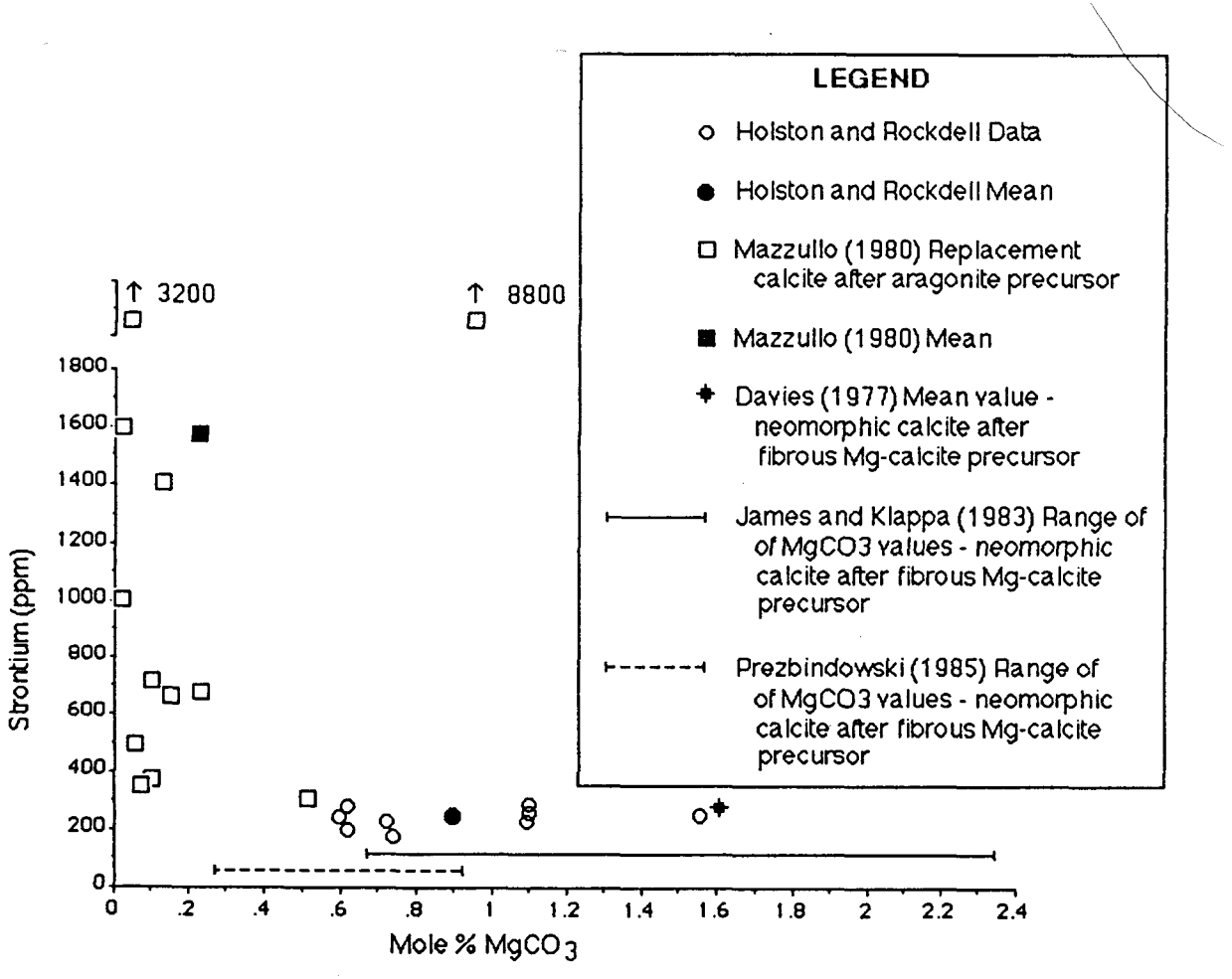


Figure 3.6. Strontium and magnesium carbonate composition of selected fibrous cement from the Holston and Rockdell formations as compared to published data for similar ancient fibrous cement.

are high relative to the manganese concentration in modern sea water (0.002 ppm; Horne, 1969) and the manganese concentration in calcite precipitated in equilibrium with modern sea water (2-5 ppm; Arnseth, personal communication). Since manganese is readily oxidized on exposure to air, it is unlikely that the average concentration would have been much greater in the marine fluids which were responsible for the precipitation of radiaxial-fibrous calcite in the Holston and Rockdell formations. However, the factors which controlled the concentration of manganese in this cement type were not established in this study.

Interpretation. Based on several lines of evidence, radiaxial-fibrous and associated cement are interpreted as syndepositional marine in origin. First, these cement types are commonly interlayered with internal marine sediment indicating a "stop-and-go" process of cement growth in the marine environment. Second, these cement types usually occur as the first cement phase, always predating equant calcite and ferroan calcite, indicating that they were precipitated early in the overall paragenetic sequence of cement and in the diagenetic history of the sediment. Third, trace element data suggests that the original mineralogy of the cement was magnesian calcite which is the dominant modern marine cement mineralogy (Bricker, 1971; Flugel, 1982). Magnesium calcite does not precipitate in the freshwater phreatic diagenetic environment. A magnesian calcite precursor is also suggested by the presence of microdolomite inclusions within fibrous cement crystals. Lohmann and Meyers (1977) suggested that microdolomite inclusions form as a result of solid-state exsolution or incongruent dissolution of

precursor magnesian calcite crystals. Thus, the presence of microdolomite inclusions in cloudy calcite is primary "evidence for a high-Mg calcite precursor, and, therefore, for a marine precipitational environment." Finally, the fabric of radiaxial-fibrous and fascicular-optic calcite cement in the Holston and Rockdell formations is identical to other examples in the geologic literature which have similarly been described as marine in origin (Davies, 1977; Kendall and Tucker, 1971, 1973; Kendall, 1977,1985).

Bladed/Prismatic Cement

Bladed cement is characterized by length:width ratios of 1.5:1 to 6:1 (Folk, 1965). This cement has elsewhere been termed "prismatic" cement (see James and Klappa, 1983). Although cement with this texture has been recognized in both modern (see James et al. 1976; and compare with the "short, closely packed, fibrous druse" cement of Purser, 1969) and ancient carbonate sediment (see Meyers, 1978; Marshall and Ashton, 1980; and James and Klappa, 1983), it has been rarely described in the geologic literature (Grover, 1981). For the remainder of this discussion, this cement will be referred to simply as "bladed" cement.

In the Holston and Rockdell formations, bladed cement is characterized by stubby (Figure 3.5D) to elongate (Figure 3.5E) crystals which vary from between 0.04 and 1.30 mm in length and between 0.03 and 0.50 mm in width. Typically, these crystals are wider at the substrate than at their distal ends but they may be "club-shaped" with the distal ends of crystals being nearly two times as wide as the proximal ends (Figure 3.5E, F, H). Bladed crystals may be either inclusion-rich or

inclusion-poor or in many cases, may exhibit two stages of growth. In two stage bladed cement, the first stage is a basal, inclusion-rich stage followed by a later inclusion-free stage (Figure 3.5G, H). The boundary between the two stages may be sharp or gradational.

Bladed cement crystals occur in both intra- and interparticle pore spaces. They may be isopachous or nonisopachous but are always oriented normal to the substrate. Bladed crystals preferentially occur on polycrystalline substrates with trilobites, ostracodes, bryozoans, brachiopods, and micrite being the most common. In many cases the cement crystals are epitaxial with the substrate. Intercrystalline boundaries are irregular to straight (planar). In both grain-supported and mud-supported rocks, there may be a lateral change from bladed cement to more fibrous crystals in some pores (Figures 3.7A, 3.5G,H). In some cavities of mud-supported lithologies, bladed cement was observed on the outer surface of ostracodes which were deposited in internal marine sediment (Figure 3.7B). In some cases, bladed cement may exhibit a competitive growth fabric with other marine cement.

Interpretation. Bladed cement in the Holston and Rockdell formations in northeastern Tennessee is interpreted as marine in origin based on the following lines of evidence. Bladed cement always occurs as the first cementing phase in these rocks (with the exception of micritic cement) indicating it form early in the diagenetic sequence. Similarly, bladed cement always occurs before clear syntaxial cement on echinoderms, equant calcite (especially in bryozoan zooecia) and Fe-calcite indicating it occurs early in the paragenetic sequence of

Figure 3.7. Petrographic features of bladed/prismatic cement, turbid syntaxial (rim) cement, and radiaxial-fibrous calcite and associated cement in the Holston and Rockdell Formations.

A. Plane light photomicrograph of an intraparticle cavity (part of the upper surface of trilobite has been removed by pressure solution) which contains both "two-stage" bladed cement (growing from the roof) and radiaxial-fibrous calcite. These cements are shown in detail in Figures 3.5G,H (p. 86). Bar scale is approximately 1.0 mm. Red House Branch. (RHB'4AS1R).

B. Photomicrograph of ostracod fragments which are isopachously rimmed by fine, bladed calcite cement. The ostracode debris was deposited with internal sediment on the floor of an irregular cavity in the Holston Formation. Bar scale is approximately 0.25 mm. Poor Valley Creek. (PVC'2C).

C. Close-up, plane light photomicrograph of turbid syntaxial cement and its host echinoderm grain. The outer rim of the echinoderm is delineated by a dark hematitic rind. Above the syntaxial cement is radiaxial-fibrous calcite and a portion of its substrate, a brachiopod. The two cements decrease uniformly in thickness as the distance between the two host grains decreases, suggesting the cements were growing simultaneously. Bar scale is approximately 0.25 mm. Red House Branch. (RHB'3BS1).

D. Photomicrograph (plane light) of clear syntaxial cement within a small void in the Rockdell Formation. The host echinoderm grains may be delineated by their turbid appearance. Bar scale is approximately 1.0 mm. Cedar Springs. (CS51).

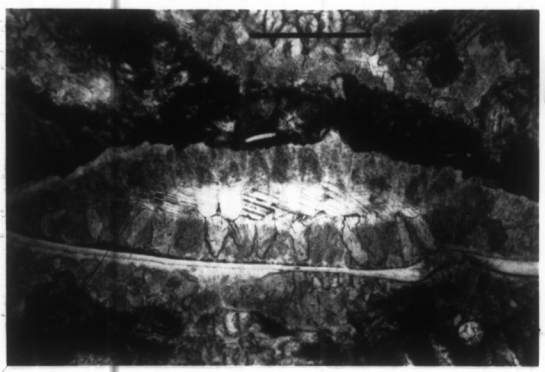
E. Plane light photomicrograph of "two-stage" syntaxial overgrowth cement in the Rockdell Formation. The initial or first stage of the cement crystal appears turbid due to inclusions within the crystal structure while the second stage of growth is generally inclusion-free. In this example, the overgrowth has engulfed two bryozoan fragments above the echinoderm grain. Bar scale is approximately 1.0 mm. Cedar Springs. (CS41).

F. Close-up photomicrograph illustrating the most common occurrence of "two-stage" syntaxial cement. The turbid stage, adjacent to the grain, is thin while the inclusion-free or clear stage is much thicker. The boundary between the two growth stages, as in this example, is commonly sharp. In this example, the clear stage is ferroan at the distal end where it partially encloses a bryozoan. Bar scale is approximately 0.25 mm. Red House Branch. (RHB'8CL).

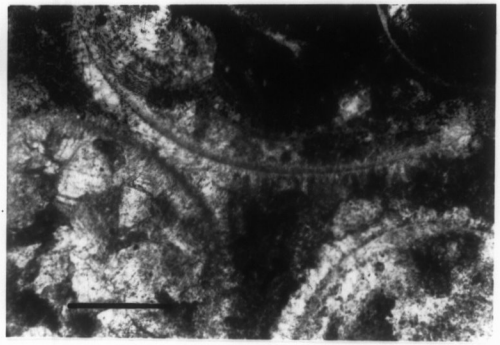
Figure 3.7 (continued)

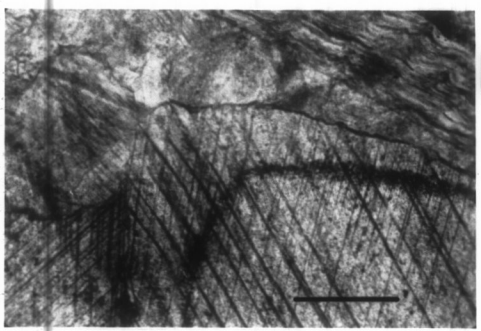
G. Close-up photomicrograph in plane light illustrating the prohibition or interference of fibrous cement formation on a bryozoan by the growth of turbid syntaxial cement on an echinoderm grain. In this example, radiaxial-fibrous calcite is only developed on the side of the bryozoan opposite the echinoderm. Syntaxial cement fills the space between the echinoderm and the bryozoan and actually poikilitically encloses the bryozoan and fibrous cement. Bar scale is approximately 0.25 mm. Red House Branch. (RHB'6BBR).

H. Photomicrograph of Figure 3.7G under crossed-nichols illustrating the extinction pattern of radiaxial-fibrous calcite on the bryozoan and the optical continuity between the echinoderm grain and its turbid overgrowth. It is clear in this example, that the development of fibrous cement has been prohibited on the bryozoan surface adjacent to the earliest overgrowth cement. Bar scale is approximately 0.25 mm. Red House Branch. (RHB'6BBR).



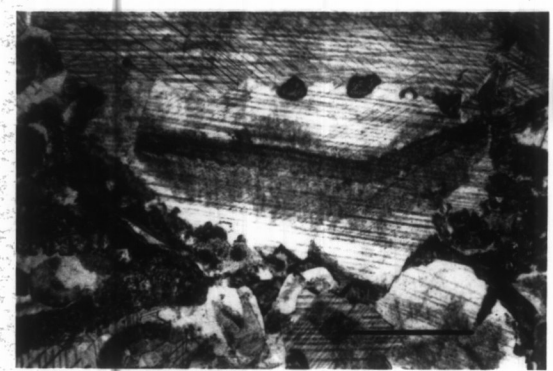
A B



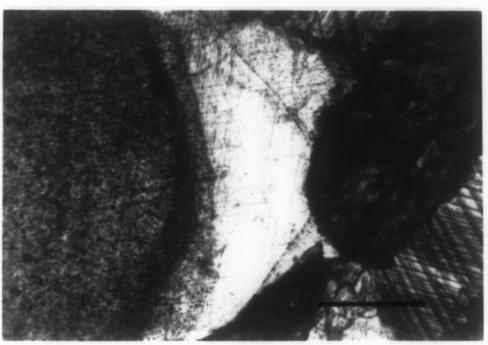


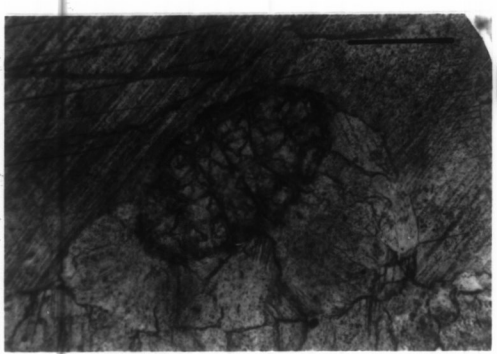
C D





E F





G H

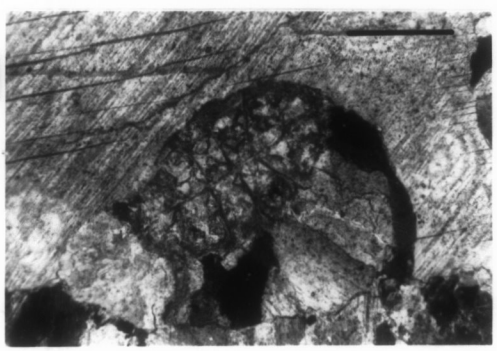


Figure 3.7
97
Jernigan, 1987

cement. In mud-supported rocks, bladed cement may exhibit a competitive growth fabric with other cement phases interpretated as marine in origin which indicates that the cement was growing at the same time and in the same environment. Bladed cement was observed on the outer surfaces of some allochems (primarily ostracodes) which were deposited within cavities in and surrounded by internal marine sediment. This line of evidence has been used elsewhere to indicate that a cement was formed prior to deposition in the marine environment (see Burgess, 1979; Walker et al., 1985). Finally, bladed cement in the Holston and Rockdell formations in northeastern Tennessee is very similar to the bladed marine cement in the Middle Ordovician limestone sequence in the Virginia Valley and Ridge described by Grover (1981) and to the "fringing" marine cement in the Holston Formation near Knoxville described by McGill (1982).

Turbid Syntaxial (rim) Cement

Overgrowth cement in optical continuity with echinoderm ossicles has been recognized since the time of Sorby (1879). Bathurst (1958) has termed this cement "rim" cement because it "evolved by rim cementation of detrital particles." Porous echinoderm grains which consist of a complex of submicrocrystalline crystals (Garrido and Blanco, 1947; Nissen, 1963) behave optically as single crystals of calcite. The overgrowth cement acquires the crystallographic orientation of the host crystal and in thin-section, host grain and overgrowth material show unit extinction.

Evamy and Shearman (1965, 1969) have extensively studied the growth history of syntaxial cement on echinoderm grains from Jurassic limestone in France and from "sub-Recent" to Pleistocene limestone in the Persian Gulf. By studying variations in the concentration of Fe^{2+} in growth zones, they were able to effectively record "the shapes of the overgrowths at various stages intheir development" (Evamy and Shearman, 1969). They observed that initial "serrated" overgrowth crystals were developed on echinoderm surfaces between canals which perforate the grain surface. These serrated crystals nucleated only on echinoderm surfaces which faced the c-crystallographic direction and were not developed on sides which paralleled the c-direction. Progressive growth in the c-direction caused the overgrowths to be elongated in that direction. In vertical sections, the number of initial crystal terminations, defined by the shape of successive cement zone boundaries, decreased away from the echinoderm surface (a result of competitive growth; see Buckley, 1951).

Evamy and Shearman (1965) noted the coarsely crystalline nature of echinoderm syntaxial overgrowths. In many cases, these overgrowths were "poikilitic" or engulfed surrounding polycrystalline grains and their fringing cement. This tendency has also been described by Lucia (1962).

In his review of processes and products which occur in diagenetic environments, Longman (1980) stated that "syntaxial overgrowths form rarely, if ever, in the marine phreatic environment" but rather form in the freshwater phreatic environment. His conclusion, however, is not

justified based on a review of the geologic literature. There have been several important studies which concluded that some syntaxial overgrowths on echinoderm grains do in fact form in the marine environment (see Evamy and Shearman, 1965; Purser, 1969, Meyers, 1974; Lohman and Meyers, 1977; Burgess, 1979; Gorur, 1979; Grover, 1981; McGill, 1982; Walker et al., 1985).

From an examination of the literature and petrographic and cathodoluminescent analysis of Cambrian, Ordovician, and Pennsylvanian age echinodermal grainstones and packstones, Walker et al. (1985) proposed eight criteria which, if developed in conjunction with syntaxial cement, would support a marine origin. These criteria included:

1. Marine borings in or encrusting marine organisms on overgrowths;

2. Overgrowths on grains which occur in a micritic matrix;

3. Oolitic coatings on the outer surface of an overgrowth;

4. Growth interference between syntaxial overgrowths and marine cement;

5. Marine cement overlying syntaxial overgrowths;

6. Compromise boundaries between syntaxial overgrowths and marine cement;

7. Triple junctions formed by the intersection of compromise boundaries between syntaxial overgrowths and marine cement; and

8. Luminescent zones which transect syntaxial overgrowths and marine cement.

Conversely, we were able to discount a marine origin for syntaxial overgrowths in rocks which did not exhibit the above criteria.

Syntaxial overgrowths on echinoderm grains in the Holston and Rockdell formations in northeastern Tennessee may be turbid (Figure 3.7C), clear (Figure 3.7D) or they may be "two stage" crystals composed of an initial turbid stage of growth and capped by a later clear (nonturbid) stage (Figure 3.7E). In the case of the two stage overgrowths, the turbid stage is usually adjacent to the host grain and is much thinner than the nonturbid stage. In many grain-supported rocks, overgrowths exhibit Fe^{2+} zoning which is revealed by staining with potassium ferricyanide. These zones are limited to early and later stages of clear syntaxial cement and to the clear stages of two stage overgrowths. Only turbid overgrowth phases are discussed in this section.

Turbid syntaxial overgrowths are very finely crystalline to coarsely crystalline. Etched thin-sections reveal that the inclusions which cause the crystals to be turbid are irregular, oval to rhombic in shape and are primarily between 2 and 20 μm in diameter. Rhombic shaped inclusions, usually the largest inclusions, are apparently microdolomite crystals (formed during mineralogic stabilization; see Lohmann and Meyers, 1977; Meyers and Lohmann, 1978). The irregular to oval shaped inclusions are usually small and difficult to resolve with a petrographic microscope but may be fluid inclusions. Inclusions are generally uniformly distributed throughout the cement. In most two stage syntaxial cement crystals, the boundary between turbid and

nonturbid zones is sharp (Figure 3.7F). In many turbid overgrowths, inclusions impart apseudopleochroism to the crystals which is typically cream to tan.

Turbid syntaxial cement is primarily limited to filling pore space immediately adjacent to the host echinoderm grain. In sections cut approximately normal to the c-axis of the host grain and thus to the c-axis of the turbid syntaxial cement, the overgrowth is 2 to 5 times thicker (relative to sections parallel to the c-axis) and may engulf parts of surrounding polycrystalline grains (Figure 3.7E, F).

In grain-supported and mud-supported lithologies which exhibit extensive cementation by radiaxial-fibrous and associated marine cement, turbid syntaxial cement appears to have interfered with or in some cases prohibited the growth of fibrous cement crystals on polycrystalline substrates such as bryozoans (Figures 3.7G, H). In other cases, turbid overgrowths exhibit polygonal growth boundaries (compromise boundaries) with fibrous marine cement on polycrystalline grains. Triple junctions commonly form where turbid overgrowths and fibrous cement fill the last remaining pore space (Figure 3.8A, B). In some instances, syntaxial cement appears to have acted as a substrate for radiaxial-fibrous calcite cement. Normally when this fabric occurs, the boundary between the two cement phases is gradational. This fabric is apparent only under crossed-polars. When the echinoderm grain is at extinction, the initial portion of the overgrowth is also extinct while the distal portion of the crystal is not at extinction. When the stage is rotated, extinction migrates toward the distal end of the overgrowth

Figure 3.8. Petrographic features of turbid syntaxial (rim) cement and micritic cement in the Holston and Rockdell Formations.

A. Close-up, plane light photomicrograph of a small void which is filled by radiaxial-fibrous calcite and turbid syntaxial (rim) cement. (The host echinoderm grain is visible at right). Compromise boundaries with corresponding triple junctions have formed by the intersection of cement crystals at the center of the cavity. These features indicate the radiaxial-fibrous calcite and turbid syntaxial cement were forming at the same time. Bar scale is approximately 0.25 mm. Red House Branch. (RHB'4AS1R).

B. Crossed-nichol photomicrograph of Figure 3.8A illustrating the syntaxial relationship between the echinoderm and the overgrowth cement. In this view, the lateral change in thickness of the fibrous crystals and the syntaxial overgrowth along the compromise boundary is apparent. Bar scale is approximately 0.25 mm. Red House Branch. (RHB'4AS1R).

C. Close-up photomicrograph (crossed-nichols) of an initial turbid syntaxial overgrowth of an echinoderm grain which appears to have acted as substrate for fibrous cement. At the distal end of the overgrowth cement, extinction has a sweeping character, similar to extinction in radiaxial-fibrous calcite crystals to the right. Compromise boundaries (with corresponding triple junction) have formed between the fibrous, distal portion of the rim cement and the radiaxial-fibrous cement crystals at right. Bar scale is approximately 0.25 mm. Red House Branch. (RHB'4AS1L).

D. Plane light photomicrograph showing what appears to be a "horseshoe-shaped" echinoderm fragment encased in turbid (syntaxial) overgrowth cement. Bar scale is approximately 1.0 mm. Red House Branch. (RHB'4AS2BR).

E. Crossed-nichol photomicrograph of Figure 3.8D. With the host echinoderm grain at extinction, the distal end of the overgrowth cement shows subcrystals which diverge away from the substrate and on rotation of the stage, sweeping extinction (in the direction opposite the rotation direction). These petrographic features are characteristic of radiaxial-fibrous calcite. Bar scale is approximately 1.0 mm. Red House Branch. (RHB'4AS2BR).

F. Photomicrograph of micrite cement lining the cavity formed by series of articulated echinoderm plates.

Figure 3.8 (continued)

The antigravitational nature of the micrite and its being devoid of fossil material suggest this micrite was precipitated in place as primary cement. Bar scale is approximately 1.0 mm. Red House Branch. (RHB'6B).

G. Photomicrograph illustrating the alternation of dense, allochem-free micrite cement with peloidal internal marine sediment within a complex cavity in the Holston Formation. The last layer of micritic cement is clearly perched in an antigravitational manner, being 1-2 times thicker at the top of the bryozoan than toward the bottom. Bar scale is approximately 1.0 mm. Red House Branch. (RHB'2AC2MR).

H. Close-up photomicrograph of Figure 3.8G showing the contrast between the dense micritic cement and the peloidal internal sediment. In this view, it is evident that th bryozoan is actually encased (coated on all sides) in micritic cement. The central portion of the cavity is filled by radiaxial-fibrous calcite cement (upper left) which used the last layer of micrite cement as a substrate. Bar scale is approximately 0.25 mm. Red House Branch. (RHB'2AC2MR).

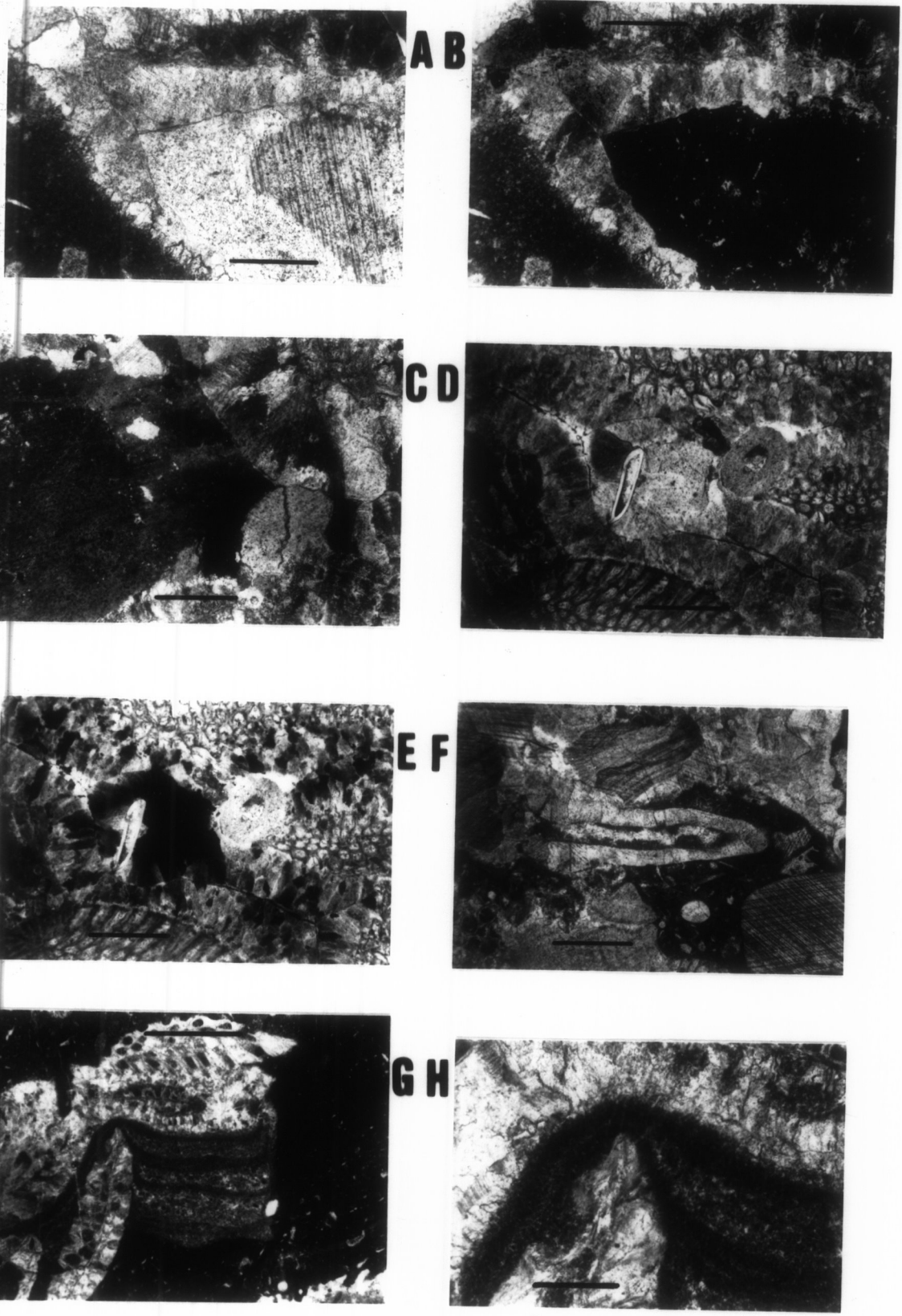

A B
C D
E F
G H

Figure 3.8
105
Jernigan, 1987

into what appear to be fibrous crystals (Figure 3.8C). Extinction in the fibrous crystals indicates that they are radiaxial-fibrous cement crystals (Figure 3.8D, E). Rarely, the boundary between the initial overgrowth and the radiaxial-fibrous cement is sharp. In such cases, the entire syntaxial cement crystal exhibits unit extinction with the host echinoderm grain while extinction in the radiaxial-fibrous calcite characteristically migrates in the direction opposite that of stage rotation.

Interpretation. Turbid syntaxial overgrowths in the Holston and Rockdell formations are interpretated as marine in origin based on several lines of evidence. First, considering growth rates and directions of the cement, turbid overgrowths have interfered with or in some cases prevented the formation of radiaxial-fibrous cement on polycrystalline substrates. This distributional feature suggests that turbid syntaxial cement was precipitated before radiaxial-fibrous crystals or they were growing at the same time. Second, in both grain- and mud-supported rocks, turbid syntaxial overgrowths have acted as substrates for radiaxial-fibrous calcite. This fabric is best explained by the overgrowth cement being precipitated in the marine environment since radiaxial-fibrous calcite is a marine precipitate. Third, polygonal growth boundaries are commonly developed between turbid syntaxial overgrowths and radiaxial-fibrous calcite. In many cases, the polygonal suture boundaries meet in the center of pores creating triple junctions. Shinn (1975) used the presence of polygonal suture boundaries between Holocene fibrous cement crystals as evidence of growth in the

phreatic environment (in his samples, the marine phreatic environment). Similarly, in the Holston and Rockdell formations, polygonal suture boundaries and triple junctions between turbid syntaxial overgrowths and radiaxial-fibrous calcite cement imply growth in the phreatic environment. Thus, since radiaxial cement forms in the marine environment, turbid syntaxial cement must also form in the marine environment. Fourth, inclusions in turbid syntaxial overgrowths are similar to inclusions in other marine cement such as radiaxial-fibrous calcite. Fifth, in two-stage syntaxial overgrowths, the turbid overgrowths always occur first and are followed by a clear, nonturbid stage. Finally, turbid syntaxial overgrowths in the Holston and Rockdell formations in northeastern Tennessee are similar to turbid syntaxial overgrowths in Middle Ordovician strata of the Virginia Valley and Ridge Province (Grover, 1981) and to the turbid syntaxial overgrowths in the Holston Formation near Knoxville, which have also been interpretated as marine in origin (McGill, 1982).

Cryptocrystalline (Micrite) Cement

Microcrystalline and submicrocrystalline cement are common in Recent reefs and their associated sediment and in intertidal settings (Land and Goreau, 1970; Logan, 1974; James et al. 1976; MacIntyre, 1977; Land and Moore, 1980). In the case of reefs, these cement types are developed in inter-reef cavities in the forereef area where water is forced through the porous reef framework. The composition of microcrystalline cement in modern reefs is commonly magnesian calcite while in intertidal settings it is aragonite.

Micrite cement in ancient rocks is an enigma. Several studies have recognized micrite cement in ancient rocks but quantifying its abundance has been difficult because of their small size and similarity to depositional lime-mud (see Davies 1977; Grover 1981; McGill, 1982). Criteria used to identify micrite cement in ancient rocks have been (1) anti-gravitational fabric, (2) massive appearance (as opposed to laminated), and (3) an absence of fossil material within the micrite.

In the present study, micrite cement was only observed in the Holston Formation. In grain-supported rocks, micrite cement is commonly developed in anti-gravitational positions in intraskeletal pores (Figure 3.8F). In general, the cement material consists of a nearly isopachous rind of dense, unfossiliferous micrite which is usually dark gray or dark red. Its distribution is irregular both in individual thin-sections and throughout the stratigraphic section. In mud-supported rocks, micrite cement is often developed in stromatactoid or irregularly shaped cavities. In some cases, the cement appears to be interlayered with internal marine sediment (Figure 3.8G). In such cases, the cement may be differentiated from depositional lime-mud by its anti-gravitational fabric, dense appearance, and unfossiliferous character. Within some cavities, micrite cement is overlain by radiaxial-fibrous and associated marine cement (Figure 3.8H).

Most micrite cement in the Holston Formation was not normally point-counted as cement due to its similarity to depositional lime-mud, small size and their overall rarity in Holston sediments. For this reason, the cement distribution data presented in Chapter 4 and in

Appendix B are somewhat misleading. Although the presence of micrite cement is supported by the data presented here, its role in the overall lithification process, especially in mud-supported lithologies, has not been established.

Interpretation. Micrite cement in the Holston Formation is interpretated as marine in origin. In grain-supported rocks, this type of cement makes up a very small portion of the overall porefilling cement (<1%) and is generally limited to intraskeletal pore spaces. In mud-supported rocks, this cement is interlayered with internal marine sediment in stromatactoid and irregularly shaped cavities. Micrite cement predates marine radiaxial-fibrous calcite cement in many cavities. A marine environment of formation is also supported by analogy with both studies of microcrystalline cement in modern reef environments and micrite cement in ancient reef and mound environments.

Meteoric Cement

Meteoric diagenesis occurs in two separate environments based on the nature of the fluids present in the pore space of a sediment: (1) the vadose environment; and (2) the meteoric (freshwater) phreatic environment (Longman, 1980). In the vadose environment, both air and meteoric water are present in the pores in varying proportions. Within this environment, water tends to be held "between grains by capillary forces or under grains as pendant drops" (Longman, 1980). Longman (1980) has separated the vadose environment into two zones which are distinguished by the dominant processes occurring within the sediment;

processes controlled by the saturation state of the pore waters with respect to calcium carbonate. The "zone of solution" at the top of the vadose zone is characterized by meteoric fluids percolating through the sediment intermittently causing extensive solution of aragonite and the formation of secondary porosity (Figure 3.9). The "zone of precipitation" generally lies below the "zone of solution" (Figure 3.9). Meteoric water in this zone is saturated with respect to calcium carbonate so that cement may be precipitated.

Vadose cement textures and fabrics reflect the distribution of water within the pores. Dunham (1971) has pointed out that if saturated water is held between grains by capillary forces, the cement formed will assume a meniscus fabric. Muller (1971) noted that when sufficient water is present, gravitational forces tend to form water droplets on the underside of grains creating "pendant" or "gravitative" cement. Thus, cementation in the vadose environment results in an uneven distribution of cement within pores. Uncommonly, continual cement precipitation may eventually fill pores completely with drusy growth calcite (Bathurst, 1958, Schroeder, 1973). Compositional zoning as revealed by staining or luminescent petrography may illustrate the above vadose fabrics distinguishing vadose from phreatic cement.

In the meteoric phreatic environment, all pores are filled with meteoric water which exhibits variable degrees of saturation with respect to calcium carbonate (Longman, 1980). The meteoric phreatic environment is bounded on top by the water table. In areas proximal to the sea, the lower boundary is gradational with marine water (which is

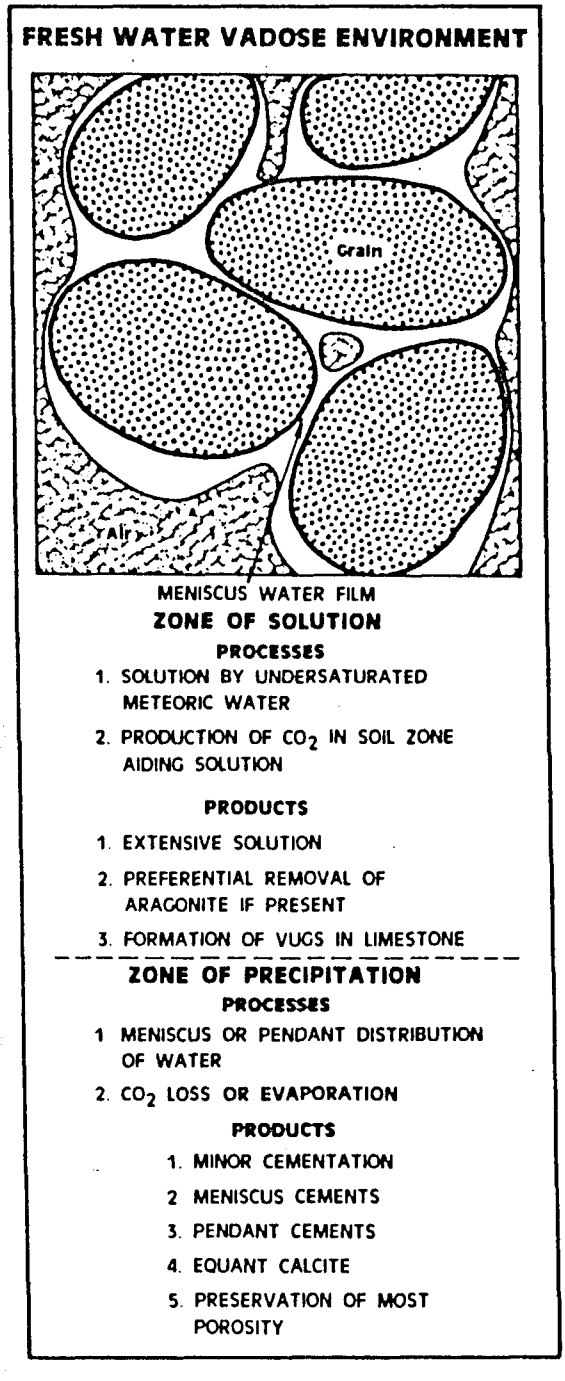
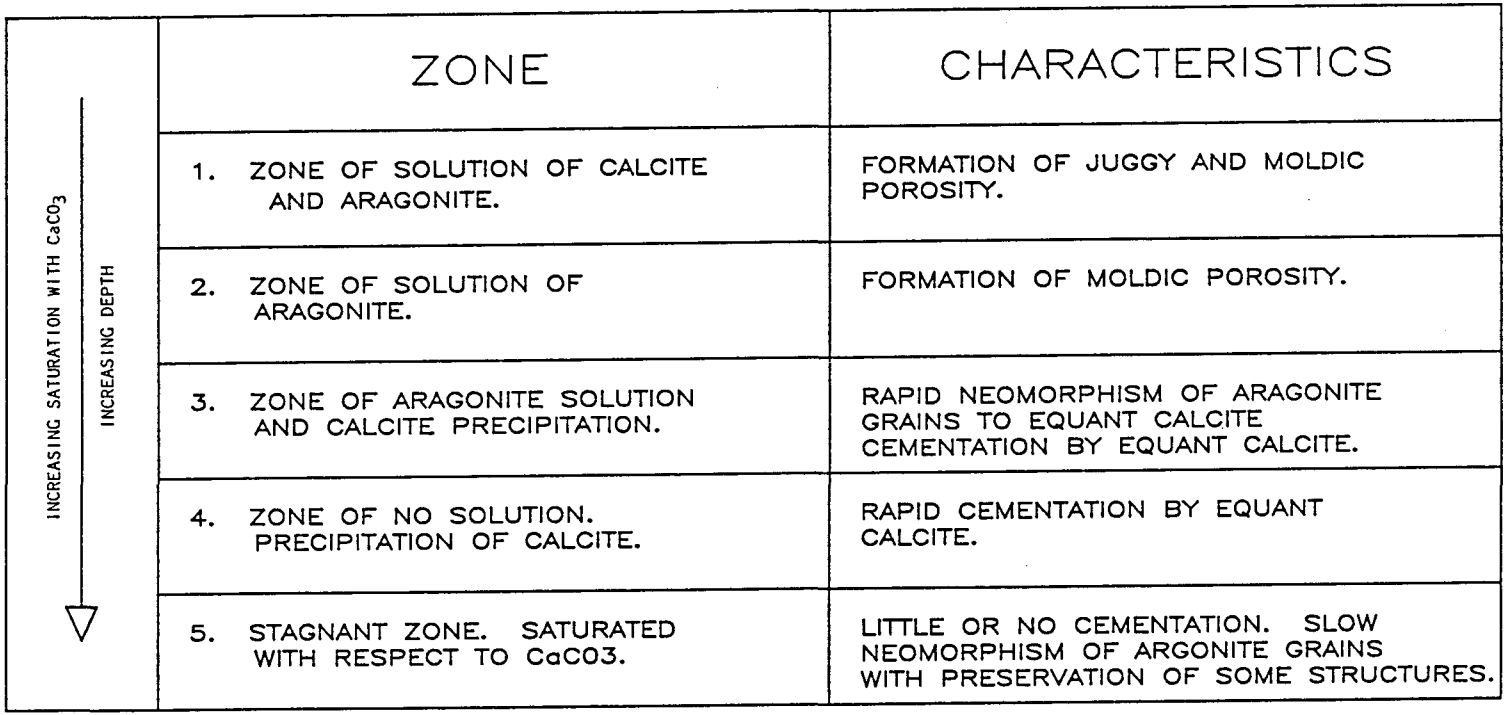


Figure 3.9. Characteristics of the vadose diagenetic environment. (From Longman, 1980).

the zone of marine-meteoric mixing). In inland areas, the lower boundary may be gradational with meteoric derived brines formed by the compaction of sediment, dehydration of clay minerals, as well as many other processes (Folk, 1974; Longman, 1980; Flugel, 1982).

Based on the assumption that as meteoric water moves downward through carbonate sediment the degree of saturation with respect to calcium carbonate increases, Longman (1980) described the "ideal" meteoric phreatic environment as consisting of five zones (Figure 3.10). The first three zones, from the top of the meteoric environment, are zones of solution. Note that initially, both aragonite and calcite may be dissolved in zone 1 but as the degree of saturation increases, calcite becomes the stable carbonate phase in zone 2. In that zone, only aragonite is dissolved. In zone 3, aragonite continues to be dissolved which continues to increase the saturation state of the meteoric water so that calcite is precipitated. Since calcite is less soluble than aragonite, the downward migrating meteoric fluid becomes saturated with respect to calcite first. Once calcite begins to precipitate, the water will never become saturated with respect to aragonite so that the dissolution-precipitation process will continue as long as aragonite is present in this third zone of solution. The processes and products which occur in the three zones of solution are summarized in Figure 3.11.

The zone immediately below the zones of solution in the meteoric phreatic environment (zone 4) is described as a "zone of no solution" by Longman (1980) (Figure 3.10). Within this zone, which is also



ZONE	CHARACTERISTICS
1. ZONE OF SOLUTION OF CALCITE AND ARAGONITE.	FORMATION OF JUGGY AND MOLDIC POROSITY.
2. ZONE OF SOLUTION OF ARAGONITE.	FORMATION OF MOLDIC POROSITY.
3. ZONE OF ARAGONITE SOLUTION AND CALCITE PRECIPITATION.	RAPID NEOMORPHISM OF ARAGONITE GRAINS TO EQUANT CALCITE CEMENTATION BY EQUANT CALCITE.
4. ZONE OF NO SOLUTION. PRECIPITATION OF CALCITE.	RAPID CEMENTATION BY EQUANT CALCITE.
5. STAGNANT ZONE. SATURATED WITH RESPECT TO CaCO3.	LITTLE OR NO CEMENTATION. SLOW NEOMORPHISM OF ARGONITE GRAINS WITH PRESERVATION OF SOME STRUCTURES.

Figure 3.10. Idealized zonation of the meteoric phreatic diagenetic environment based on the assumption that saturation of water with respect to $CaCO_3$ increased as meteoric water moves downward. Any of these zones may be small, missing or displaced within the sequence. (After Longman, 1980).

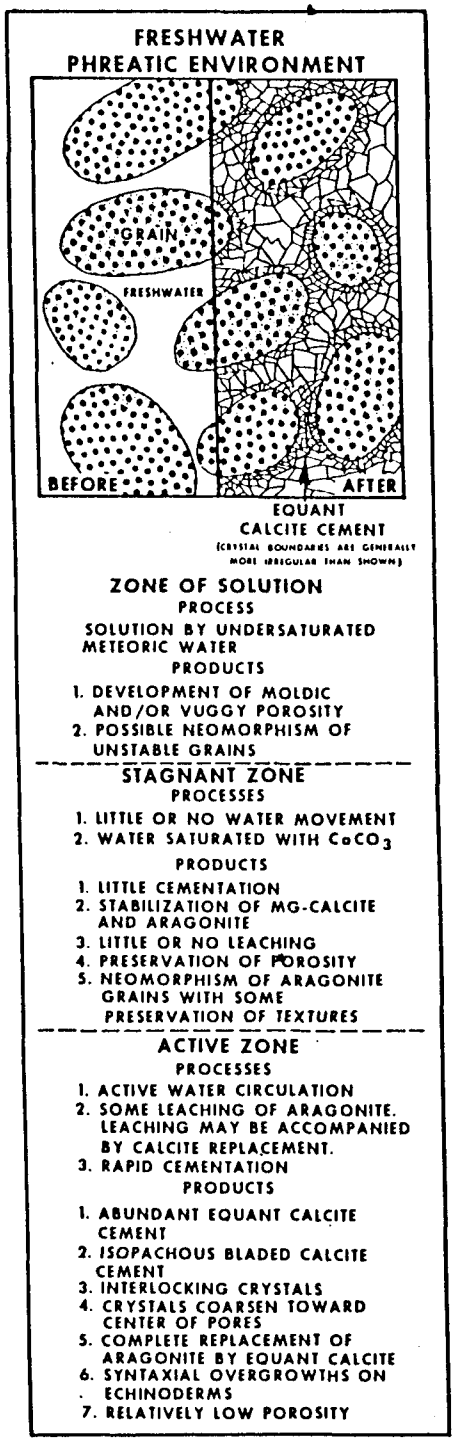


Figure 3.11. Characteristics of the freshwater phreatic diagenetic environment. (From Longman, 1980).

called the "active zone," saturated water circulates through the pores and cementation by calcite is pervasive. The dominant cement fabric formed in this zone is drusy equant calcite although initially bladed crystals may form around some grains. The progressive coarsening of calcite crystals toward the center of pores may be a distinctive characteristic of early cementation in the meteoric phreatic environment (Loucks, 1977). Syntaxial overgrowths on echinoderm grains also form in this environment (Longman, 1980; Flugel, 1982). As previously discussed in this chapter, there is strong evidence that the precipitation of syntaxial cement on monocrystalline substrates is not limited to the "active meteoric phreatic environment" but may also take place in the marine phreatic environment (see discussion of turbid syntaxial cement). A summary of the process and products of the active zone of calcite precipitation is provided in Figure 3.11.

Longman (1980) illustrated a zone of stagnant meteoric water (zone 5) which may be developed below the "active zone." Pore waters in the "stagnant zone" are saturated with respect to calcite but not aragonite. Water circulation is slow and as a result little cementation occurs. Aragonite may be recrystallized to calcite but porosity is generally preserved in this zone. Processes and products characterizing the stagnant zone are summarized in Figure 3.11.

Longman (1980) has stated that the five zones which comprise the meteoric phreatic environment, illustrated in Figure 3.10, are "ideal" and that any of the zones may be small, missing or displaced within the ideal sequence. The dominant cement fabric produced in the meteoric

phreatic environment would be unaffected by a change of the sequence. Thus, drusy equant calcite cement which is produced in the active zone of this environment is preferentially preserved. An important characteristic of cement precipitated in this environment is that the crystals are evenly distributed on the walls of pores.

The meteoric diagenetic environment "has been studied more intensively than any other diagenetic realm" (James and Choquette, 1984) (see for example, Friedman, 1964; Land, 1967, 1970, 1971; Friedman and Kolesar, 1971; Multer, 1971, Jacka and Brand, 1977; Loucks, 1977; Meyers, 1978; and Grover and Read, 1978). The review of diagenetic environments by Longman (1980) was largely a summary of earlier research. A similar review of meteoric diagenetic processes, although detailing more of the chemical parameters controlling meteoric diagenesis, has been prepared by James and Choquette (1984).

More recently, Prezbindowski (1985) has studied the effects of burial on near-surface cement, both marine and meteoric. In particular, he analyzed 17 cores taken from the Stuart City Trend, a Lower Cretaceous shelf-edge buildup complex, now buried at depths of 3300 to 5000 m. Cement textures and elemental and isotopic characteristics which reflected meteoric stabilization or precipitation in the meteoric environment were not significantly altered by burial diagenesis.

Equant (Drusy) Calcite Cement

Equant calcite cement as described previously is the dominant meteoric-derived cement (Longman, 1980, James and Choquette, 1984). Folk (1965) has characterized equant cement crystals as having length:

width ratios which average less than 1.5:1. Equant cement typically exhibits a drusy fabric or increase in crystal size toward the center of pores which effectively reduces the number of crystals distal to the substrate (Bathurst, 1971). Drusy equant calcite may also be identified by the high frequency of enfacial triple junctions (Bathurst, 1975).

Equant cement in the Holston and Rockdell formations ranges from very finely crystalline to extremely coarsely crystalline and may be developed in either of two sequences. In the Holston Formation, equant cement is primarily developed as pore central intraparticle cement within bryozoan zooecia and articulated ostracodes in grain-supported rocks (Figures 3.12A). In mud-supported rocks of the Holston Formation, equant cement is developed as intraparticle cement within bryozoan zooecia and articulated ostracodes and as interparticle cement in the center of some early diagenetic cavities and shelter voids (Figure 3.12B, C). Equant calcite may completely fill intraparticle pores (Figure 3.12A) or it may overlie an earlier bladed or fibrous cement phase. The size gradation of crystals in equant cement takes two forms. In the first form, crystal size uniformly increases away from the substrate so that the number of crystals is effectively reduced, often to the point that a single crystal fills the last remaining pore space. In the Rockdell Formation, equant cement is well developed as both intraskeletal and interparticle cement in grain- and mud-supported rocks. As in the Holston Formation, within intraparticle pores, equant cement may fill the entire pore or may overlie an initial bladed or fibrous cement (Figure 3.12D). Fine equant cement crystals may take

Petrographic features of equant (drusy) calcite and clear syntaxial (rim) cement in the Holston and Rockdell Formations.

A. Close-up, plane light photomicrograph illustrating the common intraparticle occurrence of equant calcite cement, in this case completely occluding bryozoan zooecia. Note the increase in crystal in crystal size away from the outer zooecial wall. Bar scale is approximately 0.25 mm. Red House Branch. (RHB'3D).
B. Plane light photomicrograph showing equant (drusy) calcite filling a diagenetic cavity created by decay or solution of a sponge. In this example, equant crystals completely occlude both the interior of the large, articulated ostracode within the cavity as well as the cavity itself. Bar scale is approximately 1.0 mm. Poor Valley Creek. (PVC'2C).
C. Plane light photomicrograph of a series of shelter voids created by "stacked" trilobite fragments. The upper two voids are filled by minor internal sediment and radiaxial-fibrous calcite while the large, lowermost cavity is filled by peloidal, cross-laminated internal sediment and equant calcite cement. These equant crystals have a distinctly drusy fabric with crystal size increasing from the base of the void to the top. Bar scale is approximately 1.0 mm. Red House Branch. (RHB'2D).
D. Plane-light photomicrograph of pore-central, equant calcite within and ostracode in the Rockdell Formation. In this example, the large equant crystal filling the last remaining pore space was precipitated after earlier bladed cement. Bar scale is approximately 1.0 mm. Cedar Springs. (CS41).
E. Close-up, plane light photomicrograph showing the bimodal size distribution of equant calcite crystals in a wackestone from the Rockdell Formation. The cavity wall is lined by irregularly spaced, fine crystals while the center of the void is occluded by several large crystals. In this case, there is no size gradation from the wall of the cavity to the center. Bar scale is approximately 0.25 mm. Cedar Springs. (CS49).
F. Plane light photomicrograph illustrating clear syntaxial (rim) cement overgrowing an echinoderm. The host echinoderm may be delineated by its turbid appearance at the center of the field-of-view. The syntaxial crystal has poikiolitically enclosed several bryozoan in this example. Bar scale is approximately 1.0 mm. Cedar Springs. (CS51).

Figure 3.12 (continued)

G. Left. Plane light photomicrograph illustrating the second common form of clear syntaxial (rim) cement, overgrowing turbid syntaxial cement (upper left). Right. Under crossed-nichols with the host echinoderm and the overgrowth at extinction, the pervasive nature of syntaxial cement is evident. The large Trepostome bryozoan in this field-of-view is poikilitically overgrown by the syntaxial cement. Bar scale is approximately 1.0 mm. Red House Branch. (RHB'6BBR).

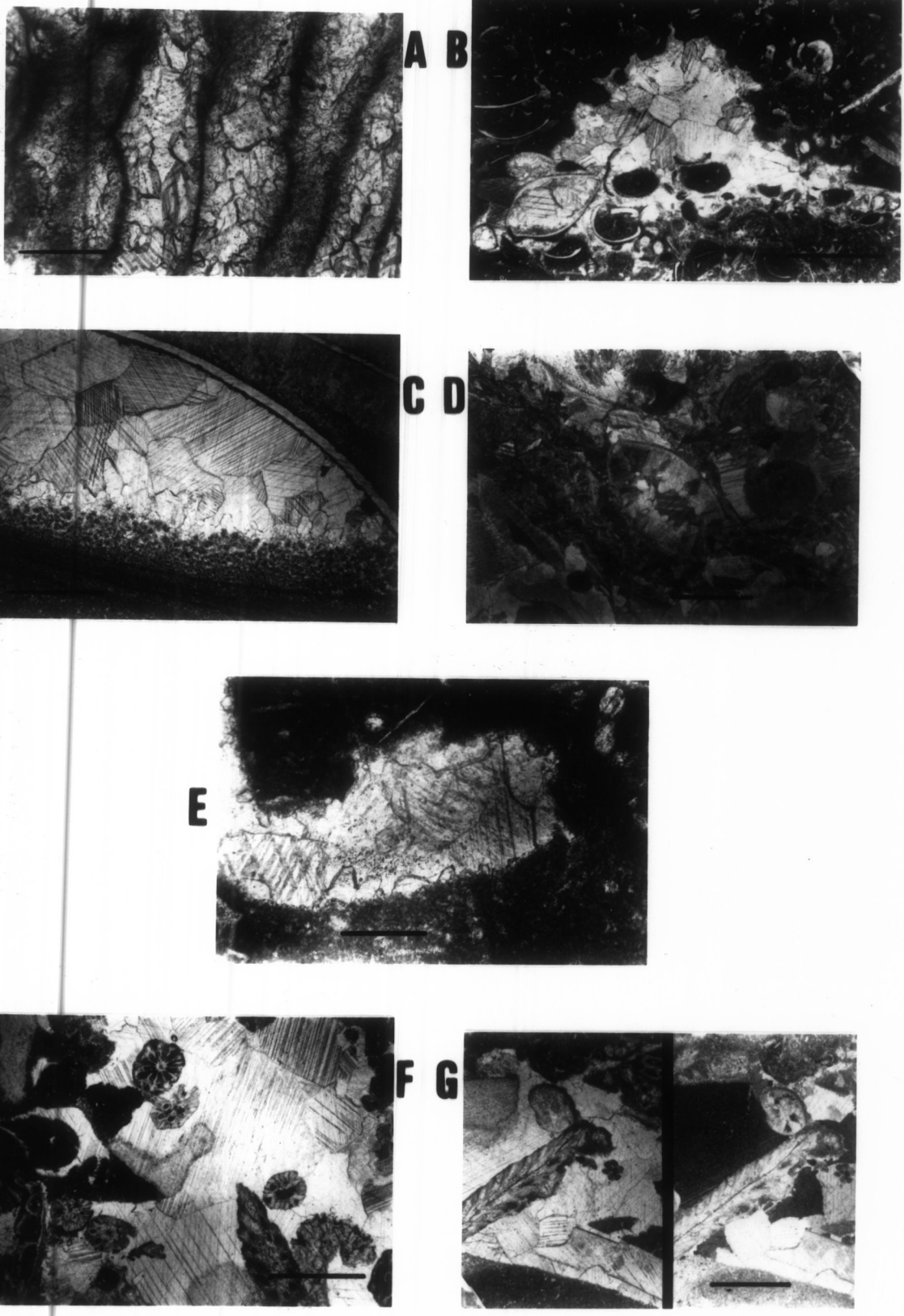

A
B
C
D
E
F
G

Figure 3.12
120
Jernigan, 1987

the first form in which they grade into coarse crystals at the center of pores as in the Holston Formation or they take a second form in which they are bimodally distributed within pores (Figure 3.12E). In this second form, initial very fine to medium crystalline cement (usually <0.1 mm) is developed at the pore walls. These initial crystals are immediately overlain by very coarsely to extremely coarsely crystalline equant cement. The boundary between the two stages is sharp. Luminescent petrography reveals that the rims of the initial small equant crystals are moderately to brightly luminescent while the center of the small crystals and the larger second stage crystals exhibit dull luminescence.

Equant calcite cement in the Holston and Rockdell formations is dominantly clear (Figures 3.12A, C). Rarely, small inclusion-rich areas may be developed within the crystals. Equant cement is developed on a variety of polycrystalline substrates including bryozoans, brachiopods, and micrite which suggests that there is no substrate specificity involved in the development of equant crystals. Contacts between substrates and equant crystals are sharp. Intercrystalline boundaries are primarily straight or planar but rarely may be slightly irregular or curved. Typically, the drusy equant mosaic is evenly distributed within pores.

Interpretation. Equant calcite cement in the Holston and Rockdell formations is interpreted as meteoric in origin based on the following lines of evidence. First, within bryozoan zooecia, articulated ostracodes and brachiopods, and in early diagenetic cavities, equant cement

commonly overlies fibrous and bladed marine cement but never exhibits a competitive growth fabric with them. Second, equant cement is commonly developed in pore central positions in both grain- and mud-supported rocks and thus, typically filled the last pore spaces. This is especially true in mud-supported rocks. Third, by analogy with equant cement in other ancient carbonate sequences, the textures and fabrics of equant cement in the Holston and Rockdell formations are typical of meteoric phreatic diagenesis (see Friedman, 1964; Land, 1967, 1970; Loucks, 1977; Jacka and Brand, 1977; Longman, 1980; and James and Choquette, 1984). In the rocks examined in the present study, equant cement is typically evenly distributed within pores suggesting that precipitation occurred in the meteoric phreatic environment rather than in the vadose environment.

Clear Syntaxial (rim) Cement

Clear syntaxial (rim) cement occurs in two separate forms in the Holston and Rockdell formations in northeastern Tennessee. As is typical for syntaxial cement, it commonly coats echinoderm grains (Figure 3.12F). Clear syntaxial cement also commonly coats turbid syntaxial cement which is a first stage rim cement (Figure 3.12G) (see previous section on turbid rim cement). In grain-supported rocks, both forms often occur together while these forms rarely occur together in mud-supported rocks.

Clear syntaxial cement ranges from fine to extremely coarsely crystalline and appear to be thicker on surfaces perpendicular to the c-axis of the host grain (Figure 3.13A). Where growth into a pore is

Figure 3.13. Petrographic features of syntaxial (rim) cement, ferroan calcite and ferroan (baroque) dolomite in the Holston and Rockdell Formations.

A. Plane light photomicrograph illustrating progressive elongation of turbid syntaxial cement and clear syntaxial cement (both nonferrous and ferrous) on an echinoderm grain in the c-crystallographic direction (vertically in this field-of-view). The host echinoderm grain may be delineated by the hematitic rind on its outer surface. Turbid syntaxial cement grows only on sides of the echinoderm perpendicular to the c-direction. Staining with potassium ferricyanide reveals that clear syntaxial cement overgrew the initial turbid stage with similar elongation in the c-direction. Bar scale is approximately 0.25 mm. Red House Branch. (RHB'8DS2R).

B. Plane light photomicrograph illustrating compositional zoning of "two-stage" syntaxial (rim) cement. The initial turbid stage (zone A) of the overgrowth (upper right of the echinoderm grain) is coated by a thin, clear stage (zone B). After a small amount of growth, the clear overgrowth becomes ferroan. Two major ferroan zones are evident (syntaxial cement zones C and D), each of which contains several subzones (see text for and explanation of cement zones A-E). Bar scale is approximately 1.0 mm. Red House Branch. (RHB'8A).

C. Plane light photomicrograph illustrating the complexity of the change in ferrous-iron content during syntaxial cement development. After an initial turbid overgrowth formed (zone A), clear syntaxial cement (zone B) overgrew it. After a short period of growth, the clear overgrowth became ferroan. Three distinct ferroan zones are apparent (zones C, D, and E). Note that the growth of this complex overgrowth is preferentially vertical in this example supporting the idea of crystalliographic control on primary growth direction. Bar scale is approximately 1.0 mm. Red House Branch. (RHB'8A).

D. Plane light photomicrograph of compositionally zoned ferroan calcite in a pore central position within an articulated ostracode. The ferroan calcite overlies turbid fibrous calcite crystals. Note the zoned syntaxial cement on the echinoderm (lower right). Bar scale is approximately 1.0 mm. Red House Branch. (RHB'6ETL).

Figure 3.13 (continued)

E. Close-up of Figure 3.13D showing the detail of zoned ferroan calcite overlying bladed calcite cement. The host ostracode grain is poikilitically enclosed by the zoned syntaxial (rim) cement. Bar scale is approximately 0.25 mm. Red House Branch. (RHB'6ETL).

F. Plane light photomicrograph showing a constructional cavity (created by an encrusting bryozoan) which has been filled by bladed calcite and later "pore central," zoned ferroan calcite. Ferroan calcite crystals in this example have a distinct drusy fabric. Bar scale is approximately 0.25 mm. Red House Branch. (RHB'8D2L).

G. Crossed-nichol photomicrograph illustrating one of the two major modes of occurrence of ferroan (baroque) dolomite in the Holston and Rockdell Formations, within major stylolitic zones. Extinction in this form of dolomite is characteristically undulatory as in this example. Bar scale is approximately 1.0 mm. Red House Branch. (RHB'3G).

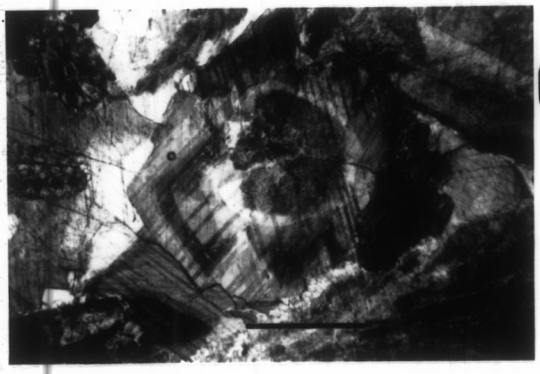
H. Crossed-nichol photomicrograph illustrating the second major mode of occurrence of ferroan (baroque) dolomite, as pore central cement with planar crystal boundaries. In this example, crystal boundaries and cleavage planes are slightly corroded. Bar scale is approximately 1.0 mm. Red House Branch. (RHB'3AB).



A



B



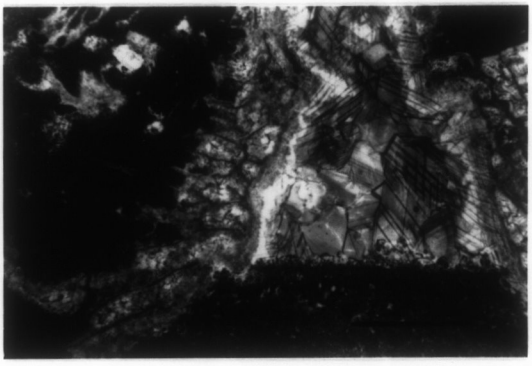
C



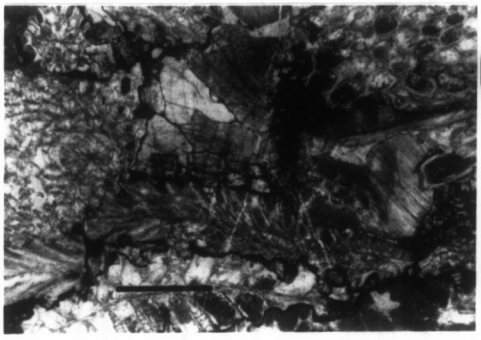
D



E



F



G



H

Figure 3.13
125
Jernigan, 1987

unimpeded, this cement tends to be pervasive, completely filling the remaining pore space (after initial marine cement). Clear syntaxial cement may partially or completely poikiliticly enclose adjacent polycrystalline grains and initial marine or meteoric cement which are nucleated on the outer surfaces of those grains (Figure 3.12F).

Compositional Zoning in Two Stage Syntaxial (Rim) Cement. In both grain- and mud-supported samples taken from more than 140 m above the lower contact of the Holston Formation at Red House Branch, two-stage syntaxial overgrowths were zoned with respect to ferrous iron. Thin-sections stained with potassium ferricyanide did not stain uniformly but rather, revealed a succession of zones stained to varying degrees indicating compositional change (Figure 3.13B, C). Boundaries between zones are always sharp and distinct.

The ideal zonation pattern consists of six different zones (A-F), illustrated in Figure 3.14. The initial turbid syntaxial cement (zone A), adjacent to the host echinoderm grain, is always nonferroan. The turbid overgrowth is followed by an initial clear, nonferroan overgrowth (zone B) which is typically thinner than zone A. Overlying the first clear, nonferroan overgrowth zone are two clear, ferroan zones which in ascending order are: (1) a light blue zone (zone C) and (2) a dark blue zone (zone D). Each of these two major ferroan zones typically contain 3-8 subzones marked by slight changes in color (Figure 3.13B, C). Depending primarily on available pore space, some samples also exhibit two additional zones (zones E and F, respectively) which followed zones A-D in time. Zone E is also ferroan and may be

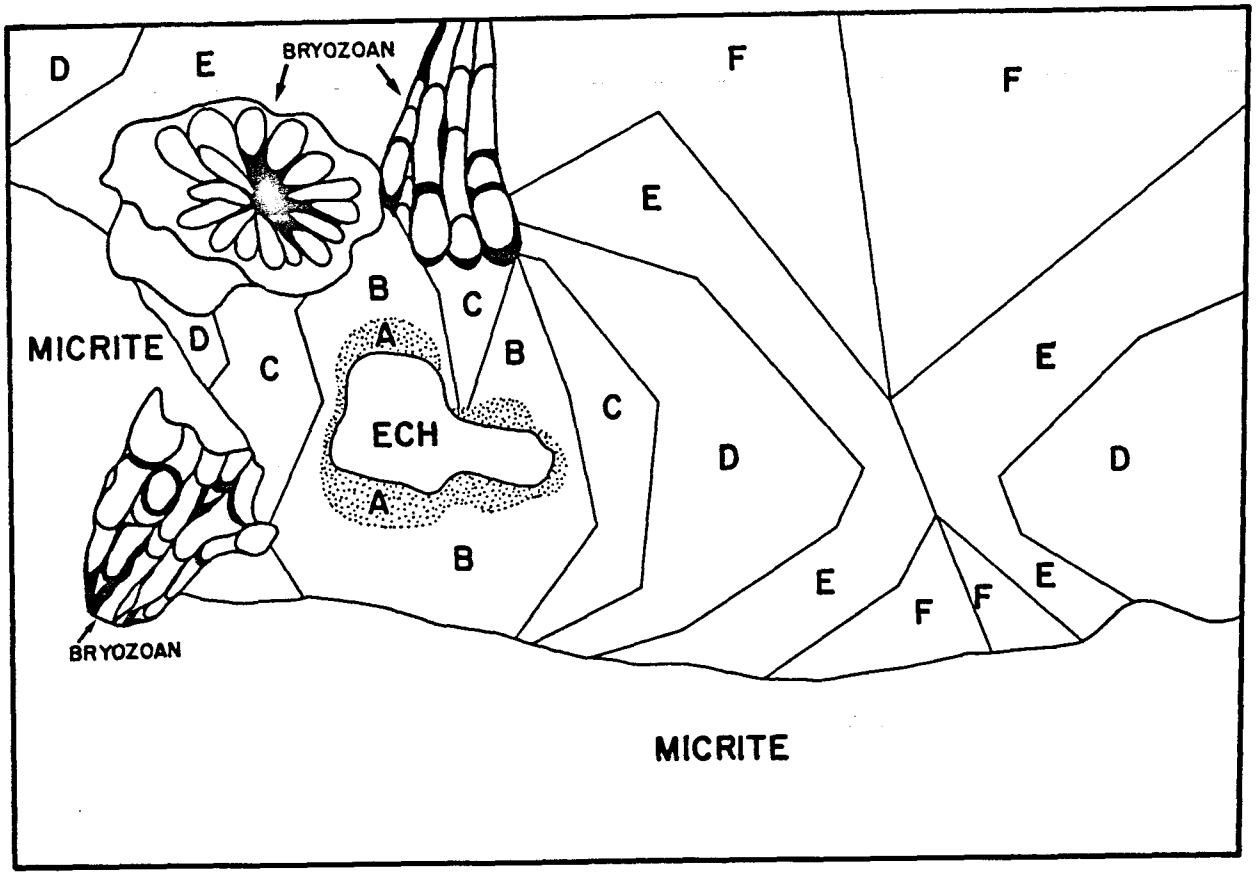


Figure 3.14. Idealized pore diagram illustrating compositional zoning in "two-stage" syntaxial as revealed by staining with potassium ferricyanide. Zones C-E usually contain several subzones. ECH--Echinoderm; A--Initial turbid overgrowth; B--Initial clear, non-ferroan overgrowth; C--Clear, light blue; D--Clear, dark blue; E--Clear, light blue or dark blue; F--Clear, nonferroan.

dark blue or light blue, depending on the sample. The last zone, zone F, is clear and nonferroan, similar to zone B.

The zonation pattern described here is an "ideal" pattern. In general, the first four zones, zones A-D, were observed in most two stage overgrowth crystals. Zones E and F were uncommon and where developed, were usually thin. There are two factors which cause these last two zones to be absent or thin, the first being the fact that zones A-D were pervasive and in most samples completely filled the interparticle pore space. Secondly, since zones E and F were thin where developed, later compactional events (solution) have often removed these last two zones in whole or in part.

Zoned ferroan syntaxial cement has been described by Evamy and Shearman (1965) although they did not offer an origin for the iron in the cement. Oldershaw and Scoffin (1967) and Oldershaw (1971) demonstrated a linear relationship between ferroan calcite and the presence of clay minerals in some Silurian and Mississippian limestone units in England. Further, they demonstrated that the volume of pore filling ferroan calcite is systematically reduced with distance away from stylolites, shale seams and shale beds in the rocks they examined. Their data suggest that "iron may have been carried into the sedimentary environment with clay minerals . . . and later redistributed in ferrous form during precipitation" of ferroan calcite (Oldershaw, 1971). Flugel (1982) has stated that "calcites containing ferrous iron are probably precipitated in the (meteoric) phreatic zone where interstitial water has a low Eh" because under oxidizing conditions, iron is

present in ferric form which will not substitute into the calcite structure. The reducing conditions needed for ferroan calcite formation suggests that this type of cement may form in the stagnant zone of the meteoric phreatic environment.

Ferroan syntaxial overgrowth cement in the Holston and Rockdell formations probably formed under similar conditions as those proposed by Flugel (1982) for ferroan calcite. It probably precipitated after shallow burial from stagnant meteoric water with a low Eh or after substantial burial in the deep-burial environment. There are two possible sources for the iron in this cement.

First, the red coloration of micrite in the Holston Formation shows that ferric iron was present in the oxidizing conditions of the depositional environment. After burial, circulation may have been restricted so that pore waters may have become reducing. Under reducing conditions and changes in temperature, pressure and pH with depth, some of the iron from complex iron oxides already within the sediment may have been mobilized and redistributed into precipitating syntaxial cement. A second possible source for the iron is basinal shale to the southeast, which was undergoing compaction. Fluids released from the clay minerals at depth during compaction may have migrated shelfward carrying with them ferrous iron. It is significant to note that zoned, two stage, syntaxial cement was observed only at the most basinward locality, Red House Branch. The limited occurrence of ferroan overgrowths to the most basinward locality would be expected if the source of iron was compacting basinal shale. The change from clear, nonferroan

syntaxial cement (zone B) to ferroan syntaxial cement zones with different concentrations of iron (zones C-E), back to nonferroan syntaxial cement (zone F) may reflect varying Eh conditions within the sediment over time.

Interpretation. Clear syntaxial (rim) cement is interpreted as meteoric phreatic in origin based on the following lines of evidence. First, clear syntaxial cement overlies turbid syntaxial cement which is marine in origin, but was never observed competing for space with any marine cement. In all samples examined in this study, clear syntaxial cement always occurred as the second stage of two stage syntaxial cement. Second, clear syntaxial cement in the Holston and Rockdell formation is similar to clear syntaxial cement described by Grover (1981) in Middle Ordovician strata in the Virginia Valley and Ridge which was also interpreted as meteoric phreatic in origin. Finally, the ferroan nature of clear syntaxial cement on echinoderm grains at the shelf margin (Red House Branch) implies precipitation from meteoric water of low Eh (Flugel, 1982). Reducing conditions could have developed in the sediments after shallow burial in the "stagnant meteoric phreatic zone" as described by Longman (1980).

Ferroan Calcite (Fe-Calcite)

In the Holston and Rockdell formation at Red House Branch and in the Holston Formation at Poor Valley Creek, ferroan calcite occurs as clear, equant crystals which exhibit either a drusy or nondrusy fabric (note that Fe-calcite does not occur in the Rockdell Formation at the

two shelfward Rockdell localities, Cedar Springs and Evans Ferry). Staining with potassium ferricyanide distinguishes ferroan calcite from nonferroan equant cement. Ferroan calcite crystals are fine to coarsely crystalline in grain-supported rocks and fine to extremely coarsely crystalline in mud supported rocks. In grain-supported rocks, this cement normally occurs as late stage (pore central) intraparticle equant cement and along with ferroan "baroque" dolomite, is the last cementing phase (Figure 3.13D, E) (see following section on ferroan "baroque" dolomite). Host grains for ferroan calcite in grain-supported rocks are primarily bryozoans and articulated brachiopods. It may also occur in shelter voids created by curvilinear (in cross-section) skeletal grains such as brachiopod valves and trilobites (Figure 3.13F). In grain-supported rocks, ferroan calcite is rarely developed as interparticle cement primarily because of the pervasive nature of syntaxial cement in these rocks. In mud-supported rocks, the bulk of the ferroan calcite occurs as pore central cement inside stromatactoid and irregularly shaped cavities. On outcrop, cement crystals appear pinkish which may be the result of manganese within the calcite structure (Table 3.3). Crystals are extremely coarse within these cavities and they always overlie an initial fibrous marine cementing phase (radiaxial-fibrous or fascicular-optic calcite).

Interpretation. There are two possible explanations or origins for ferroan calcite cement in the Holston and Rockdell formations in northeastern Tennessee. First, they could have formed from the same ferrous iron bearing meteoric fluids responsible for the zoned ferroan

Table 3.3. Trace element composition of ferroan calcite cement from selected samples from the Holston Formation. Duplicate analyses are noted in parentheses.

Sample No.	Sr (ppm)	Mg (ppm)	mole% $MgCo_3$	Mn (ppm)	mole% $MnCo_3$
RHB'2J	116	2060	0.85	903 (800)	0.16
PVC'2A	151	2060	0.85	410 (535)	0.07
PVC'2G	143	2180	0.90	336	0.06
PVC'2J	229	1450	0.60	480	0.90
Average	160	1938	0.80	532	0.10

syntaxial cement previously discussed. In such a case, they would have formed in meteoric water of low Eh and slow circulation rates, conditions which would have typically developed in the stagnant meteoric phreatic zone (Longman, 1980). Iron which was included in ferroan calcite crystals may have been present in the depositional environment or may have been derived from dewatering of clay minerals in the basin. Some ferroan calcite crystals in mud-supported rocks from the Rockdell Formation at Red House Branch (samples RHB'-8D, RHB'-8E, and RHB'-8F) exhibit zoning similar to the zoning in the clear stage of two stage syntaxial cement in Holston and Rockdell grain-supported rocks. The similarity in zonation pattern in the tow ferroan cement phases suggests they may have originated from similar fluids.

A much later time of formation of ferroan calcite is suggested by a positive correlation between authigenic quartz and ferroan calcite in the Holston and Rockdell formations at Red House Branch (see Appendix C). Authigenic quartz in these rocks is low in abundance but replaces both allochems and late diagenetic products (clear syntaxial cement). The correlation between these two rock constituents, then, suggests they both developed very late in the diagenetic history of these rocks.

There is also petrographic evidence which suggests that the pore central ferroan calcite cement in mud-supported rocks of the Holston Formation at Poor Valley Creek was the result of fluids which entered the rocks through fractures that developed during late diagenesis after significant lithification or during Late Paleozoic to Early Mesozoic

tectonism. Most samples examined in this study exhibited fractures filled with ferroan calcite which were oriented normal to bedding and truncate all diagenetic features except the last major set of stylolites (stylolites which were oriented at a slight angle to bedding). In one sample from Poor Valley Creek (PVC'-2D), a large fracture was observed which truncated all depositional and diagenetic features in the rock except pore central ferroan calcite within a large cavity. Examination of this sample in hand specimen suggests that the center of the cavity remained open until very late in the diagenetic history of this sample or possibly even more remarkable, until Late Paleozoic to Early Mesozoic structural deformation.

Ferroan (Baroque) Dolomite

Ferroan "saddle" dolomite (baroque dolomite) occurs as cement in both grain- and mud-supported rocks of the Holston and Rockdell formations at Poor Valley Creek and Red House Branch. This variety of dolomite is characterized by a warped crystal lattice which causes undulatory extinction. In samples from the Holston and Rockdell, ferroan dolomite crystals are turbid with inclusions. In most cases, the inclusions are unidentifiable, but staining reveals that micron-sized calcite inclusions are present in some crystals. All ferroan dolomite crystals observed in samples from the Holston and Rockdell formations are pseudopleochroic from tan to brown. Commonly, crystals are euhedral to subhedral and range in size from finely to very coarsely crystalline.

In many samples, ferroan dolomite appears to be associated with major stylolitic zones (Figure 3.13G, p. 123). In such cases, ferroan dolomite crystals are concentrated in and immediately adjacent to stylolites and decrease in abundance away from the stylolitic seams. This is primary evidence that large stylotlites were major conduits to lateral fluid migration during diagenesis. In grain-supported rock, ferroan dolomite occurs as pore central cement with planar grain boundaries (Figure 3.13H) or often exhibiting a poikilitic fabric with surrounding allochems. Stylolites may or may not be present in these grain-supported rocks.

Interpretation. Ferroan "saddle" dolomite in the Holston and Rockdell formations in northeastern Tennessee is interpreted as a primary cementing phase precipitated during late stages of diagenesis. The presence of micron-sized calcite inclusions in some ferroan dolomite crystals could be used as evidence of a replacement origin for this form of dolomite (i.e., relict calcite remaining from the original calcite precursor). However, there is no other evidence to support a replacement origin for the dolomite. Grain boundaries are consistently planar in nature. In grain-supported rocks, ferroan dolomite is always pore central or poikiliticly encloses allochems and cement and was never observed cross-cutting depositional fabric. The observed calcite inclusions could have formed by exsolution processes in disordered primary ferroan dolomite at elevated temperatures.

Radke and Mathis (1980) have determined that saddle dolomite may be used as a geothermometer as it is indicative of elevated

temperatures between 60°-150°C. The observation that saddle dolomite forms only at such temperatures and only occurs as pore central cement and associated with major stylolitic seams in both the Holston and Rockdell formations suggests that ferroan "saddle" dolomite developed in the late stages of diagenesis in the deep burial environment. The minimum depth of burial required for the formation of this form of dolomite using a standard geothermal gradient of 25°C/Km would have been 2.4 Km. This figure is obviously highly speculative. The true geothermal gradient may have been much higher due to the tectonic activity to the southeast.

CHAPTER 4

CEMENT ABUNDANCE AND DISTRIBUTION

Introduction

Environmental studies of Middle Ordovician rocks in East Tennessee, conducted in the 1970s and early 1980s, recognized the variety of diagenetic materials in these rocks. Those studies, however, were not structured to "map" or quantify the regional distribution of these diagenetic rock constituents. This is the first study which has sought to understand the stratigraphic variability of carbonate cement types on a regional scale (McGill, 1982, however, studied the variation in occurrence of carbonate cement in the Holston Formation near Knoxville, Tennessee). This study has shown that regional trends in cementation in the Ordovician sequence may be present and may be delineated through petrographic and geochemical analysis. To some degree, however, this study is only a model illustrating the overall complexity of diagenesis in Middle Ordovician carbonate rocks in East Tennessee and the enormous amount of this sequence which remains to be studied in detail.

The first part of this chapter concerns the cement abundance in the Holston and Rockdell formations by lithofacies. Second, the abundance of cement types at each of the four localities used in this study is presented. Third, cement abundances are presented relative to the abundance of depositional grains (allochems) in each rock (i.e., grain-supported and mud-supported rocks) followed by discussion of the

regional trends in cementation from shelf margin to on-shelf environments. Next, the observed stratigraphic trends in cementation at Red House Branch and Cedar Springs are discussed. Finally, the relative paragenetic sequence of carbonate cement in the Holston and Rockdell formations is outlined.

Cement Abundance and Distribution

Table 4.1 illustrates the distribution of cement in the Holston and Rockdell formations by lithofacies based on constituent analysis of 75 thin-sections. Syntaxial cement is not separated by type (turbid or clear). In both grain-supported lithologies of the Rockdell Formation, the dominant cementing phase is syntaxial cement on echinoderm grains, averaging 31% of the rock volume (approximately 86% of total cement) in the bryozoan-echinoderm grainstone/packstones and 19% (approximately 63% of total cement) in bryozoan-echinoderm packstones. Equant calcite is the second most common cement type. Bladed/prismatic cement and radiaxial-fibrous and associated cement are relatively less important, both in terms of their relatively low overall abundance and their decreasing abundance shelfward (discussed later) (Table 4.1). Ferroan calcite accounts for an average of 4.8% of the rock volume (approximately 16% of total cement) in bryozoan-echinoderm packstones in the Rockdell Formation but it is limited in occurrence to the Red House Branch locality as has been previously described (Table 4.1). The high abundance of ferroan calcite in this lithofacies is explained by the pervasiveness of this cement type at the Red House Branch locality.

Table 4.1. Distribution of carbonate cement by lithofacies in the Holston and Rockdell formations. The letter "n" at the top of each column indicates the number of thin-sections analyzed from tthat lithofacies. Note that Ferroan calcite and Ferroan (Baroque) dolomite occur in the Rockdell Formation only at Red House Branch.

	Rockdell Formation			Holston Formation		
	n = 8 Bryozoan-Echinoderm Grainstone/ Packstones	n = 14 Bryozoan-Echinoderm Packstones	n = 13 Bryozoan-Wackestones	n = 15 Bryozoan-Echinoderm Grainstone/ Packstones	n = 10 Echinoderm Bryozoan-Packstones	n = 15 Bryozoan-Wackestone/ Boundstones
	Radiaxial-Fibrous Calcite and Associated Cement					
Range	0.00-2.05	0.00-13.90	0.00-19.18	0.00-41.28	0.00-32.78	0.00-45.60
Average	0.46	1.75	2.78	10.73	13.67	14.89
	Bladed-Prismatic Cement					
Range	0.53-4.64	0.18-4.41	0.00-1.20	0.00-7.65	0.00-4.57	0.00-4.22
Average	1.65	1.34	0.25	2.57	1.32	1.68
	Syntaxial Cement					
Range	20.90-39.47	3.56-30.90	0.00-6.71	0.75-28.92	0.74-27.52	0.00-13.30
Average	30.98	18.96	1.35	18.66	9.50	2.98
	Equant (Drusy) Calcite Cement					
Range	0.26-4.81	0.36-15.49	0.12-18.46	0.00-10.86	0.00-17.13	0.17-9.28
Average	2.07	6.30	5.72	3.97	5.43	3.88
	(RHB only)	Ferroan Calcite Cement				
Range	0.13-1.86	1.19-11.29	0.25-4.14	0.00-7.50	0.00-4.92	0.00-3.99
Average	0.97	4.82	1.73	1.07	1.01	0.40
	(RHB only)	Ferroan (Baroque) Dolomite				
	n = 4	n = 3	n = 4			
Range	0.00-0.12	0.00-0.12	0.00-7.55	0.00-6.10	0.00-16.35	0.00-3.92
Average	0.03	0.04	3.83	1.09	2.26	0.28

Equant calcite is the predominant cement in the bryozoan wackestone lithofacies of the Rockdell Formation, accounting for an average of 5.7% of the rock volume (approximately 63% of total cement) in this lithofacies (Table 4.1). This cement phase is primarily developed in irregularly shaped cavities in lime-mud mounds at the on-shelf localities as will be described later. Ferroan (baroque) dolomite, radiaxial-fibrous calcite and associated cement, and ferroan calcite follow equant calcite in importance in the bryozoan wackestone lithofacies (Table 4.1). Their relative abundance reflects the predominance of these cementing phases in bryozoan wackestones exposed at Red House Branch. Syntaxial overgrowth cement is the fifth most abundant cementing phase in this lithofacies, accounting for an average of only 1.4% of the rock volume (approximately 10% of total cement) in this lithofacies (Table 4.1). The low abundance of syntaxial cement in the bryozoan wackestones reflects the relatively low abundance of echinoderm debris in this lithofacies.

Syntaxial overgrowth cement is the dominant cement type in Holston echinoderm-bryozoan grainstone/packstones, averaging 18.7% of the rock volume (approximately 55% of total cement) (Table 4.1). Radiaxial-fibrous and associated cement are the second most common cement types in this lithofacies, averaging 10.7% of the rock volume (approximately 25% of total cement). Conversely, radiaxial-fibrous and associated cement are the most abundant cement types in the echinoderm-bryozoan packstone lithofacies, averaging 13.7% of the rock volume (approximately 41% of total cement) (Table 4.1). Syntaxial overgrowth cement

represents the second most abundant cement type in this lithofacies, averaging 9.5% of the rock volume (approximately 33% of total cement). The difference in the relative abundance of syntaxial and radiaxial-fibrous cement between these two grain-supported lithofacies probably reflects the difference in their depositional environments. The echinoderm-bryozoan packstone lithofacies represents deeper-water conditions and in most cases is associated with lime-mud mounds (Ruppel and Walker, 1982). These deposits accumulated in "weakly agitated conditions" allowing cementation by fibrous cement similar to that observed in modern and ancient reef environments (Ruppel and Walker, 1982) (see James et al., 1976; Ginsburg and James, 1976; and Davies 1977). The echinoderm-bryozoan grainstone/packstone lithofacies represents an environment which was episodically turbulent as evidenced by abrasion of grains and low abundance of microcrystalline matrix material (see Chapter 2). Early formed fibrous crystals would have had less chance to be preserved in this environment. Equant calcite is the third most common cement type in grain-supported rocks of the Holston Formation (Table 4.1). As noted previously, this cement is primarily limited to intraparticle pores of bryozoans, articulated brachiopods and ostracodes. The two least important cement types in Holston grain-supported rocks are ferroan calcite and bladed/prismatic cement, respectively (Table 4.1).

Radiaxial-fibrous and associated cement are the most common cement types in Holston bryozoan wackestone/boundstones, averaging 14.9% of the rock volume (approximately 53% of total cement) (Table 4.1). As

noted previously, these cement types are primarily developed in depositional and early diagenetic cavities on polycrystalline substrates. The predominance of fibrous marine cement in the bryozoan wackestone/-boundstone lithofacies illustrates the cavernous nature of these masses as well as their early lithification in the marine environment (Bathurst, 1959, 1980). Equant calcite is the second most abundant cement type in Holston wackestone/boundstones, averaging 3.9% of the rock volume (approximately 20% of total cement) (Table 4.1). Equant calcite is common as pore central cement within bryozoan zooecia but also is developed as pore central cement in large stromatactoid and irregularly shaped cavities. Syntaxial overgrowth cement is the third most common cement type in these rocks (Table 4.1). By visual estimate, over 75% of the syntaxial cement in this lithofacies is turbid and marine in origin. Ferroan calcite and bladed/prismatic cement represent the two least important cement types in this lithofacies (Table 4.1).

Figures 4.1-4.4 illustrate the distribution of cement types by volume percentage abundance at each of the four outcrop localities used in this study. Syntaxial cement is not separated by type (turbid or clear). Marine cement (radiaxial-fibrous calcite and associated cement, turbid rim cement, and bladed/prismatic cement) is best developed in the Holston and Rockdell formations at Red House Branch and Poor Valley Creek and, in most samples, represent the predominant cement phases (Figures 4.1, 4.2). Radiaxial-fibrous and associated cement are much less abundant at the two on-shelf localities, Cedar

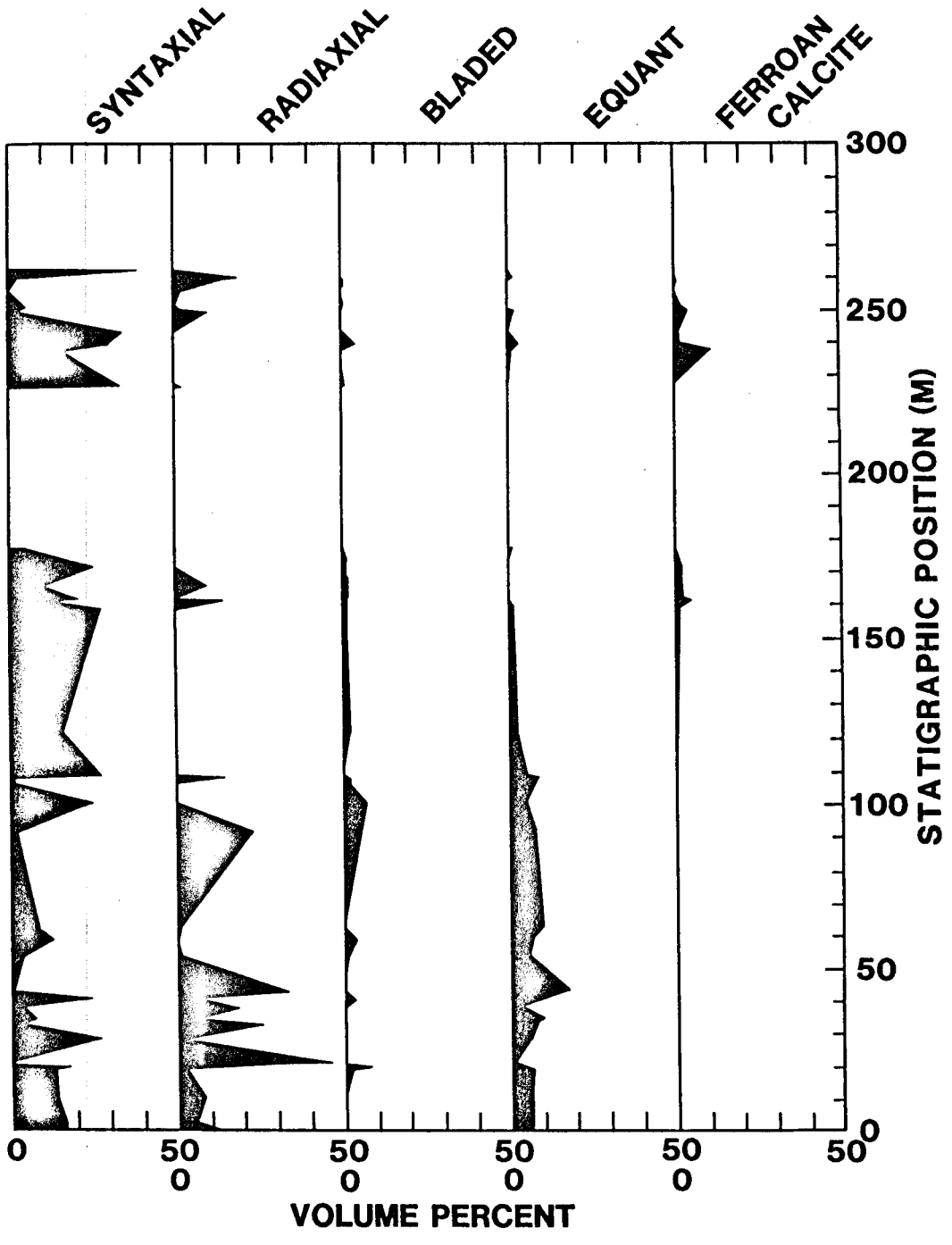


Figure 4.1. Percent volume abundance of cement types at Red House Branch versus stratigraphic position. The vertical scale is 0-300 m and the horizontal scale is 0-50 volume percent.

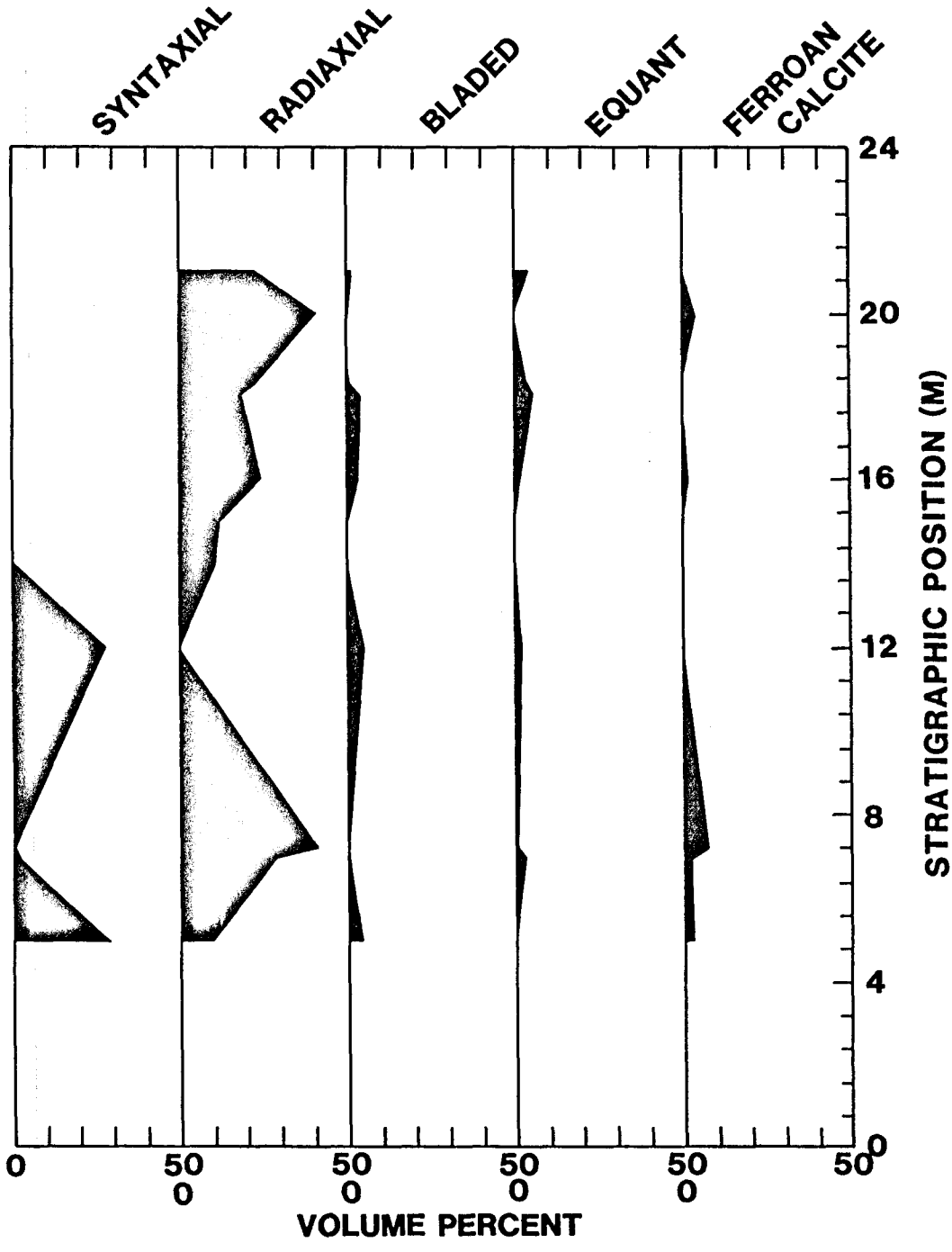


Figure 4.2. Percent volume abundance of cement types at Poor Valley Creek versus stratigraphic position. The vertical scale is 0-24 m and the horizontal scale is 0-50 volume percent.

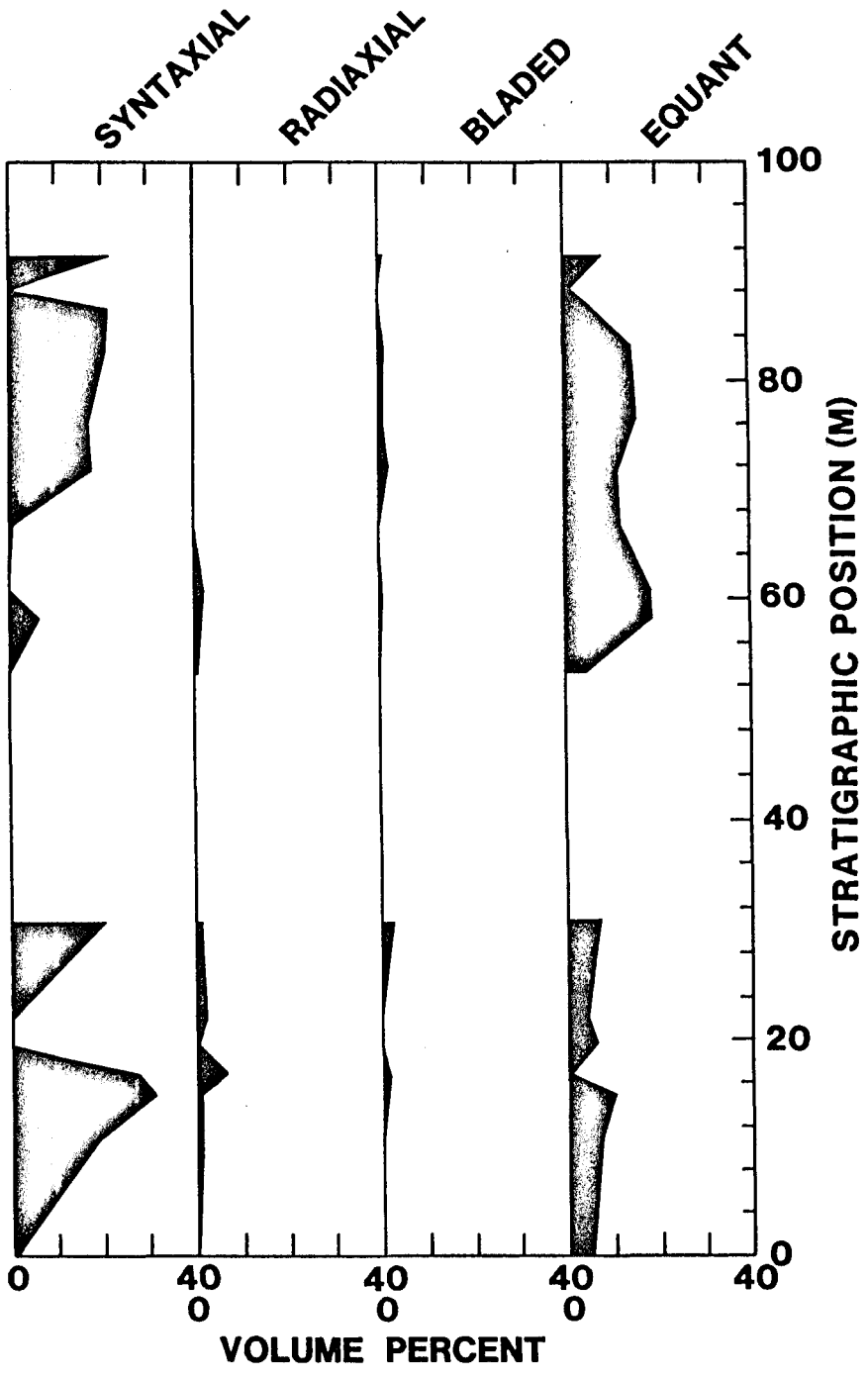


Figure 4.3. Percent volume abundance of cement types at Cedar Springs versus stratigraphic position. The vertical scale is 0-100 m and the horizontal scale is 0-40 volume percent. Ferroan calcite does not occur at this locality.

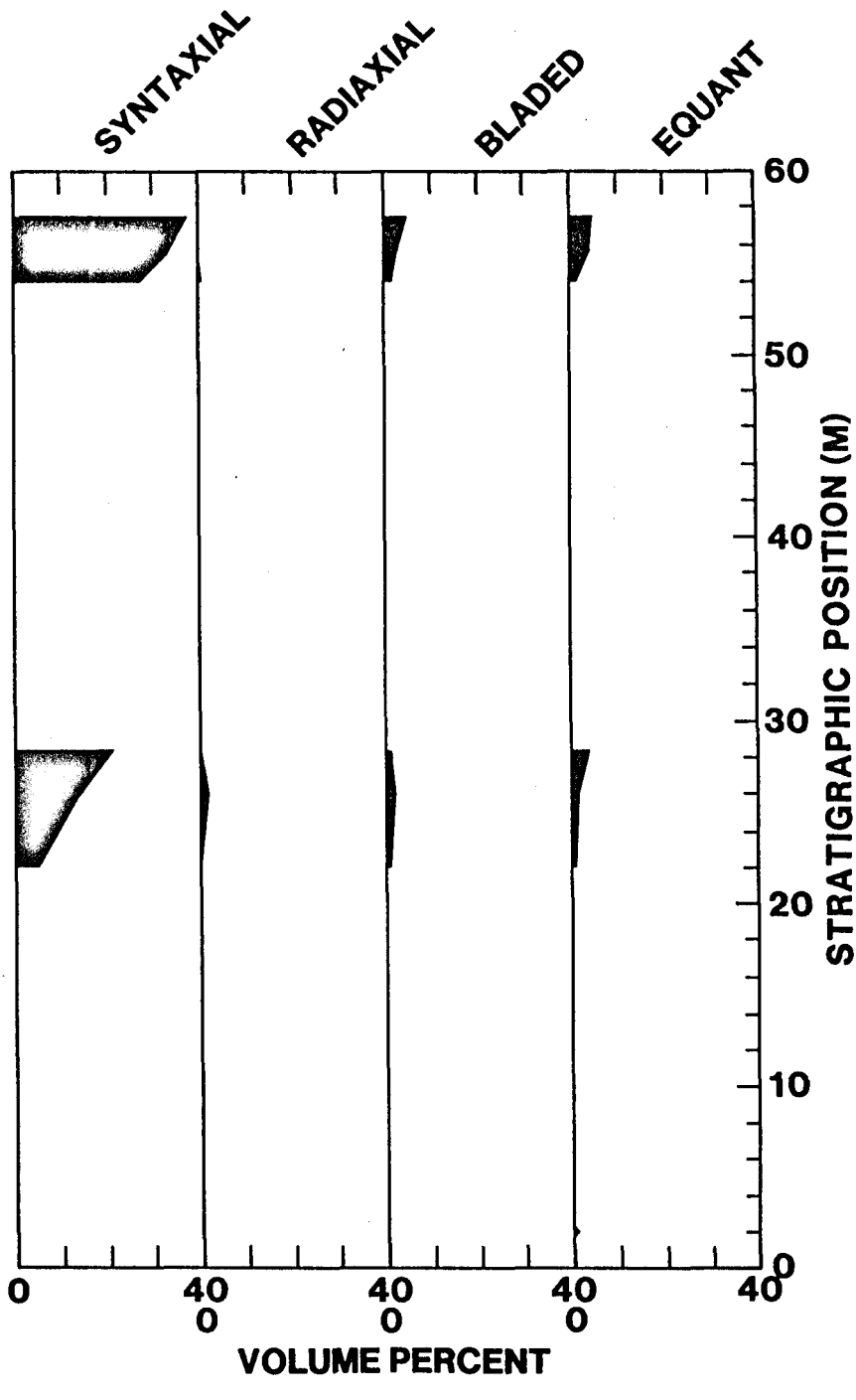


Figure 4.4. Percent volume abundance of cement types at Evans Ferry versus stratigraphic position. The vertical scale is 0-60 m and the horizontal scale is 0-40 volume percent. Ferroan calcite does not occur in this locality.

Springs and Evans Ferry (Figures 4.3, 4.4). Turbid syntaxial cement is also less abundant at these localities, but in over 90% of the grain-supported samples examined, two stage overgrowths are developed with a thin, initial turbid phase adjacent to the host echinoderm grain followed by a much thicker, clear phase. Meteoric cement (clear syntaxial overgrowth cement and equant calcite) generally is best developed at Cedar Springs and Evans Ferry (Figure 4.3, 4.4).

Figures 4.1-4.4 also illustrate an inverse relationship between syntaxial cement on echinoderm grains and radiaxial-fibrous calcite and associated cement. This relationship is also supported by a slight negative correlation between these two cement types at Red House Branch (see Appendix C). Conversely, there is a positive relationship between echinoderm syntaxial cement and bladed/prismatic cement at all localities except Red House Branch (compare Figures 4.1-4.4 with Appendix C). These relationships may help explain an apparent discrepency between petrographic observation and statistical correlation of cement substrate preference. In samples which exhibit extensive cementation by radiaxial-fibrous calcite or an associated cement, it appears to be preferentially developed on bryozoans primarily because they are the most common and largest polycrystalline allochem in those samples. However, these two variables, bryozoans and radiaxial-fibrous calcite, are never positively correlated with each other in the constituent analysis data set or its subsets (outcrops, rock types, etc.; see Appendix C). The explanation for this apparent discrepancy is that the values of radiaxial-fibrous cement in the constituent analysis data set

are not normally distributed. Many samples which contain abundant bryozoans exhibited little or no cementation by radiaxial-fibrous calcite or its associated cement. In those samples, bladed/prismatic cement and turbid syntaxial cement are the dominant marine cement types.

Figures 4.5 and 4.6 are ternary diagrams which illustrate the relative cement abundances in Holston and Rockdell formation grain-supported and mud-supported rocks, respectively. In both figures, samples from the Rockdell Formation are separated into two groups: (1) Rockdell samples from the shelf margin locality (Red House Branch); and (2) Rockdell samples from well on-shelf (Cedar Springs and Evans Ferry). In these figures, radiaxial-fibrous calcite and associated cement have been combined with bladed/prismatic cement and comprise the left end-member on the diagram. Turbid and clear syntaxial overgrowth cement are combined in these figures and make up the top end-member and clear equant calcite is represented in the right end-member. Samples which plot to the left in these diagrams have undergone substantial submarine cementation while samples which plot on the right side have undergone greater cementation in the meteoric environment. Those samples which plot at the top (near the Syntaxial Cement apex) represent samples which have undergone both marine and freshwater diagenesis, because syntaxial overgrowths on echinoderms (especially in shelf marginal samples) usually consist of an initial turbid marine phase followed by a later clear meteoric phase.

Figure 4.5. Relative cement abundance in Holston and Rockdell Formations grain-supported rocks. Rockdell samples are separated into two groups based on depositional position relative to the Middle Ordovician shelf margin. Syntaxial overgrowth cement includes both turbid and clear overgrowths in this diagram.

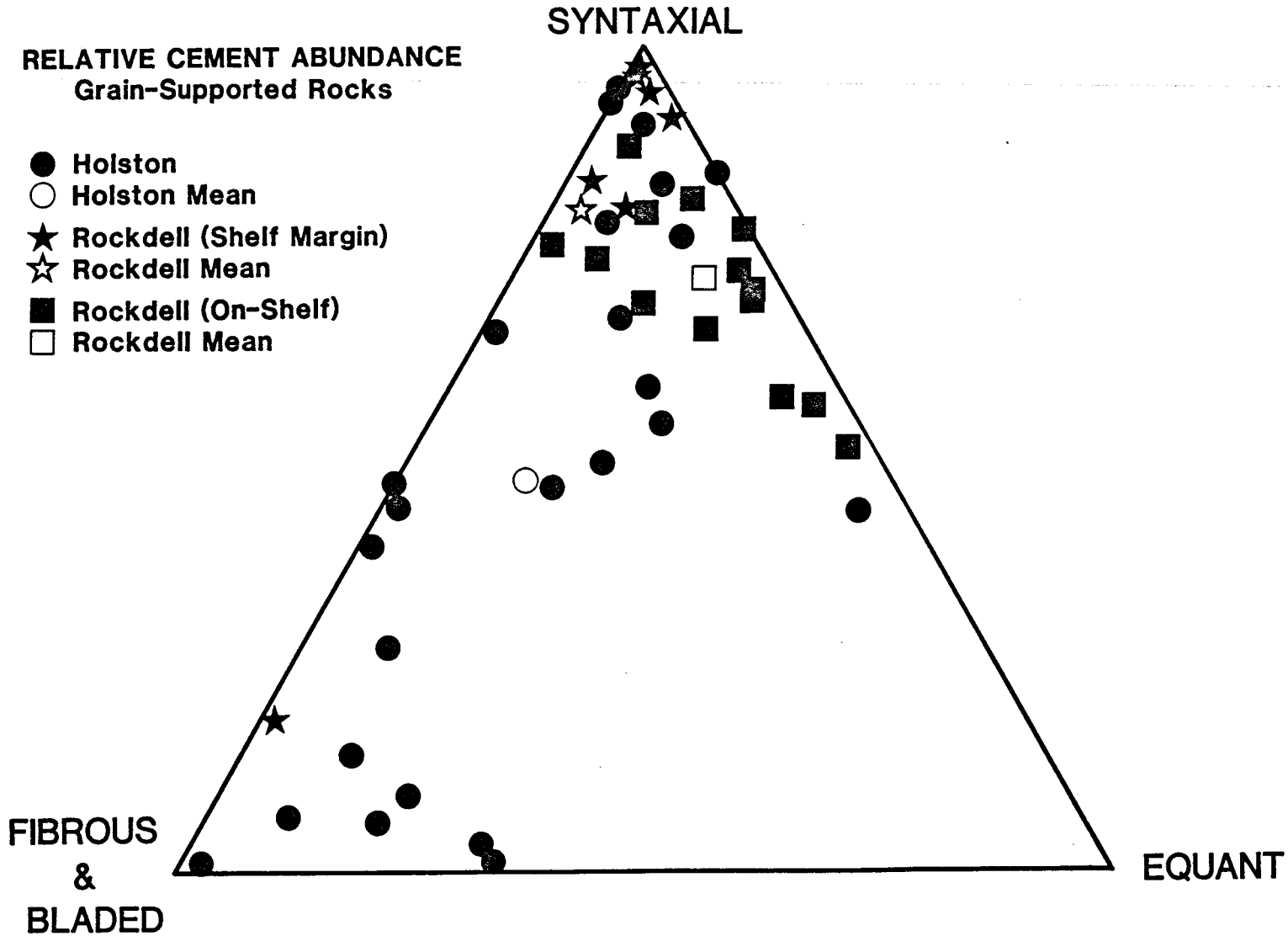
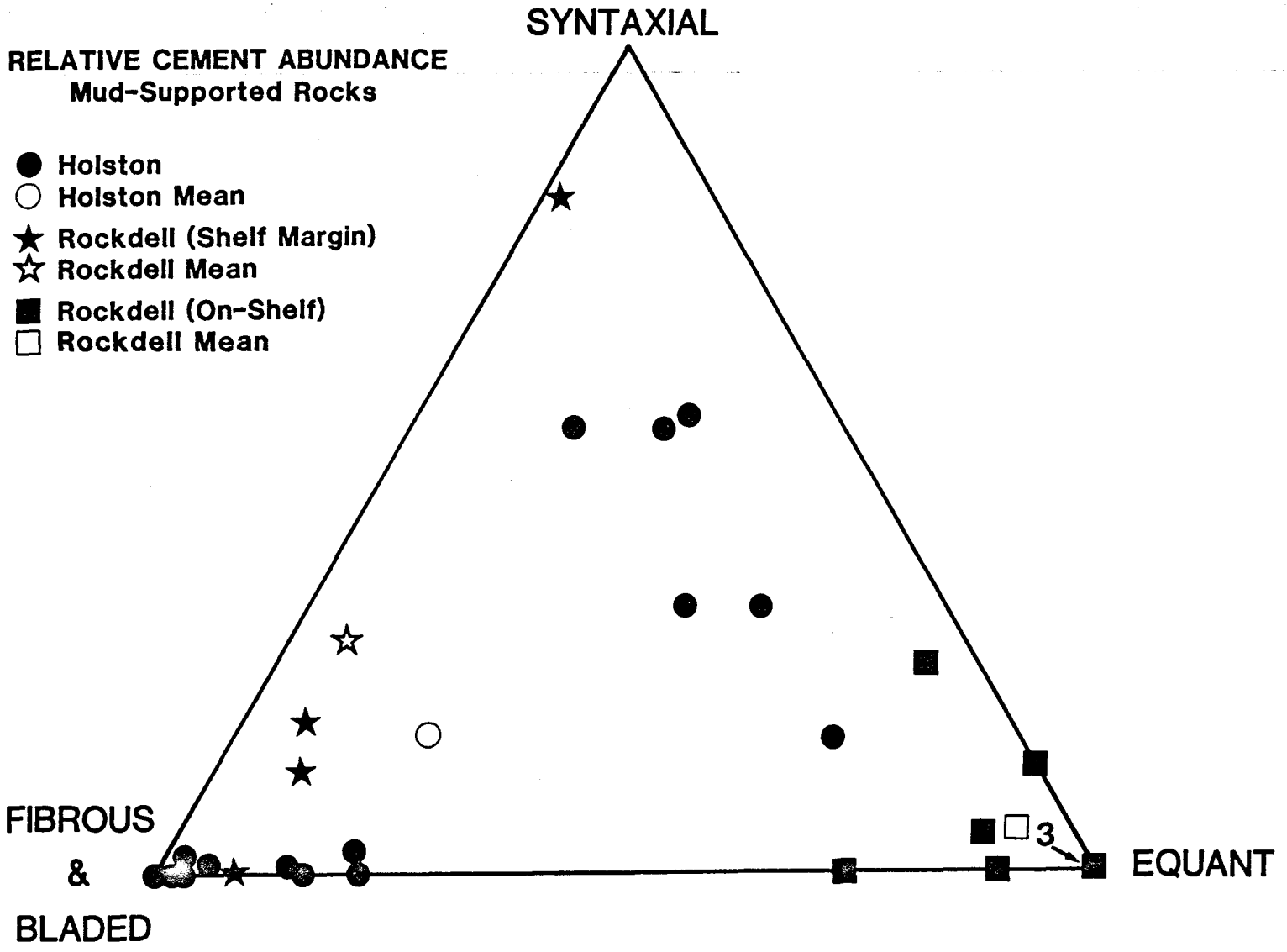

SYNTAXIAL
RELATIVE CEMENT ABUNDANCE
Grain-Supported Rocks
Holston
Holston Mean
Rockdell (Shelf Margin)
Rockdell Mean
Rockdell (On-Shelf)
Rockdell Mean
FIBROUS
&
BLADED
EQUANT

Figure 4.6. Relative cement abundance in Holston and Rockdell Formations mud-supported rocks. Rockdell samples are separated into two groups based on depositional position relative to the Middle Ordovician shelf margin. Syntaxial overgrowth cement includes both turbid and clear overgrowth in this diagram.


SYNTAXIAL
RELATIVE CEMENT ABUNDANCE
Mud-Supported Rocks
Holston
Holston Mean
Rockdell (Shelf Margin)
Rockdell Mean
Rockdell (On-Shelf)
Rockdell Mean
FIBROUS
&
BLADED
3
EQUANT

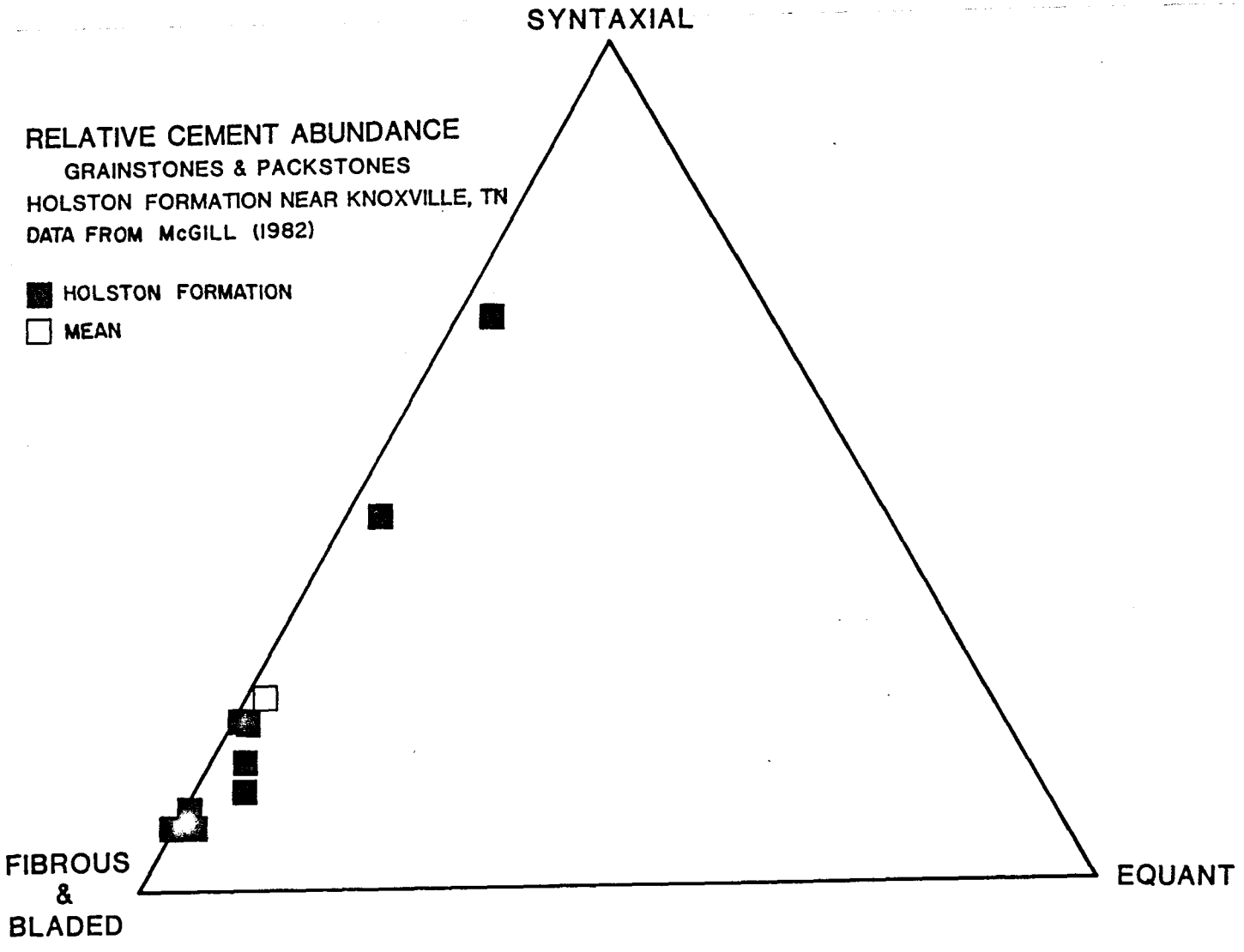
The grainstone/packstone and packstone lithofacies of the Holston and Rockdell formations are represented in Figure 4.5. It appears that Holston samples may represent two distinct populations: (1) samples which exhibit >50% fibrous and bladed cement and; (2) samples which exhibit <50% fibrous and bladed cement. These two populations generally reflect samples which occur adjacent to lime-mud mounds (>50% fibrous and bladed cement) and samples which are away from lime-mud mounds (<50% fibrous and bladed cement). For the remainder of this discussion, however, Holston samples will be treated as a single population. Samples from the Rockdell formation near the shelf margin plot near the syntaxial overgrowth end-member but note that one sample plots well out of that field near the fibrous-bladed end-member. Samples from the Rockdell Formation at the on-shelf localities all plot in the upper one-half (>50% syntaxial cement) of the diagram and always below 22% fibrous and bladed cement. It is important to note that the syntaxial cement in these on-shelf Rockdell samples is primarily the clear meteoric variety or may have a thin initial turbid zone. The means of each population have also been plotted in Figure 4.5. From this figure, it is apparent that sediment deposited at or near the shelf margin underwent greater submarine cementation than similar sediment deposited well on-shelf.

Similar relationships are apparent in Figure 4.6 which represents the Rockdell Formation bryozoan wackestone lithofacies and the Holston Formation bryozoan wackestone/boundstone lithofacies. Holston samples again plot in two fields: (1) samples which contain >75% fibrous and

bladed cement and; (2) samples which contain <30% fibrous and bladed cement. These two populations actually represent lime-mud mound samples which contain abundant depositional and early diagenetic cavities (>75% fibrous and bladed cement) and samples which are noncavernous (<30% fibrous and bladed cement). Again, Holston samples will be treated as one population. Most Rockdell samples from the shelf margin plot near the fibrous and bladed cement end-member while Rockdell samples from the on-shelf localities plot near the equant calcite end-member. The means of each population have also been plotted on Figure 4.6. As in Figure 4.5, it is apparent that toward the basin, there is a substantial increase in the amount of marine cement within similar lithologies in the Holston and Rockdell formations.

If the observed trend from meteoric dominated cementation on-shelf to marine dominated cementation at the shelf margin is real, then it should be reflected in samples from similar rocks deposited even closer to the basin. McGill (1982) studied the cementation history of the Holston Formations near Knoxville, focusing primarily on the grain-supported lithofacies. Relative cement abundance data from her Alcoa Highway section (shelf margin to slightly down-slope) have been plotted in Figure 4.7. By comparison to Figure 4.5, rocks from the Holston Formation exposed at Alcoa Highway exhibit even more extensive cementation by fibrous and bladed marine cement than rocks of the Holston and Rockdell formation which were taken from the shelf margin localities in northeastern Tennessee. These additional data further support the trend toward greater marine cementation toward the basin.

Figure 4.7. Relative cement abundance in Holston Formation grainstones and packstones near Knoxville, Tennessee. Data for this diagram derived from McGill's (1982) constituent analysis of samples from the Alcoa Highway section. Syntaxial overgrowth cement includes both turbid and clear overgrowths in this diagram.

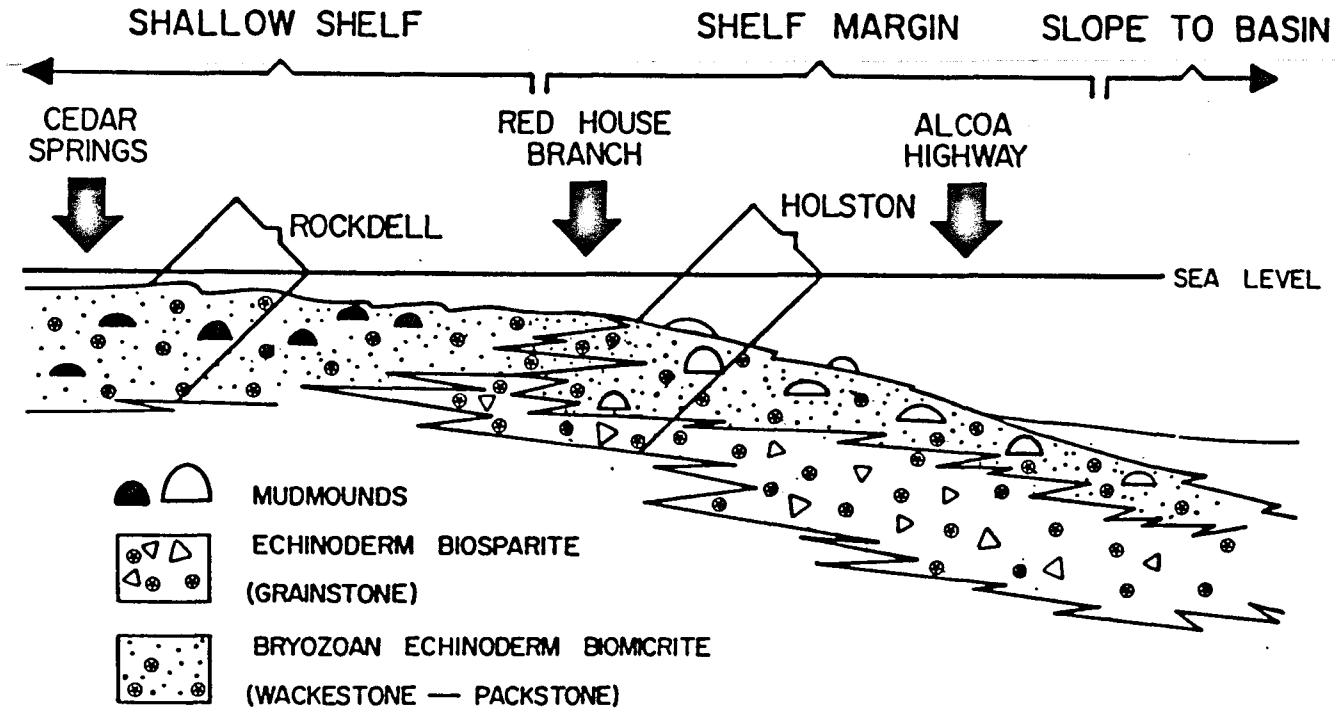

SYNTAXIAL
RELATIVE CEMENT ABUNDANCE
GRAINSTONES & PACKSTONES
HOLSTON FORMATION NEAR KNOXVILLE, TN
DATA FROM McGILL (1982)
HOLSTON FORMATION
MEAN
FIBROUS
&
BLADED
EQUANT

Qualitatively, it appears that less marine cementation toward the shelf may have allowed a greater degree of early compaction in Rockdell sediment in northeastern Tennessee (Jernigan and Walker, 1985). McGill has noted that early compaction was a minor phenomenon in the Holston Formation at the Alcoa Highway section. The overall trend in cementation and early compaction from on-shelf to shelf margin is discussed in the next chapter, but summarized herein Figure 4.8.

The abundance of marine cement in samples from the Holston and Rockdell formations at the shelf margin may be explained by greater tidal pumping of seawater through sediment deposited in shelf marginal environments. As noted in modern carbonate shelf marginal environments, marine cementation occurs where seawater is forced through sediment by the action of waves and tides (Shinn, 1971; Schroeder, 1972; James et al., 1976; Matthews, 1974). Shelfward, due to more restricted hydrodynamic conditions (because of the dampening effect of the shelf margin), sediment of the Rockdell Formation was subjected to reduced tidal and wave flushing of seawater through pores and thus developed less marine cement.

Stratigraphic Patterns of Cementation

An important question resulting from this thesis is: Are there any regional stratigraphic cementation patterns which might be recognizable using petrographic constituent analysis data? Using the data collected in this thesis and additional data collected in the Summer, 1986, a feasibility study was undertaken to examine this question



CEDAR SPRINGS	RED HOUSE BRANCH	ALCOA HIGHWAY
__ METEORIC DOMINATED CEMENTATION	__ MARINE DOMINATED CEMENTATION	__ MARINE DOMINATED CEMENTATION
__ EARLY COMPACTION COMMON	__ MINOR EARLY COMPACTION	__ MINOR EARLY COMPACTION

Figure 4.8. Idealized cross-section across the Middle Ordovician carbonate shelf in northeastern East Tennessee illustrating the relative position of the Cedar Springs, Red House Branch, and Alcoa Highway sections relative to the shelf margin and the tends in compaction and cementation across the shelf.

(Walker, Jernigan, Johnson, and Foreman, 1986). The Red House Branch and Cedar Springs localities were used to examine this question because these two localities were sampled most thoroughly. Figure 4.9 illustrates the stratigraphic relationships between the Holston and Rockdell formations at these two localities. It is important to note that the lower part of the Holston Formation at Red House Branch is older than the lower part of the Rockdell Formation at Cedar Springs and is correlative to the uppermost Five Oaks and the lowermost Lincolnshire formations at Cedar Springs. Note also that the upper contact of the Rockdell Formation is slightly older at Red House Branch than at Cedar Springs.

Table 4.2 lists the diagenetic environment of formation of carbonate cement types as discussed in Chapter 3. Cement data derived from constituent analysis of each sample from Red House Branch and Cedar Springs were tabulated using this environmental scheme. Visual estimates were used to determine the volume percentage of turbid syntaxial cement in each sample in order to make the data more accurate. The volume percentage of each cement category was compared, then, from locality to locality.

Figure 4.10 shows the 3x3 moving average curves of the volume percentages of the three major cement categories (marine, meteoric, and burial derived) versus stratigraphic level at Red House Branch. Also in this figure is a 3x3 moving average of total-cement volume percentage versus stratigraphic level. It is evident from this illustration, that some stratigraphic units are dominated by marine

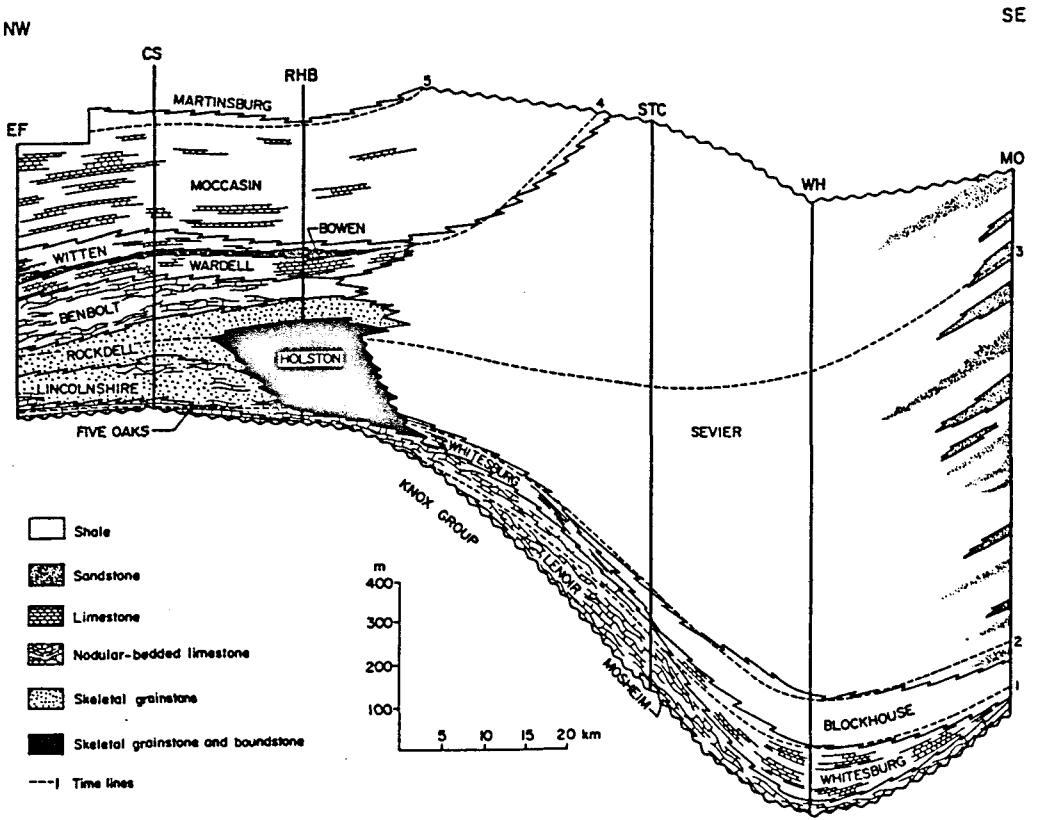


Figure 4.9. Stratigraphic cross-section drawn through the Copper Creek allochthon illustrating the stratigraphic relationships between the Holston and Rockdell formations at Cedar Springs (CS) and Red House Branch (RHB). The lower part of the Holston Formation at Red House Branch is older than the lower part of the Rockdell Formation at Cedar Springs. (From Ruppel and Walker, 1982).

Table 4.2. Diagenetic environment of formation of carbonate cement types in the Holston and Rockdell formations in northeastern Tennessee. The texture and fabric of each cement type is discussed in detail in Chapter 3.

Cement Type	Marine	Freshwater	Deep-burial
Baroode dolomite			X
Bladed/prismatic calcite	X		
Clear syntaxial calcite		X	
Equant (brusy) calcite		X	
Fascicular-octic calcite	X		
Ferroan calcite (pore-central)			X
Radial fibrous calcite	X		
Radiaxial fiber calcite	X		
Turbid syntaxial calcite	X		

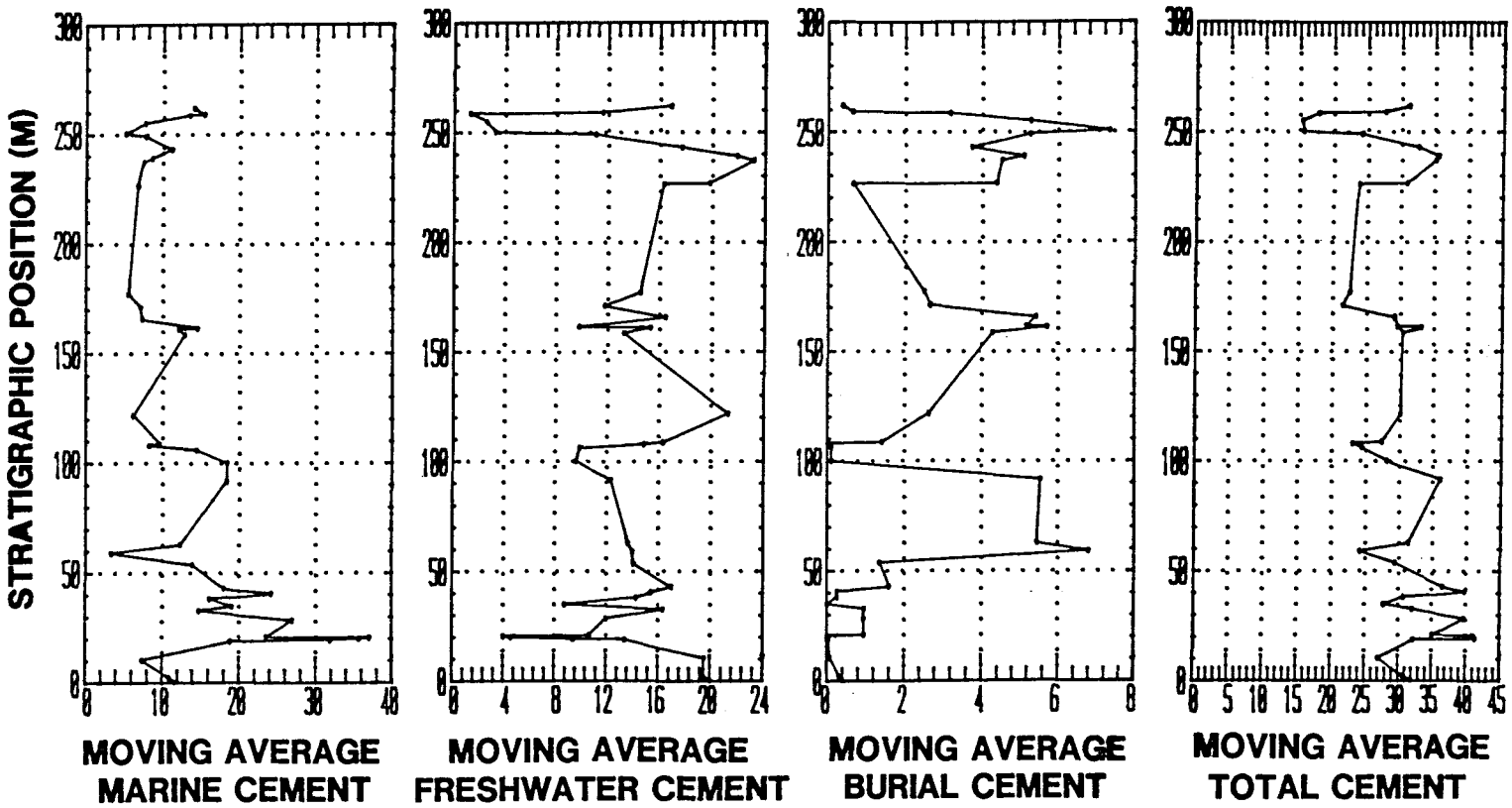


Figure 4.10. 3 x 3 moving averages of marine, freshwater, and burial cements versus stratigraphic position in the Holston and Rockdell Formations at Red House Branch. The fourth curve shows the moving average of total cement.

cement, others by meteoric cement, and still other units characterized by unusually high volumes of burial cement. Table 4.3 shows the stratigraphic distribution of cement zones illustrated in Figure 4.10. The most important conclusion which could be drawn from Figure 4.10 and Table 4.3 is the presence at Red House Branch of several repeated cement-zone sequences or cycles, each consisting of three parts: (1) a lowermost interval which contains abundant marine cement, (2) a middle interval in which cement derived from meteoric fluids is dominant, and (3) an uppermost interval characterized by a high volume of cement derived from burial fluids. There is only one possible exception to the observed pattern. The minor burial cement peak between 20 and 35 m actually represents only 1.0% by volume and falls in a zone dominated by marine cement. Otherwise, the cyclical cementation pattern is clear.

Figure 4.11 shows the 3x3 moving average curves of the three types of cement (marine, meteoric,and burial derived) versus stratigraphic level in the Rockdell Formation at Cedar Springs. A plot of the 3x3 moving average of total cement versus stratigraphic level at Cedar Springs is also provided. The stratigraphic patterns of cementation are less clear here, due primarily to the smaller sample size from this section. As discussed previously in this chapter, the abundance of marine cement is greatly reduced in the Rockdell Formation at the shelfward localities, however, it is interesting to note the presence of a marked "peak" in marine cement abundance at 10-20 m above the lower contact of the Rockdell Formation (Figure 4.11). Cement derived

Table 4.3. Stratigraphic range of cement zones in the Holston and Rockdell Formations at Red House Branch.

Stratigraphic Zone	Dominant Cement Type		
	Marine	Freshwater	Burial
265 m		X	
260–264 m	X		
240–260 m			X
160–240 m		X	
160 m	X		
130–160 m			X
100–130 m		X	
90–100 m	X		
60–80 m			X
40–60 m		X	
20–35 m			? X ?
15–40 m	X		
0–15 m		X	

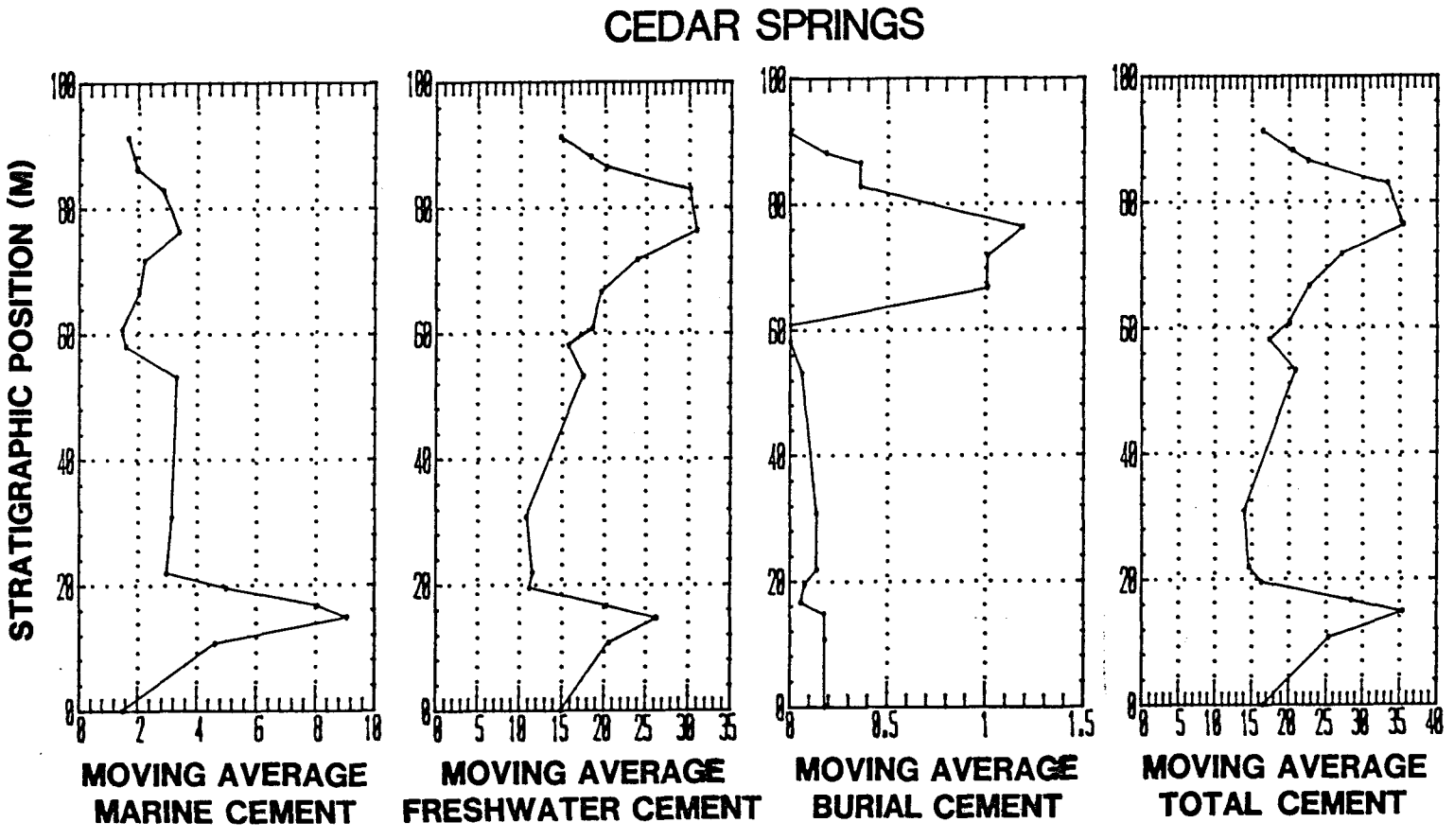


Figure 4.11. 3 x 3 moving averages of marine, freshwater, and burial cements versus stratigraphic position in the Rockdell Formation at Cedar Springs. The fourth curve shows moving average of total cement.

from meteoric fluids is characteristically abundant at Cedar Springs, but peaks at 0.5 m, 20-24 m, 56-64 m, and approximately 91 m. The abundance of burial cement at Cedar Springs appears to peak in two separate intervals, 20-30 m and 65-80 m. These "peaks" are considerably smaller than burial cement peaks at Red House Branch (Figure 4.10) and the actual maximum volume percentages are almost an order of magnitude smaller. However, the two burial peaks at Cedar Springs may correspond in time to the upper two burial cement peaks at Red House Branch, since they occur at approximately the same stratigraphic levels (see Figure 4.9). Johnson (in preparation) has determined that an earlier burial cement peak occurs stratigraphically below the Rockdell Formation at Cedar Springs in the Lincolnshire Formation. That peak may be equivalent to the first burial cement peak in the Holston Formation at Red House Branch. Because of the coarse sampling interval at Cedar Springs, more sampling is needed to confirm this conclusion.

The corresponding burial cemented zones at Red House Branch and Cedar Springs may mark the stratigraphic routes of basin derived fluids. As compaction of sediment deposited in the shale basin proceeded to the southeast in mid late-Paleozoic time, fluids generated by dewatering of clay minerals probably flowed northwestward toward the Ordovician shelf sequence (an area of lower lithostatic pressure). These basinal "brines" could have most readily penetrated shelf marginal sediment with the greatest remaining macro-porosity,the sediment that now contain substantial amounts of burial cement. This hypothesis

is supported by two lines of evidence. First, burial cement is substantially more abundant at Red House Branch than at Cedar Springs, which would be expected if the basinal fluids were flowing from the shelf marginal sequence toward the shelf sequence. Second, the "peaks" in burial cement occur at approximately the same stratigraphic levels at the two localities.

It is not clear what controls the cementation cycles delineated in this study. The marine cemented intervals may represent times of marine transgression followed by sea level drop and meteoric dominated cementation. Turbulent bottom conditions may have limited marine cementation in some zones,allowing for greater cementation in the meteoric environment. The relatively higher bathymetric position at Cedar Springs may have subjected sediments at that locality to more intense cementation during any sea level low stand. Also, because the Cedar Springs section is thinner, the entire sequence may have been subjected to freshwater alteration more than once shortly after deposition. Clearly, for more complete interpretations, more data are needed. This study, however, indicates that fluid flow pathways and the timing of fluid migration may be delineated.

Paragenetic Sequence of Cements

Figure 4.12 details the relative timing of formation of the various cement phases described in this chapter. In the marine environment, microcrystalline cement formed first in intraparticle pores and

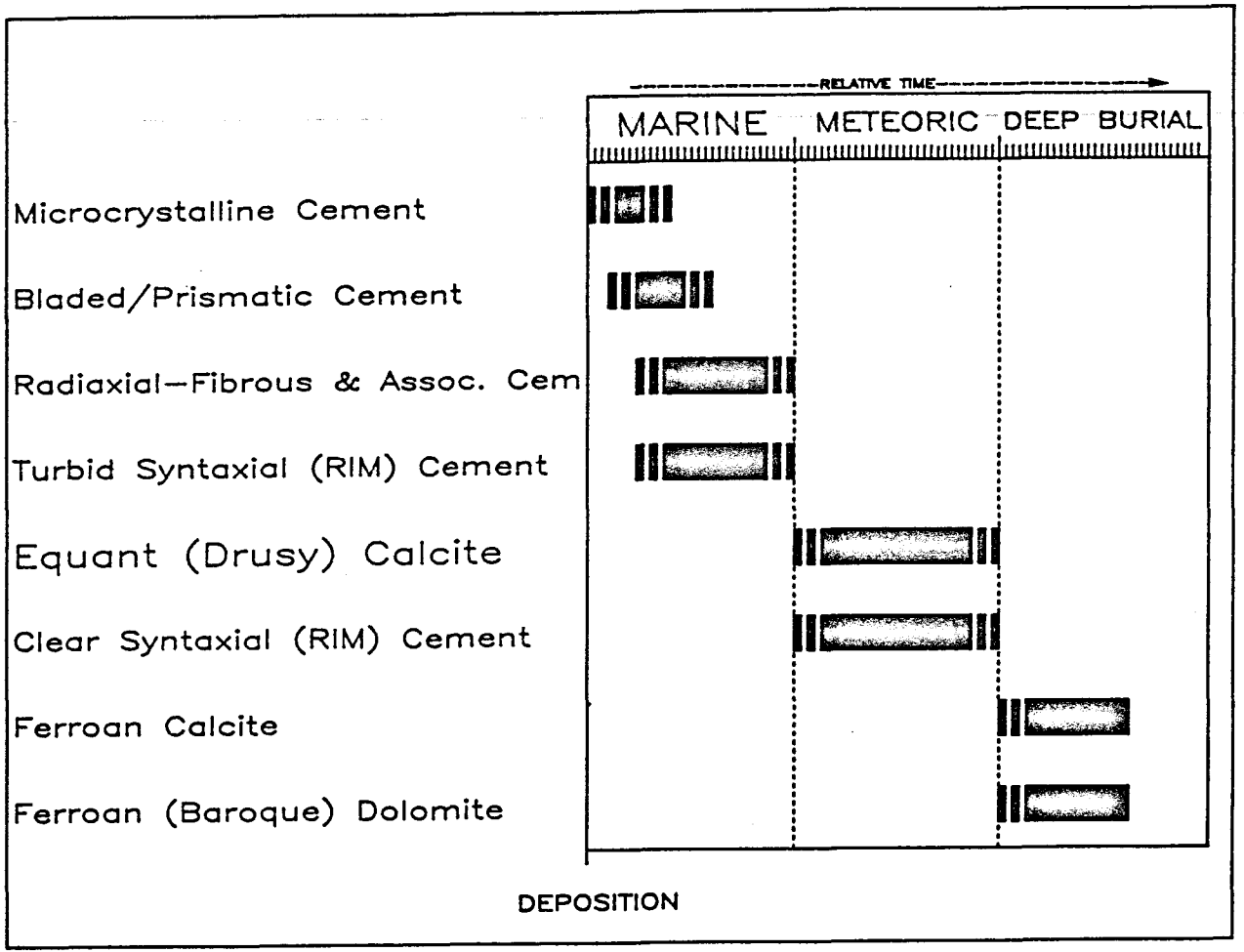


Figure 4.12. Summary of the paragenetic sequence of carbonate cements in the Holston and Rockdell Formations in northern East Tennessee.

depositional cavities. Bladed/prismatic cement formed second and may have overlaped in time with microcrystalline cement but formed in both intraparticle and interparticle pores. Radiaxial-fibrous calcite and its associated cement and turbid syntaxial overgrowth cement formed next. These two cement groups are the dominant marine cement types in the Holston and Rockdell formations. They always developed after microcrystalline cement but may be coeval with bladed/prismatic cement in some samples.

Clear syntaxial overgrowth cement and clear equant calcite cement both formed in the meteoric diagenetic environment. These cement types are largely coeval, but in echinoderm-rich sediment, clear syntaxial cement was the preferred cement phase. In these rocks, clear syntaxial cement may fill all remaining pore space or may even poikilitic1y enclose surrounding polycrystalline grains, a characteristic of syntaxial cement noted in other carbonate sequences (see Lucia, 1962; Evamy and Shearman, 1965). Ferroan calcite, which is probably formed after burial, postdates all other cement phases except the ferroan syntaxial cement zones on some echinoderms in the Holston Formation at Red House Branch and Poor Valley Creek.

CHAPTER 5

RELATIVE TIMING OF NONCEMENTATION DIAGENETIC EVENTS

Introduction

The cementation history of carbonate rocks, especially the "early" cementation history, strongly influences the effect other diagenetic processes have on these rocks (Flugel, 1982). For example, early (marine) cementation may inhibit or diminish the effects of compaction on carbonate sand by making the sediment rigid, reducing grain-to-grain movement. This chapter briefly summarizes the diagenetic features observed petrographically in terms of their time of formation relative to the formation of the seven cement phases discussed in Chapters 3 and 4.

Figures 5.1 and 5.2 illustrate the relative sequence of diagenetic events, including cementation, in grain- and mud-supported rocks of the Holston and Rockdell formations, respectively. The following discussion describes the diagenetic features illustrated in these figures in the following order: (1) macroboring and micritization; (2) stromatactoid and irregular (nonstromatactoid) cavity formation and internal sedimentation; (3) mineralogic stabilization; (4) neomorphism; (5) dolomitization; (6) silicification; (7) compaction; and (8) fracturing. For a comprehensive discussion of the cementation history of these rocks, see Chapters 3 and 4.

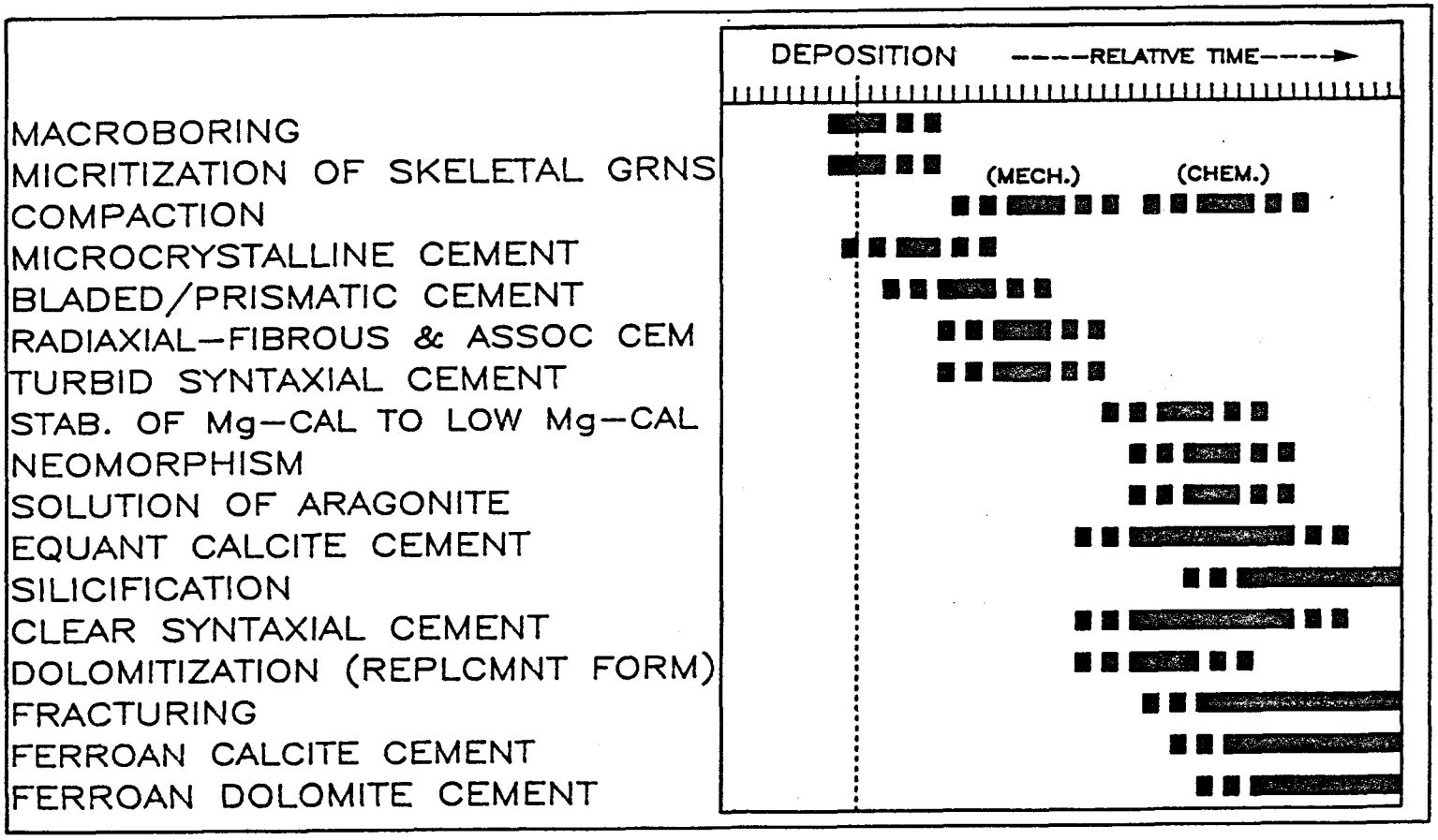


Figure 5.1. Sequence of diagenetic events in grain-supported rocks of the Holston and Rockdell Formations.

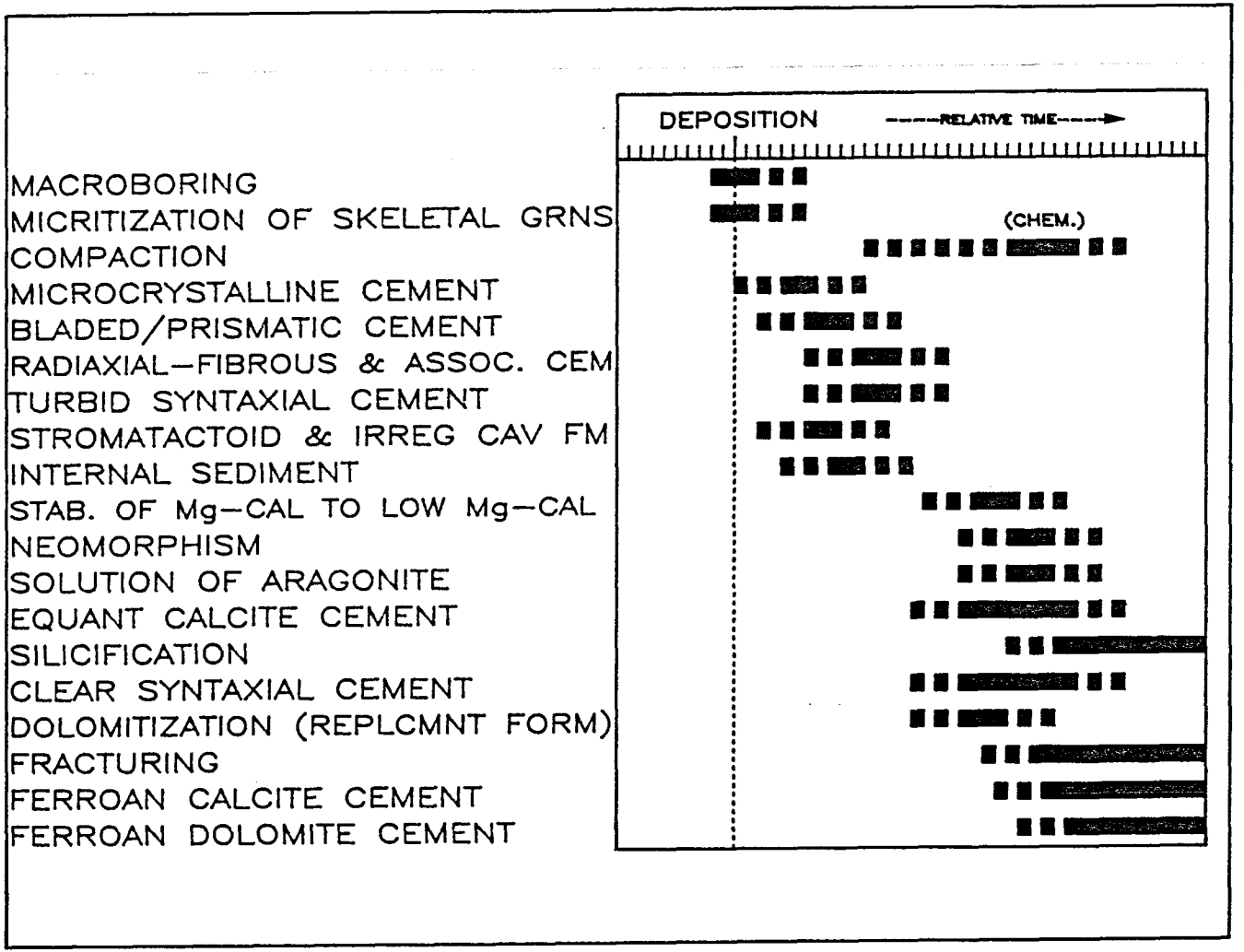


Figure 5.2. Sequence of diagenetic events in mud-supported rocks of the Holston and Rockdell Formations.

Macroboring and Micritization

Macroborings are those borings which are large enough to be resolved petrographically at low-power (>5 μm in diameter). Micritization involves a series of bores, adjacent to each other, which are too small to be resolved petrographically at low-power (generally <5 μm in diameter). These two features are ubiquitous in the Holston and Rockdell formations in northeastern Tennessee. Macroborings were best developed in echinoderm debris where they were commonly in-filled by micrite. They were also observed on trilobites and ostracodes and in lithified internal sediments within stromatactoid cavities of Holston and Rockdell formation mud-supported rocks. Trilobites, ostracodes, mollusc fragments and echinoderm debris commonly showed evidence of micritization.

As pointed out in Chapter 2, both the Holston and Rockdell formations in northeastern Tennessee contain calcareous algae, although this group is rare in the Holston Formation. Moore (1977) has pointed out that near Knoxville, pelmatozoan debris in the Holston Formation is bored by endolithic algae or fungi. Undoubtedly, algae and/or fungi are responsible for the majority of the macroboring and micritization of skeletal grains and lithified internal sediment (probably fungi within internal cavities because of the low light intensity) in these rocks. Further indirect evidence for algal activity, especially in mud-supported rocks of the Holston Formation, is the abundance of irregular micro-inclusions in carbonate cement which Moore (1977) interpreted as organic matter. These inclusions create "banded" cement

crystals similar to the banded cement described by Schroeder (1972) within Bermuda cup-reefs. The inclusion bands in the latter case represent the remains of filamentous algae which aid precipitation of cement by taking CO_2 out of sea water. Similar processes may have occurred within some of the Holston Formation reef bodies and flanking grain-supported lithologies to create the inclusion bands in fibrous cement which were described in Chapter 3.

Stromatactoid and Irregular Cavity Formation

Ruppel (1979) studied the form and occurrence of stromatactis in mud-supported rocks of the Holston and Rockdell formations in northeastern Tennessee in detail. He found that stromatactis occurs in three basic forms. Type I stromatactis consists of discontinuous, tabular (2-3 cm in length) cavities which have an undulatory to planar base and digitate roof. These stromatactoid cavities may be filled by either equant calcite or radiaxial-fibrous calcite. Ruppel (1979) stated that Type I stromatactis only occurs in the Holston Formation but during the present study, Type I stromatactis was also observed in the Rockdell Formation at Red House Branch. Type II stromatactis consists of discontinuous, irregularly shaped cavities which are always in-filled by radiaxial-fibrous calcite. Type II stromatactisis "invariably associated with bryozoans" and only occurs in the Holston Formation (Ruppel, 1979). Type III stromatactis is the most common stromatactis form in northeastern Tennessee and occurs in both the Holston and Rockdell formations. This form consists of a series of tabular, elongate (5-20 cm in length) cavities in-filled with inclusion-rich

radiaxial-fibrous calcite which alternates with layers of sparsely fossiliferous lime-mud. Cavities have smooth to slightly undulatory bases and slightly digitate roofs. Both the tabular cavities and the intercalated lime-mud layers average 10 mm in thickness. Type III stromatactis masses may range in size from 0.5-6.0 m in long dimension and from 0.1-1.0 m in thickness. The importance of Ruppel's (1979) characterization of stromatactis types is that the wide variety of forms of stromatactis argues against a single origin for all stromatactis structures in northeastern Tennessee.

Ferrigno (1973) and Ruppel (1979) have discussed the various hypotheses of stromatactis formation. However, the most plausible explanation, at least for Type I and Type III stromatactis, has been provided by Bathurst (1980). Bathurst noted that the micritic laminae of most stromatactis structures have smooth tops and irregular bottoms and in many cases, show evidence of "brittle fracture of thin crusts." By analogy with Holocene submarine cemented crusts (indurated at the surface with decreasing induration downward; see Shinn, 1969) he proposed that stromatactis structures result from cement in-filling of a "system of cavities which developed between submarine cemented crusts on a carbonate mud mound." Turbulent water conditions, down-slope slumping and bioerosion were proposed as mechanisms for removing less indurated sediment between cemented crusts resulting in a network of cavities (Bathurst, 1980).

Bourque and Gignac (1983) have suggested that Bathurst's (1980) model cannot apply to all stromatactis mounds. They suggested that

sponges played an important role in the formation of some Paleozoic stromatactis mounds. In their model, stromactactoid cavities were created in two ways. The primary mechanism of cavity formation was the "system of growth cavities" created by the sponge network responsible for mound formation. Other cavities could have originated from the decay of "local uncemented sponge tissue." As in Bathurst's (1980) model, the characteristic smooth floor and digitate roof of stromatactoid cavities were accounted for by internal sedimentation and collapse of uncemented roof material.

It is evident that stromatactis in the Holston and Rockdell formations formed early in the overall diagenetic sequence. Most stromatactoid cavities were in-filled by alternating internal marine sediment, microcrystalline cement and radiaxial-fibrous calcite cement, all of which developed early in the diagenetic sequence. If the cemented-crust process, proposed by Bathurst (1980) is responsible for the majority of the stromatactoid structures in the Holston and Rockdell Formations, it is evident that the processes he proposed recurred over time. Multiple cavity generations occur in individual stromatactoid masses and these masses have a wide stratigraphic occurrence at the two shelf margin localities, Poor Valley Creek and Red House Branch. In one sample from a stromatactis mound in the Holston Formation at Red House Branch, an in situ sponge was observed flooring one large stromatactoid cavity. The spicule network, now replaced by equant calcite cement, was well preserved so that at least in this one sample (RHB'-2K), there is evidence that sponges were in place prior to the formation of

stromatactoid cavities and may have acted to enhance cavity formation. Alternatively, the sponge might have lived in the already formed cavity. It is interesting to note that in samples from the Holston and Rockdell formations at Red House Branch, the volume percentage of sponge spicules disseminated in the lime-mud matrix is abnormally high (see Appendix B). Bourque and Gignac (1983) observed similar trends in spicule occurrence in Silurian sponge constructed stromatactis mounds in Quebec. Although the actual number of stromatactis mound samples examined in this study was small, the evidence suggests that sponges might have played a more important role in stromatactoid mound and cavity development in the Holston and Rockdell formations in East Tennessee than has previously been suggested.

The largest cavities in mud-supported lithologies of the Holston and Rockdell formations are irregular in shape and range in size from about 1 cm to 1-2 m in diameter. These cavities are commonly in-filled by dark-red to gray,peloidal internal sediment (which may be graded), fossil debris, and/or cement. These cavities may also be filled with orthocone cephalopods. On outcrop, it appears that the boundary between the cavity fill material and the lime-mud matrix is very irregular and may be marked by clay seams, stylolites, or hard grounds. The majority of these cavities were not constructional in origin (i.e., they were not voids created by growth of a skeletal framework). More likely, the abundant irregular cavities in Holston and Rockdell lime-mud mounds were created by destructional processes such as erosion or solution. The evidence for either mode of formation of these cavities, however, is equivocal.

There are two possible erosional processes which could have been responsible for the irregularly shaped cavities. As in stromatactoid cavities, they might represent areas slightly below the mound surface which were unlithified but still connected to circulating waters. At some later time, this uncemented material might have been winnowed, leaving behind an irregular void surrounded by lithified lime-mud. This process would be analogous to the process of cavity formation in lithoherms in the Straits of Florida described by Neuman et al. (1977). These cavities might also have formed as a result of bioerosion by some unknown group of organisms.

A solutional origin for these cavities is supported by their large size and highly irregular shape. Because the cavities are filled by internal sediment and fossil material, the solution model of formation would require reexposure to the marine environment after the cavities formed in the meteoric environment. No other evidence for exposure and resubmergence was observed; further data is needed to support this model of cavity formation. From the evidence collected in this study, it is impossible to determine which of the processes described here (or some other process) was the principal mechanism of formation. It is possible that all of the processes described here played an active role in the formation of these cavities.

Mineralogic Stabilization and Neomorphism

Carbonate sediment consisting of grains and cement with metastable mineralogies undergoes a series of changes when exposed to the meteoric

diagenetic environment. The first of these is mineralogic stabilization, which includes both the inversion of magnesian calcite to calcite (without destroying the original texture of the grain or cement; Richter, 1979) and the solution of aragonite and reprecipitation of calcite (polymorphic transformation; Bathurst, 1975). In the ideal meteoric diagenetic environment which is undersaturated with respect to calcium carbonate, aragonite and the various phases of calcite are all soluble but to differing degrees. In terms of relative solubilities of these carbonate phases are related by the following relationship (from highest to lowest solubility) (James and Choquette, 1984):

Mg-calcite (>12 mole% $MgCO_3$) > aragonite

and Mg-calcite (12 mole% $MgCO_3$) > Mg-calcite (<12 mole% $MgCO_3$)

> calcite

Based on these thermodynamic solubilities, allochems and cement composed of calcite with >12 mole percent $MgCO_3$ should begin stabilization before solution of aragonite allochems and matrix when exposed to meteoric water. Based on Quaternary to late Tertiary carbonate sediment of the Mediterranean region, Gavish and Friedman (1969) determined that stabilization of magnesian calcite begins before solution of aragonite. As illustrated in Figures 5.1 and 5.2 (pp. 171 and 172), stabilization of magnesian calcite to calcite may have been largely coeval with solution of aragonite but probably began first.

Neomorphism, as used in this thesis, primarily refers to aggrading neomorphism (Folk, 1965; Bathurst, 1975). In this process, finely

crystalline carbonate grains (micrite) are replaced by coarser-grained crystals (microspar and pseudospar). As is evident from the constituent analysis data in Appendix B, microspar is most abundant in mud-supported rocks but there is no apparent pattern to its occurrence. Pseudospar has a similarly "patchy" distribution in the Holston and Rockdell formations but may rarely be relatively abundant in both grain- and mud-supported rocks. Longman (1977) has determined that in the Bromide Formation (Middle Ordovician) of Oklahoma, shale beds which contain chlorite and montmorillonite attracted magnesium ions from the surfaces of micrite grains and allowed them to recrystallize to microspar. Neomorphism of Bromide Formation micrite was found to have occurred after burial. Neomorphism in the Holston and Rockdell formations probably also occurred after some degree of burial. Basinal shale exposed near the shelf margin localities and dispersed terrigenous material within on-shelf Rockdell strata may have been responsible for the formation of microspar and pseudospar observed in the Holston and Rockdell formations.

Dolomitization

Dolomite occurs in the Holston and Rockdell formations in two forms. The finely to very coarsely crystalline ferroan dolomite cement, described in Chapter 3, is volumetrically the dominant form. That variety of dolomite will not be discussed here. Dolomite also occurs as finely crystalline, euhedral to subhedral rhombs within the micritic matrix of mud-supported rocks and in micritic areas of some

grain-supported rocks. This form of dolomite is difficult to distinguish petrographically, but may be delineated by staining thin-sections with Alizarin red-S.

The origin of finely crystalline matrix dolomite in these rocks is problematic. Although grains do not appear abraded, it is impossible to rule out the possibility that the dolomite is allochthonous. Thus, this form of dolomite may actually be "detrital" dolomite. Johnson (in preparation), however, has determined that the dominant original mineralogy of micrite in the Holston and Rockdell formations in northeastern Tennessee was probably magnesian calcite. The magnesium from that magnesian calcite may have been liberated during mineralogic stabilization in the meteoric environment and changed the porewater chemistry to allow precipitation of finely crystalline dolomite within the micrite matrix. In this second case, the dolomite would have been formed in situ.

Silicification

Replacement silica occurs in the Holston and Rockdell formations in two forms. At the on-shelf localities, Cedar Springs and Evans Ferry, it appears as spherulitic chalcedony and microcrystalline granular quartz (terms after Wilson, 1966). In samples from these two localities, bryozoans, brachiopods, echinoderms and turbid and clear syntaxial cement were the primary materials which were replaced.

At the shelf margin localities, euhedral to subhedral quartz crystals (authigenic quartz) were observed replacing micrite, bryozoans,

trilobites, echinoderms and turbid and clear syntaxial cement. In basal sections, euhedral quartz crystals averaged 0.10 mm in diameter but crystals as large as 0.16 mm in diameter were observed. Longitudinal sections through quartz crystals revealed that the average crystal length was 0.25 mm but crystals as long as 0.45 mm were observed. In most basal sections, crystal centers were turbid while crystal rims were clear.

The source of replacement silica within rocks of the Holston and Rockdell formations was probably abundant siliceous sponge spicules in the sediment. Two possible mechanisms for the leaching of silica and replacement allochems and cement are possible. Meteoric or burial fluids, undersaturated with respect to silica may have migrated through the sediment before all porosity was occluded. These fluids could have effectively leached silica from the sediment and redistributed it by replacement of primary allochems and cement. Silica-rich fluids capable of replacing carbonate may also have been derived through pressure solution of silica-rich sediment. No matter what mechanism was responsible for redistributing silica within these rocks, it occurred relatively late in the diagenetic sequence.

Compaction

Compaction of Holston and Rockdell formation sediment occurred over a continuum from mechanical compaction (grain breakage) to chemical compaction (which usually resulted in pervasive stylolitization). Mechanical compaction is well developed only in grain supported

lithologies of the Holston and Rockdell formations. In most cases, only curvilinear grains such as trilobites and brachiopods exhibited grain breakage. Mechanical compaction apparently was not an active process during early diagenesis because only rarely was marine cement observed on fractured surfaces. More commonly, the area within a fracture was in-filled by clear syntaxial cement from an adjacent echinoderm fragment.

Chemical compaction occurred under greater stress conditions (relative to simple grain breakage) and resulted in solutional grain contacts or "grain boundary stylolites" (sutured, longitudinal or concavo-convex grain contacts; terms after Bhattacharyya and Friedman, 1979) and pervasive stylolitization. Sutured, longitudinal and concavo-convex grain contacts were best developed ingrain-supported rocks which are dominantly cemented by syntaxial cement. In these rocks, curvilinear grains such as trilobites were initially fractured by compaction against an adjacent syntaxially cemented echinoderm. Continued compaction of the two grains caused solution and the formation of a sutured grain contact.

Most grain- and mud-supported rocks in the Holston and Rockdell formations exhibited extensive stylolitization. In the Holston Formation, the stylolitic seams were generally heavily iron stained while those in Rockdell samples were not. Stylolites in grain-supported rocks were typically sutured-seams and stylolites in mud-supported rocks were generally nonsutured seams (terms after Wanless, 1979). Stylolites in the Holston and Rockdell formations appear to cross-cut

all depositional and diagenetic features except the latest large-scale fractures. Fractures in-filled by ferroan calcite are usually off-set by the major stylolitic seams in both grain- and mud-supported rocks. Large-scale fractures which are in-filled by angular rock fragments and "ground-up" rock material always cross-cut the same major stylolites.

Overall, compaction apparently was not an important diagenetic process in Holston and Rockdell sediment until the formation of meteoric cement. Qualitatively, mechanical compaction was more prominent in skeletal sand deposited well on-shelf because petrographically, it appeared that grain breakage was more common in Rockdell samples from Cedar Springs and Evans Ferry than in Holston and Rockdell samples from Poor Valley Creek and Red House Branch.

Fracturing

It is evident from the previous discussion of compaction that there appear to be two sets of fractures in both grain- and mud-supported rocks of the Holston and Rockdell formations. The first set of fractures was always in-filled by ferroan calcite and as described previously, seldom cross-cut the major stylolites in the rocks examined in this study. The ferroan calcite filled fractures were generally nearly normal to bedding. A second set of fractures which was generally dark in color and filled with rock fragments and matrix material was also observed in these rocks (primarily in sample from Poor Valley Creek and Red House Branch). These fractures never were off-set by stylolites and were randomly oriented with respect to bedding.

The ferroan calcite-filled fractures formed late in the diagenetic sequence as evidenced by their cross-cutting all depositional and diagenetic features except major stylolites and grain and matrix-filled fractures. The late occurrence of the ferroan calcite-filled fracture set suggests that they formed after burial. The second fracture set formed after all depositional and diagenetic features. The angular rock fragments and matrix material which commonly in-fill these fractures suggest that they may be tectonic in origin rather than the product of carbonate diagenesis.

CHAPTER 6

SUMMARY AND CONCLUSIONS

1. In northeastern Tennessee, the Holston and Rockdell formations both consist of three somewhat intergradational lithofacies. The Holston consists of the echinoderm-bryozoan grainstone-packstone, bryozoan wackestone-boundstone, and echinoderm-bryozoan packstone lithofacies. Echinoderm-bryozoan grainstone-packstones are somewhat analogous to the skeletal sand bank deposits in the Lower Holston Formation near Knoxville, Tennessee while the bryozoan wackestone-boundstones and echinoderm-bryozoan packstones are collectively similar to the upper part of the Holston Formation near Knoxville: reef core and flank deposits. The Rockdell Formation consists of the bryozoan-echinoderm grainstone-packstone, bryozoan-echinoderm packstone, and bryozoan wackestone lithofacies. The grainstone-packstone lithofacies represents on-shelf, skeletal sand deposits while the packstones were deposited in "thickets" created by ramose bryozoans and pelmatozoan echinoderms (Ruppel and Walker, 1982). Rockdell wackestones were deposited as a series of isolated lime-mud mounds within the complex of skeletal sand (grainstone-packstones and packstones). (Ruppel and Walker, 1982).

2. Petrographic analysis of samples from the Holston and Rockdell formations has allowed the distinction of the following eight cement categories:

(1) Radiaxial-fibrous calcite and associated cement;

(2) Bladed/prismatic calcite cement;

(3) Turbid (inclusion-rich) syntaxial (rim) overgrowth cement;

(4) Cryptocrystalline (micrite) calcite cement;

(5) Equant (drusy) calcite cement;

(6) Clear syntaxial (rim) overgrowth cement;

(7) Ferroan calcite cement;

(8) Ferroan (baroque) dolomite cement.

Based on different combinations of several lines of evidence, radiaxial-fibrous calcite and associated cement, bladed/prismatic calcite cement, turbid syntaxial overgrowth cement, and cryptocrystalline (micrite) calcite cement are interpreted as syndepositional, early marine in origin. This evidence includes trace elemental composition of radiaxial-fibrous calcite, cement development both before and after deposition of internal marine sediment, superposition within pores and cavities (cement stratigraphy), inclusions of microdolomite within cement crystal structures (suggesting a magnesian calcite precursor), and comparison of cement texture, fabric, and occurrence to examples in the geologic literature. Equant (drusy) calcite and clear syntaxial (rim) cement are interpreted as meteoric in origin because they always postdate marine cement, occur in a pore central position (equant calcite), are devoid of inclusions, and are similar to other meteoric cement in the geologic literature.

Ferroan calcite (including the ferroan part of clear syntaxial cement) and ferroan (baroque) dolomite cement, which co-occur as the last cementing phases, formed after burial under reducing conditions in

the stagnant meteoric phreatic zone or much later within the deep burial (phreatic) environment. Since baroque dolomite only forms in elevated temperatures and both cement types occur in the same relative positions in these rocks, a deep origin is suggested for both.

3. Constituent analysis (Appendix B) suggests that grain-supported rocks from the Holston Formation may be divided into two separate groups: (1) rocks which exhibit >50% fibrous and bladed cement; and (2) rocks which exhibit <50% fibrous and bladed cement. These two populations generally reflect samples which occur adjacent to lime-mud mounds and those which occur away from lime-mud mounds, respectively. Holston wackestone-boundstones also may be divided into two populations: (1) cavernous mound samples which contain substantially >75% fibrous and bladed cement; and (2) noncavernous mound samples which contain <30% fibrous and bladed cement. Both grain- and mud-supported rocks from the Rockdell Formation may be divided into two distinct populations based on the abundance of marine cement within each sample. However, these two populations also reflect the difference in locality (i.e., Rockdell at the shelf margin versus Rockdell on-shelf).

Marine cement (radiaxial-fibrous calcite and associated cement, turbid syntaxial cement, and bladed/prismatic cement) is best developed at the shelf margin (Red House Branch and Poor Valley Creek) and in most samples, represents the predominant cementing phases. Meteoric derived cement is best developed on-shelf in the Rockdell Formation where marine cement is much less abundant. Thus, there are two inverse cement gradients from the shelf interior to the shelf margin,

marine cement increases in abundance basinward and meteoric cement decreases in abundance basinward.

It is clear that some depositional units at the different study localities were dominated by either marine, meteoric, or burial cementation. Preliminary analyses of this phenomenon, presented here and in Walker et al. (1986), suggest that these "cement units" or "zones" do not occur randomly within the section, but rather occur repetitively in series: (1) marine dominated; (2) meteoric dominated; followed by (3) burial dominated. Data presented here do not prove the existence of this repetitive series on a regional scale, but they do suggest that the timing of fluid flow (from basin toward the shelf) through carbonate sediment may be "mappable" based on the diagenetic products produced by these fluids. These "units" may also serve as guides to small-scale sea-level fluctuations through time.

4. Cementation in the Holston and Rockdell formations largely controlled the development of other diagenetic processes. Although their timing overlaps somewhat, the paragenetic sequence of marine cement is as follows: (1) microcrystalline (micrite) cement; (2) bladed/prismatic cement; and (3) turbid syntaxial (rim) cement and radiaxial-fibrous calcite and associated cement. Other diagenetic processes which occurred in the marine environment, in order of apparent earliest occurrence, are: (1) macroboring and micritization of skeletal grains; (2) stromatactoid and irregular cavity formation; (3) internal sedimentation; and (4) mechanical compaction (grain-supported rocks).

Equant (drusy) calcite and clear syntaxial (rim) cement formed at about the same time in the meteoric diagenetic environment. Diagenetic processes accompanying meteoric cementation, in order of apparent earliest occurrence, are: (1) mineralogic stabilization (magnesian calcite to low-magnesian calcite); (2) dolomitization (finely crystalline dolomite in matrix micrite); (3) solution of aragonite; (4) neomorphism; and (5) silicification (replacement by both chalcedony and authigenic quartz).

Ferroan calcite (including ferroan zones of clear syntaxial (rim) cement)and ferroan (baroque) dolomite developed under reducing conditions and probably elevated temperatures after burial. Diagenetic processes co-occurring with these cement types include: (1) fracturing; (2) silicification (replacement by both chalcedony and authigenic quartz); (3) chemical compaction.

LIST OF REFERENCES

LIST OF REFERENCES

Badiozamani, K., MacKenzie, F. T., and Thorstensen, D. C., 1977, Experimental carbonate cementation: salinity, temperature and vadose-phreatic effects: Jour. Sed. Petrology, v. 47, p. 529-542.

Ball, M. M., 1976, Carbonate sand bodies of Florida and the Bahamas: Jour. Sed. Petrology, v. 556-591.

Banner, F. T., and Wood, G. V., 1964, Recrystallization in microfossiliferous limestones: Geol. Jour., v. 4, p. 21-34.

Bathurst, R. G. C., 1958, Diagenetic fabrics in some British Dinantian limestones: Liverpool Manchester Geol. Jour., v. 2, p. 11-36.

Bathurst, R. G. C., 1959a, Diagenesis in Mississippian calcilutites and pseudobreccias: Jour. Sed. Petrology, v. 29, p. 365-376.

Bathurst, R. G. C., 1959b, The cavernous structure of some Mississippian Stromatactis reefs in Lancashire, England: Jour. Geol., v. 67, p. 506-521.

Bathurst, R. G. C., 1964a, Diagenesis and paleoecology: A survey, IN Imbrie, J., and Newell, N. D., eds., Approaches to Paleoecology: Wiley, New York, p. 319-344.

Bathurst, R. G. C., 1964b, The replacement of aragonite by calcite in the molluscan shell wall, IN Imbrie, J., and Newell, N. D., eds., Approaches to Paleoecology: Wiley, New York, p. 357-376.

Bathurst, R. G. C., 1966, Boring algae, micrite envelopes and lithification ofmolluscan biosparites: Jour. Geol., v. 5, p. 15-32.

Bathurst, R. G. C., 1975, Carbonate Sediments and Their Diagenesis: Elsevier,Amsterdam, 658 p.

Bathurst, R. G. C., 1980, Stromatactis--Origin related to submarine-cemented crusts in Paleozoic mud mounds: Geology, v. 8, p. 131-134.

Benedict, G. L., 1977, Stop 3--Lenoir, Holston, and Ottosee formations: shallow shelf lagoon, deeper shelf, and shelf marginal environments, IN Ruppel, S. C.,and Walker, K. R., eds., The Ecostratigraphy of the Middle Ordovician of the Southern Appalachians: The Univ. of Tenn., Knoxville, Dept. Geol. Sci. Studies in Geoloy, No. 1, p. 52-59.

Benedict, G. L., and Walker, K. R., 1978, Paleobathymetric analysis in Paleozoic sequences and its geodynamic significance: Amer. Jour. Sci., v. 278, p. 579-607.

Black, W. W., 1952, The origin of the supposed tufa bands in Carboniferous reef limestones: Geol. Mag., v. 89, p. 195-200.

Bond, G., 1950, The nomenclature of Lower Carboniferous "reef" limestones in the North of England: Geol. Mag., v. 87, p. 267-278.

Borowski, W. S., 1982, Petrology, depositional environments, and stratigraphicanalysis of a part of the Middle Ordovician Chickamauga Group limestones near Clinton, Tennessee: unpubl. M.S. thesis, The Univ. of Tennessee, Knoxville, 239 p.

Bourque, P., and Gignac, H., 1983, Sponge-constructed stromatactis mud mounds, Silurian of Gaspe, Quebec: Jour. Sed. Petrology, v. 53, p. 521-532.

Brand, U., and Veizer, J., 1981, Chemical diagenesis of a multicomponent carbonate system--2: Stable isotopes: Jour. Sed. Petrology, v. 51, p. 987-999.

Breland, F. C., 1980, Stratigraphic, paleoenvironmental and echinoderm distribution patterns in an unfaulted Middle Ordovician (Chickamauga Group) shelf edge to on-shelf transect in East Tennessee: unpubl. Ph.D. dissertation, The Univ. of Tennessee, Knoxville, 217 p.

Bricker, O. P., ed., 1971, Carbonate Cements: Johns Hopkins University Press, Baltimore, Md., 376 p.

Buckley, H. E., 1951, Crystal Growth: New York, Wiley, 571 p.

Burgess, C. J., 1979, The development of a Lower Jurassic carbonate tidal flat, Central High Atlas, Morocco, 2: Diagenetic history: Jour. Sed. Petrology, v. 49, p. 413-428.

Cantrell, D. L., 1982, Anatomy, diagenesis, and geochemistry of a Middle Ordovician oolite shoal, eastern Tennessee: unpubl. M.S. thesis, The Univ. of Tennessee, Knoxville, 153 p.

Cantrell, D. L., and Walker, K. R., 1985, Depositional and diagenetic patterns, ancient oolite Middle Ordovician, eastern Tennessee: Jour. Sed. Petrology, v. 55, p. 518-531.

Cooper, B. N., 1944, Geology and mineral resources of the Burkes Garden quadrangle, Virginia: Virginia Geol. Survey Bull. 60, p. 39-92.

Cooper, B. N., 1945, Industrial limestones and dolomites in Virginia: Clinch Valley district: Virginia Geol. Surv. Bull. 66, 259 p.

Cooper, B. N., and Cooper, G. A., 1946, Lower Middle Ordovician stratigraphy of the Shenandoah Valley, Virginia: Geol. Soc. Amer. Bull., v. 57, p. 35-114.

Cooper, B. N., and Prouty, C. E., 1943, Stratigraphy of the lower Middle Ordovician of Tazewell County, Virginia: Geol. Soc. Amer. Bull., v. 43, p. 819-886.

Cooper, G. A., 1956, Chazyan and related brachiopods: Smithsonian Inst. Misc. Collections, Pt. 1, 1024 p.

Cotter, E., 1966, Limestone diagenesis and dolomitization in Mississippian carbonate banks in Montana: Jour. Sed. Petrology, v. 36, p. 764-774.

Davies, G. R., 1977, Former magnesian calcite and aragonite submarine cements in upper Paleozoic reefs of the Canadian Arctic A summary: Geology, v. 5, p. 11-15.

Davies, G. R., and Krouse, H. R., 1975, Carbon and oxygen isotopic compositionof Late Paleozoic calcite cements, Canadian Arctic archipelago--preliminary results and interpretation: Geol. Soc. Canada Paper 75-1, Part B, p. 215-220.

Dickson, J. A. D., 1966, Carbonate identification and genesis as revealed by staining: Jour. Sed. Petrology, v. 36, p. 491-505.

Diehl, W. W., 1982, Depositional environments and paleoecology of the Middle and Upper Ordovician Martinsburg Formation of Grainger County, Tennessee: unpubl. M.S. thesis, The Univ. of Tennessee, Knoxville, 242 p.

Dixon, E. E. L., 1921, The geology of the country around Pembroke and Tenby: London, Mem. Geol. Survey.

Dravis, J., 1979, Rapid and widespread generation of Recent oolitic hardgrounds on a high energy Bahamian platform, Eleuthera Bank, Bahamas: Jour. Sed. Petrol., v. 79, p. 195-208.

Dunham, R. J., 1962, Classification of carbonate rocks according to depositional texture, IN Ham, W. E., ed., Classification of Carbonate Rocks--A Symposium: Amer. Assoc. Petroleum Geologists Mem. 1, p. 108-121.

Evamy, B. D., and Shearman, D. J., 1965, The development of overgrowths from echinoderm fragments: Sedimentology, v. 5, p. 211-233.

Evamy, B. D., and Shearman, D. J., 1969, Early stages in development of overgrowths on echinoderm fragments in limestones: Sedimentology, v. 12, p. 317-322.

Ewing, E. L., 1985, Environmental sedimentology of the lower Middle Ordovician in the Lay School section, Hogskin Valley, Grainger County, Tennessee: unpubl. M.S. thesis, The University of Tennessee, Knoxville, 333 p.

Ferrigno, K. F., 1973, Paleoecology of the reefs of the Holston Formation: unpubl. Ph.D. dissertation, The Univ. of Tennessee, Knoxville, 142 p.

Fischer, A. G., 1981, Climatic oscillations in the Biosphere, IN Nitecki, M., ed., Biotic Crises in Ecological and Evolutionary Time: Acad. Press, New York, p. 103-131.

Flugel, E., 1982, Microfacies Analysis of Limestones: Berlin-NewYork, Springer-Verlag, 633 p.

Folk, R. L., 1962, Petrography and origin of the Silurian Rochester and McKenzie shales, Morgan County, West Virginia: Jour. Sed. Petrology, v. 32, p. 539-578.

Folk, R. L., 1965, Some aspects of recrystallization in ancient limestones, IN Pray, L. C., and Murray, R. C., eds., Dolomitization and Limestone Diagenesis: Soc. Econ. Paleontologist and Mineralogists Spec. Pub. 13, p. 13-48.

Folk, R. L., 1974, The natural history of calcium carbonate: Effect of magnesium content and salinity: Jour. Sed. Petrology, v. 44, p. 40-53.

Frank, J. R., Carpenter, A. B., and Oglesby, T. W., 1982, Cathodoluminescence and composition of calcite cement in the Taum Sauk Limestone (Upper Cambrian), southeast Missouri: Jour. Sed. Petrology, v. 52, p. 631-638.

Friedman, G. M., 1964, Early diagenesis and lithification in carbonate sediments: Jour. Sed. Petrology, v. 34, p. 777-813.

Friedman, G. M., Amiel, A. J., and Schneidermann, N., 1974, Submarine cementation in reefs: Example from the Red Sea: Jour. Sed. Petrology, v. 44, p. 816-825.

Friedman, G. M., and Kolesar, P. T., 1971, Fresh-water carbonate cements, IN Bricker, O. P., ed., Carbonate Cements: Johns Hopkins University Press, Baltimore, Md., p. 122-123.

Garrido, J. and Blanco, J., 1947, Structure cristalline des piquants d'Oursin: Compt. Rend., v. 224, p. 485.

Garrison, R. E., 1972, Inter- and intrapillow limestones of the Olympic Peninsula, Washington: Jour. Geol., v. 80, p. 310-322.

Ginsburg, R. N., 1957, Early diagenesis and litification of shallow-water carbonate sediments in south Florida, IN LeBlanc, R. J., and Breeding, J. G., eds., Regional Aspects of Carbonate Deposition: Soc. Econ. Paleontologists and Mineralogist Spec. Pub. 5, p. 80-99.

Ginsburg, R. N., and James, N. P., 1976, Submarine botryoidal aragonite in Holocene reef limestones, Belize: Geology, v. 4, p. 431-436.

Ginsburg, R. N., Shinn, E. A., and Schroeder, J. H., 1967, Submarine cementation and internal sedimentation within Bermuda reefs (abs.): Geol. Soc. Amer. Spec. Paper 115, p. 78-79.

Given, R. K., and Lohmann, K. C., 1985, Derivation of the original isotopic composition of Permian marine cements: Jour. Sed. Petrology, v. 55, p. 430-439.

Given, R. K., and Lohmann, K. C., 1986, Isotopic evidence for early meteoric diagenesis of the reef facies, Permian Reef Complex of West Texas and New Mexico: Jour. Sed. Petrology, v. 56, p. 183-193.

Gorur, N., 1979, Downward development of overgrowths from echinoderm fragmentsin a submarine environment: Sedimentology, v. 26, p. 605-608.

Grover, G. A., 1981, Cement types and cementation patterns of Middle Ordovician ramp-to-basin carbonates, Virginia: unpubl. Ph.D. dissertation, Virginia Polytechnic Institute and State University, Blacksburg, 219 p.

Grover, G. A., and Read, J. F., 1978, Fenestral and associated vadose diagenetic fabrics of tidal flat carbonates, Middle Ordovician, New Market Limestone, southwestern Virginia: Jour. Sed. Petrology, p. 453-473.

Hanor, J. S., 1978, Precipitation of beachrock cements: mixing of marine and meteoric waters vs. CO2-degassing: Jour. Sed. Petrology, v. 48, p. 489-501.

Harrison, R. S., 1974, Near-surface subaerial diagenesis of Pleistocene carbonates, Barbados, West Indies: unpubl. Ph.D dissertation, Brown Univ., 332 p.

Harrison, R. S., 1975, Porosity in Pleistocene grainstones from Barbados: someprelimin aly observations: Canadian Petroleum Geologists Bull., v. 23, p. 383-392.

Horne, R. A., 1969, Marine Chemistry: The Structure of Water and the Chemistry of the Hydrosphere: Wiley-Interscience, New York, 153 p.

Hudson, J. D., 1962, Pseudo-pleochroic calcite in recrystallized shell limestones: Geol Mag., v. 99, p. 492-500.

Hudson, J. D., and Coleman, M. L., 1978, Submarine cementation of the Scheck Limestone conglomerate (Jurassic, Austria): Isotopic evidence: N. Jb. Geol. Palaont. Mh., v. 1978, p. 534-544.

Hudson, R. G., 1933, The scenery and geology of north-west Yorkshire: Geologists' Assoc. London Porc., v. 44, p. 228-255.

Jacka, A. D., and Brand, J. P. 1977, Biofacies and development and differential occlusion of porosity in a Lower Cretaceous (Edwards) reef: Jour. Sed. Petrology, v. 47, p. 366-382.

James, N. P., 1974, Diagenesis of scleractinian corals in the subaerial vadose environment: Jour. Paleontol., v. 48, p. 785-795.

James, N. P., and Choquette, P., 1983, Diagenesis 6. Limestones--The seafloor diagenetic environment: Geoscience Canada, v. 10, p. 162-179.

James, N. P., and Choquette, P., 1984, Diagenesis 9. Limestones--The meteoric diagenetic environment: Geoscience Canada, v. 11, p. 161-194.

James, N. P., and Ginsburg, R. N., 1979, The Seaward Margin of Belize Barrier and Atoll Reefs: Int. Assoc. Sedimentologists Spec. Pub. 3, 191 p.

James, N. P., Ginsburg, R. N., Marszalek, D. S., and Choquette, P. W., 1976, Facies and fabric specificity of early subsea cements in shallow Belize (British Honduras) reefs: Jour. Sed. Petrology, v. 46, p. 523-544.

James, N. P., and Klappa, C. F., 1983, Petrogenesis of early Cambrian reef limestones, Labrador, Canada: Jour. Sed. Petrology, v. 53, p. 1051-1096.

Jernigan, D. G., and Walker, K. R., 1985, Comparison of early diagenetic features in the Middle Ordovician Holston and Rockdell formations of East Tennessee (abs.): Geol. Soc. Amer. Abst. with Programs, v. 17, No. 2, p. 97, Southeastern Section, Knoxville, TN.

Johnson, R. E., In preparation, Diagenesis and trace element geochemistry of Lower Middle Ordovician shelf, shelf-edge and slope lithofacies in East Tennessee: unpubl. Ph.D. dissertation, The Univ. of Tennessee, Knoxville.

Keith, A., 1895, U.S. Geol. Surv. Atlas, Knoxville, Folio 16.

Kendall, A. C., 1977, Fascicular-optic calcite: A replacement of bundled acicular carbonate cements: Jour. Sed. Petrology, v. 47, p. 1056-1062.

Kendall, A. C., 1985, Radiaxial fibrous calcite: A reappraisal, IN Schneidermann, N., and Harris, P. M., eds., Carbonate Cements: Soc. Econ. Paleontologists and Mineralogists Spec. Pub. 36, p. 59-77.

Kendall, A. C., and Tucker, M. E., 1971, Radiaxial fibrous calcite as a replacement after syn-sedimentary cement: Nature Phys. Sci., v. 232, p. 162-163.

Kendall, A. C., and Tucker, M. E., 1973, Radiaxial fibrous calcite: A replacement after acicular carbonate: Sedimentology, v. 20, p. 365-389.

Krumbein, W., 1942, Criteria for subsurface recognition of unconformities: Amer. Assoc. Petroleum Geologists Bull., v. 26, p. 36-62.

Land, L. S., 1967, Diagenesis in skeletal carbonates: Jour. Sed. Petrology, v. 37, p. 914-930.

Land L. S., 1970, Phreatic versus vadose meteoric diagenesis of limestones, evidence from a fossil water table: Sedimentology, v. 14, p. 175-185.

Land, L. S., 1971, Submarine lithification of Jamaican reefs, IN Bricker, O. P., ed., Carbonate Cements: Johns Hopkins University Press, Baltimore, Md., p. 59-62.

Land, L. S., 1973, Contemporaneous dolomitization of middle Pleistocene reefs by meteoric water, North Jamaica: Bull. Marine Sci., v. 23, p. 64-92.

Land L. S., and Goreau, T. R., 1970, Submarine lithification of Jamaican reefs: Jour. Sed. Petrology, v. 40, p. 457-462.

Land, L. S., and Moore, C. H., 1980, Lithification, micritization and syndepositional diagenesis of biolithites on the Jamaican island slope: Jour. Sed. Petrology, v. 40, p. 357-371.

Lees, A., 1964, The structure and origin of the Walusortian (Lower Carboniferous) "reefs" of West-Central Eire: Royal Soc. London Philos. Trans., v. 247, p. 483-531.

Logan, B. W., 1974, Inventory of diagenesis in Holocene-Recent carbonate sediments, Shark Bay, Western Australia, IN Logan, B. W., Read, J. F., Hagan, G. M., Hoffman, P., Brown, R. G., Woods, P. J., and Gebelein, C. D., Evolutionand Diagenesis of Quaternary Carbonate Sequences, Shark Bay, Western Australia: Amer. Assoc. Petroleum Geologists Mem. 22, p. 140-194.

Lohmann, K. C., and Meyers, W. J., 1977, Microdolomite inclusions in cloudy prismatic calcites: A proposed criterion for former high magnesium calcites: Jour. Sed. Petrology, v. 48, p. 475-488.

Lohmann, K. C., in press, Covariant carbon and oxygen isotopic trends in calcitized marine cements - estimation of marine isotopic signatures: Jour. Sed. Petrology.

Longman, M. W., 1980, Carbonate diagenetic textures from near- surface diagenetic environments: Bull. Am. Assoc. Petrol. Geol., v. 64, p. 461-487.

Loucks, R. G., 1977, Porosity development and distribution in shoal-water carbonate complexes - subsurface Pearsall Formation (Lower Cretaceous), south Texas: Texas Univ. Bur. Econ. Geol. Rep. Inv., v. 89, p. 97-126.

Lucia, F. J., 1962, Diagenesis of a crinoidal sediment: Jour. Sed. Petrology, v. 32, p. 848-865.

MacIntyre, I. G., 1977, Distribution of submarine cement in a modern Caribbeanfringing reef, Galeta Point, Panama: Jour. Sed. Petrol., v. 47, p. 503-516. MacKenzie, F. T., and Bricker, O. P., 1971, Cementation of sediments by carbonate minerals, IN Bricker, O. P., ed., Carbonate Cements: Johns Hopkins University Press, Baltimore, Md., p. 239-246.

MacKenzie, F. T., and Pigott, J. D., 1981, Tectonic controls of Phanerozoic sedimentary rock cycling: Jour. Geol. Soc. London, v. 138, p. 183-196.

Macqueen, R. W., and Ghent, E. D., 1970, Electron microprobe study of magnesium distribution in some Mississippian echinoderm limestones from Western Canada: Canadian Jour. Earth Sciences, v. 7, p. 1308-1317.

Marshall, J. D., and Ashton, M., 1980, Isotopic and trace element evidence for submarine lithification of hardgrounds in the Jurassic of eastern England: Sedimentology, v. 27, p. 271-290.

Marshall, J. F., and Davies, P. J., 1981, Submarine lithification on windward reef slopes: Capricorn-Bunker Group, Southern Great Barrier Reef: Jour. Sed. Petrol., v. 51, p. 953-960.

Mattes, B. W., and Mountjoy, E.W., 1980, Burial dolomitization of the Upper Devonian Miette buildup, Jasper National Park, Alberta, IN Zenger, D. H., Dunham, J. B., and Ethington, R. L., eds., Concepts and Models of Dolomitization: Soc. Econ. Paleontologists and Mineralogists Spec. Pub. 28, p. 259-297.

Matthews, R. K., 1967, Diagenetic fabrics in biosparites from the Pleistocene of Barbados, West Indies: Jour. Sed. Petrology, v. 37, p. 1147-1153.

Matthews, R. K., 1968, Carbonate diagenesis: equilibration of sedimentary mineralogy to the subaerial environment; coral cap of Barbados, West Indies: Jour. Sed. Petrology, v. 38, p. 1110-1119.

Matthews, R. K., 1974, A process approach to diagenesis of reefs and reef associated limestones, IN Laporte, L. F., ed., Reefs in Space and Time, Selected Examples From the Recent and Ancient: Soc. Econ. Paleontologists and Mineralogists Spec. Pub. 18, p. 234-256.

Mazzullo, S. J., 1980, Calcite pseudospar replacive of marine acicular aragonite and implications for aragonite cement diagenesis: Jour. Sed. Petrology, v. 50, p. 409-423.

Mazzullo, S. J., and Cys, J. M., 1979, Marine aragonite seafloor growths and cements in Permian phylloid algal mounds, Sacramento Mountains, New Mexico: Jour. Sed. Petrol., v. 49, p. 917-936.

McGill, M. M., 1982, Study of diagenesis of a portion of the Holston Limestone: paragenesis of cements and evaluation of geochemistry: unpubl. M.S. thesis, The Univ. of Tennessee, Knoxville, 103 p.

Mckee, E. D., and Weir, G. W., 1953, Terminology for stratification and cross-stratification in sedimentary rocks: Geol. Soc. Amer. Bull., v. 64, p. 381-390.

McLaughlin, R. E., 1973, Observations on the biostratigraphy of Knox County, Tennessee and vicinity, IN The Geology of Knox County, Tennessee: Tenn. Div. Geol. Bull., v. 70, p. 25-62.

McWilliams, E. B., 1975, Paleoenvironmental analysis of the Chapman Ridge Sandstone (Middle Ordovician) in the area of Knoxville, Tennessee: unpubl. M.S. thesis, The Univ. of Tennessee, Knoxville, 109 p.

Meyers, W. J., 1974, Carbonate cement stratigraphy of the Lake Valley Formation (Mississippian) Sacramento Mountains, New Mexico: Jour. Sed. Petrology, v. 44, p. 837-861.

Meyers, W. J., 1977, Chertification in the Mississippian Lake Valley Fm., Sacramento Mts., New Mexico: Sedimentology, v. 24, p. 75-105.

Meyers, W. J., 1978, Regional cementation patterns in Mississippian limestones of southwestern New Mexico: Sedimentology, v. 25, p. 371-400.

Meyers, W. J., 1980, Compaction in Mississippian skeletal limestones southwestern New Mexico: Jour. Sed. Petrology, v. 50, p. 457-474.

Meyers, W. J., and Hill, B. E., 1983, Quantitative studies of compaction in Mississippian skeletal limestones, New Mexico: Jour. Sed. Petrology, v. 53, p. 231-242.

Meyers, W. J., and Lohmann, K. C., 1978, Microdolomite-rich syntaxial cements--Proposed meteoric-marine mixing zone phreatic cements from Mississippian limestones, New Mexico: Jour. Sed. Petrology, v. 48, p. 475-488.

Milici, R. C., 1973, The stratigraphy of Knox County, Tennessee, IN The Geology of Knox County, Tennessee: Tenn. Div.Geol. Bull., v. 70, p. 9-24. Milici, R. C., and Smith, J. W., 1969, Stratigraphy of the Chickamauga Supergroup in its type area: Georgia Dept. Mines, Mining and Geol. Bull. 80, p. 1-35.

Milliken, K. L., and Pigott, J. D., 1977, Variation of oceanic Mg/Ca ratio through time--Implications for the calcite sea (abs.): Geol. Soc. Amer. Abstracts with Programs, South-Central Meeting, p. 64-65.

Milliman, J. D., 1966, Submarine lithification of carbonate sediments: Science, v. 153, p. 994-997.

Milliman, J. D., 1971, Carbonate lithification in the deep sea, IN Bricker, O. P., ed., Carbonate Cements: Johns Hopkins University Press, Baltimore, Md., p. 95-102.

Moldovanyi, E. P., and Lohmann, K. C., 1982, Isotopic identifications of diagenetic environments, Sligo Formation, Southeast Texas (abs.): Geol. Soc. Amer. Abstracts with Programs, v. 14, No. 7, p. 568.

Multer, H. G., 1971, Cementation and recrystallization of Miami Limestone ooids, In Bricker, O. P., ed., Carbonate Cements: Johns Hopkins University Press, Baltimore , Md., p. 139-140.

Murray, R. C., and Pray, L. C., 1965, Dolomitization and limestone diagenesis--an introduction, IN Pray, L. C., and Murray, R. C., eds., Dolomitization and Limestone Diagenesis, A Symposium: Soc. Econ. Paleontologists and Mineralogists Spec. Pub. 13, p. 1-2.

Nelson, H. F., Brown, C. W., and Brineman, J. H., 1962, Skeletal limestone classification, IN Hamm, W. E., ed., Classification of Carbonate Rocks: Amer. Assoc. Petroleum Geologists Memoir 1, p. 224-252.

Newell, N. D., 1955, Depositional fabric in Permian reef limestones: Jour. Geol., v. 63, p. 301-309.

Nissen, H., 1963, Rontgengefugeanalyse am Kalzit von Echinodermen-skeletten: Neues Jahrb. Geol. Palaontol. Abhandl., v. 117, p. 230-234.

Oldershaw, A. E., 1971, The significance of ferroan and non-ferroan calcite cements in the Halkin and Wenlock Limestones (Great Britain), IN Bricker, O. P., ed., Carbonate Cements: Johns Hopkins University Press, Baltimore Md., p. 225-232.

Oldershaw, A. E., 1967, The source of ferroan and non-ferroan calcite cements in the Halkin and Wenlock Limestones: Jour. Geol., v. 5, p. 309-320.

Orme, G. R., and Brown, W. W. M., 1963, Diagenetic fabrics in the Avonian limestones of Derbyshire and North Wales: Proc. Yorks. Geol. Soc., v. 34, p. 51-66.

Parkinson, D., 1935, The geology and topography of the knolls in Bolland (Bowland), Lancs. and Yorks.: Geologists' Assoc. London Proc., v. 46, p. 97-120.

Pigott, J. D., 1981, Global tectonic control of secular variations in Phanerozoic sedimentary rock/ocean/atmospheric chemistry (abs.): Amer. Assoc.Petroleum Geologists Bull., v. 65, p. 963.

Pingitore, N. E., 1976, Vadose and phreatic diagenesis: processes, products and their recognition in corals: Jour. Sed. Petrology, v. 46, p. 985-1006.

Popp, B. N., Sandberg, P. A., and Anderson, T. F., 1981, Coordinated textural isotopic and elemental analysis of constituents in some Middle Devonian limestones (abs.): Geol. Soc. Amer. Abst. with Programs, v. 13, p. 531. Powers, M. C., 1954, A new roundness scale for sedimentary particles: Jour. Sed. Petrology, v. 23, p. 117-119.

Pratt, B. R., 1982, Stromatolitic framework of carbonate mud-mounds: Jour. Sed. Petrology, v. 52, p. 1203-1227.

Prezbindowski, D. R., 1985, Burial cementation--Is it important? A case study, Stuart City Trend, South Central Texas, IN Schneidermann, N., and Harris, P. M., eds., Carbonate Cements: Soc. Econ. Paleontologists and Mineralogists Spec. Pub. 36, p. 241-264.

Prouty, C. E., 1946, Lower Middle Ordovician of southwest Virginia and northeast Tennessee: Amer. Assoc. Petroleum Geologists Bull., v. 30, p. 1140-1191.

Purdy, E. G., 1968, Carbonate diagenesis: A review: Geol. Romana, v. 7, p. 183-228.

Purser, B. H., 1969, Syn-sedimentary marine lithification of Middle Jurassic limestones in the Paris Basin: Sedimentology, v. 12, p. 205-230.

Rodgers, J., 1953, Geologic map of East Tennessee with explanatory text: Tenn. Div. Geol.Bull., v. 58, part 2, p. 64-99.

Ross, R. J., Jaanusson, V., and Friedman, I., 1975, Lithology and origin of Middle Ordovician calcareous mudmound of Meiklejohn Peak Southern Nevada: U. S. Geol. Survey Professional Paper 871, 48 p.

Ruppel, S. C., 1977, The Chickamauga Limestone--a complex mosaic of supratidal to subtidal carbonate shelf environments, IN Ruppel, S. C., and Walker, K. R., eds., The Ecostratigraphy of the Middle Ordovician of the Southern Appalachians: The Univ. of Tenn., Knoxville, Dept. Geol. Sci. Studies in Geology No. 1, p. 39-48.

Ruppel, S. C., 1979, The stratigraphy, carbonate petrography, and depositional environments of the Chickamauga Group (Middle Ordovician) of northern East Tennessee: unpubl. Ph.D. dissertation, The Univ. of Tennessee, Knoxville, 231 p.

Ruppel, S. C., Broadhead, T. W., and Walker, K. R., 1980, Stop 2--Cedar Springs, IN Walker, K. R., Broadhead, T. W., and Keller, F. B., eds., Middle Ordovician Carbonate Shelf to Deep Water Basin Deposition in the Southern Appalachians: The Univ. of Tenn., Knoxville, Dept. Geol. Sci. Studies in Geology, No. 4, p. 34-45.

Ruppel, S. C., and Walker, K. R., 1982, Sedimentology and distinction of carbonate buildups: Middle Ordovician, East Tennessee: Jour. Sed. Petrology, v. 52, p. 1055-1071.

Ruppel, S. C., and Walker, K. R., 1984, Petrology and depositional history of a Middle Ordovician carbonate platform: Chickamauga Group, northeastern Tennessee: Geol. Soc. Amer. Bull., v. 95, p. 568-583.

Safford, J. M., 1869, Geology of Tennessee: State of Tennessee, Nashville, 550 p.

Sandberg, P. A., 1975a, Bryozoan diagenesis: bearing on the nature of the original skeleton of rugose corals: Jour. Paleontology, v. 49, p. 587-606.

Sandberg, P. A., 1975b, New interpretations of Great Salt Lake ooids and of ancient non-skeletal carbonate mineralogy: Sedimentology, v. 22, p. 497-537.

Sandberg, P. A., 1983, An oscillating trend in Phanerozoic non-skeletal carbonate mineralogy: Nature, v. 305, p. 19-22.

Sandberg, P. A., 1985, Aragonite cements and their occurrence in ancient limestones, IN Schneidermann, N., and Harris, P. M., eds., Carbonate Cements: Soc. Econ. Paleontologists and Mineralogists Spec. Pub. 13, p. 33-57.

Sandberg, P. A., and Hudson, J. D., 1983, Aragonite relic preservation in Jurassic calcite-replaced bivalves: Sedimentology, v. 30. p. 879-892.

Sandberg, P. A., and Popp, B. N., 1981, Pennsylvannian aragonites from southeastern Kansas--Environmental and diagenetic implications: Amer. Assoc. Petroleum Geologists Bull., v. 65, p. 985

Sandberg, P. A., Schneidermann, N., and Wunder, S. J., 1973, Aragonite ultrastructural relics in calcite-replaced Pleistocene skeletons: Nature Phys. Sci., v. 245, p. 133-134.

Sander, B., 1951, Contributions to the Study of Depositional Fabrics--Rhythmically Deposited Triassic Limestones and Dolomites (English translation by E. B. Knopf): Tulsa, Amer. Assoc. Petroleum Geologists, 207 p.

Schroeder, J. H., 1972, Fabrics and sequences of submarine carbonate cements in Holocene Bermuda cup reefs: Geol. Rdsch., v. 61, p. 708-730.

Schroeder, J. H., 1973, Submarine and vadose cements in Pleistocene Bermuda reef rock: Sed. Geology, v. 10, p. 179-204.

Schwarzacher, W., 1961, Petrology and structure of some Lower Carboniferous reefs in northwestern Ireland: Amer. Assoc. Petroleum Geologists Bull., v. 45, p. 1481-1503.

Sears, S. O., and Lucia, F. J., 1980, Dolomitization of northern Michigan Niagara reefs by brine refluxion and freshwater/seawater mixing, IN Zenger, D. H., Dunham, J. B., and Ethington, R. L., eds., Concepts and Models of Dolomitization: Soc. Econ. Paleontologists and Mineralogists Spec. Pub. 28, p. 215-237.

Shanmugam, G., 1978, The stratigraphy, sedimentology, and tectonics of the Middle Ordovician Sevier Shale Basin in East Tennessee: unpubl. Ph.D. dissertation, The Univ. of Tennessee, Knoxville, 222 p.

Shanmugam, G., and Walker, K. R., 1978, Tectonic significance of distal turbidites in the Middle Ordovician Blockhouse and lower Sevier formations in East Tennessee: Amer. Jour. Sci., v. 278, p. 551-578.

Shanmugam, G., and Walker, K. R., 1980, Sedimentation, subsidence and evolution of a foredeep basin in the Middle Ordovician, Southern Appalachians: Amer. Jour. Sci., v. 280, p. 479-496.

Shanmugam, G., and Walker, K. R., 1983, Anatomy of the Middle Ordovician Sevier Shale basin, eastern Tennessee: Sediment. Geol., v. 34, p. 315-337.

Shinn, E. A., 1969, Submarine lithification of Holocene carboante sediments inthe Persian Gulf: Sedimentology, v. 12, p. 109-144.

Shinn, E. A., 1971, Holocene submarine cementation in the Persian Gulf, IN Bricker, O. P., ed., Carbonate Cements: Johns Hopkins University Press, Baltimore Md., p. 63-65.

Shinn, E. A., 1975, Polygonal cement sutures from the Holocene: a clue to recognition of submarine diagenesis (abs.): Amer. Assoc. Petroleum Geologists-Soc. Econ. Paleontologists and Mineralogists Ann. Mtg. Abs., v. 2, p. 68. Sickafoose, D. K., 1979, The ecostratigraphy of the lower Middle Ordovician and paleoecology of Porterfieldian and Wildernessian biotas at Evans Ferry, Tennessee: unpubl. MS thesis, Univ. of Tenn., Knoxville, 185 p.

Sickafoose, D. K., and Broadhead, T. W., 1980, Stop 1--Evans Ferry, IN Walker, K. R., Broadhead, T. W., and Keller, F. B., eds., Middle Ordovician Carbonate Shelf to Deep Water Basin Deposition in the Southern Appalachians: The Univ. of Tenn., Knoxville, Dept. Geol. Sci., Studies in Geology, No. 4, p. 22-34.

Simonson, J. C. B., 1985, The stratigraphy, carbonate petrology, depositional environments, and paleoecology of the Middle Ordovician Moccasin Formation near Thorn Hill, Tennessee: unpubl. M.S. thesis, The Univ. of Tennessee, Knoxville, 279 p.

Sippel, R. F., and Glover, E. D., 1964, The solution alteration of carbonaterocks, the effects of temperature and pressure: Geochim. Cosmochim. Acta, v. 28, p. 1401-1417.

Sorby, H. C., 1879, The structure and origin of limestones: Proc. Geol. Soc. London, v. 35, p. 56-95.

Steinen, R. P., 1974, Phreatic and vadose diagenetic modifications of Pleistocene limestone: petrographic observations from subsurface of Barbados, West Indies: Amer. Assoc. Petroleum Geologists Bull., v. 58, p. 1008-1024.

Stephenson, J. P., 1973, Paleoenvironmental analysis of the Lenoir Limestone of southern Knox County, Tennessee: unpubl. M.S. thesis, Univ. of Tenn., Knoxville, 99 p.

Swingle, G. C., 1964, Elevation of the Chickamauga Limestone to Group status in East Tennessee (abs): Tennessee Acad. Sci. Jour., v. 39, p. 66.

Taylor, J. C. M., and Illing, L. V., 1971, Variation in Recent beachrock cements, Qatar, Persian Gulf, IN Bricker, O. P., ed., Carbonate cements: Johns Hopkins University Press, Baltimore, Md., p. 32-35.

Tebbutt, G., 1975, Paleoecology and diagenesis of Pleistocene limestone on Ambergris Cay: Amer. Assoc. Petroleum Geologists, Studies in Geol., v. 2, p. 297-331.

Twenhofel, W. H., Bridge, J., Cloud, P. E., Cooper, B. N., Cooper, G. A., Cummings, E. R., Cullison, J. S., Dunbar, C. O., Kay, G. M., Liberty, B. A., McFarlan, A. C., Rodgers, J., Whittington, H. B., Wilson, C. W., 1954, Correlation of the Ordovician formations of North America: Geol. Soc. Amer. Bull., v. 65, p. 247-298.

Vail, P. R., Mitchum, J. R., and Thompson, S., 1977, Seismic stratigraphy and global changes in sea-level, part 4, IN Peyton, C. E., ed., Seismic Stratigraphy: Amer. Assoc. Petroleum Geologists Memoir 26, p. 83-97.

Walker, K. R, 1977a, A brief introduction to the ecostratigraphy of the Middle Ordovician of Eastern Tennessee, IN Ruppel, S. C., and Walker, K. R., eds., The Ecostratigraphy of the Middle Ordovician of the Southern Appalachians: The Univ. of Tenn., Knoxville, Dept. Geol. Sci. Studies in Geology No. 1, p. 12-17.

Walker, K. R., 1977b, Stop 4--Upper Holston Formation: bryozoan/pelmatozoan reefs, IN Ruppel, S. C., and Walker, K. R., eds., The Ecostratigraphy of the Middle Ordovician of the Southern Appalachians: The Univ. of Tenn., Knoxville, Dept. Geol. Sci. Studies in Geology No. 1, p. 60-65.

Walker, K. R., 1980a, Introduction to the stratigraphy and paleoenvironments of the Middle Ordovician of Tennessee, IN Walker, K. R., Broadhead, T. W., and Keller, F. B., eds., Middle Ordovician Shelf to Deep Water Basin Deposition in the Southern Appalachians: The Univ. of Tenn., Knoxville, Dept. Geol. Sci. Studies in Geology, No. 4, p. 4-12.

Walker, K. R., 1980b, Stop 4--Holston and Chapman Ridge formations: shelf-edgeskeletal sand banks, organic buildups and quartose-sand-wave environments, IN Walker, K. R., Broadhead, T. W., and Keller, F. B., eds., Middle Ordovician Shelf to Deep Water Basin Deposition in the Southern Appalachians: The Univ. of Tenn., Knoxville, Dept. Geol. Sci. Studies in Geology, No. 4, p. 57-65.

Walker, K. R., and Ferrigno, K. F., 1973, Major Middle Ordovician reef tract in East Tennessee: Amer. Jour. Sci., v. 273-A (Cooper Volume), p. 294-325.

Walker, K. R., and Diehl, W. W., 1985, The role of marine cementation in the preservation of Lower Paleozoic assemblages: Trans. Royal Soc. London B311, p. 143-153.

Walker, K. R., Jernigan, D. G., and Weber, L. J., 1985, Diagenetic environments of syntaxial cement formation as a function of geologic age (abs.): Geol. Soc. Amer. Abst. with Programs, v. 17, No. 7, p. 742.

Walker, K. R., Jernigan, D. G., Johnson, R. E., and Foreman, J. L., 1986, Prediction of fluid flow pathways and timing in Paleozoic carbonate sequences: Appalachian Basin Industrial Associates Program, v. 11, p. 143-160.

Walls, R. A., Mountjoy, E. W., and Fritz, P., 1979, Isotopic composition anddiagenetic history of carbonate cements in Devonian Golden Spike reef, Alberta, Canada: Geol. Soc. Amer. Bull., v. 90, p. 963-982.

Weiss, E. A., 1981, Environmental sedimentology of the Middle Ordovician and paleoecology of a portion of the Witten Formation at Solway, Tennessee: unpubl. M.S. thesis, The Univ. of Tennessee, Knoxville, 229 p.

Weyl, P. K., The solution kinetics of calcite: Jour. Geol., v. 66, p. 163-176.

Wilkinson, B. H., 1982, Cyclic cratonic carbonates and Phanerozoic calcite seas: Jour. Geol. Ed., v. 30, p. 189-203.

Wilkinson, B. H., Janecke, S. U., and Brett, C. E., 1982, Low-magnesian calcite marine cement in Middle Ordovician hardgrounds from Kirkfield, Ontario: Jour. Sed. Petrol., v. 52, p. 47-58.

Wilson, J. L., 1975, Carbonate Facies in Geologic History: Springer-Verlag, Berlin-New York, 471 p.

Zankel, H., 1971, A model of sedimentation and diagenesis in a Triassic Reef, IN Bricker, O. P., ed., Carbonate Cements: Johns Hopkins University Press, Baltimore, Md., p. 189-192.

APPENDICES

APPENDIX A

DESCRIPTION OF MEASURED SECTIONS

MEASUREMENT CONVENTIONS

BED THICKNESS, after McKee and Weir (1953) as modified by Powers (1953).

Very thick-bedded	greater than 1.0 m
Thick-bedded	0.3-1.0 m
Medium-bedded	0.1-0.3 m
Thin-bedded	0.03-0.1 m
Very thin-bedded	0.01-0.03 m
Laminated	0.003-0.01 m
Thin-laminated	less than 0.003 m

GRAIN SIZE

Thin-section (cement crystal size)

Extremely coarsely crystalline	greater than 4.0 mm
Very coarsely crystalline	1.0-4.0 mm
Coarsely crystalline	0.25-1.0 mm
Medium crystalline	0.062-0.25 mm
Finely crystalline	0.016-0.062 mm
Very finely crystalline	0.004-0.016 mm

Field description

Coarse-grained	grains visible to the unaided eye and readily identifyable (approximately greater than 1 mm)
Medium-grained	grains visible; not readily identifyable (approximately 0.25-1.0 mm)
Fine-grained	grains visible only with hand lens (approximately 0.1-0.25 mm)
Very fine-grained	grains not visible even with hand lens (generally less than 0.1 mm)

LOCALITY 1--EVANS FERRY

Approximately 62.0 m of the Rockdell Formation are exposed along the"new" road cut on U.S. 25E approximately 5.9 km (3.7 miles) northwest of Thorn Hill, Grainger County, Tennessee (SW 1/4, SE 1/4, E 1/2, Howard Quarter Quadrangle). Rockdell samples from the study of Sickafoose (1979) were used in the present study. See Sickafoose (1979) for a detailed description of section at this locality. Sample numbers are given below with stratigraphic position within the measured

section. All measurements are relative to the lower contact of the Rockdell Formation.

SAMPLE NO.	STRAT. POS.	SAMPLE NO.	STRAT. POS.
EF'18	0.50 m	EF'34	37.50 m
EF'19	2.00 m	EF'35	40.00 m
EF'20	3.00 m	EF'36	42.50 m
EF'21	4.50 m	EF'37	44.00 m
EF'22	8.00 m	EF'38	44.50 m
EF'23	9.50 m	EF'39	47.50 m
EF'24	12.50 m	EF'40	49.00 m
EF'25	15.50 m	EF'41	49.50 m
EF'26	17.50 m	EF'42	50.00 m
EF'27	19.50 m	EF'43	51.50 m
EF'28	21.50 m	EF'44	53.50 m
EF'29	23.50 m	EF'45	54.00 m
EF'30	26.00 m	EF'46	55.50 m
EF'31	28.50 m	EF'47	57.50 m
EF'32	31.00 m	EF'48	59.50 m
EF'33	33.50 m	EF'49	61.50 m

LOCALITY 2--CEDAR SPRINGS

Approximately 99.4 m of the Rockdell Formation are exposed along Cedar Springs Creek and in pastures on either side of Cedar Springs Church Road, approximately 4.8 km (3.0 miles) northeast of Thorn Hill, Grainger County, Tennessee on State Route 66 (SW 1/4, SW 1/4, SW 1/4, Swan Island Quadrangle). This section has been measured and described by Ruppel (1979) and Johnson (in prep.). Samples used in the present study are from the study of Johnson (in prep.). Sample numbers are given below with stratigraphic position within the measured section. All measurements are relative to the lower contact of the Rockdell Formation. The reader is referred to Ruppel (1979) and Johnson (in prep.) for complete descriptions and detailed measurements.

SAMPLE NO.	STRAT. POS.	SAMPLE NO.	STRAT. POS.
CS-37	0.10 m	CS-51	58.20 m
CS-38	4.50 m	CS-52	60.90 m
CS-40	10.80 m	CS-53	66.70 m
CS-41	14.80 m	CS-54	71.80 m
CS-43	16.70 m	CS-55	76.40 m
CS-42	19.60 m	CS-58	83.00 m
CS-44	22.00 m	CS-59	86.60 m
CS-45	30.90 m	CS-57	88.20 m
CS-49	53.20 m	CS-60	91.40 m

LOCALITY 3--POOR VALLEY CREEK

Approximately 38.4 m of the Holston Formation are exposed on the southwest side of the Poor Valley Creek embayment of Cherokee Lake immediately southeast of the US 11W bridge, approximately 2.30 km (1.43 mi.) east of the intersection of US 11W and State Route 31 (Flat Gap Road) in Hawkins County at Mooresburg, Tennessee (N 1/2, SE 1/4, NW 1/6, Russellville Quadrangle). The middle portion of the Holston Formation at this locality has been covered by renovation of the bridge across the embayment, allowing only the lowermost portion of the Holston to be sampled. This locality is covered by water during high-water stages of the Cherokee Lake (May through September). Sample numbers are given along with stratigraphic position within the measured section. All measurements are relative to the lower contact of the Holston Formation.

UNIT	THKN.	CUM. THKN.	DESCRIPTION
1	13.5	13.5	Very fine to coarse grained grainstone to packstone. Carbonate mud content increases up-section while the lower portion of the unit is mud-free grainstone. These lower grainstones appear to be dominated by bryozoans which are surrounded by radiaxial fibrous cement--this feature is conspicuous in outcrop. Bedding parallel stylolitization is common and produces an apparent layering of bryozoans. Outcrop is discontinuous. SAMPLES: PVC'-1A, 5.0 m; PVC'-1B, 7.0 m; PVC'-1B2, 7.2 m; PVC'-1C, 12.0 m.
2	8.5	22.0	Brick red, very fine-grained limestone (reef core). Reef flank sediments are not developed possibly due to weathing. Massive-bedding indistinct and discontinuous. Contains abundant encrusting bryozoans and large cephaloplods. Stomatactis is developed subparallel to bedding in the middle of the unit. Cavities with internal sediment fill, botryoidal cement (radiaxial fibrous) linings and minor fossil debris are common. Radiaxial cement appears to have nucleated on cavity walls and on allochem projecting into the cavities. Large cephalopods are commonly found within these cavities. The thickness of this unit is highly variable laterally. Radiaxial fibrous cement appears to sometimes be associated with fossil allochems (Trilobites?--Sample Number--shows this feature--Cut

			thin-section to examine the relationship between the allochems and the cement). This unit grades into the overlying unit. SAMPLES: PVC'-2A; PVC'-2B; PVC'-2C; PVC'-2D; PVC'-2E; PVC'-2F; PVC'-2G; PVC'-2F;; PVC'-2G; PVC'-2H; PVC'-2I; PVC'-2J.
3	16.4	38.4	Similar to Unit 1 except the mud content appears to be much greater throughout this unit as compared to Unit 1. Stylolitization is common in this unit--appears to be bedding parallel stylolitization. Massive bedded. SAMPLES: PVC'-3, 27.0 m; PVC'-3A, 33.0 m; PVC'-3B, 38.0 m.

LOCALITY 4--RED HOUSE BRANCH

Approximately 165.0 m of the Holston Formation and 42.4 m of the Rockdell Formation are exposed along both sides of the Red House Branch Embayment of Cherokee Lake, southeast of US 11W on the southwest side of the Lakemont Cabin Area in Hawkins County at Mooresburg, Tennessee (NE 1/4, NW 1/4, Russellville Quadrangle). The entrance to the Lakemont Cabin Area is on the south side of US 11W, approximately 4.76 kilometers (2.96 mi.) east of the intersection of State Route 31 (Flat Gap Road). Section is discontinuous at this locality. A complete section was obtained by measuring on both sides of the embayment. Portions of this section are covered by water during high-water stages of Cherokee Lake (May-September). Sample numbers are given along with stratigraphic position within the measured section. All measurements are relative to the lower contact of the Holston Formation.

UNIT	THKN.	CUM. THKN.	DESCRIPTION
1	16.0	16.0	[HOLSTON] Pinkish gray to brownish gray, medium to coarse grained limestone (grainstone). Massive bedded. Large ramose bryozoans and pelmatozoan ossicles abundant. Cross-bedding is well developed. Deformation is intense in this unit--on polished surface and especially in thin-section the grains are characterized by grain boundary stylolites. It appears that much of the the matrix material has been removed through deformation.This unit grades into the overlying unit as the micrite (present in the upper 5.0m of Unitl) content increases. The lower contact between the Holston and underlying Lenoir Formation is sharp and generally stylolitic.

			SAMPLES: RHB'-LC, at lower contact; RHB'-1, 0.5 m; RHB'-1A, 2.5 m; RHB'-1B, 10.5 m; RHB'-1C, 14.0 m.
2	7.0	23.0	[HOLSTON] Dark red to brick red, very fine grained limestone (reef core). Contains extremely abundant encrusting bryozoans. Straight cephalopods and coiled cephalopods are common locally within this unit. This unit is very similar to Unit 2 at Poor Valley Creek which is located along strike, 2.2 km to the southwest. The thickness of the unit appears to be variable laterally. Cavities lined by bryozoans, infilled with botryoidal cement/equant druse (pore central) and floored by internal sediment are common. These features are conspicuous on outcrop. Stromatactis is well developed within this unit with individual buildups varying in size from 0.10 m to >2.0 m in diameter. Flanking calcarenites (reef flank) which are adjacent to the mud mounds within this unit are well developed (generally packstones). Grades into the overlying unit. SAMPLES: RHB'-2A; RHB'-2B; RHB'-2C; RHB'-2D; RHB'-2E; RHB'-2F; RHB'-2G; RHB'-2H; RHB'-2I; RHB'-2J, RHB'-2K.
	5.0	28.0	COVERED INTERVAL
3	41.0	69.0	[HOLSTON] Cream to buff, pink to brick red, coarse-grained limestone containing varying amounts of carbonate mud and abundant, rather large ramose bryozoans and echinoderm ossicles. Unit appears layered due in part to stylolitization but also to normal breaks in bedding. Grainstones and packstones within this unit are distinctly cross-laminated. This unit also contains relatively small (10cm diameter), "isolated" mud-mounds throughout. These mud-mounds generally increase in size up-section. Deformational features are distinct within this unit with small faults (stylolitization perpendicular to bedding?) and fractures common. Unit exhibits patches or "lenses" which are brachiopod rich--an unusual feature for the Holston Formation in general. These areas are distinct on outcrop by color (purple and white due to iron staining and cementation) and the abundant cement associated with these "patches" of brachiopods.

			SAMPLES: RHB'-3A, 28.5 m; RHB'-3B, 32.8 m; RHB'-3C, 35.0 m; RHB'-3D, 38.3 m; RHB'-3E, 40.7 m; RHB'-3F, 43.0 m; RHB'-3G, 53.8 m; RHB'-3H, 59.2 m; RHB'-3I, 63.0 m; RHB'-3J, 67.0 m.
	21.0	90.0	COVERED INTERVAL
4	21.0	111.0	[HOLSTON] Lithologically similar to unit 3. Stylolites(approximately parallel to bedding) are abundant. Grades into the overlying unit. SAMPLES: RHB'-4A, 91.9 m; RHB'-4B, 100.4 m; RHB'-4C, 106.3 m; RHB'-4D, 108.3 m; RHB'-4E, 109.0 m.
5	29.0	140.0	[HOLSTON] Poorly exposed--consist of a mixture of pink, very fine-grained limestone and pink to gray coarse-grained limestone. Stylolites abundant. The deep red coloration characteristic of the Holston Formation is not developed in this unit or further up-section. SAMPLES: RHB'-5A, 122.0 m.
6	51.0	191.0	[HOLSTON] Cream to buff, medium to coarse-grained limestone (generally packstones). The unit becomes somewhat pinkish upward from base of unit. The pinkish color is associated with patches of lime mud. Dominant allochems appear to be echinoderms and bryozoans. The unit is generally massive but occasionally displays layering similar to that seen in Unit 3. SAMPLES: RHB'-6A, 159.0 m; RHB'-6B, 161.4 m; RHB'-6C, 162.0 m; RHB'-6D, 166.0 m; RHB'-6E, 171.5 m; RHB'-6F, 177.6 m.
	30.0	221.0	COVERED INTERVAL
7	7.4	228.4	[ROCKDELL] Cream to light gray, medium to coarse-grained limestone. This unit is superficially similar to Unit 6 except this unit exhibits a fetid odor when broken similar to the Rockdell Formation at Evans Ferry. SAMPLES: RHB'-7A, 226.5 m; RHB'-7B, 227.0 m.
8	35.0	263.4	[ROCKDELL] Greenish gray to brownish grey to grey, very fine grained (lime-mud) limestone containing abundant encrusting bryozoans and echinoderms. Pelmatozoan holdfasts are conspicuously well preserved throughout the micrite

rich areas. This unit contains several "lenses and patches" of light grey to cream, medium to coarse grained bryozoan-pelmatozoan grainstone and packstone. The micritic areas represent lime-mud mounds whereas the coarse-grained lithologies represent environments of higher current regime lateral to these mud-mounds--flanking grainstones and packstones. The grainstone and packstone areas are characteristically cross-laminated. At approximately 4.0 m from the upper contact, stromatactis build-ups are fairly well developed. (Ruppel's sample RHB 10-2). This stromatactis is developed on both sides of the Red House Branch embayment, the area described here, but also along strike to the northeast (approximately 0.4 miles northeast of the Red House Branch embayment on the northeast side of the Lakemont Cabin Area). This is the first Rockdell locality at which stromatactis has been described. The unit exhibits a strong fetid odor when broken - similar to the Rockdell at Evans Ferry. The is upper contact with the overlying Benbolt Formation is relatively sharp.

SAMPLES: RHB'-8A, 237.4 m; RHB'-8B, 239.4 m; RHB'-8C, 243.4 m; RHB'-8D, 249.4 m; RHB'-8E, 250.8 m; RHB'-8F, 255.4 m; RHB'-8G, 258.9 m; RHB'-8H, 259.4 m; RRB'-8J, 259.9 m; RHB'-8K, 262.1 m.

APPENDIX B

PETROGRAPHIC CONSTITUENT ANALYSIS DATA

Table B.1. Variables observed in constituent analysis. Section thicknesses are measured in meters from the lower contact of the Holston Formation at Red House Branch and Poor Valley Creek and from the lower contact of the Rockdell Formation at Cedar Springs and Evans Ferry. Section numbers (section no.) are as follows: 1 = Evans Ferry; 2 = Cedar Springs; 3 = Poor Valley Creek; and 4 = Red House Branch. Dunham rock types are as follows: 1 = grainstone; 2 = packstone; 3 = wackestone; 4 = mudstone; and 5 = boundstone.

Sample No.	Stratigraphic Position	Section No.	Dunham Rock Type	Echinoderms	Bryozoans	Trilobites	Ostracodes	Brachiopods	Molluscs	Algae	Sponges and Debris	Algally Coated Grains	Intraclasts	Peloids	Micrite	Microspar	Pseudospar	Dolomite	Stylocumulate	Indeterminate Fossils	Replacement Silica	Internal Sediment	Fractures	Opaques	Terrigenous Clastics	Syntaxial Overgrowth Cement	Radiaxial-Fibrous, Fascicular-Optic, Radial Fibrous Calcite	Bladed/Prismatic Cements	Equant Calcite	Ferroan Calcite	Micritic Cement
RHB1	0.50	4	1	21.65	37.99	0.11	0.56	0.00	0.00	0.00	0.00	0.00	0.00	0.00	0.00	0.00	0.00	0.68	1.01	2.93	0.00	0.00	0.00	0.00	0.00	16.46	12.84	0.79	5.97	0.00	0.00
RHB1AR	2.50	4	1	29.43	33.56	1.08	0.98	0.69	0.00	0.00	0.00	0.00	0.00	0.00	0.00	1.77	0.00	0.10	2.07	2.26	0.00	0.00	0.00	0.00	0.00	16.44	4.92	0.69	6.00	0.00	0.00
RHB1B	10.50	4	2	34.10	30.69	0.22	0.00	1.21	0.00	0.00	0.00	0.00	0.00	0.00	0.44	1.21	0.00	0.11	1.21	2.75	0.00	0.00	0.00	0.00	0.00	13.97	8.14	0.00	5.94	0.00	0.00
RHB2A	19.00	4	5	5.04	15.88	0.32	0.11	0.11	0.21	0.00	9.12	0.00	0.00	1.61	34.12	1.39	0.00	0.00	1.18	0.43	0.21	5.47	0.11	0.00	0.00	13.30	2.46	2.25	6.65	0.00	0.00
RHB2CTR	19.50	4	2	22.11	24.83	0.85	0.00	0.34	0.00	0.00	0.00	0.00	0.00	0.00	2.04	0.00	0.17	0.00	2.89	1.70	0.00	0.00	1.19	0.00	0.00	17.35	18.20	7.65	0.68	0.00	0.00
RHB2CBL	20.00	4	2	7.60	17.74	1.17	0.00	1.17	0.00	0.00	0.00	0.00	0.00	0.00	7.41	0.78	3.70	0.00	3.70	1.36	0.00	0.00	0.00	0.00	0.00	15.20	29.24	5.65	5.26	0.00	0.00
RHB2JS1	20.50	4	5	2.29	16.04	0.12	0.97	0.00	0.72	0.00	2.41	0.00	0.24	0.36	25.93	0.97	1.57	0.00	3.62	1.09	0.00	15.68	6.39	0.00	0.00	0.00	12.67	4.22	4.70	0.00	0.00
RHB2K	21.00	4	4	0.00	0.35	0.00	0.18	0.00	0.00	0.00	7.39	0.00	0.00	0.00	32.57	0.53	0.18	0.00	2.99	0.18	0.00	6.87	2.64	0.00	0.00	0.00	45.60	0.00	0.53	0.00	0.00
RHB3AT	28.50	4	2	22.76	22.09	0.67	0.27	0.13	0.00	0.00	0.00	0.00	0.00	0.00	5.22	1.07	0.27	2.81	8.03	1.87	0.00	0.00	0.00	0.00	0.00	0.00	2.55	0.00	5.49	0.00	0.00
RHB3BS1	32.80	4	2	11.16	24.04	4.91	0.27	0.93	0.00	0.00	0.00	0.00	0.00	0.00	14.87	1.06	0.46	0.00	4.78	1.06	0.00	0.00	0.27	0.00	0.00	3.32	24.71	0.00	7.44	0.00	0.00
RHB3C	35.00	4	5	9.85	21.06	1.70	0.23	1.59	0.00	0.00	0.00	0.00	0.00	0.34	30.24	3.40	3.17	0.00	3.28	1.02	0.00	0.00	0.91	0.00	0.00	7.47	6.23	0.23	9.28	0.00	0.00
RHB3DS1B	38.30	4	1	21.11	21.11	0.24	0.12	0.36	0.97	0.00	0.00	0.00	0.00	0.60	15.08	3.62	3.02	0.00	7.00	1.09	0.00	0.00	0.97	0.00	0.00	3.62	17.74	0.36	3.01	0.00	0.00
RHB3ER	40.70	4	2	13.89	32.58	2.27	0.00	0.13	0.00	0.00	0.00	0.00	0.00	0.13	1.26	0.51	0.88	0.76	2.40	1.77	0.00	0.00	0.00	0.00	0.00	23.74	5.68	3.16	10.86	0.00	0.00
RHB3FS2	43.00	4	2	1.84	32.04	0.37	0.00	0.00	0.00	0.00	0.00	0.00	0.00	0.00	10.87	1.66	0.00	0.00	2.03	0.18	0.00	0.00	0.37	0.00	0.00	0.74	32.78	0.00	17.13	0.00	0.00
RHB3G	53.80	4	3	3.69	35.08	0.36	0.00	0.00	0.00	0.00	0.00	0.00	0.00	0.12	25.80	7.13	2.14	3.92	8.56	0.00	0.00	0.00	2.02	0.00	0.00	3.57	1.19	0.95	5.35	0.12	0.00
RHB3HL	59.20	4	3	12.04	23.11	0.49	0.12	0.00	0.00	0.00	0.00	0.00	0.00	0.00	21.29	14.72	1.09	0.00	0.00	0.36	0.00	0.00	4.38	0.00	0.00	12.41	0.00	3.53	6.45	0.00	0.00
RHB3IR	63.00	4	2	3.53	30.94	0.59	0.00	0.00	0.00	0.00	0.00	0.00	0.00	0.00	17.53	8.00	0.94	16.35	2.71	0.35	0.00	0.00	0.35	0.00	0.00	8.24	0.94	0.00	9.53	0.00	0.00
RHB4AS1R	91.90	4	2	9.27	25.59	2.74	0.52	1.57	0.00	0.00	0.00	0.00	0.00	0.00	12.79	1.70	4.83	0.00	2.61	0.91	0.00	0.00	0.65	0.00	0.00	2.22	22.84	4.57	7.18	0.00	0.00
RHB4BS2	100.40	4	2	30.30	27.17	1.36	0.00	0.68	0.00	0.00	0.00	0.00	0.00	0.00	0.54	0.27	2.04	0.00	0.27	0.82	0.00	0.00	0.00	0.00	0.00	24.46	0.00	6.79	5.03	0.27	0.00
RHB4C	106.30	4	3	6.41	23.80	1.36	0.37	0.25	0.00	0.00	0.00	0.00	0.00	0.86	35.51	11.10	4.81	0.00	2.71	0.62	0.00	0.00	1.23	0.00	0.00	1.85	0.00	2.10	7.03	0.00	0.00
RHB4DL	108.30	4	2	5.51	24.55	0.72	0.12	0.12	0.00	0.00	0.00	0.00	0.00	1.80	24.67	1.80	6.23	0.00	8.02	0.84	0.00	0.00	0.00	0.00	0.00	0.96	14.49	2.16	8.02	0.00	0.00
RHB4ER	109.00	4	2	21.51	28.81	4.91	1.23	0.30	0.00	0.00	0.00	0.00	0.00	0.00	5.16	1.13	1.01	0.00	2.01	1.13	0.00	0.00	0.00	0.00	0.00	27.67	0.00	0.00	5.04	0.00	0.00
RHB5A	122.00	4	2	28.60	37.87	0.00	0.35	0.12	0.00	1.76	0.00	0.00	0.00	0.00	2.70	0.70	0.00	3.63	6.10	0.23	0.00	0.00	0.00	0.00	0.00	16.06	0.00	1.30	1.98	0.59	0.00
RHB6ABR	139.00	4	2	30.10	13.27	0.12	0.12	0.00	0.00	0.00	0.00	0.00	0.00	1.11	0.00	6.51	9.34	3.32	2.46	1.72	0.37	0.00	0.00	0.00	0.00	27.52	0.00	1.35	1.47	1.23	0.00
RHB6BBR	161.40	4	2	28.29	15.74	0.25	0.37	0.00	0.00	0.00	0.00	0.00	0.00	1.35	0.00	14.64	3.81	0.98	0.00	0.37	0.62	0.00	0.00	0.00	0.00	12.79	13.90	1.47	0.49	4.92	0.00
RHB6C	162.00	4	2	32.20	22.44	0.85	0.37	0.00	0.00	0.00	0.00	0.00	0.24	0.00	1.22	3.17	0.24	6.10	3.17	0.73	0.00	0.00	3.78	0.00	0.00	21.46	0.00	1.58	0.00	2.44	0.00
RHB6DM	166.00	4	2	29.71	9.67	0.95	0.12	0.00	0.12	0.00	0.00	0.00	0.60	0.24	14.68	14.08	1.31	0.36	3.34	1.79	0.00	0.00	0.00	0.00	0.00	10.15	9.30	1.91	0.00	1.47	0.00
RHB6ETL	171.50	4	2	31.99	14.65	0.00	0.22	0.22	0.00	0.00	0.00	0.00	1.57	0.34	4.03	6.94	0.56	3.47	3.47	0.34	0.00	0.00	3.24	0.00	0.00	25.39	0.00	1.34	0.00	2.23	0.00
RHB6FR	177.60	4	3	17.72	23.02	0.45	0.00	0.00	0.56	0.00	0.79	0.56	1.35	0.23	39.05	6.09	1.24	0.11	0.11	0.00	0.00	0.00	0.23	0.00	0.00	4.52	0.79	1.58	1.47	0.11	0.00
RHB7AS2	226.50	4	2	35.39	19.69	0.12	0.36	0.00	0.36	0.00	0.00	0.00	1.93	0.24	4.23	4.83	1.57	0.12	1.21	3.50	0.00	0.00	0.00	0.00	0.00	20.90	2.05	1.32	0.72	1.45	0.00
RHB7BB	227.00	4	2	28.86	19.73	0.94	0.00	0.00	0.00	0.00	0.00	0.00	1.34	0.00	1.74	2.01	0.13	0.00	5.91	2.68	0.00	0.00	0.00	0.00	0.00	33.83	0.27	0.67	1.21	0.13	0.34
RHB8A	237.40	4	2	13.16	22.33	0.00	0.00	2.23	0.12	0.00	0.00	0.24	1.06	0.00	16.33	2.00	1.06	0.12	2.94	1.29	7.05	0.00	0.24	0.00	0.00	16.92	0.00	0.24	1.41	11.29	0.00
RHB8B	239.40	4	2	18.92	15.22	0.14	0.57	0.00	0.00	0.00	0.00	0.00	0.14	0.00	16.50	1.71	3.98	0.00	1.28	2.13	0.00	0.00	0.14	0.00	0.00	29.88	0.00	4.41	2.98	1.99	0.00
RHB8CL	243.40	4	2	25.13	21.03	0.13	0.00	0.40	0.00	0.13	0.00	0.26	0.66	0.13	5.29	0.66	0.00	0.00	7.80	0.66	0.26	0.00	0.00	0.13	0.00	34.52	0.13	0.53	0.26	1.86	0.00
RHB8DS1	249.40	4	3	2.01	10.87	0.59	0.12	0.12	0.12	0.24	2.36	0.00	0.35	1.42	47.64	8.63	2.01	3.19	0.00	0.35	0.00	2.25	0.00	0.00	0.00	2.48	9.81	0.35	0.95	4.14	0.00
RHB8E	250.80	4	3	8.73	26.26	0.12	0.48	0.36	0.24	0.00	1.20	0.12	0.24	0.48	31.53	4.68	1.08	4.56	7.67	1.32	0.00	0.00	1.56	0.00	0.00	6.00	0.00	1.20	0.12	2.04	0.00
RHB8FS1	255.40	4	3	1.92	4.44	0.00	0.24	0.00	0.00	0.00	7.91	0.00	0.00	0.96	61.03	6.95	1.44	7.55	1.92	1.08	0.00	0.00	0.12	0.00	0.00	0.48	2.40	0.72	0.36	0.48	0.00
RHB8G	258.90	4	2	11.05	24.47	0.24	0.12	1.19	0.36	0.00	0.36	0.00	0.00	1.07	24.58	7.96	2.38	0.00	4.39	1.07	0.00	0.00	0.59	0.00	0.00	3.56	13.90	1.19	0.36	1.19	0.00
RHB8HW2R	259.40	4	4	0.50	0.25	0.00	0.12	0.00	0.00	0.00	6.35	0.00	0.00	1.99	53.92	14.20	0.25	0.00	0.87	0.37	0.00	0.00	0.00	0.00	0.00	0.00	19.18	0.00	1.74	0.25	0.00
RHB8KL	262.10	4	1	35.61	15.28	0.89	0.00	1.19	0.00	0.00	0.00	0.00	0.00	0.00	0.00	0.00	0.00	0.00	4.45	1.48	0.00	0.00	0.00	0.00	0.00	39.47	0.00	0.90	0.30	0.45	0.00
PVC1AB	5.00	3	2	5.92	34.49	0.17	0.35	0.00	0.00	0.00	0.00	0.00	0.00	0.00	1.92	4.88	0.70	1.92	0.00	2.96	0.00	0.00	0.00	0.00	0.00	28.92	10.10	4.36	0.52	2.79	0.00
PVC1B1	7.00	3	2	6.13	41.51	0.71	0.00	0.14	0.00	0.00	0.00	0.00	0.00	0.00	3.28	4.99	2.14	0.00	2.00	1.43	0.00	0.00	0.00	0.00	0.00	2.57	28.96	0.57	3.14	2.43	0.00
PVC1B2L	7.20	3	2	0.94	39.59	0.75	0.00	0.00	0.00	0.00	0.00	0.00	0.00	0.00	0.75	0.00	0.19	0.00	4.32	1.31	0.00	0.00	0.00	0.56	0.00	0.75	41.28	0.94	1.13	7.50	0.00
PVC1C	12.00	3	2	22.86	27.35	0.68	0.27	0.27	0.00	0.00	0.00	0.00	0.00	0.00	1.63	1.77	0.95	0.27	3.27	2.18	0.00	0.00	2.86	0.14	0.00	28.02	0.00	5.03	2.45	0.00	0.00
PVC2C	14.00	3	3	2.06	1.09	2.42	1.81	0.12	0.00	0.00	16.81	0.12	0.00	0.48	28.17	1.09	0.97	0.24	7.98	1.21	0.00	7.26	16.57	0.00	0.00	0.24	11.00	0.12	0.24	0.00	0.00
PVC2D	15.00	3	3	0.73	2.92	1.71	0.12	0.12	0.24	0.00	13.40	0.00	0.00	0.12	49.82	3.05	0.12	0.00	3.65	0.85	0.00	5.12	5.36	0.00	0.00	0.00	12.06	0.24	0.37	0.00	0.00
PVC2ES2	16.00	3	3	0.61	11.21	0.85	3.17	0.00	0.24	0.00	2.92	0.00	0.00	0.37	26.43	1.72	1.58	0.00	3.78	1.58	0.00	12.18	1.22	0.12	0.00	0.37	24.60	3.65	1.58	1.83	0.00
PVC2AC1MR	18.00	3	4	5.04	12.90	0.00	0.25	0.86	0.00	0.00	2.09	0.00	0.00	0.25	32.92	7.49	0.37	0.00	2.46	0.49	0.00	5.04	0.12	0.00	0.00	0.74	18.96	4.18	5.90	0.00	0.00
PVC2AC2MR	18.30	3	4	6.37	9.73	1.51	0.00	0.35	0.23	0.00	0.70	0.00	0.00	0.58	39.75	2.78	0.93	0.00	1.04	0.35	0.00	7.18	0.46	0.00	0.00	0.23	23.29	0.70	3.83	0.00	0.00
PVC2G	20.00	3	4	0.83	12.15	1.83	0.50	0.00	0.33	0.00	2.33	0.00	0.00	0.00	19.30	1.16	0.33	0.00	2.16	0.83	0.00	2.66	9.65	0.33	0.00	0.00	41.27	0.17	0.17	3.99	0.00
PVC2H	21.00	3	4	0.24	27.36	0.00	0.37	0.00	0.00	0.00	4.65	0.00	0.00	0.00	23.13	0.49	0.61	0.00	2.45	2.08	0.00	8.32	0.12	0.00	0.00	0.00	23.26	1.35	4.65	0.00	0.00
CS37	0.10	2	3	9.16	4.95	0.74	0.99	0.25	0.25	2.97	0.00	0.00	0.00	0.00	14.85	34.16	2.23	0.00	18.56	4.21	0.00	0.00	0.00	0.50	0.50	0.74	0.00	0.00	4.95	0.00	0.00
CS40	10.80	2	2	23.79	12.34	2.15	0.36	0.18	0.00	2.68	0.00	1.97	0.00	1.43	6.26	9.84	3.76	0.36	3.22	3.40	0.54	0.00	0.18	0.36	0.00	18.96	0.72	0.36	7.16	0.00	0.00
CS41	14.80	2	2	19.62	11.28	0.69	0.33	0.17	0.00	0.00	0.00	0.00	0.00	0.17	13.54	0.17	0.35	0.17	6.94	3.82	0.00	0.00	0.00	0.00	0.00	30.90	0.52	1.04	10.07	0.00	0.00
CS43	16.70	2	2	24.54	12.32	0.55	0.18	0.18	0.00	0.37	0.00	0.00	1.29	1.29	11.03	6.99	2.21	0.00	0.74	2.39	0.00	0.00	0.00	0.00	0.00	27.39	6.43	1.47	0.74	0.00	0.00
CS42	19.60	2	3	0.68	21.49	0.00	0.23	0.00	0.23	0.00	0.00	0.00	0.00	0.23	51.13	13.57	1.36	0.00	3.39	0.90	0.00	0.00	0.00	0.23	0.00	0.00	0.00	0.00	6.56	0.00	0.00
CS44	22.00	2	3	6.93	9.67	0.00	0.00	0.00	0.00	0.69	0.46	0.00	0.00	0.00	48.50	18.94	2.54	0.23	1.39	1.62	0.00	0.92	2.31	0.00	0.00	0.00	1.62	0.00	4.39	0.00	0.00
CS45	30.90	2	2	27.19	6.08	0.36	0.36	0.00	0.36	0.00	0.00	0.00	1.07	0.18	13.42	7.69	3.58	0.18	3.94	4.47	0.00	0.00	0.00	0.18	0.00	20.39	0.72	2.50	7.33	0.00	0.00
CS49	53.20	2	3	2.49	10.88	0.00	0.23	0.00	0.00	1.36	0.00	0.00	0.00	0.00	52.61	24.49	0.23	0.00	0.00	2.72	0.00	0.23	0.00	0.00	0.00	0.23	0.45	0.00	4.08	0.00	0.00
CS51	58.20	2	3	9.59	8.15	0.24	0.00	0.24	0.24	0.00	0.00	0.00	0.00	0.72	51.80	0.00	0.00	0.00	0.96	1.44	0.00	0.00	0.00	0.00	0.00	6.71	0.96	0.48	18.46	0.00	0.00
CS52	60.90	2	4	0.00	3.34	0.00	0.00	0.24	0.00	0.00	0.00	0.00	0.00	0.72	41.53	0.00	28.64	0.00	3.58	1.43	0.00	0.00	0.00	0.00	0.00	0.00	1.67	0.48	18.38	0.00	0.00
CS53	66.70	2	3	2.98	9.40	0.46	0.46	0.00	0.00	0.00	0.23	0.00	0.00	0.00	46.56	24.31	0.46	0.00	0.69	1.61	0.00	0.00	0.00	0.00	0.00	0.92	0.00	0.00	11.93	0.00	0.00
CS54	71.80	2	2	16.86	16.48	0.38	0.76	0.57	0.19	0.00	0.00	0.00	0.00	0.00	10.61	17.23	1.70	3.03	0.57	0.00	0.00	0.00	0.00	0.00	0.00	18.18	0.19	1.89	11.36	0.00	0.00
CS55	76.40	2	2	12.31	13.99	0.56	0.19	0.37	0.19	0.00	0.37	0.00	0.00	0.56	22.01	8.58	1.12	0.00	2.43	3.36	0.00	0.00	0.00	0.00	0.00	17.54	0.00	0.93	15.49	0.00	0.00
CS58	83.00	2	2	12.94	14.36	0.53	0.89	0.18	0.00	0.18	0.00	0.00	0.00	0.89	13.30	12.94	2.66	0.53	1.24	2.13	0.00	0.00	0.00	0.00	0.00	21.10	0.18	2.74	14.72	0.00	0.00
CS59	86.60	2	2	35.71	8.97	1.47	0.18	0.37	0.00	0.00	0.00	0.00	0.00	0.92	0.00	4.58	10.26	1.47	0.55	4.03	3.66	0.00	0.00	0.00	0.00	21.61	0.00	0.18	6.04	0.00	0.00
CS57	88.20	2	4	0.47	1.40	0.00	0.00	1.16	0.00	0.00	0.00	0.00	0.00	1.63	51.86	37.44	1.86	0.00	0.00	2.09	0.00	0.00	0.47	0.23	0.00	0.00	0.00	0.00	1.40	0.00	0.00
CS60	91.40	2	2	18.82	23.99	1.11	0.92	0.37	0.00	0.00	0.00	0.00	0.00	0.00	7.75	9.96	0.92	0.00	2.21	2.58	0.00	0.00	0.00	0.00	0.00	21.96	1.11	1.11	8.30	0.00	0.00
EF19	2.00	1	3	7.48	1.50	1.07	1.50	0.00	0.00	0.85	8.12	0.21	0.00	1.50	30.77	19.66	13.46	0.00	7.28	4.27	0.21	0.00	1.07	0.00	0.00	0.00	0.00	0.00	1.07	0.00	0.00
EF28	21.50	1	2	13.14	2.46	2.09	1.11	0.61	0.12	0.61	8.23	0.25	0.37	0.25	27.27	9.34	3.93	8.60	10.57	3.32	0.12	0.00	1.60	0.49	0.00	3.81	0.25	0.61	0.86	0.00	0.00
EF30	24.00	1	2	25.83	15.99	0.62	0.86	0.74	0.25	0.62	0.00	0.62	0.98	0.98	10.46	5.78	4.43	0.12	8.36	5.04	0.37	0.00	0.00	0.12	0.00	13.28	1.60	1.60	1.35	0.00	0.00
EF31	28.50	1	2	25.85	8.78	0.37	1.46	0.37	0.37	2.80	1.46	5.61	1.10	0.49	5.61	4.02	3.78	0.37	0.37	5.24	0.73	0.00	5.49	0.00	0.00	20.98	0.37	0.73	3.66	0.00	0.00
EF45	54.00	1	2	32.61	16.30	1.69	0.68	0.12	0.24	1.93	0.00	0.24	0.36	0.24	1.21	3.99	2.17	0.00	3.50	3.14	0.12	0.00	0.48	0.00	0.00	27.42	0.72	1.69	1.33	0.00	0.00
EF46	55.50	1	2	25.91	14.79	1.27	1.43	0.95	0.00	1.11	0.00	0.32	0.32	0.00	2.07	0.95	2.38	0.48	0.16	3.82	0.00	0.00	3.50	0.00	0.00	33.39	0.16	2.70	4.29	0.00	0.00
EF47A	57.50	1	2	18.91	5.47	0.66	0.50	1.99	0.00	0.66	0.00	0.17	0.00	0.00	1.00	2.99	2.99	4.48	7.79	5.64	0.00	0.00	0.00	0.00	0.00	37.31	0.00	4.64	4.81	0.00	0.00

APPENDIX C

CORRELATION COEFFICIENT OF THE CONSTITUENT ANALYSIS DATA

Correlation coefficients listed in the following tables were generated for the constituent analysis dataset (Appendix B) and subsets of that dataset using the correlation matrix procedure in the microcomputer program Statgraphics. Correlation coefficients listed in all tables except C.2 are those which were ≥0.65 or ≤-0.65. Correlation coefficients in Table C.2 (Evans Ferry samples only) are those from the matrix which were ≥0.80 or ≤-0.80 because of the small sample size at that locality (7).

Table C.1. All constituent analysis data (75 samples).

Variables	Correlation Coefficient
1) SYNTAXIAL CEMENT/ECHINODERMS	0.761
2) SYNTAXIAL CEMENT/MICRITE	-0.707
3) FERROAN CALCITE/REPLACEMENT SILICA	0.659

Table C.2. Evans Ferry samples (7 samples).

Variables	Correlation Coefficient
1) BRYOZOANS/ECHINODERMS	0.913
2) SPONGES/ECHINODERMS	-0.860
3) SPONGES/BRYOZOANS	-0.809
4) ONCOIDS/ALGAE	0.818
5) INTRACLASTS/MOLLUSCS	0.881
6) MICRITE/ECHINODERMS	-0.850
7) MICRITE/SPONGES	0.960
8) MICROSPAR/ECHINODERMS	-0.809
9) MICROSPAR/SPONGES	0.843
10) MICROSPAR/PELOIDS	0.825
11) MICROSPAR/MICRITE	0.899
12) PSEUDOSPAR/PELOIDS	0.875
13) PSEUDOSPAR/MICROSPAR	0.948
14) UNIDENTIFIED FOSSILS/TRILOBITES	-0.924

Table C.2 (continued)

Variables	Correlation Coefficient
15) REPLACEMENT SILICA/MOLLUSCS	0.815
16) REPLACEMENT SILICA/ONCOIDS	0.894
17) REPLACEMENT SILICA/INTRACLASTS	0.830
18) OPAQUES/DOLOMITE	0.823
19) SYNTAXIAL CEMENT/SPONGES	-0.849
20) SYNTAXIAL CEMENT/MICRITE	-0.939
21) SYNTAXIAL CEMENT/MICROSPAR	-0.848
22) BLADED CEMENT/BRACHIOPODS	0.903
23) BLADED CEMENT/SYNTAXIAL CEMENT	0.857
24) EQUANT CEMENT/SYNTAXIAL CEMENT	0.814

Table C.3. Cedar Springs samples (17 samples).

Variables	Correlation Coefficient
1) TRILOBITES/ECHINODERMS	0.706
2) ONCOIDS/TRILOBITES	0.709
3) INTRACLASTS/ECHINODERMS	0.681
4) MICRITE/ECHINODERMS	-0.844
5) MICRITE/TRILOBITES	-0.733
6) STYLOCUMULATE/ALGAE	0.667
7) REPLACEMENT SILICA/TRILOBITES	0.709
8) FRACTURES/INTERNAL SEDIMENT	0.943
9) OPAQUES/ALGAE	0.707
10) OPAQUES/STYLOCUMULATE	0.724
11) TERRIGENOUS CLASTICS/ALGAE	0.710
12) TERRIGENOUS CLASTICS/STYLOCUMULATE	0.909
13) TERRIGENOUS CLASTICS/OPAQUES	0.669
14) SYNTAXIAL CEMENT/ECHINODERMS	0.839
15) SYNTAXIAL CEMENT/MICRITE	-0.837
16) BLADED CEMENT/SYNTAXIAL CEMENT	0.700

Table C.4. Poor Valley Creek samples (11 samples)

Variables	Correlation Coefficient
1) SPONGES/BRYOZOANS	-0.689
2) ONCOIDS/SPONGES	0.739
3) MICRITE/BRYOZOANS	-0.860
4) MICROSPAR/BRACHIOPODS	0.697
5) STYLOCUMULATE/SPONGES	0.729
6) STYLOCUMULATE/ONCOIDS	0.797
7) UNIDENTIFIED FOSSILS/MICRITE	-0.662
8) UNIDENTIFIED FOSSILS/DOLOMITE	0.711
9) INTERNAL SEDIMENT/BRYOZOANS	-0.664
10) INTERNAL SEDIMENT/OSTRACODES	0.690
11) INTERNAL SEDIMENT/PELOIDS	0.810
12) INTERNAL SEDIMENT/MICRITE	0.695
13) FRACTURES/TRILOBITE	0.828
14) FRACTURES/SPONGES	0.761
15) FRACTURES/ONCOIDS	0.822
16) FRACTURES/STYLOCUMULATE	0.707
17) SYNTAXIAL CEMENT/ECHINODERMS	0.736
18) SYNTAXIAL CEMENT/DOLOMITE	0.763
19) SYNTAXIAL CEMENT/UNIDENTIFIED FOSSILS	0.753
20) BLADED CEMENT/SYNTAXIAL CEMENT	0.703
21) EQUANT CEMENT/BRACHIOPODS	0.692
22) FERROAN CALCITE/OPAQUES	0.860
23) FERROAN CALCITE/RADIAXIAL-FIBROUS CALCITE	0.718

Table C.5. Red House Branch samples (40 samples).

Variables	Correlation Coefficient
1) MICRITE/ECHINODERMS	-0.741
2) MICRITE/SPONGES	0.678
3) MICRITE/PELOIDS	0.698
4) SYNTAXIAL CEMENT/ECHINODERMS	0.739
5) SYNTAXIAL CEMENT/MICRITE	-0.694
6) FERROAN CALCITE/REPLACEMENT SILICA	0.821

Table C.6. All Holston Formation samples (40 samples).

Variables	Correlation Coefficient
1) SYNTAXIAL CEMENT/ECHINODERMS	0.704
2) SYNTAXIAL CEMENT/MICRITE	-0.676
3) FERROAN CALCITE/OPAQUES	0.728

Table C.7. All Rockdell Formation samples (35 samples).

Variables	Correlation Coefficient
1) ONCOIDS/ALGAE	0.638
2) INTRACLASTS/ECHINODERMS	0.612
3) FRACTURES/ONCOIDS	0.722
4) TERRIGENOUS CLASTICS/STYLOCUMULATE	0.668
5) SYNTAXIAL CEMENT/ECHINODERMS	0.825
6) SYNTAXIAL CEMENT/MICRITE	-0.847
7) FERROAN CALCITE/REPLACEMENT SILICA	0.885

Table C.8. All grainstones and packstones (47 samples).

Variables	Correlation Coefficient
1) ONCOIDS/ALGAE	0.742
2) RADIAXIAL-FIBROUS CALCITE/SYNTAXIAL CEMENT	-0.682
3) FERROAN CALCITE/REPLACEMENT SILICA	0.710

Table C.9. Holston grainstones and packstones (25 samples).

Variables	Correlation Coefficient
1) RADIAXIAL-FIBROUS CALCITE/ECHINODERMS	-0.686
2) RADIAXIAL-FIBROUS CALCITE/SYNTAXIAL CEMENT	-0.749
3) FERROAN CALCITE/OPAQUES	0.682

Table C.10. Rockdell Grainstones and packstones (22 samples).

Variables	Correlation Coefficient
1) ONCOIDS/ALGAE	0.786
2) MICRITE/ECHINODERMS	-0.769
3) DOLOMITE/SPONGES	0.823
4) FRACTURES/OSTRACODES	0.708
5) FRACTURES/ONCOIDS	0.781
6) OPAQUES/SPONGES	0.670
7) SYNTAXIAL CEMENT/MICRITE	-0.743
8) FERROAN CALCITE/REPLACEMENT SILICA	0.952

Table C.11. All wackestones, mudstones, and boundstones (28 samples).

Variables	Correlation Coefficient
1) INTRACLASTS/ONCOIDS	0.868
2) STYLOCUMULATE/ALGAE	0.758
3) UNIDENTIFIED FOSSILS/ALGAE	0.671
4) TERRIGENOUS CLASTICS/ALGAE	0.937
5) TERRIGENOUS CLASTICS/STYLOCUMULATE	0.770
6) TERRIGENOUS CLASTICS/OPAQUES	0.717

Table C.12. Holston wackestones, mudstones, and boundstones (15 samples).

Variables	Correlation Coefficient
1) SPONGES/BRYOZOANS	-0.679
2) ONCOIDS/ECHINODERMS	0.665
3) INTRACLASTS/ECHINODERMS	0.676
4) INTRACLASTS/ONCOIDS	0.959
5) STYLOCUMULATE/DOLOMITE	0.652
6) REPLACEMENT SILICA/PELOIDS	0.787
7) FERROAN CALCITE/OPAQUES	0.996

Table C.13. Rockdell wackestones, mudstones, and boundstones (13 samples).

Variables	Correlation Coefficient
1) OSTRACODES/TRILOBITES	0.834
2) ONCOIDS/OSTRACODES	0.755
3) MICRITE/TRILOBITES	-0.657
4) MICRITE/OSTRACODES	-0.723
5) MICRITE/ALGAE	-0.790
6) STYLOCUMULATE/OSTRACODES	0.685
7) STYLOCUMULATE/ALGAE	0.873
8) STYLOCUMULATE/MICRITE	-0.908
9) UNIDENTIFIED FOSSILS/OSTRACODES	0.782
10) UNIDENTIFIED FOSSILS/ALGAE	0.700
11) UNIDENTIFIED FOSSILS/MICRITE	-0.685
12) UNIDENTIFIED FOSSILS/STYLOCUMULATE	-0.656
13) REPLACEMENT SILICA/TRILOBITES	0.693
14) REPLACEMENT SILICA/OSTRACODES	0.783
15) REPLACEMENT SILICA/ONCOIDS	0.858
16) INTERNAL SEDIMENT/INTRACLASTS	0.718
17) OPAQUES/ALGAE	0.736
18) OPAQUES/STYLOCUMULATE	0.692
19) TERRIGENOUS CLASTICS/ALGAE	0.939
20) TERRIGENOUS CLASTICS/MICRITE	-0.727
21) TERRIGENOUS CLASTICS/STYLOCUMULATE	0.868
22) TERRIGENOUS CLASTICS/OPAQUES	0.831
23) SYNTAXIAL CEMENT/MOLLUSCS	0.652

Table C.13 (continued)

Variables	Correlation Coefficient
24) BLADED CEMENT/MICROSPAR	-0.687
25) BLADED CEMENT/DOLOMITE	0.743
26) BLADED CEMENT/SYNTAXIAL CEMENT	0.683
27) FERROAN CALCITE/INTRACLASTS	0.980
28) FERROAN CALCITE/INTERNAL SEDIMENT	0.787

APPENDIX D

ATOMIC ABSORPTION SPECTROPHOTOMETRY

Atomic Absorption Procedures

Sample Selection

Atomic absorption spectrophotometry was used to determine the concentrations of three minor elements in radiaxial-fibrous and pore central equant cement. The minor elements analyzed were strontium, magnesium, and manganese. Data derived from these analyses were used to help infer original mineralogies of these two cements. All cement samples were taken from large cavities in mud-supported lithologies of the Holston and Rockdell formations. Samples were selected based on the following criteria:

1. Cement type;
2. Size of the cement crystals;
3. Distance away from late diagenetic/tectonic fractures; and
4. "Unaltered" appearance in hand specimen.

Methods

Each specimen to be sampled was rinsed in tap water, air dried and rinsed again in deionized water. Selected cement crystals were "micro-sampled" using carbide steel dental drill bits mounted in a Jensen vertical milling machine. This technique provided a finely powdered sample which was collected in small sampling vials. To obtain enough material to analyze, several holes were drilled in the cement mosaic, giving an averaged sample. Radiaxial-fibrous cement in sample PVC-2A was drilled proximal to the substrate and at the distal end of the crystals providing two samples from that cavity filling mosaic. Five

drill bits were used in the sampling process, each being washed after use in a 25% (volume/volume) acetic acid solution, rinsed in deionized water, and allowed to air dry.

The total sample weight before dissolution was 0.10 gm, weighed to the nearest 0.01 gm using a Mettler balance. The sample was dissolved in 5 ml of 25% (volume/volume) acetic acid in a 100 ml beaker. The solution was allowed to digest for 8 hours and was then filtered into a separate 100 ml beaker. The solution was brought up to 10 ml by adding additional 25% acetic acid.

The weight of insoluble residue on the filter paper was obtained by weighing each filter paper used in the filtration process to the nearest 0.01 gm on a Mettler balance prior to use. After filtration, the filter paper was oven-dried and reweighed. The original weight of each paper was subtracted from the second weight giving the weight of insoluble residue for each sample. The weight of insoluble material was subtracted from the original sample weight of 0.10 gm yielding the amount of sample in solution. A total of 13 differentcement samples were collected and prepared using this technique. Nine of the samples were taken from radiaxial-fibrous calcite cement and 4 were pore central equant calcite. Duplicate solutions were prepared for 4 samples, 2 radiaxial-fibrous cement samples and 2 equant calcite samples.

Control Data

Samples were prepared and analyzed in conjunction with a larger suite of samples being identically prepared and analyzed by Eric Johnson at the University of Tennessee, Department of Geological

Sciences. To insure accurate machine calibration, blank solutions (25% acetic acid) were run after every third sample and standard solutions were run periodically while analyzing the suite of samples. The 4 duplicate solutions were run with the other samples in an attempt to test the precision or reproducibility of the sample preparation technique.

Johnson (in prep.) has calculated the precision of the analyses for strontium, magnesium and manganese based on the entire suite of samples he analyzed. Using samples which had replicate analyses for strontium, magnesium and/or manganese, he calculated the relative percent error for each sample. The mean relative percent error for analyses of either strontium, magnesium ormanganese was then calculated. Precision data used in the calculations and the mean relative percent error are given in Table D-1. Results of the analyses are summarized in Table D-2.

Table D-1. Precision data for strontium, magnesium and manganese. This table lists the relative percent error of individual analyses of samples for a particular element. The mean relative percent error, listed below, has been calculated from the data presented here.

relative% Sr	relative% Mg	relative% Mn
2	3	10
2	15	7
7	12	7
6	10	5
9	10	3
8	8	7
14	9	19
17	12	2
2	3	3
6	3	3
6	4	3
3	2	3
5	3	1
4	2	2
6	3	2
8	1	3
3	4	2
2	6	1
3	2	2
7	3	2
6	9	1
7	2	1
16	3	2
12	3	3
4	2	3
13	4	2
4	8	
9	2	
6	2	
3	3	
MEAN ±7 relative%	±5 relative%	±4 relative%

Table D.2. Atomic absorption spectrophotometry data. Duplicate analyses are noted in parentheses. RHB-2H and RHB-8H represent Holston and Rockdell stromatactis, respectively. PVC-2A(I) was taken proximal to the substrate and PVC-2A (II) was taken distal to the substrate.

SAMPLE NO.	Sr (ppm)	Mg (ppm)	Mn (ppm)
Radiaxial-Fibrous Calcite			
RHB-2J	230	2640	100 (157)
RHB-2H	250	3760	124
RHB-8H	256	2670	93
PVC-2A(I)	289	2670	226
PVC-2A(II)	180	1800	140
PVC-2F	280	1500	100
PVC-2G	200	1500	104
PVC-2J	230	1750	249 (225)
PVC-2K	240	1450	143
Pore Central Equant Calcite			
RHB-2J	116	2060	903 (800)
PVC-2A	151	2060	410 (535)
PVC-2G	143	2180	336
PVC-2J	229	1450	480

VITA

Dana Gregory Jernigan was born on March 14, 1960 in Knoxville, Tennessee. He attended public school in Knoxville and was graduated from Bearden Senior High School in June 1978. He entered The University of Tennessee, Knoxville in July 1978, majoring in Liberal Arts. On December 11, 1982, Greg married the former Cheryl Lynn Wade of Knoxville and the following Spring, was graduated with honors from the University of Tennessee, Knoxville with a Bachelor of Arts in Geology.

In June 1983, Greg enrolled in the graduate program in the Department of Geological Sciences, The University of Tennessee, Knoxville and in December 1983, received a Teaching Assistantship. In December 1984, he was awarded a Carden Fellowship with the Department of Geological Sciences. Greg was graduated from The University of Tennessee, Knoxville in August 1987 with a Master of Science in Geology.

At the time of this writing, Greg was a member of the American Association of Petroleum Geologists, the Society of Economic Paleontologist and Mineralogists, and Sigma Gamma Epsilon. He was employed under contract to Martin Marietta Energy Systems, Inc. in Oak Ridge, Tennessee, working in the Remedial Action Program at Oak Ridge National Laboratory.